UMCEE 00-10

May 2001

VERIFICATION OF GIRDER DISTRIBUTION FACTORS FOR STEEL GIRDER BRIDGES

PROJECT 2000-0341 DIR

Report submitted to the Michigan Department of Transportation

Andrzej S. Nowak and Junsik Eom

Department of Civil and Environmental Engineering
University of Michigan
Ann Arbor, Michigan 48109-2125

TESTING AND RESEARCH SECTION
CONSTRUCTION AND TECHNOLOGY DIVISION
RC-1393

Technical Report Documentation Page

1. Report No. RC-1393	2. Government Accession No.	3. Recipient's Catalog No.
4. Title and Subtitle Verification of girder distribution factors for steel girder bridges		5. Report Date April 2001
7. Author(s) Andrzej S. Nowak and Junsik Eom		6. Performing Organization Code
9. Performing Organization Name and Address University of Michigan 2340 GG Brown Bldg. Ann Arbor, MI 48109-2125		8. Performing Org Report No. UMCEE 00-10
12. Sponsoring Agency Name and Address Michigan Department of Transportation Construction and Technology Division P.O. Box 30049 Lansing, MI 48909		10. Work Unit No. (TRAIS) 11. Contract/Grant No. Project 2000-0341 DIR
15. Supplementary Notes		13.Type of Report& Period Covered Final Report 14. Sponsoring Agency Code

16. Abstract

The Report documents the field testing and finite element analysis of steel girder bridges with spans from 10 to 45 m. A total of six bridges were instrumented and loaded with heavy 11-axle trucks. In addition, truck survey was carried out to determine the frequency of simultaneous occurrence of two trucks in-lane and side-by-side. The field tests confirmed that the code specified GDF's, for a single lane and for two-lane traffic, are conservative. An advanced finite element (FEM) analysis was performed using ABAQUS. The actual bridge behavior was modeled by assuming a partial fixity of the supports (fixed hinges and restrained rotation). For the design of new bridges, it is recommended to use AASHTO LRFD (1998) GDF's. For evaluation of existing steel girder bridges, it is recommended to use AASHTO LRFD (1998) GDF's specified for a single lane even for two lane structures, because of a reduced probability of a simultaneous occurrence of two heavy trucks side-by-side. The field study also confirmed previous findings related to the dynamic load factors (DLF). Therefore, for evaluation of existing steel girder bridges it is recommended to use DLF = 0.10 for two lane loading, and DLF = 0.20 for a single truck load case.

17. Key Words steel girder bridges, girder distribution factors, dynamic load factors, finite element analysis		18. Distribution Statement No restrictions. This document is available to the public through the Michigan Department of Transportation	
19. Security Classification (report) Unclassified	20.Security Classification (page) Unclassified	21. No of Pages	22. Price

DISCLAIMER

The contents of this report reflect the views of the authors, who are responsible for the facts and the accuracy of the information presented herein. This document is disseminated under the sponsorship of the Michigan Department of Transportation, in the interest of information exchange. The Michigan Department of Transportation assumes no liability for the contents or use thereof.

Executive Summary

The Report documents the field testing and analysis of steel girder bridges with spans from 10 to 45 m. The objective of the tests was to provide a basis for recommended girder distribution factors (GDF) for interior girders and dynamic load factors (DLF), suitable for evaluation of existing bridges. In addition, truck survey was carried out to determine the frequency of simultaneous occurrence of two trucks in-lane and side-by-side.

A total of six bridges were instrumented and loaded with heavy 11-axle trucks. The results were obtained for one truck and two trucks side-by-side. The vehicles were moving at crawling speed for the static load measurement and at a regular speed for the dynamic load measurement. Two truck positions were considered for each case: close to the curb and center of the traffic lane. The strains for both trucks are practically the same, which confirms the repeatability of the results. The measured maximum strains were also the same for crawling speed and a regular speed. The tested bridges were all simply supported structures. The maximum measured strain was less than 200 με. Lower than expected strain values were due to partial fixity of supports, and flexural stiffness of the deck slab, sidewalks, parapets and curbs.

The field study confirmed previous findings related to the dynamic load factors (DLF). The test results showed that DLF for a single truck is about 0.20. For two trucks side-by-side, DLF is less than 0.10 for all the tested bridges. Therefore, for evaluation of existing steel girder bridges it is recommended to use DLF = 0.10 for two lane loading, and DLF = 0.20 for a single truck load case.

An advanced finite element (FEM) analysis was performed using ABAQUS. Three models were used, one with simply supported girders, the other one with restraints imposed on horizontal movements of

girders, and the third one with spring elements simulating a partial fixity of supports. The spring constants in the latter were determined using the test data. The FEM results are compared with the test results. It was observed that the most important and difficult task is the selection of the boundary conditions (in particular support conditions). The actual bridge behavior was modeled by assuming a partial fixity of the supports (fixed hinges and restrained rotation).

The field tests confirmed that the code specified GDF's, for a single lane and for two lane traffic, are conservative, for both AASHTO LRFD (1998) and AASHTO Standard (1996). For the design of new bridges, it is recommended to use AASHTO LRFD (1998) GDF's. The truck survey confirmed that the probability of a simultaneous occurrence of two fully loaded truck side-by-side is negligible. Therefore, for evaluation of existing steel girder bridges, it is recommended to use AASHTO LRFD (1998) GDF's specified for a single lane even for two lane structures, because of a reduced probability of a simultaneous occurrence of two heavy trucks side-by-side.

There were continued problems with wireless transmitters (interference, poor connections, range), and the system had to be returned for repairs. There is still a need for further field trials. The measurement of deflection using the optical device by Noptel provided good results. However, there is a need to purchase additional units to measure the deflection at several points simultaneously (only one unit was available for this project).

TABLE OF CONTENTS

Note:

Intentionally left blank

Acknowledgments

The presented research has been sponsored by the Michigan Department of Transportation which is gratefully acknowledged. The authors thank the technical staff of the Michigan DOT, Roger Till, Sudhakar Kulkarni, David Juntunen, Steven Beck and other members of TAG for their useful comments, discussions and support.

The project team received help from other researchers, current and former students and staff of the University of Michigan. In particular, thanks are due to Dr. Chris Eamon, Dr. Ahmet Sanli, Dr. Maria Szerszen, Taejun Cho, Gerard Gaal, David Ferrand, Jose Romero, and Huron High School students Karol Szerszen and Jakub Szerszen. They were involved in field instrumentation, measurements, and processing of the results.

The field survey of multiple presence of trucks was carried out by Jose Romero.

Thanks are due to the Michigan State Police for their cooperation.

The realization of the research program would not be possible without in kind support of the Michigan DOT and the University of Michigan. Measurements were taken using equipment purchased by the University of Michigan.

Note:

Intentionally left blank

1. INTRODUCTION AND LITERATURE SURVEY

1.1 Introduction

The objective of this study is validation of the code–specified girder distribution factors (GDF) and dynamic load factors (DLF) for short and medium span girder bridges (spans 10-40 m) by field tests. Field testing is an increasingly important topic in the effort to deal with the deteriorating infrastructure, in particular this applies to bridges and pavements. There is a need for accurate and inexpensive methods for diagnostics, verification of load distribution, and determination of the actual load carrying capacity. A considerable number of Michigan bridges were constructed in 1950's and 1960's. Many of them show signs of deterioration. In particular, there is a severe corrosion on many steel and concrete structures. By analytical methods, some of these bridges are not adequate to carry the normal highway traffic. However, the actual load carrying capacity is often much higher than what can be determined by analysis, due to more favorable load sharing, effect of non-structural components (parapets, railing, sidewalks), and other difficult to quantify factors. Field testing can reveal the hidden strength reserve and thus verify the adequacy of the bridge.

There is a growing need for developing efficient procedures for evaluation of the actual load spectra, load distribution, actual strength and predict the remaining life of the structure. There is a need to verify if the currently used girder distribution factors (GDF) are too conservative. Girder distribution factors (GDF) are very important in evaluation of existing bridges. Extensive analytical studies performed in conjunction with the development of AASHTO LRFD Code indicated that GDF's specified by the AASHTO Standard Specifications (1996) are often inaccurate, in some cases the specified values are overly conservative, and in other cases they are too permissive. Knowledge of the accurate GDF's is needed to determine the actual value of live load (truck load) for

bridge girders. Overestimation of GDF's can have serious economic consequences, as deficient bridges must be repaired or rehabilitated.

Furthermore, the GDF's specified in AASHTO were derived for HS-20 trucks. On the other hand, the live load in Michigan is often governed by 11 axle trucks. Therefore, there is a need to determine the GDF's for 11 axle vehicles loaded to the legal limit.

The analytical derivation of GDF's has limitations. The advanced structural analysis is based on the finite element method (FEM). The currently available computer procedures allow for a very high degree of mathematical accuracy. However, the limitation, even for the latest generation of FEM programs, is the accuracy of input data, in particular, boundary conditions. The actual support conditions are difficult to represent analytically. Hinge-roller supports can be partially fixed (frozen) due to corrosion, accumulation of debris, and presence of a heavy diaphragm over the support. Non-structural components such as sidewalks, curbs and parapets contribute to the overall stiffness, and it is difficult to estimate this contribution analytically.

1.2 Literature review

The literature available on the subject of girder distribution factors and dynamic load factors was summarized in the report UMCEE 99-13 submitted by the Project Team to the Michigan DOT. The basic analytical studies on GDF were carried out as part of NCHRP Project by Imbsen and Associators, with the results summarized by Zokaie at al. (1991). The researchers at the University of Michigan also carried out an extensive analysis which led to the conclusion that the GDF's specified by the AASHTO Standard (1996) are considerably conservative for larger spans and girder spacings. The latest reference is a book by O'Connor and Shaw (2000) which provides a very good summary of bridge load models. This book contains detailed summary about bridge loads from

an international perspective, including current codes of practice in the various countries. It covers various kinds of loads, including vehicular loads, pedestrian loads, railing loads, wind loads, and earthquake loads. It contains the design philosophies regarding the loads and bridges. The possible modes of failure are also covered in this book.

The available dynamic load models were also summarized in report UMCEE 99-13 submitted to MDOT. It was observed that DLF decreases for heavier trucks, and it is further reduced for two trucks side-by-side (multiple presence).

A stochastic model for multilane traffic effects on bridges was proposed by Croce and Salvatore (2001). Their model was based on an equilibrium renewal process of vehicle arrivals. The results are presented for different span length and for traffic condition.

Note:

Intentionally left blank

2. SELECTED BRIDGES

This study is focused on steel girder bridges with simply supported spans from 10 to 40 m. These structures constitute 65% of bridges in Michigan. It was observed that many steel girder bridges are considered deficient and in need of repair or replacement due to insufficient live load carrying capacity. In 1997 and 1999, twelve bridge tests were performed to determine the GDF's for fully loaded Michigan trucks with 10 and 11 axles. The results of these tests are documented in the previous reports (Nowak et al. 1998 and 2000). However, it is recognized that there is still a need for more tests of steel girder bridges with spans 10-40 m. A considerable number of short span steel girder bridges can be saved by evaluation using a more accurate value of GDF. Analytical studies also point to a reduced conservatism in code-specified GDF's for shorter spans.

In this study, the selection of bridges was based of the following criteria:

- Structural type and material; steel girder bridges.
- Span length; short spans between 10 m and 20 m, and spans longer than 30 m.
- Number of lanes; two lane bridges were considered.
- Skewness; Bridges with skew angle of more than 15 degrees were excluded.
- Accessibility; some structures could not be considered because of difficult access for testing equipment, in particular due to deep water or excessive height. Bridges over major highways were also excluded due to difficult traffic control during instrumentation and testing.
- Traffic volume; very busy bridges were not considered because of the expected difficulties with traffic control. Therefore, only bridges with an average daily traffic of 12,000 were selected.

More than a hundred bridges were inspected to verify their feasibility for load test. Finally, six bridges were selected for this study as listed in Table 2.1.

Table 2.1. Selected Bridges.

MDOT ID Number	Location (County)	Tested Span (m)	Number of Girders	Girder Spacing (m)	Year of Construction	Skew Angle	Operating Rating (kN)	ADT
B02-46071	Lenawee	15.2	9	1.57	1947	0	1,005	2,500
B01-30071	Hillsdale	10.6	10	1.40	1948	15	1,094	3,300
B01-58041	Monroe	16.7	8	1.79	1953	10	1,237	4,400
S11-25032	Genesse	38.4	7	2.21	1972	0	1,023	2,000
B02-23041	Eaton	10.6	9	1.57	1949	0	1,343	4,000
B01-47041	Livingston	42.6	6	2.85	1986	15	1,050	12,000

3. LOAD TESTING PROCEDURE

3.1 Instrumentation and data acquisition

The strain transducers were attached to the lower and/or upper surface of the bottom flange of steel girders at midspan (Figure 3.1), depending on the accessibility. In addition, they were installed on selected girders at the ends to measure the moment restraint provided by the supports, and at intermediate span locations to measure variation in moment along the span. For some bridges, the deflection of the most loaded girder was measured using the optical device (PSM-R) manufactured by Noptel, Co. in Finland. This device is suitable for long distance remote displacement measurements. It is based on a combined LED transmitter and opto-electronic receiver that measures the position of the reflector or prism attached to the target.

Strain transducers were connected to the SCXI data acquisition system from the National Instruments. The data acquisition mode is controlled from the external PC notebook computer, and acquired data are processed and directly saved in PC's hard drive (Figure 3.2).

The data acquisition system consists of a four slot SCXI-1000 chassis, one SCXI-1200 data acquisition module and two SCXI-1100 multiplexers. Each multiplexer can handle up to 32 channels of input data. The current system is capable of handling 64 channels of strain or deflection inputs. Up to 32 additional channels can be added if required. A portable field computer is used to store, process and display the data on site. A typical data acquisition setup is shown in Figure 3.2. The data from all instruments is collected after placing the trucks in desired positions or while trucks are passing on the bridge. For the normal speed tests, a sampling rate of 300 per second was used for calculation of dynamic effects. This is equivalent to 11.4 samples per meter at a truck speed of 95 km/h. The real time responses of all transducers are

displayed on the monitor during all stages of testing, assuring the safety of the bridge load test.

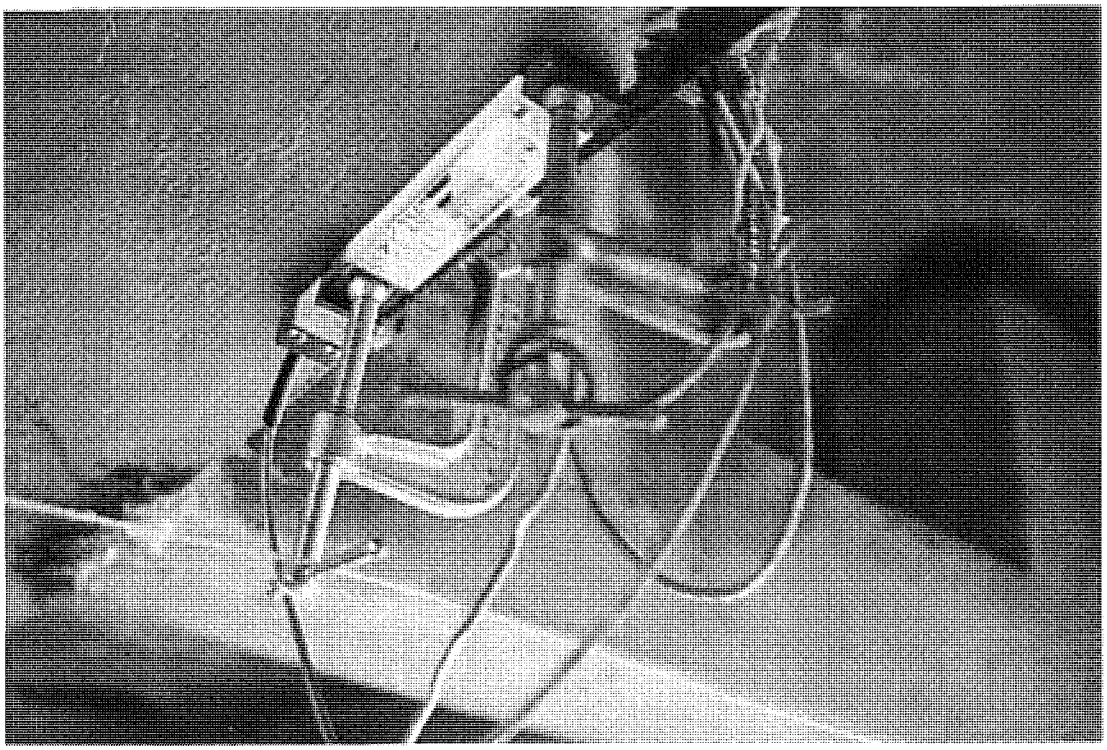

Figure 3.1. Removable Strain Transducer Mounted to the Lower Flange.

One of the objectives of the project was verification of reliability and usability of wireless transmitters as a replacement for cables connecting the strain transducers and the main computer unit.

The wireless transmitters were purchased in 1997, but lab test showed they were not working properly and they were fixed by the manufacturer several times. Prior to the field tests in 2000, the equipment was again tested by University of Michigan research team, and was found not fully functional. Therefore, it was returned to the manufacture for further modifications.

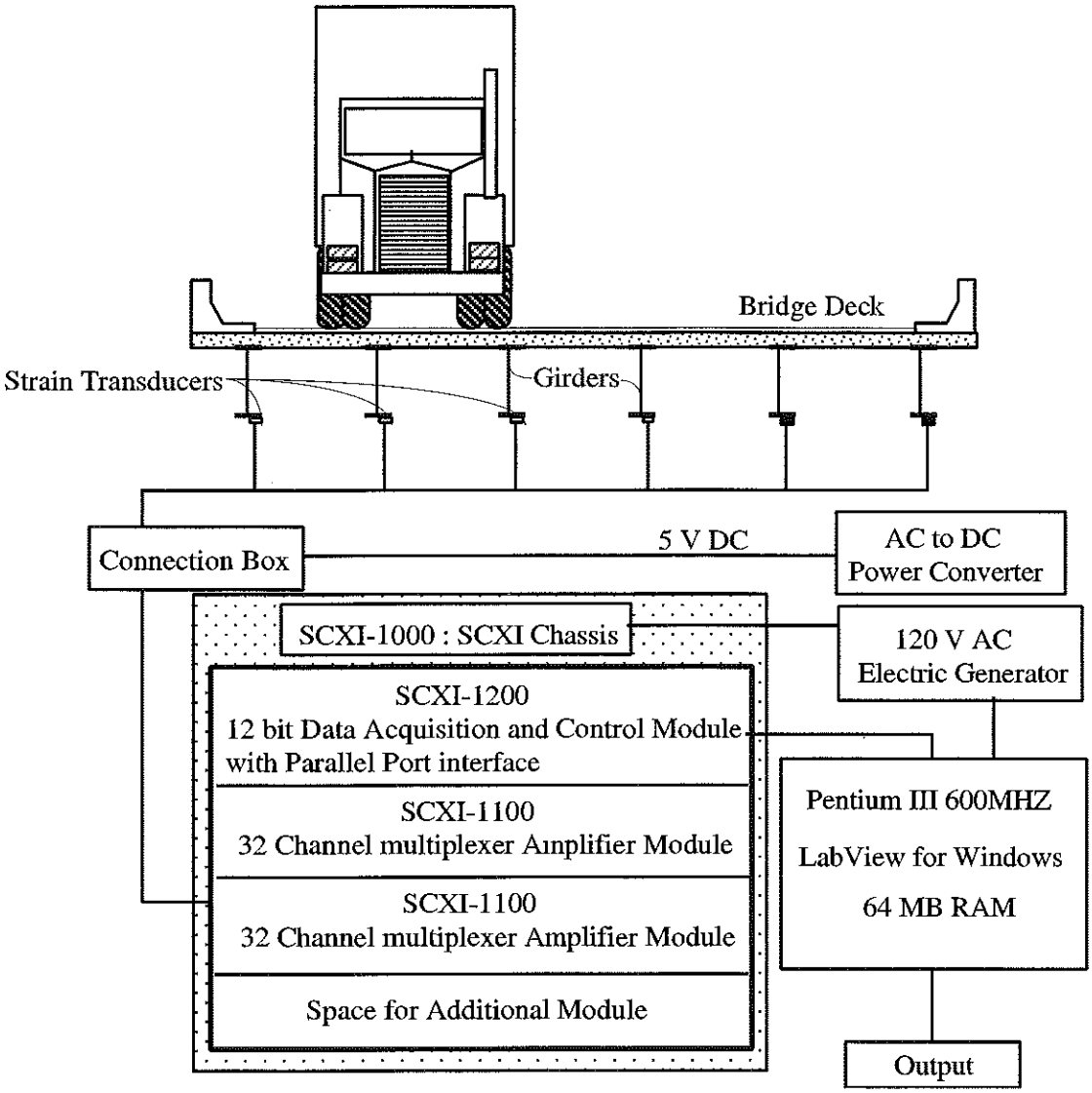

Figure 3.2. SCXI Data Acquisition System Setup.

3.2 Test loads for load distribution tests

Strain data for calculation of the girder distribution factors and dynamic load factors were taken from bottom-flanges of girders in the middle of a span. The measurements were taken under passages of one and two vehicles, each being a three-unit 11-axle truck with known weight and axle configuration. The actual axle weights of the test trucks were measured at the weigh stations prior to the test for all bridges.

Strain data was used to calculate load distribution and dynamic load factors. Superposition of strain data for single trucks was compared to the results obtained for two trucks side-by-side, as the verification of the linear-elastic behavior of the bridge.

Trucks were driven over the bridge at crawling speed as static load and at normal speed to obtain dynamic effect on the bridge. For each location, normal speed was the maximum possible speed for the test truck. Table 3.1 shows typical sequence of test runs. Lane 1 indicates north or west lane, and lane 2 indicates south or east lane, depending on the orientation of the tested bridge.

Table 3.1. Sequence of Typical Test Runs for All Bridges.

Run Number	Trucks	Lane	Position in Lane	Truck Speed
1	Truck A	1	Center	Crawling Speed
2	Truck A	1	Curb	Crawling Speed
3	Truck B	1	Center	Crawling Speed
4	Truck B	1	Curb	Crawling Speed
5	Truck B	1	Center	Normal Speed
6	Truck A	1	Center	Normal Speed
7	Truck A	2	Center	Crawling Speed
8	Truck A	2	Curb	Crawling Speed
9	Truck B	2	Center	Crawling Speed
10	Truck B	2	Curb	Crawling Speed
11	Truck B	2	Center	Normal Speed
12	Truck A	2	Center	Normal Speed
13	Truck A and B	1 and 2	Center	Crawling Speed
14	Truck B and A	1 and 2	Center	Crawling Speed
15	Truck A and B	1 and 2	Center	Normal Speed
16	Truck B and A	1 and 2	Center	Normal Speed

3.3 Load distribution factor and dynamic load factor calculation from test results

Collected strain data from the tests were processed to identify dynamic load and girder distribution factors. Girder Distribution Factors (GDF) are calculated from the maximum static strain obtained from the static loading at each girder at the same section along the length of the bridge. Ghosn *et al.* (1986) assumed that GDF was equal to the ratio of the static strain at the girder to the sum of all the static strains. Stallings and Yoo (1993) used the weighted strains to account for different section moduli of the girders. Accordingly, GDF for the *i*-th girder, GDF_i, can be derived as follows:

$$GDF_i = \frac{M_i}{\sum_{j=1}^{k} M_j} = \frac{ES_i\varepsilon_i}{\sum_{j=1}^{k} ES_j\varepsilon_j} = \frac{\frac{S_i}{S_1}\varepsilon_i}{\sum_{j=1}^{k}\frac{S_j}{S_1}\varepsilon_j} = \frac{\varepsilon_i w_i}{\sum_{j=1}^{k}\varepsilon_j w_j} \qquad (3\text{-}1)$$

where M_i = bending moment at the *i*-th girder; E = modulus of elasticity; S_i = section modulus of the *i*-th girder; S_1 = typical interior section modulus; ε_i = maximum bottom-flange static strain at the *I*-th girder; w_i = ratio of the section modulus of the *i*th girder to that of a typical interior girder; and k = number of girders. When all girders have the same section modulus (that is, when weigh factors, w_i, are equal to one for all girders), Eq. (3-1) is equivalent to that of Ghosn *et al.* (1986). Because of edge stiffening effect due to curbs and barrier walls, the section modulus in exterior girders is slightly greater than in interior girders. In other words, the weigh factors, w_i, for exterior girders are greater than one. Therefore, from Eq. (3-1), the assumption of the weigh factors, w_i, equal to one will cause slightly overestimated girder distribution factors in interior girders and underestimated girder distribution factors in exterior girders. In this study, the weigh factors, w_i, are assumed to be one.

For two trucks side-by-side, the girder distribution factors calculated from Eq. (3-1) must be multiplied by two to be comparable with the bridge code because the AASHTO code specified girder distribution factors are based on the effect of one truck load.

Dynamic load factors (DLF's) are defined in several ways, as discussed in previous studies (Paultre *et al.* 1992; Bakht and Pinjarkar 1989). In this study, the dynamic load factor was taken as the ratio of the maximum dynamic strain and the maximum static strain (Figure 3.3):

$$DLF = \frac{\varepsilon_{dyn}}{\varepsilon_{stat}} \tag{3-2}$$

where ε_{dyn} = absolute maximum dynamic strain under the vehicle traveling at normal speed; and ε_{stat} = maximum equivalent static strain from normal speed test, obtained by filtering out the dynamic portion. Collected data are filtered by applying some numerical procedures, such as averaging filtering technique, to increase the signal-to-noise ratio, and to reduce the effect of random, and non-periodic noise.

Dynamic load factor is calculated for all instrumented girders. However, for comparison with the code specified DLF, it is necessary to consider DLF corresponding to the largest static strains, because this is the governing case.

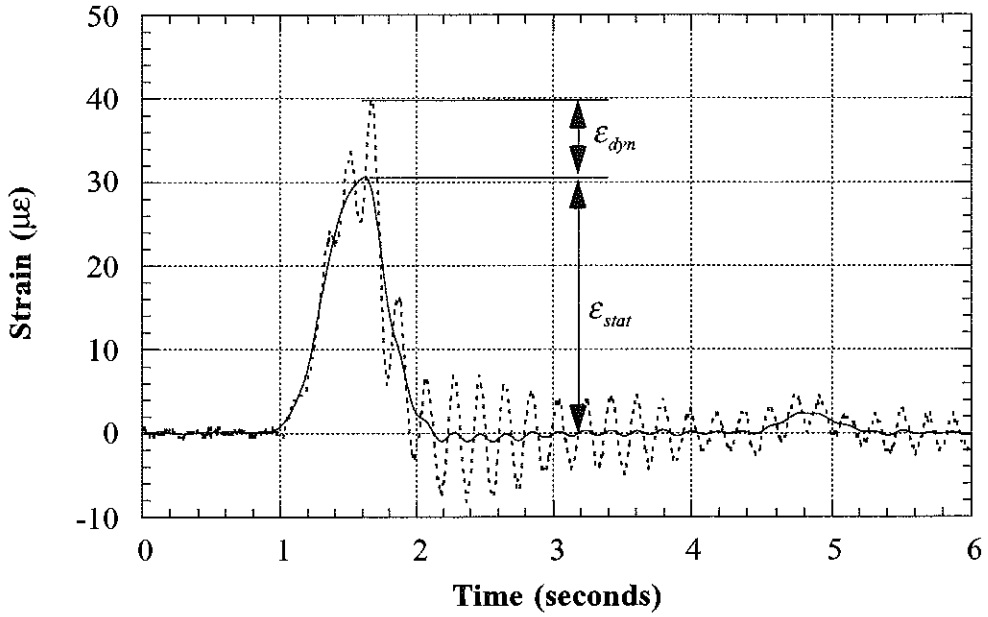

Figure 3.3. Dynamic and Static Strain under a Truck at Highway Speed.

Note:

Intentionally left blank

4. SPECIFIED LOAD DISTRIBUTION FACTORS AND DYNAMIC LOAD FACTORS

Measured girder distribution factors (GDF) and dynamic load factors (DLF) are compared in tables and figures with the values calculated according to the current design codes. Throughout the report, distribution factors are expressed in terms of axle load for the full truck rather than a line of wheel loads for the half truck. For the bending moment in interior girders, the AASHTO Standard (1996) specifies GDF's as follows. For steel girder and prestressed concrete girder bridges, with one lane, GDF is:

$$GDF = \frac{S}{4.27} \tag{4-1}$$

and for steel and prestressed concrete girder bridges, with multi lanes,

$$GDF = \frac{S}{3.36} \tag{4-2}$$

where S = girder spacing (m).

The AASHTO LRFD Code (1998) specifies GDF as a function of girder spacing, span length, stiffness parameters, and bridge skew. For the bending moment in interior girders with one lane loading, GDF is:

$$GDF = \left\{0.06 + \left(\frac{S}{4300}\right)^{0.4}\left(\frac{S}{L}\right)^{0.3}\left(\frac{K_g}{Lt_s^3}\right)^{0.1}\right\}\left\{1 - c_1(\tan\theta)^{1.5}\right\} \tag{4-3}$$

and for multi lane loading:

$$GDF = \left\{0.075 + \left(\frac{S}{2900}\right)^{0.6}\left(\frac{S}{L}\right)^{0.2}\left(\frac{K_g}{Lt_s^3}\right)^{0.1}\right\}\left\{1 - c_1(\tan\theta)^{1.5}\right\} \tag{4-4}$$

$$c_1 = 0.25\left(\frac{K_g}{Lt_s^3}\right)^{0.25}\left(\frac{S}{L}\right)^{0.5} \qquad \text{for } 30° < \theta < 60° \tag{4-5}$$

$$c_1 = 0 \qquad \text{for } \theta < 30° \qquad (4\text{-}6)$$

where S = girder spacing (mm); L = span length (mm); $K_g = n(I + Ae_g^2)$; t_s = thickness of concrete slab (mm); n = modular ratio between girder and slab materials; I = moment of inertia of the girder (mm^4); A = area of the girder (mm^2); e_g = distance between the centers of gravity of the girder and the slab (mm); and θ = skew angle in degrees. Because the term $K_g / (Lt_s^3)$ can imply more accuracy than exists for bridge evaluation, it is recommended that they be taken as 1.0. In this report, however, actual values of the term $K_g / (Lt_s^3)$ are used in calculation of girder distribution factors. The AASHTO LRFD (1998) formulas have been developed based on a NCHRP Project 12-26 (Zokaie *et al.* 1991). The method includes the longitudinal stiffness parameter, K_g, and the span length, L, in addition to the girder spacing, S. AASHTO Guide for Load Distribution (1994) specifies similar load factors to those of AASHTO LRFD (1998).

Most bridge design codes specify the dynamic load as an additional static live load. In the AASHTO Standard (1996), dynamic load factors are specified as a function of span length only:

$$\text{DLF} = \frac{50}{3.28\text{L} + 125} \dagger 0.30 \qquad (4\text{-}7)$$

where DLF = dynamic load factor (maximum 30 percent); and L= span length (m). This empirical equation has been used since 1944. In the AASHTO LRFD (1998), live load is specified as a combination of HS20 truck (AASHTO 1996) and a uniformly distributed load of 9.3 kN/m. The dynamic load factor is equal to 0.33 of the truck effect, with no dynamic load applied to the uniform loading.

5. FINITE ELEMENT ANALYSIS

The field test results were compared with analytical computations. The analysis was performed using ABAQUS finite element program available at the University of Michigan. Material and other structural parameters are based on the collected information about the bridge supplemented with engineering judgement.

5.1. Types of finite element models for bridges

In the finite element analysis, the geometry of a bridge superstructure can be idealized in many different ways. The following types of models are used:

- Plane grillage model,
- 3-dimensional grillage model,
- 2-dimensional model with shell elements for slab and beam elements for girders,
- 3-dimensional model with shell elements for slab and beam elements for girders,
- 3-dimensional model with shell elements for slab and girders,
- 3-dimensional model with solid elements for slab and shell elements for girders.

For this study, a three-dimensional finite element method (FEM) was applied to investigate the structural behavior of the considered bridges. The concrete slab is modeled using isotropic, eight node solid elements, with three degrees of freedom at each node. The girder flanges and web are modeled using three-dimensional, quadrilateral, four node shell elements with six degrees of freedom at each node (Tarhini and Frederic 1992). The structural effects of the secondary members, such as sidewalk and parapet, are also taken into account in the finite element analysis models.

5.2 Boundary conditions

All investigated bridges were designed as simply supported. However, in older structures, corrosion of the bearings often causes additional constraints for both rotations and longitudinal displacements. It was observed, as also reported by other authors (Bakht and Jaeger 1988, Schultz et al. 1995), that even slight changes in boundary conditions have considerable effect on the results.

Therefore, three cases of boundary conditions were considered in the FEM models, as shown in Figure 5.1. In (a), the supports are represented by a hinge at one end, and a roller at the other end. In (b), it was assumed that both supports are hinged, with no movement in longitudinal (horizontal) direction. In (c), the supports are assumed to be partially frozen, by applying elastic spring elements to the top and bottom flanges, with stiffness represented by K values. The magnitude of stiffness K was calibrated using field measurements.

5.3 Applied Loads

The load was applied in form of two 11-axle, three unit trucks, the same as those used in field tests. The input data included axle loads and axle spacings.

The trucks were positioned as in the field test. The transverse position of the trucks was as measured during the actual test. The longitudinal position of trucks was calculated as the position producing the maximum bending moment at midspan, where the strain transducers were located. Theoretically, the maximum bending moment for simple span bridges does not occur at midspan. However, the difference is very small, usually less than 2 percent. Therefore, the strain transducers were attached at midspan for all tested bridges. Bending

moment at the midspan is calculated using influence curves for the bridge span treated as a simply supported beam.

After determining the truck position on the bridge, concentrated loads are linearly distributed to adjacent nodes based on the location of the load.

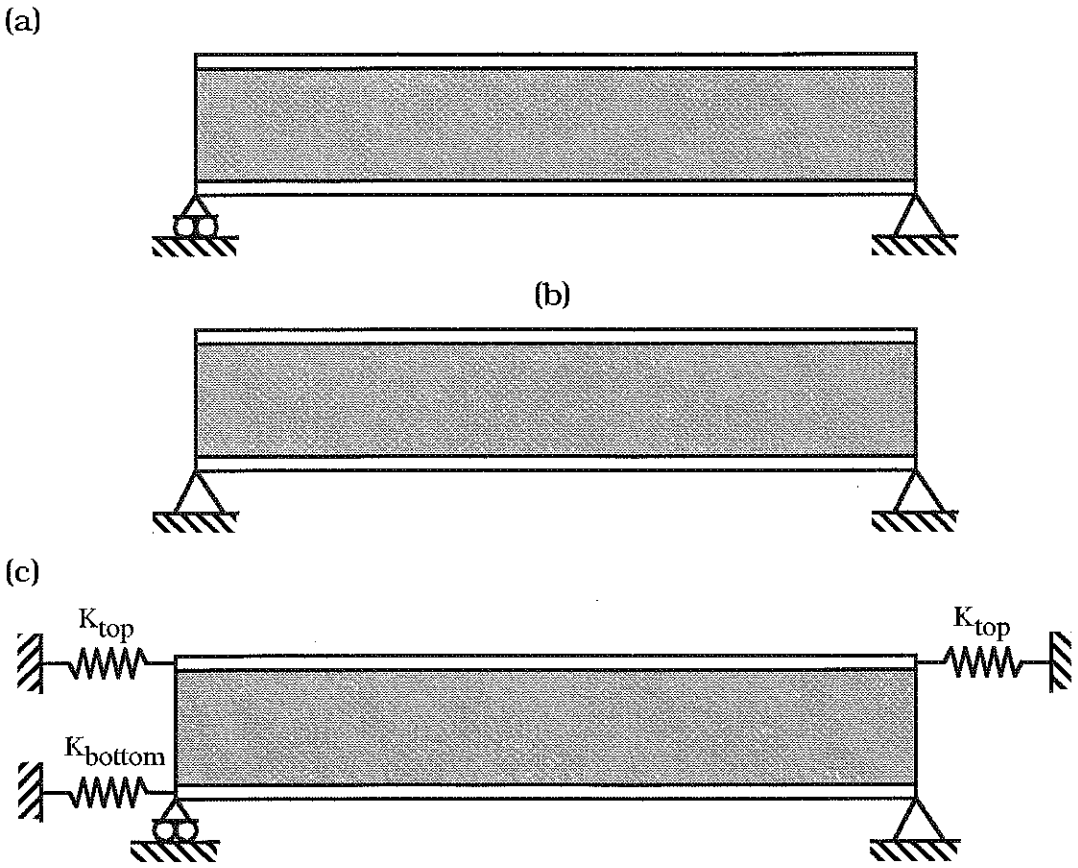

Figure 5.1. Three Cases of Boundary Conditions used in the Finite Element Analysis: (a) Bridge With Simple Supports, (b) Bridge with Hinged Supports at both the lower ends, (c) Bridge with Partially Fixed Supports.

Note:

Intentionally left blank

6. BRIDGE ON M-52 OVER BLACK CREEK, LENAWEE COUNTY (B02-46071, M52/BC)

6.1 Description

This bridge was built in 1947 and it is located on M-52 over Black Creek in Lenawee County, Michigan. It is a single span, simply supported structure, designed as a non-composite section. The total span length is 15.2 m, without any skew. It has nine steel girders spaced at 1.57 m, as shown in Figure 6.1. The bridge has one lane in each direction and it carries an average daily traffic (ADT) of 2,500. The speed limit on this bridge is 89 km/h. The operating load rating is 1,005 kN, according to the Michigan Structure Inventory.

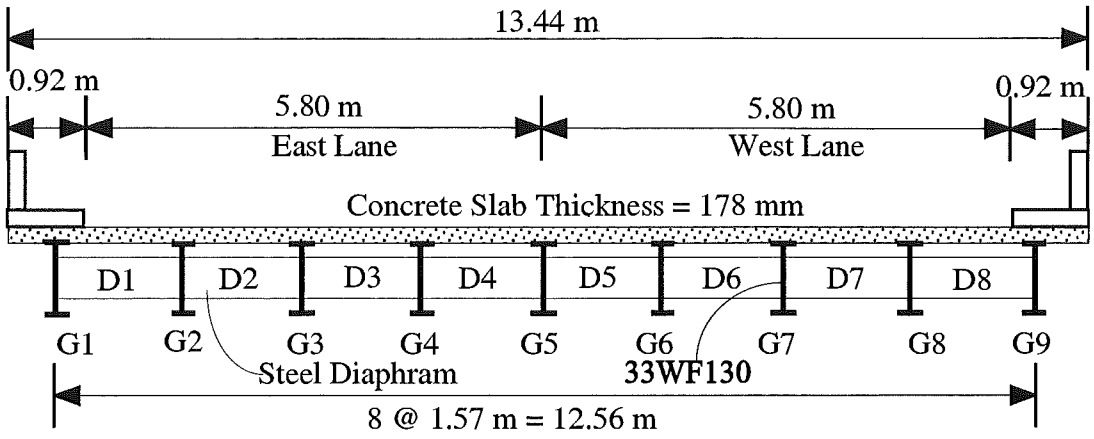

Figure 6.1. Cross-Section of the Bridge M52/BC (B02-46071).

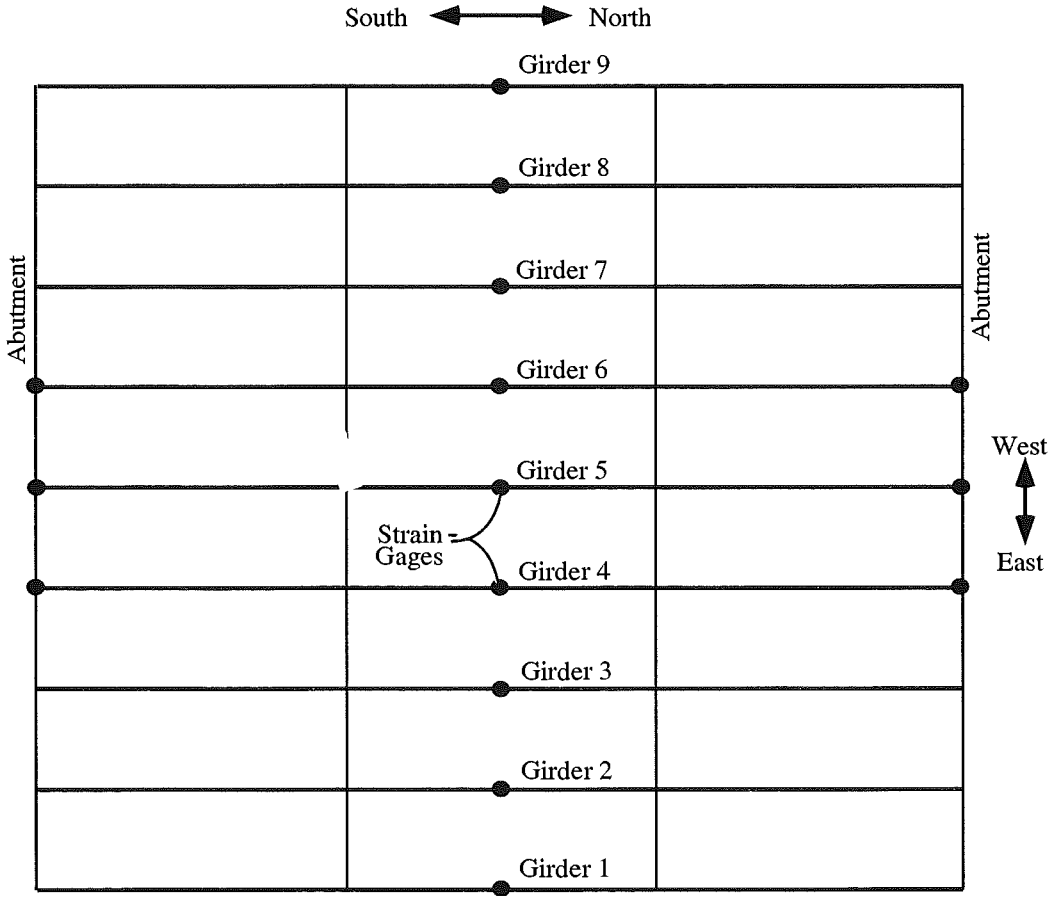

Figure 6.2. Strain Gage Locations in Bridge M52/BC (B02-46071).

6.2 Instrumentation

Strain transducers were installed on the bottom flanges of girders at midspan and at selected support locations, as shown in Figure 6.2. The test equipment was installed on July 12, 2000. The bridge test was performed on July 13, 2000.

6.3. Load cases

The girder distribution factors (GDF) and dynamic load factors (DLF) were calculated using the strains measured at midspan. The bridge was loaded with two 11-axle trucks (three-unit vehicles).

The truck A and truck B have gross weights of 639 kN and 632 kN, with wheelbases of 15.53 m and 15.37 m, respectively. Truck configurations are shown in Figures 6.3 and 6.4.

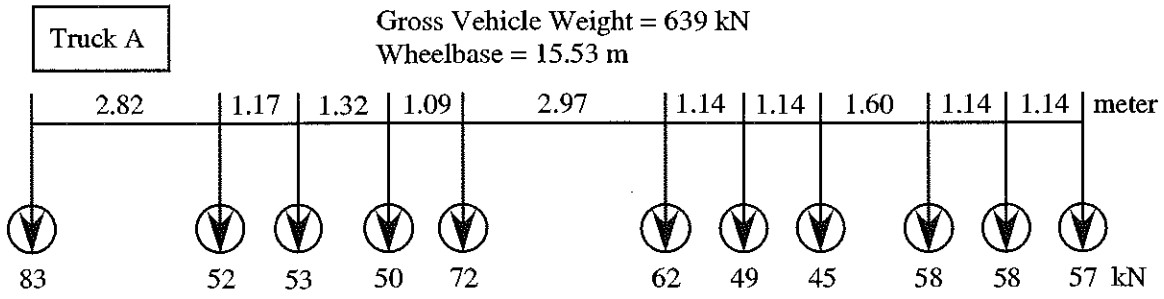

Figure 6.3. Truck A Configuration, Bridge M52/BC (B02-46071).

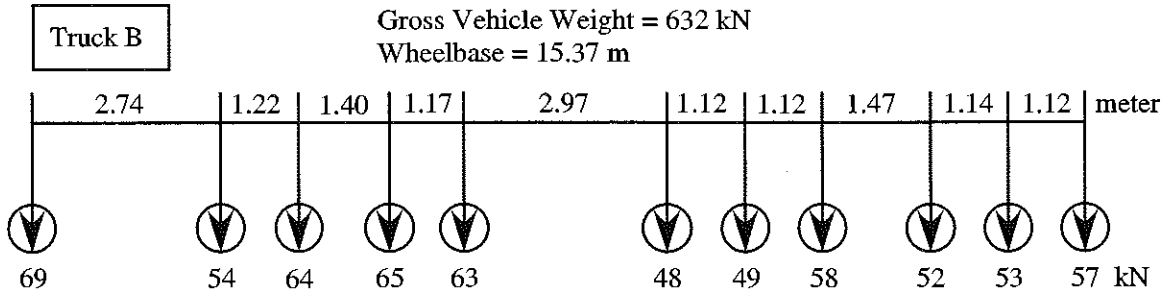

Figure 6.4. Truck B Configuration, Bridge M52/BC (B02-46071).

A total of 16 load cases were considered, as shown in Table 6.1. First each truck was driven by itself at the center of one lane, at crawling speed. Then, the same truck was driven close to the curb. The runs in the center of the lane were repeated at a normal highway speed. The same was repeated for the other lane. Finally, two trucks were driven simultaneously, side-by-side, at crawling speed and normal highway speed. For side-by-side cases, the runs were repeated after the trucks switched lanes, i.e. first truck A was in West lane, and B in East lane, then truck A was in East lane, and B in West lane.

Table 6.1. Sequence of Test Runs, Bridge M52/BC (B02-46071).

Run#	Truck	Lane Side	Position in Lane	Truck Speed
1	Truck A	East	Center	Crawling
2	Truck A	East	Curb	Crawling
3	Truck B	East	Center	Crawling
4	Truck B	East	Curb	Crawling
5	Truck B	East	Center	42 km/h
6	Truck A	East	Center	45 km/h
7	Truck A	West	Center	Crawling
8	Truck A	West	Curb	Crawling
9	Truck B	West	Center	Crawling
10	Truck B	West	Curb	Crawling
11	Truck B	West	Center	37 km/h
12	Truck A	West	Center	45 km/h
13	Truck A and B	both	Center	Crawling
14	Truck B and A	both	Center	Crawling
15	Truck A and B	both	Center	36 km/h
16	Truck B and A	both	Center	30 km/h

6.4. Analysis results

A three-dimensional finite element method (FEM) was applied to investigate the structural behavior of the bridge M52/BC (B02-46071). The concrete slab was modeled with isotropic, eight node solid elements, with three degrees of freedoms at each node. The girder flanges and web were modeled using three-dimensional, quadrilateral, four node shell elements with six degrees of freedom at each node. The structural effects of the secondary members, such as the sidewalk and parapet, were also taken into account in the finite element analysis models.

Three cases of the boundary conditions are considered, as described earlier in this Report. The partially frozen supports were modeled using spring elements as shown in Figure 6.6.

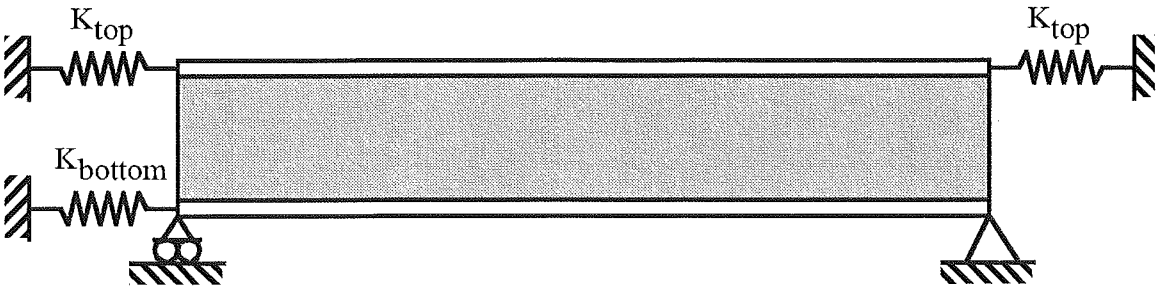

Figure 6.6. Modeing of Support Partial Fixity in Finite Element Analysis.

The mesh of the FEM model is shown in Figure 6.7. Figure 6.8 presents a deformed shape of the bridge loaded with two trucks side-by-side. Figure 6.9 illustrates the distribution of the loads simulating two truck side-by-side.

Strains calculated for the three considered models are shown in Figure 6.10 for two trucks side-by-side (Run 13). Also shown are the experimental results. The FEM results show that the maximum strain at the most heavily loaded girder is about 170 με for the model with simple support, while the maximum strain recorded from the test is about 125 με. When the spring elements are used with the K constants adjusted

according to the test results (K_{top} = 60,000 kN/m and K_{bottom}=120,000 kN/m), then the FEM results become very close to the test results. This confirms the presence of some degree of fixity of supports.

Figure 6.11 presents the deflection obtained from the three different FEM models. It shows that the maximum deflection under two truck loading is about 4.2 mm, for the FEM model with the partial support fixity.

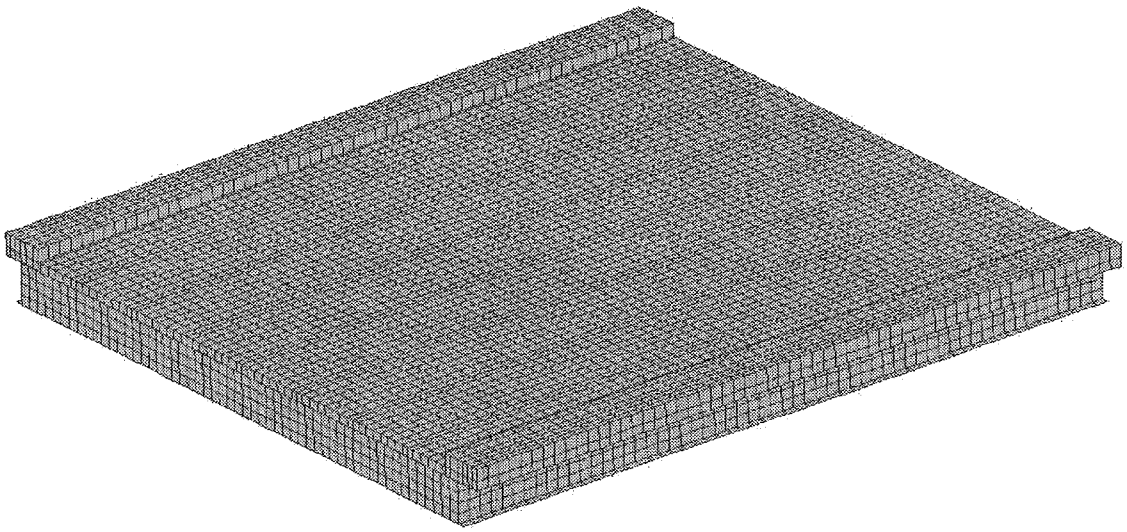

Figure 6.7. The Mesh of the Finite Element Model.
M52/BC (B02-46071).

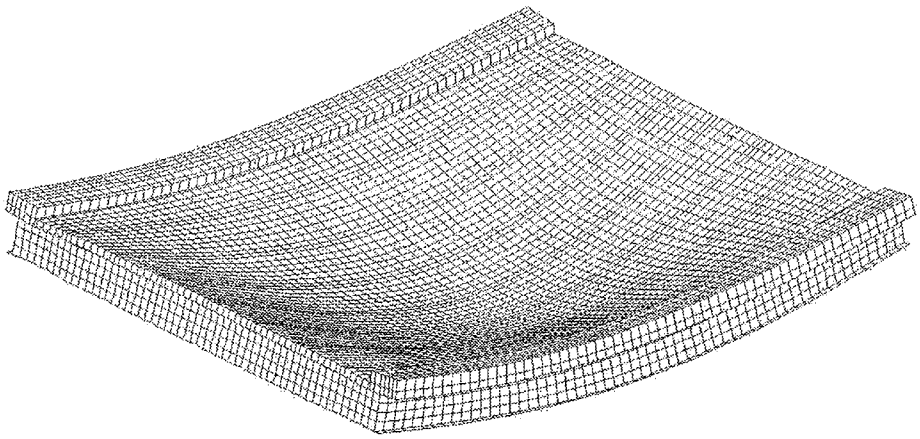

Figure 6.8. The Deformed Shape of the Bridge under Two Lane Loading.
M52/BC (B02-46071).

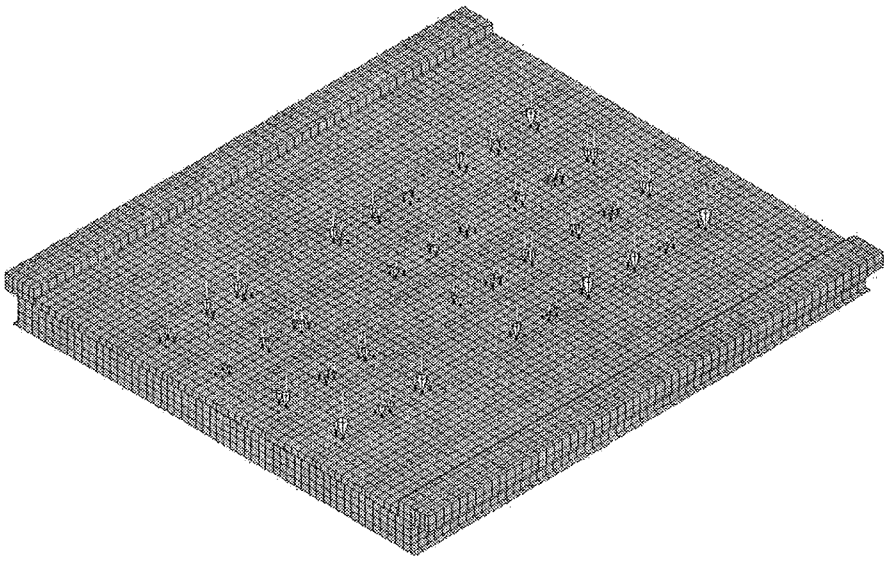

Figure 6.9. Truck Load Distribution for Two Lane Loading
M52/BC (B02-46071).

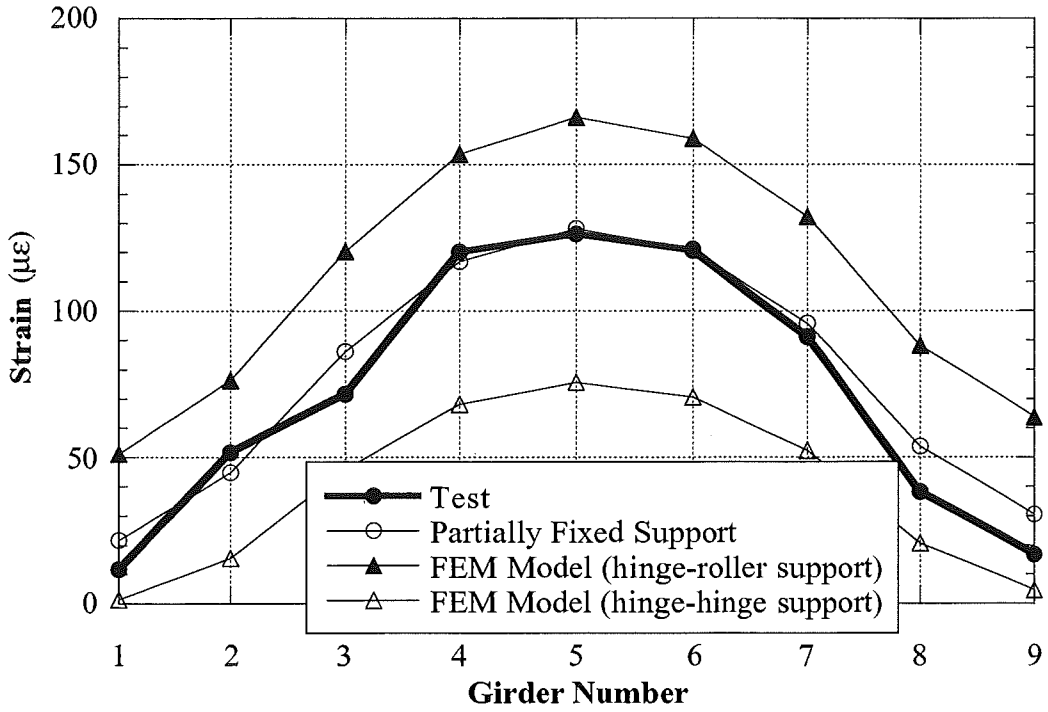

Figure 6.10. Strain from the FEM Analysis Compared with the Test Results for Two Lane Loading, M52/BC (B02-46071).

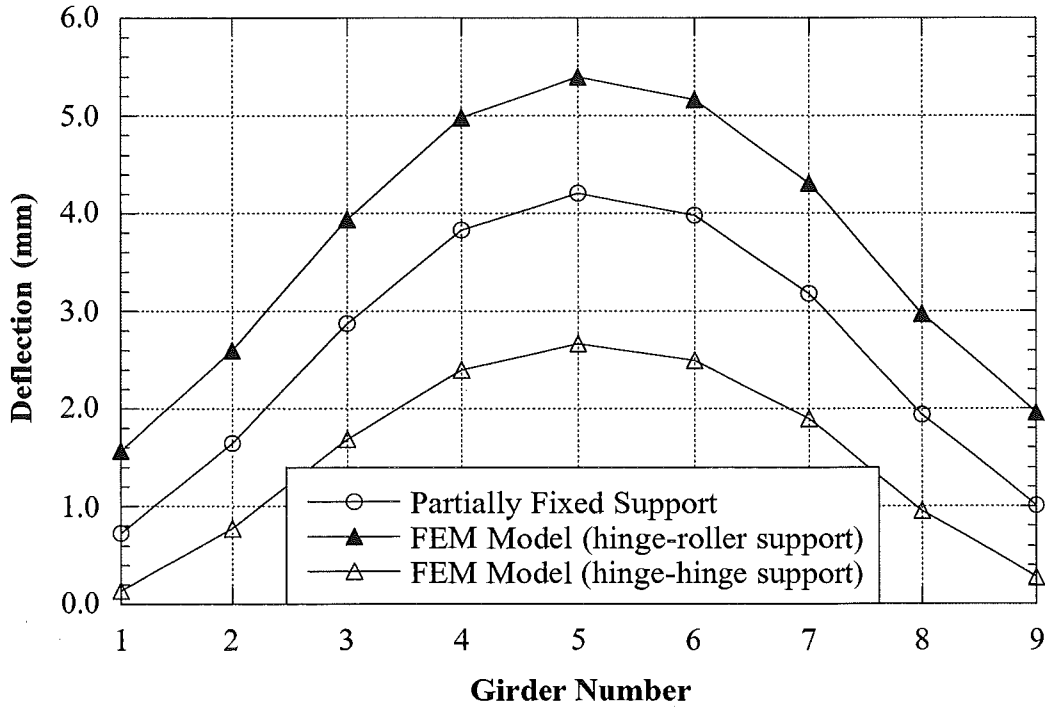

Figure 6.11. Deflection from the FEM Analysis for Two Lane Loading M52/BC (B02-46071).

6.5. Test results

The resulting strains and GDF's are shown in Figures 6.12 through 6.16. Figures 6.12 to 6.14 present the results of all crawling-speed (static) tests. Figures 6.12 to 6.13 present static strains and GDF's for one truck on the bridge. The maximum strain due to a single truck is about 100 με. This corresponds to about 20 MPa.

Figure 6.14 shows static strains and GDF's from side-by-side static load tests. For two vehicles side-by-side the maximum strain is about 130 με (which corresponds to 26 MPa). The superposition of strains due to a single truck in West and East lanes produces almost the same results as strain due to two trucks side-by-side.

For two trucks side-by-side, the girder distribution factor for girder i is determined using Eq. (3-1). For comparison, GDF are also calculated according to AASHTO Standard (1996) and AASHTO LRFD Code (1998). Two cases were considered, a single lane loaded, and two lanes loaded. The resulting GDF's are shown in Figures 6.12 through 6.16.

The results indicate that code-specified GDF's are conservative. A single lane GDF specified in AASHTO LRFD (1998) is also sufficient for two lane load cases for this bridge. However, a single lane GDF specified in AASHTO Standard (1996) is not enough for two lane load cases for this bridge. However, the absolute values of the strains are less than 130 με for the heaviest load case (two fully-loaded trucks side-by-side). Therefore, the total load effect per girder estimated using GDF specified for single lane in AASHTO Standard (1996) is also conservative (less than design value).

Figures 6.15 and 6.16 shows the resulting strain and distribution factors from normal speed tests. There is practically no difference between the crawling speed and normal speed results.

Dynamic load factor is defined in section 3.3. In Figure 6.17, DLF's are plotted for all load cases involving normal speed (no dynamic load was measured for crawling speed runs). Dynamic load factors for exterior girders are high because the static strains in these girders are very low. In other words, large values of DLF in exterior girders correspond to load cases with a single truck in the opposite lane (resulting in very low static strain).

The relationship between DLF and static and dynamic strains is shown in Figure 6.18. The open circles correspond to static strain, ε_{stat}, and black solid squares correspond to dynamic strain, ε_{dyn}. For each static strain value (open circle), the corresponding dynamic strain is denoted by solid square (the numbers of circles and squares are same). Dynamic strains remain nearly constant, while static strains increase as truck loading increases. This results in large dynamic load factors for low static strains. It is clear from the Figure 6.18 that dynamic strains does not exceed 20 $\mu\varepsilon$ for all the cases while the static strain can exceed 120 $\mu\varepsilon$ in normal speed test. DLF corresponding to the maximum strain caused by two trucks side-by-side, is less than 0.10 at girder No. 5, the most heavily loaded girder.

The strains were also measured close to the support. The results are shown in Figures 6.19 and 6.20. Negative strain values indicate the strains recorded at the bottom flanges near supports were in compression, due to the partial fixity of support. The strain values near the support were measured when the loads caused the maximum strain at the midspan. As shown in the figures, the levels of support fixity are highly unpredictable. Even in a bridge, each girder has different support behavior.

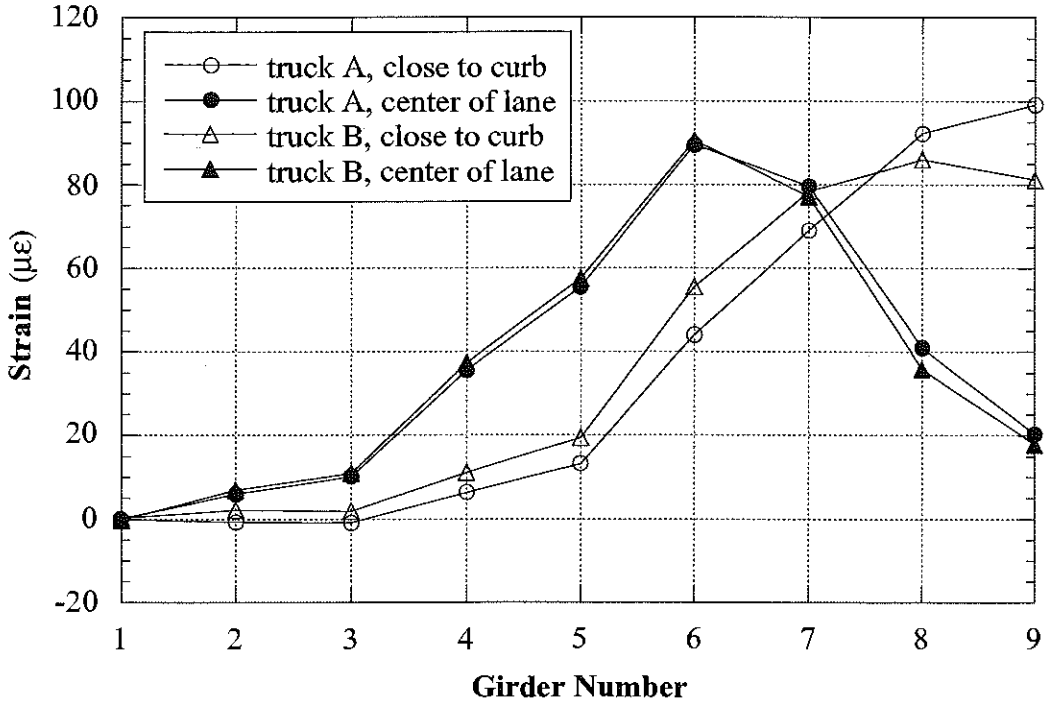

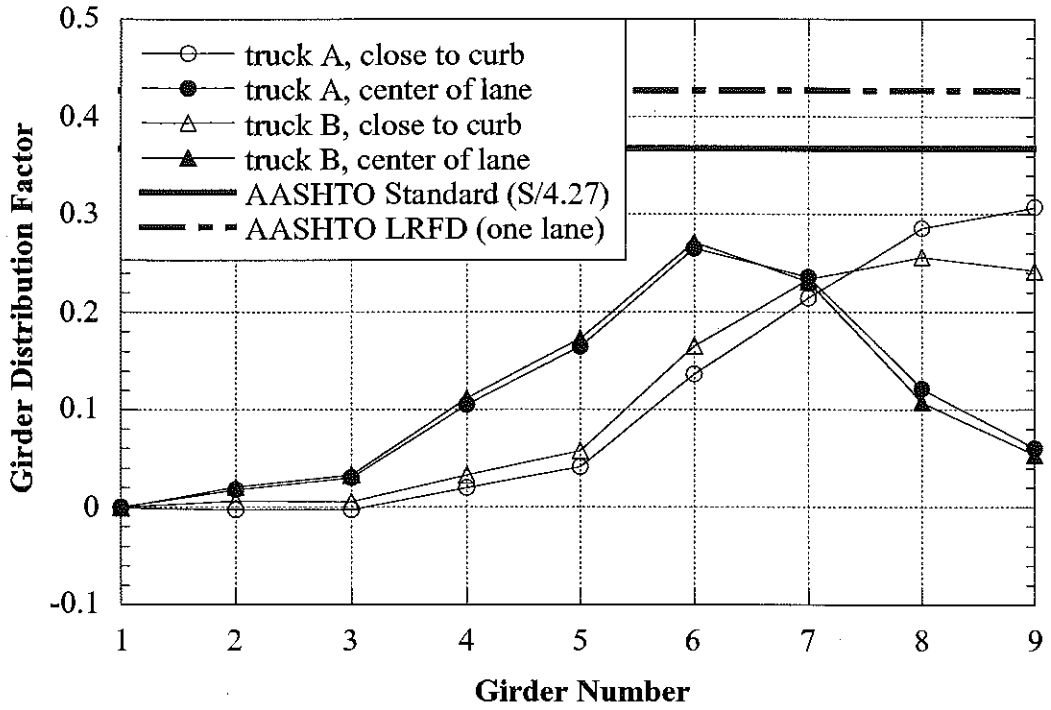

Figure 6.12. West Lane, Crawling Speed, M52/BC (B02-46071).

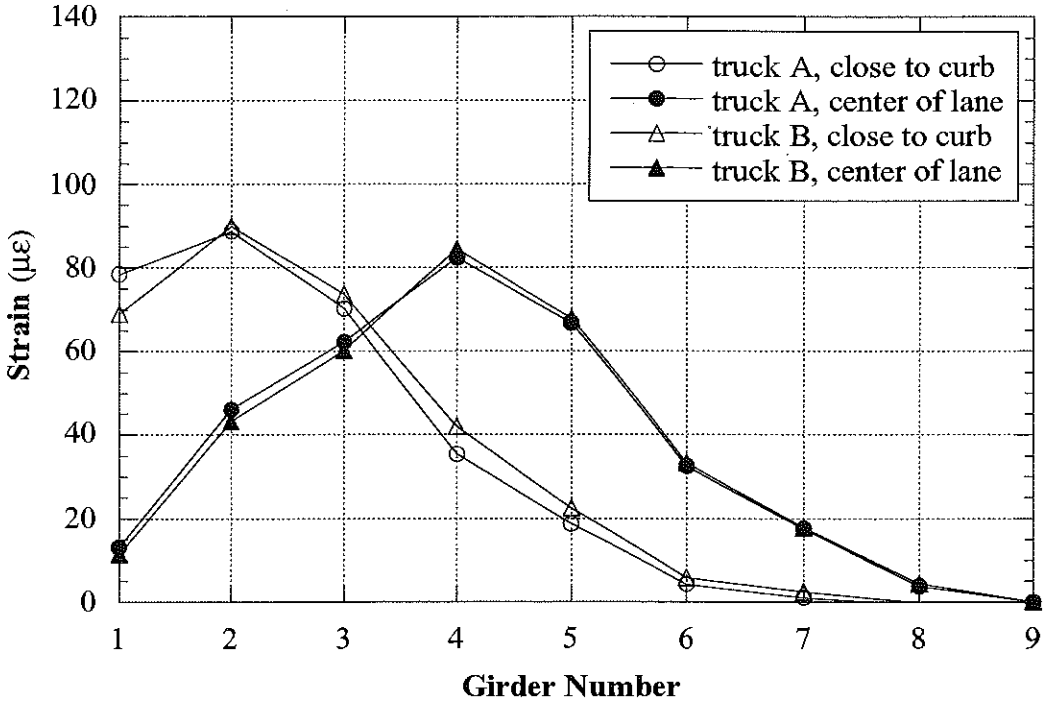

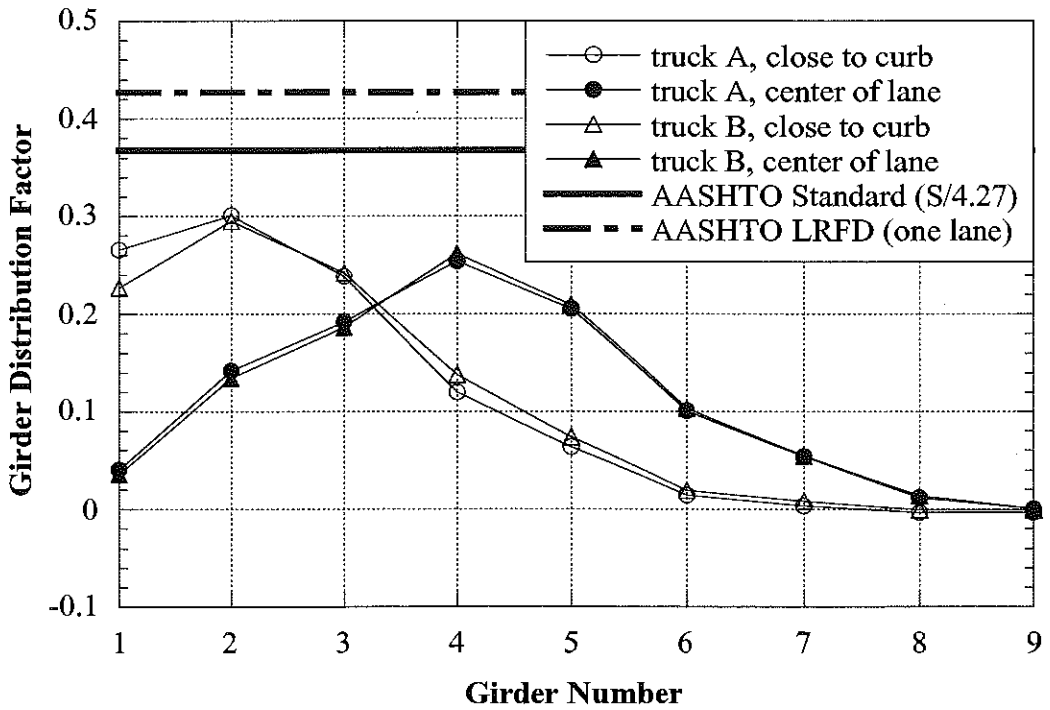

Figure 6.13. East Lane, Crawling Speed, M52/BC (B02-46071).

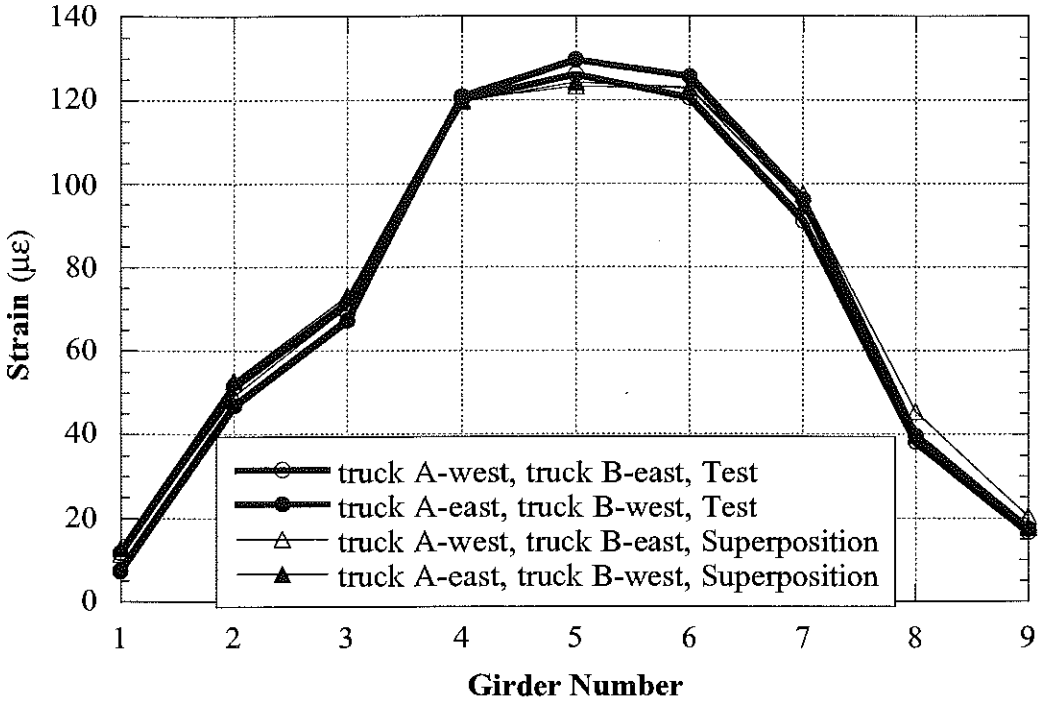

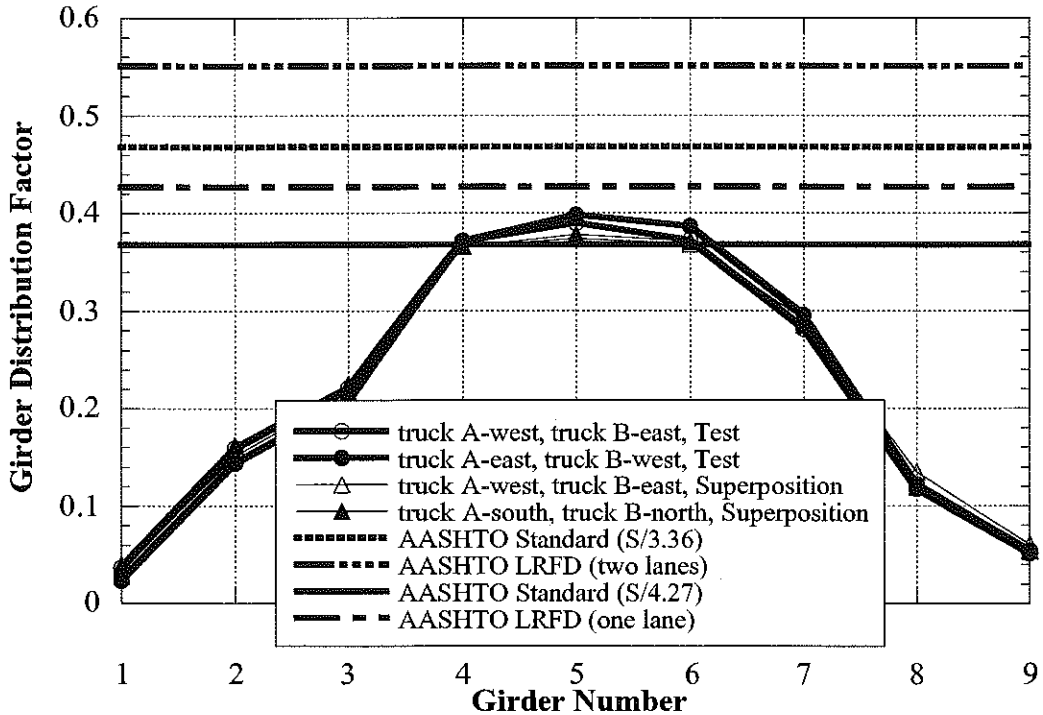

Figure 6.14. Side-by-Side Loading, Center of Lane, Crawling Speed, M52/BC (B02-46071).

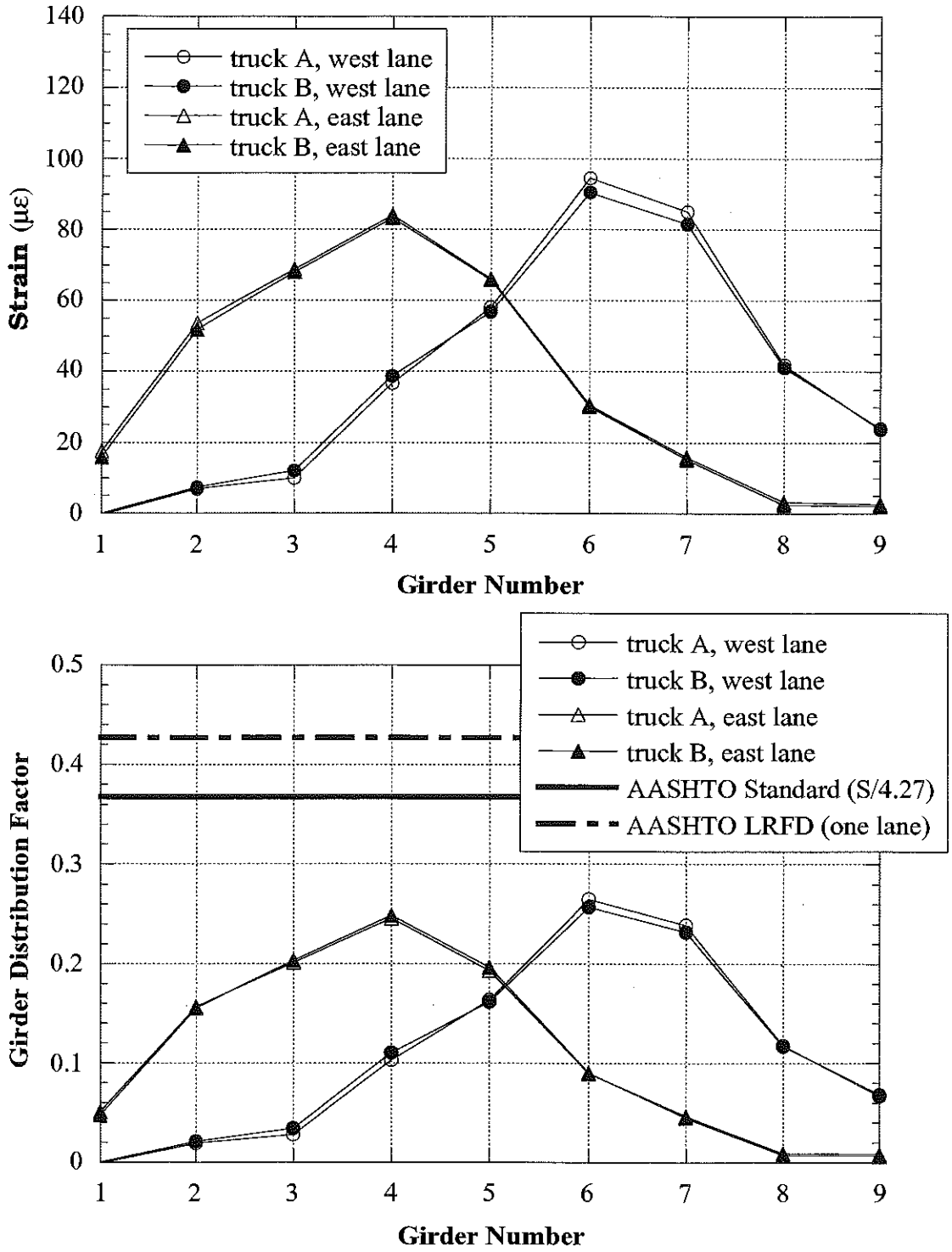

Figure 6.15. Strain and GDF under One Truck Loading at Regular Speed, M52/BC (B02-46071).

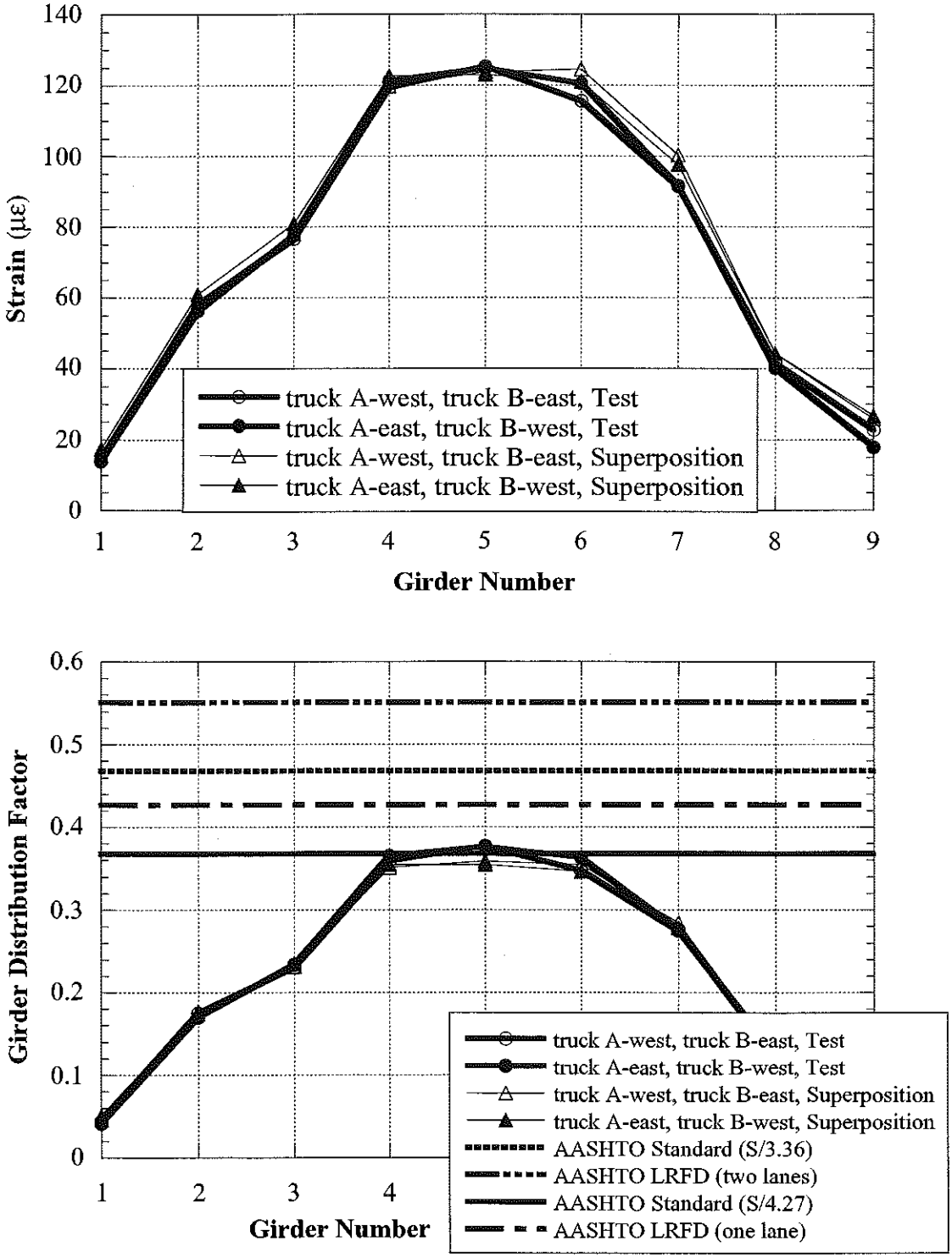

Figure 6.16. Strain and GDF under Side-by-Side Loading at Regular Speed, M52/BC (B02-46071).

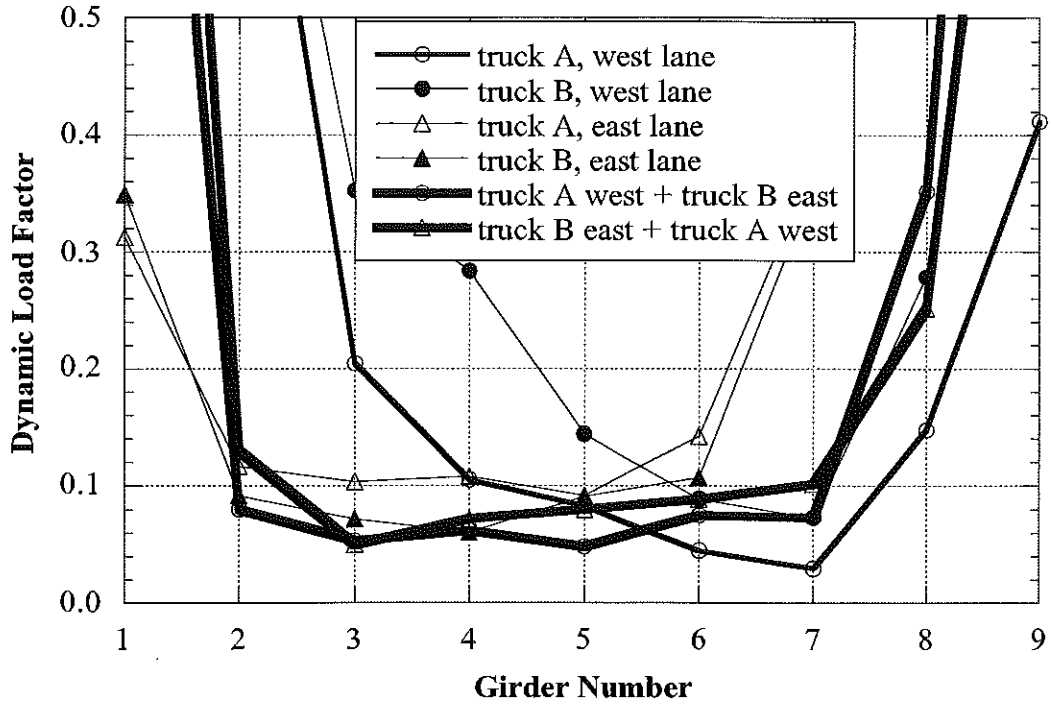

Figure 6.17. Dynamic Load Factors, M52/BC (B02-46071).

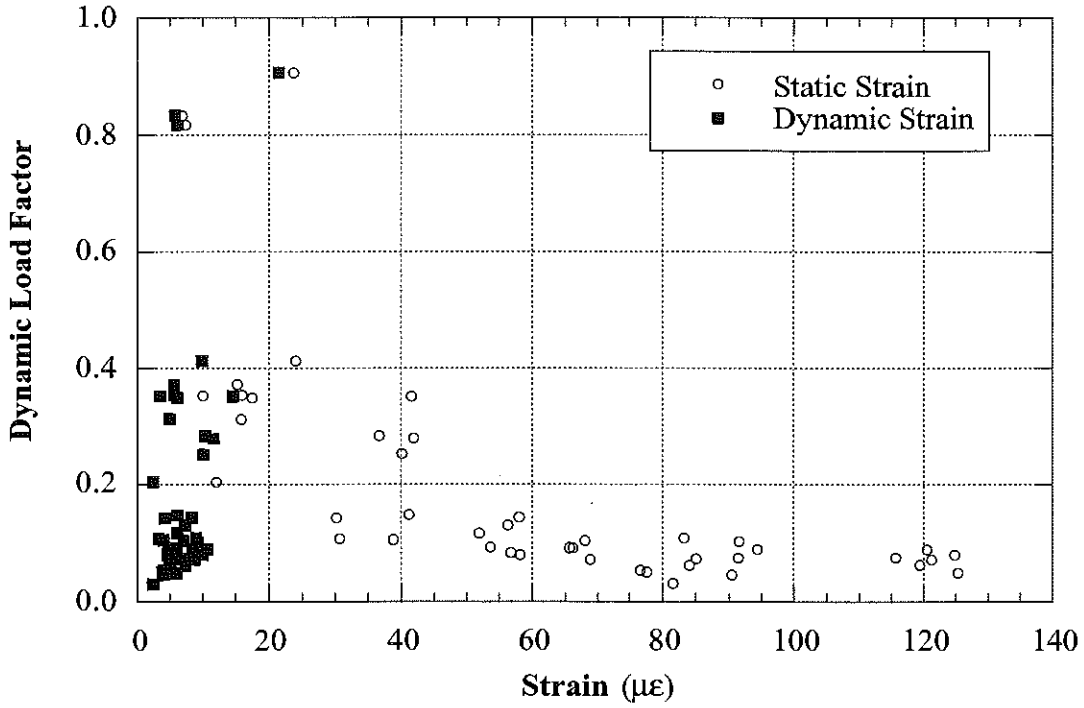

Figure 6.18. Strain vs. Dynamic Load Factors, M52/BC (B02-46071).

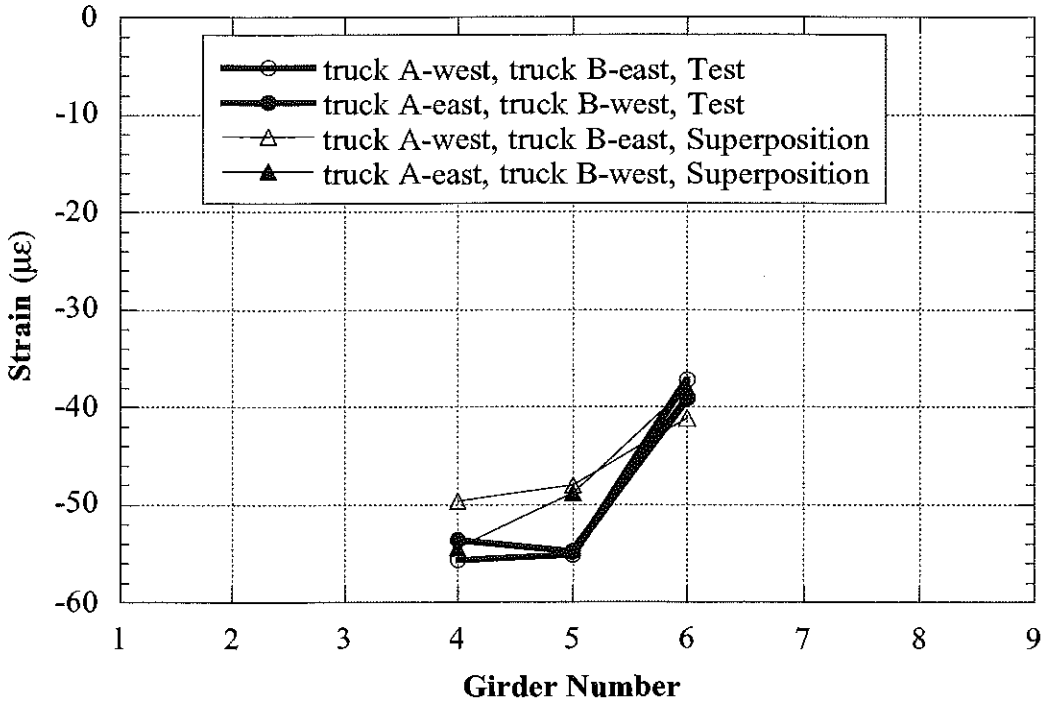

Figure 6.19. Strains at North End, Side-by-Side Loading, Crawling Speed, M19/ M52/BC (B02-46071).

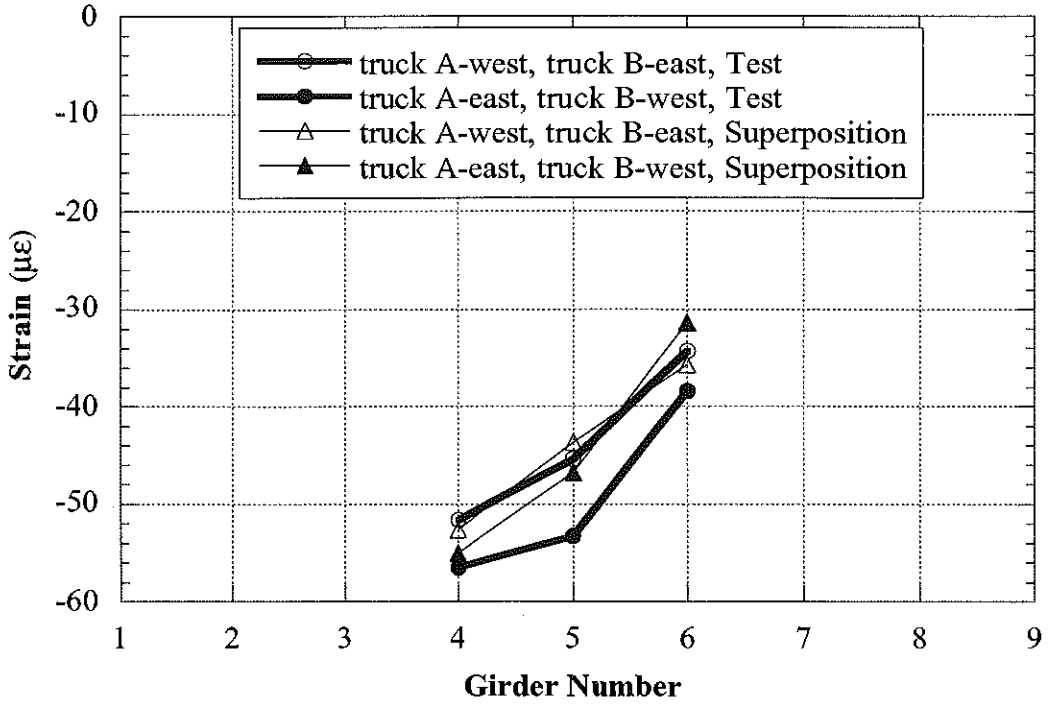

Figure 6.20. Strains at South End, Side-by-Side Loading, Crawling Speed, M52/BC (B02-46071).

Note:

Intentionally left blank

7. BRIDGE ON US-127 OVER BLANCHARD (TOAD) DRAIN, HILLSDALE COUNTY (B01-30071, US127/BD)

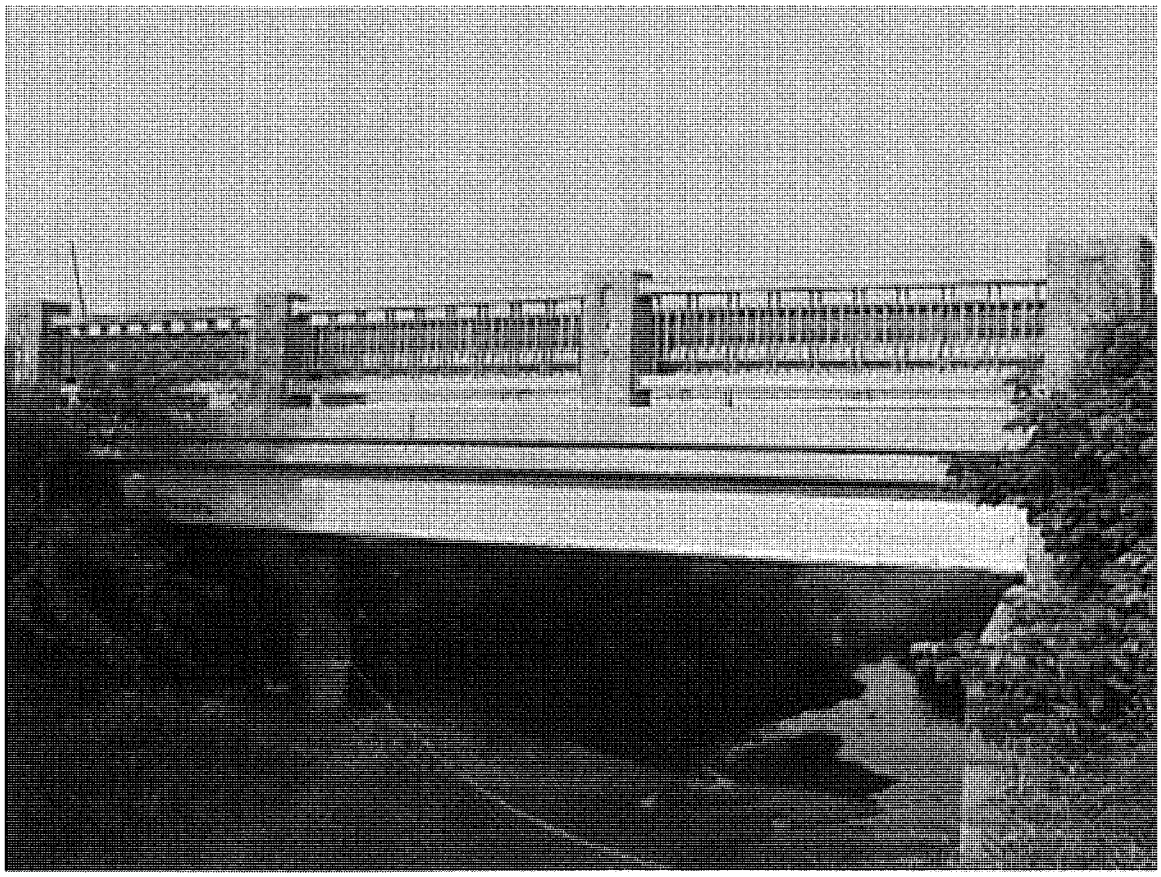

7.1 Description

This bridge was built in 1948 and it is located on US-127 over Blanchard (Toad) Drain in Hillsdale County, Michigan. It is a single span, simply supported structure, designed as a non-composite section. The total span length is 10.6 m, with skew of 15 degrees. It has ten steel girders spaced at 1.40 m, as shown in Figure 7.1. The bridge has one lane in each direction and it carries an average daily traffic (ADT) of 3,300. The speed limit on this bridge is 89 km/h. The operating load rating is 1,094 kN, according to the Michigan Structure Inventory.

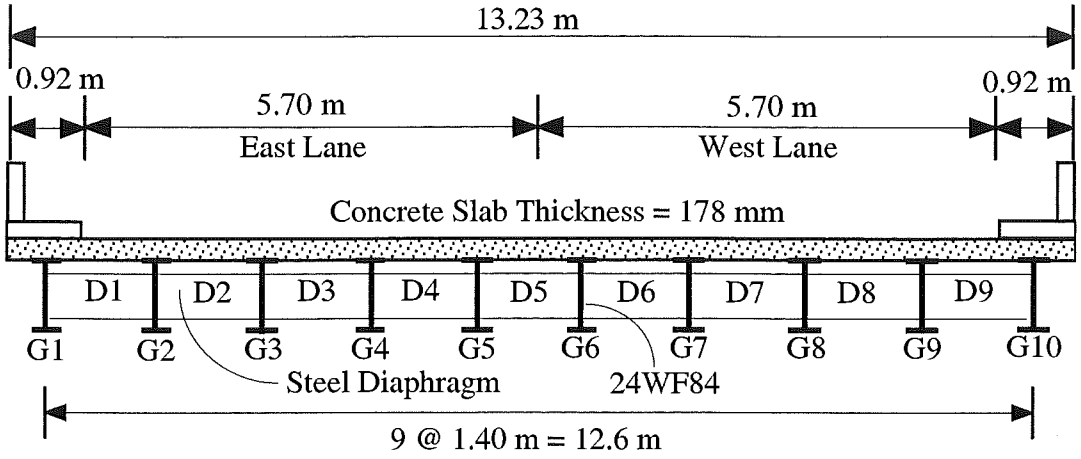

Figure 7.1. Cross-Section of the Bridge US127/BD (B01-30071).

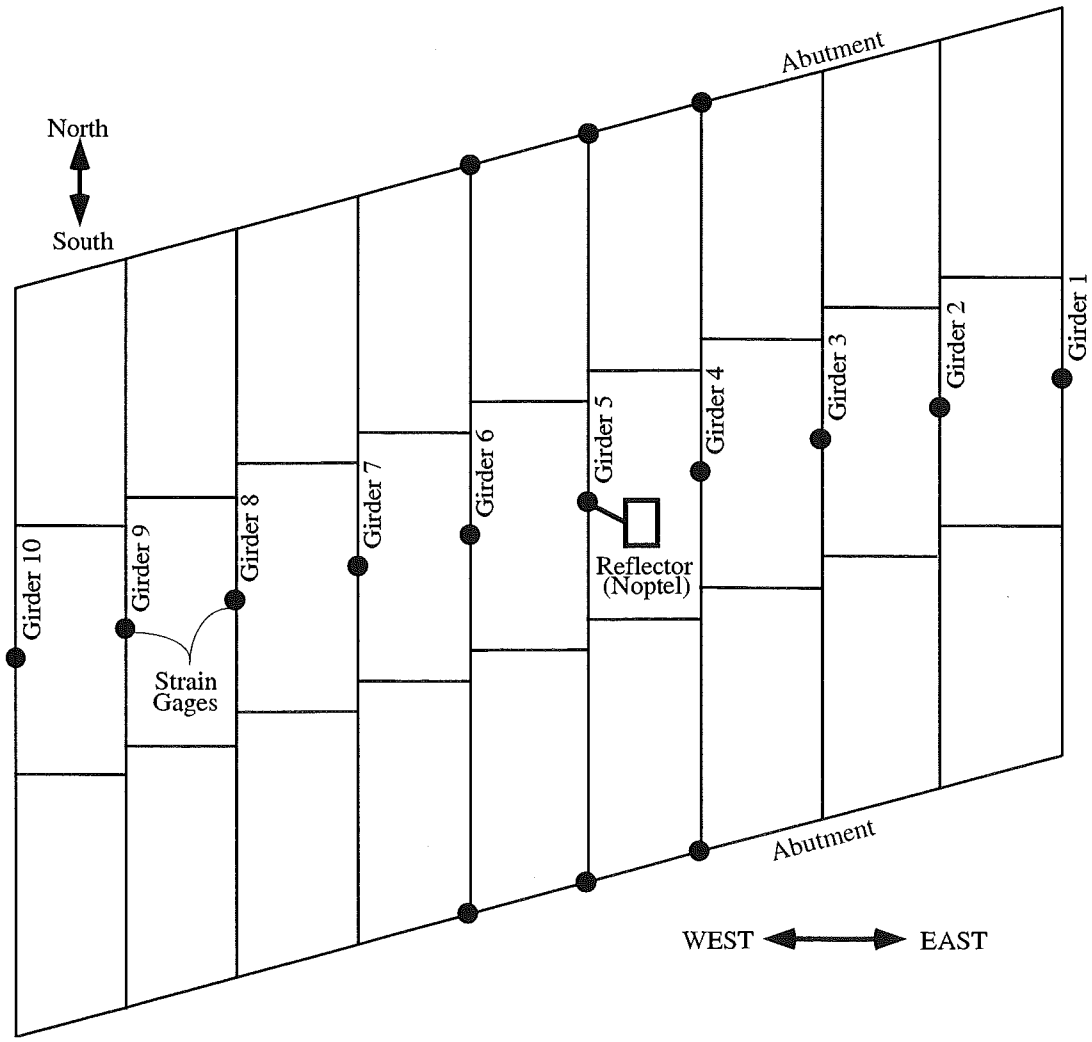

Figure 7.2. Strain Gage Locations in Bridge Bridge US127/BD (B01-30071).

7.2 Instrumentation

Strain transducers were installed on the bottom flanges of girders at midspan and at selected support locations, as shown in Figure 7.2. The reflector for the PSM-R device from Noptel was installed at the girder No. 5 to measure deflection. The test equipment was installed on July 26, 2000. The bridge test was performed on July 27, 2000.

7.3 Load cases

The girder distribution factors (GDF) and dynamic load factors (DLF) were calculated using the strains measured at midspan. The bridge was loaded with two 11-axle trucks (three-unit vehicles).

The truck A and truck B have gross weights of 651 kN and 678 kN, with wheelbases of 17.41 m and 17.05 m, respectively. Truck configurations are shown in Figures 7.3 and 7.4.

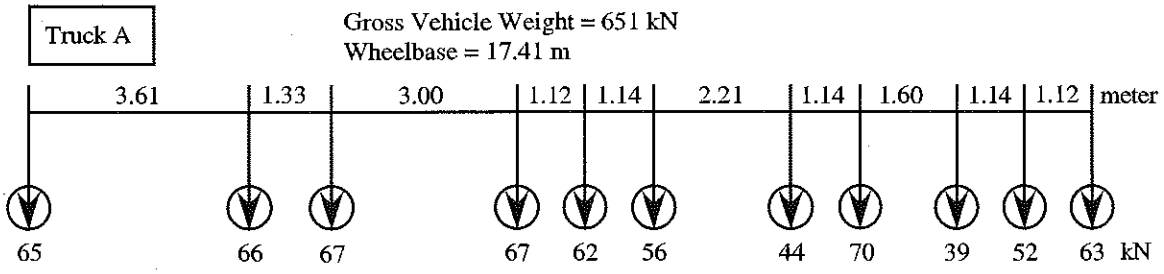

Figure 7.3. Truck A Configuration, Bridge US127/BD (B01-30071).

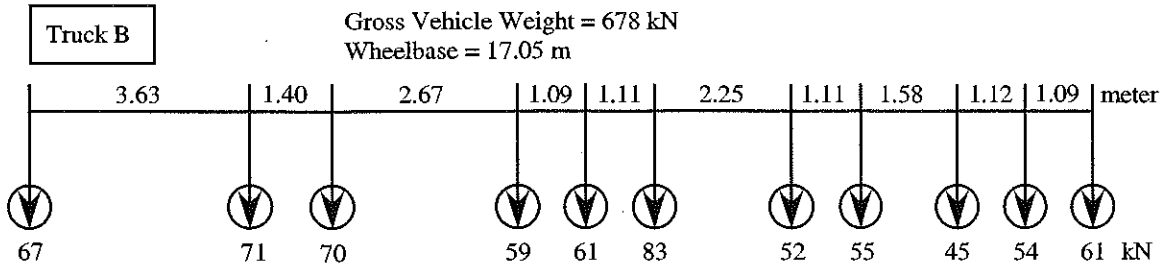

Figure 7.4. Truck B Configuration, Bridge US127/BD (B01-30071).

A total of 16 load cases were considered, as shown in Table 7.1. First each truck was driven by itself at the center of one lane, at crawling speed. Then, the same truck was driven close to the curb. The runs in the center of the lane were repeated at a normal highway speed. The same was repeated for the other lane. Finally, two trucks were driven simultaneously, side-by-side, at crawling speed and normal highway speed. For side-by-side cases, the runs were repeated after the trucks switched lanes, i.e. first truck A was in West lane, and B in East lane, then truck A was in East lane, and B in West lane.

Table 7.1. Sequence of Test Runs, Bridge US127/BD (B01-30071).

Run#	Truck	Lane Side	Position in Lane	Truck Speed
1	Truck A	West	Center	Crawling
2	Truck A	West	Curb	Crawling
3	Truck B	West	Center	Crawling
4	Truck B	West	Curb	Crawling
5	Truck B	West	Center	41 km/h
6	Truck A	West	Center	42 km/h
7	Truck A	East	Center	Crawling
8	Truck A	East	Curb	Crawling
9	Truck B	East	Center	Crawling
10	Truck B	West	Curb	Crawling
11	Truck B	West	Center	41 km/h
12	Truck A	West	Center	39 km/h
13	Truck A and B	both	Center	Crawling
14	Truck B and A	both	Center	Crawling
15	Truck A and B	both	Center	41 km/h
16	Truck B and A	both	Center	41 km/h

7.4. Analysis results

A three-dimensional finite element method (FEM) was applied to investigate the structural behavior of the bridge US127/BD (B01-30071). The concrete slab was modeled with isotropic, eight node solid elements, with three degrees of freedoms at each node. The girder flanges and web were modeled using three-dimensional, quadrilateral, four node shell elements with six degrees of freedom at each node. The structural effects of the secondary members, such as the sidewalk and parapet, were also taken into account in the finite element analysis models.

Three cases of the boundary conditions are considered, as described earlier in this Report. The partially frozen supports were modeled using spring elements as shown in Figure 7.6.

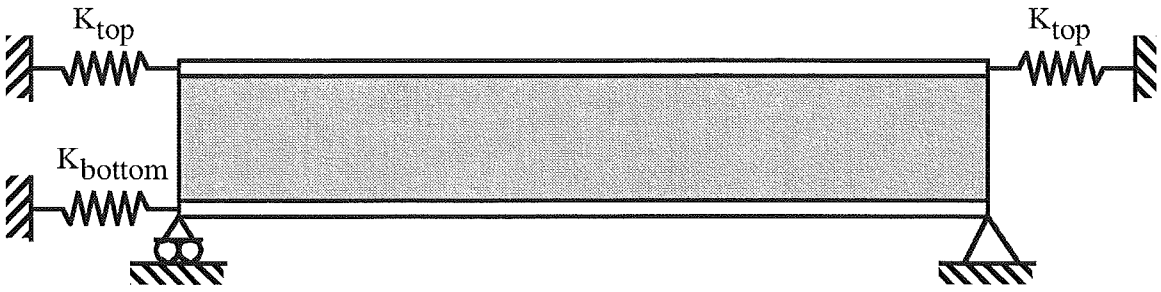

Figure 7.6. Modeing of Support Partial Fixity in Finite Element Analysis.

The mesh of the FEM model is shown in Figure 7.7. Figure 7.8 presents a deformed shape of the bridge loaded with two trucks side-by-side. Figure 7.9 illustrates the distribution of the loads simulating two truck side-by-side.

Strains calculated for the three considered models are shown in Figure 7.10 for two trucks side-by-side (Run 13). Also shown are the experimental results. The FEM results show that the maximum strain at

the most heavily loaded girder is about 170 με for the model with simple support, while the maximum strain recorded from the test is about 135 με. When the spring elements are used with the K constants adjusted according to the test results (K_{top} = 60,000 kN/m and K_{bottom}=120,000 kN/m), then the FEM results become very close to the test results. This confirms the presence of some degree of fixity of supports.

Figure 7.11 presents the deflection obtained from the three different FEM models. It shows that the maximum deflection under two truck loading is about 3 mm, for the FEM model with the partial support fixity.

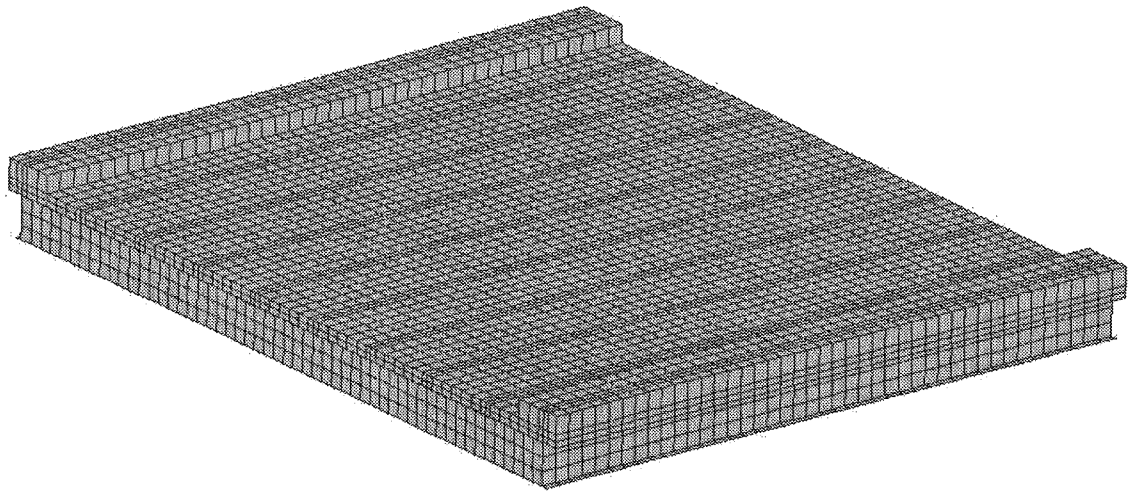

Figure 7.7. The Mesh of the Finite Element Model.
US127/BD (B01-30071).

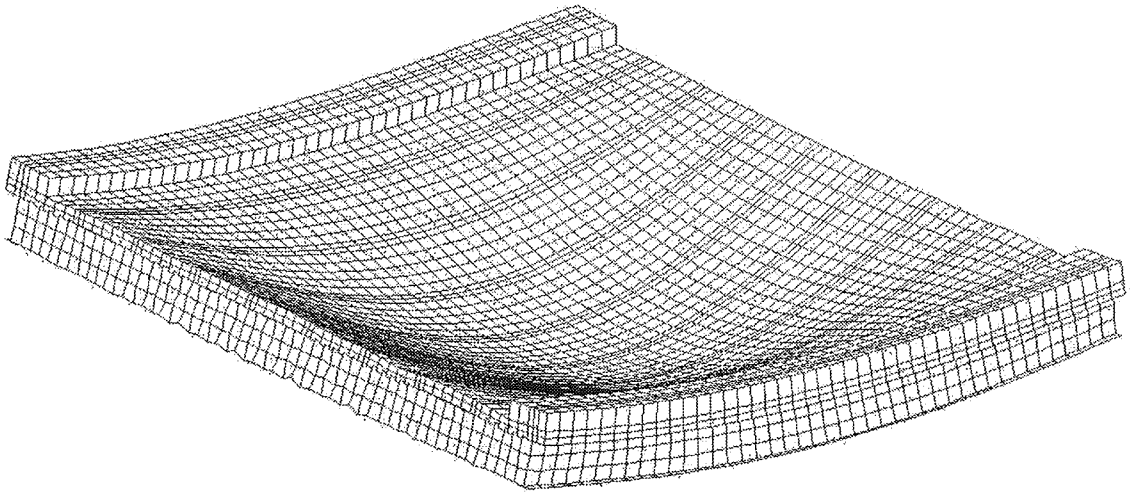

Figure 7.8. The Deformed Shape of the Bridge under Two Lane Loading. US127/BD (B01-30071).

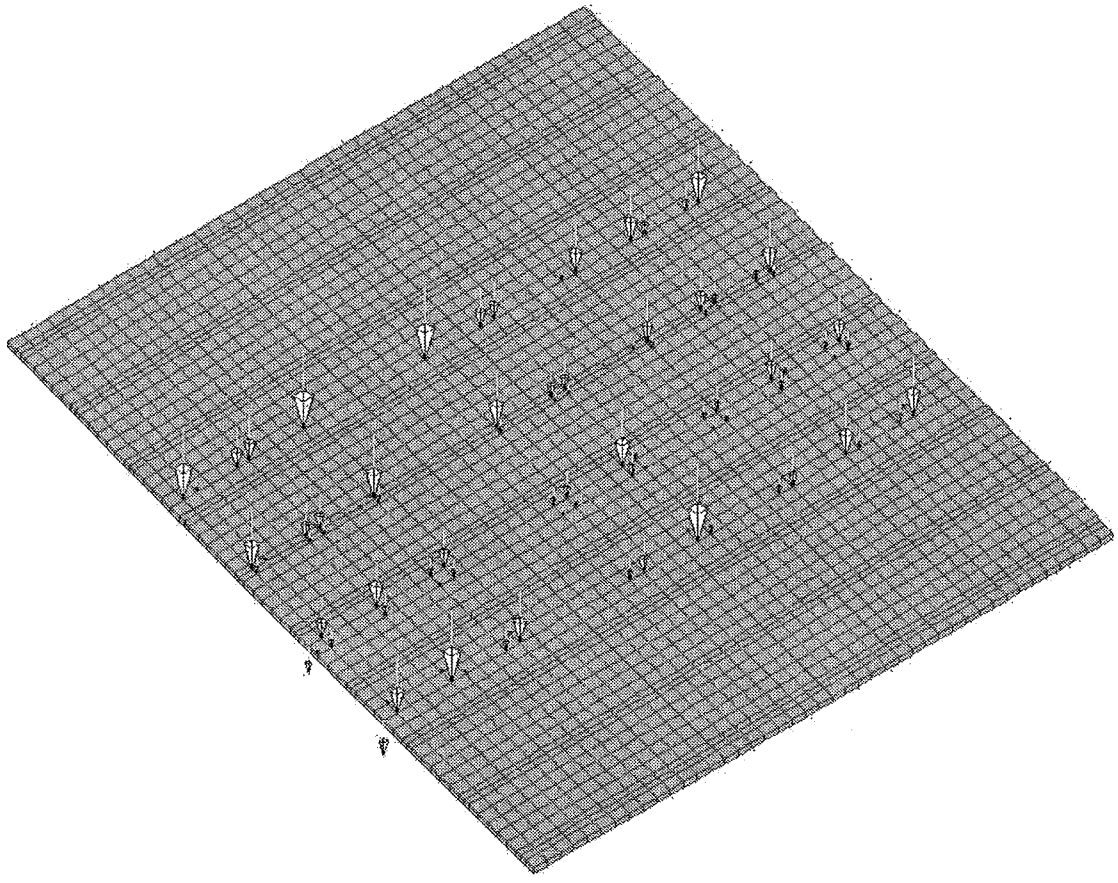

Figure 7.9. Configuration of Load Distribution under Two Lane Loading US127/BD (B01-30071).

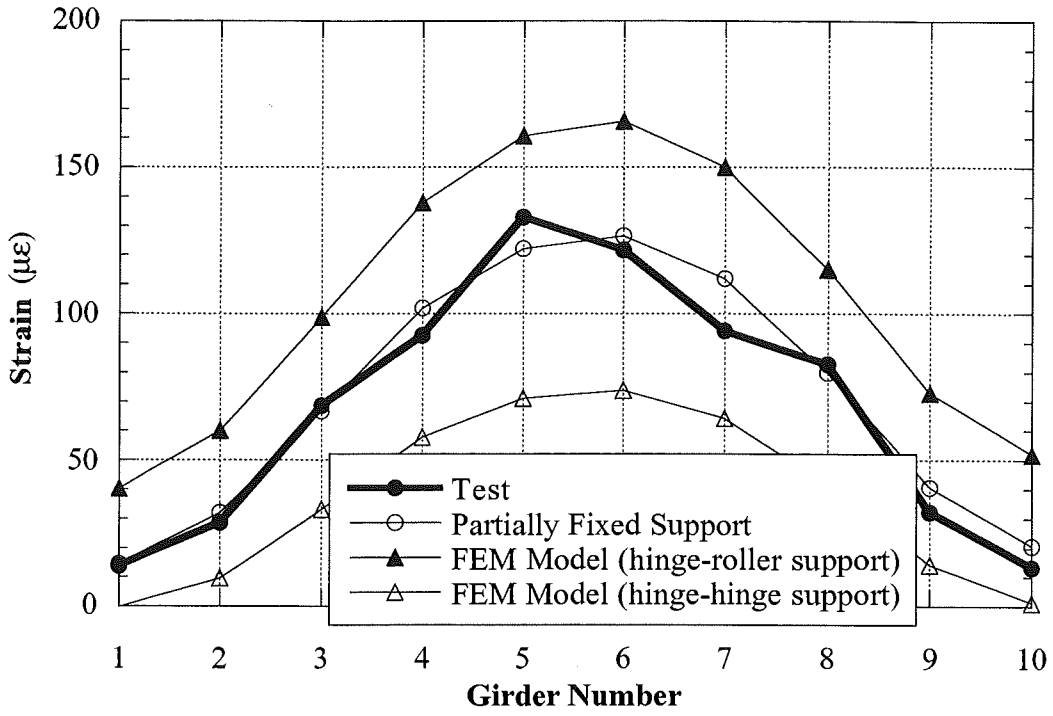

Figure 7.10. Strain from the FEM Analysis Compared with the Test Results for Two Lane Loading, US127/BD (B01-30071).

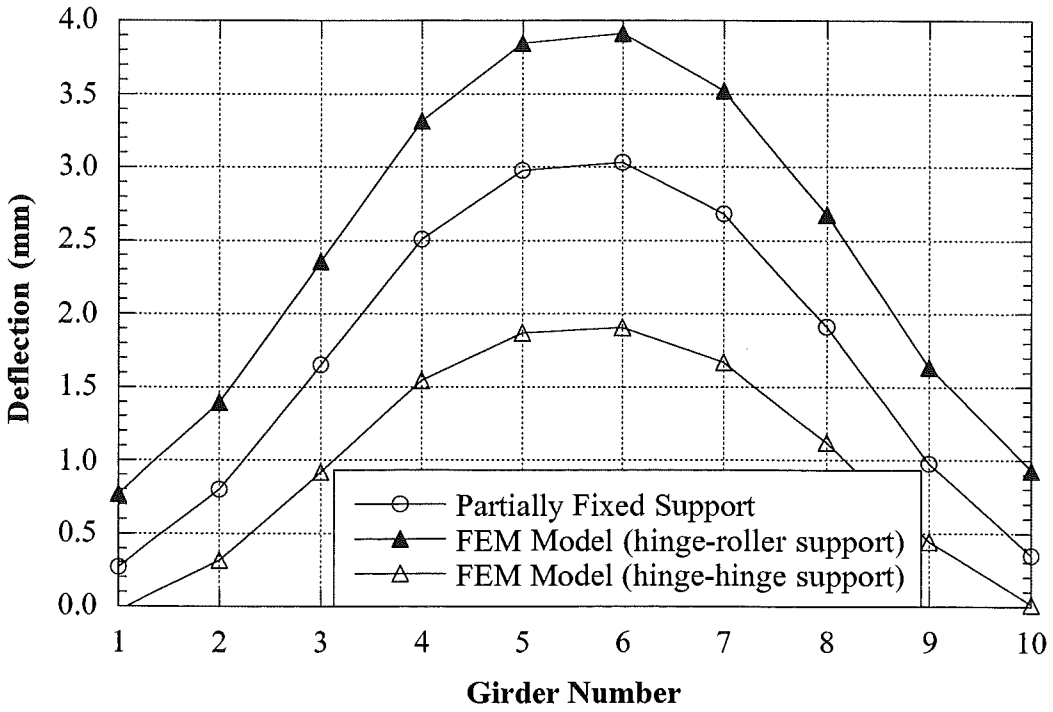

Figure 7.11. Deflection from the FEM Analysis for Two Lane Loading US127/BD (B01-30071).

7.5. Test results

The resulting strains and GDF's are shown in Figures 7.12 through 7.16. Figures 7.12 to 7.14 present the results of all crawling-speed (static) tests. Figures 7.12 to 7.13 present static strains and GDF's for one truck on the bridge. The maximum strain due to a single truck is about 80 με. This corresponds to about 16 MPa.

Figure 7.14 shows static strains and GDF's from side-by-side static load tests. For two vehicles side-by-side the maximum strain is about 140 με (which corresponds to 28 MPa). The superposition of strains due to a single truck in West and East lanes produces almost the same results as strain due to two trucks side-by-side.

For two trucks side-by-side, the girder distribution factor for girder i is determined using Eq. (3-1). For comparison, GDF are also calculated according to AASHTO Standard (1996) and AASHTO LRFD Code (1998). Two cases were considered, a single lane loaded, and two lanes loaded. The resulting GDF's are shown in Figures 7.12 through 7.16.

The results indicate that code-specified GDF's are conservative. A single lane GDF specified in AASHTO LRFD (1998) is also sufficient for two lane load cases for this bridge. However, a single lane GDF specified in AASHTO Standard (1996) is not enough for two lane load cases for this bridge. However, the absolute values of the strains are less than 140 με for the heaviest load case (two fully-loaded trucks side-by-side). Therefore, the total load effect per girder estimated using GDF specified for single lane in AASHTO Standard (1996) is also conservative (less than design value).

Figures 7.15 and 7.16 shows the resulting strain and distribution factors from normal speed tests. There is practically no difference between the crawling speed and normal speed results.

Dynamic load factor is defined in section 3.3. In Figure 7.17, DLF's are plotted for all load cases involving normal speed (no dynamic load was measured for crawling speed runs). Dynamic load factors for exterior girders are high because the static strains in these girders are very low. In other words, large values of DLF in exterior girders correspond to load cases with a single truck in the opposite lane (resulting in very low static strain).

The relationship between DLF and static and dynamic strains is shown in Figure 7.18. The open circles correspond to static strain, ε_{stat}, and black solid squares correspond to dynamic strain, ε_{dyn}. For each static strain value (open circle), the corresponding dynamic strain is denoted by solid square (the numbers of circles and squares are same). Dynamic strains remain nearly constant, while static strains increase as truck loading increases. This results in large dynamic load factors for low static strains. It is clear from the Figure 7.18 that dynamic strains does not exceed 20 $\mu\varepsilon$ for all the cases while the static strain can exceed 120 $\mu\varepsilon$ in normal speed test. DLF corresponding to the maximum strain caused by two trucks side-by-side, is less than 0.10 at girder No. 5 and 6, the most heavily loaded girders.

The strains were also measured close to the support. The results are shown in Figures 7.19 and 7.20. Negative strain values indicate the strains recorded at the bottom flanges near supports were in compression, due to the partial fixity of support. The strain values near the support were measured when the loads caused the maximum strain at the midspan. As shown in the figures, the levels of support fixity are highly unpredictable. Even in one bridge, each girder has different support behavior.

Girder No. 5 was instrumented with remote deflection measurement device manufactured by Noptel. The reflector was installed

at midspan. The result is shown in Table 7.2. The maximum deflection recorded during the test is 3.0 mm for girder number 5. In FEM analysis, about 3 mm of deflection was obtained for run 13 when the supports were assumed to be partially fixed, which is very close to the test results (2.8 mm). This indicates the partial fixity exists at the supports of the bridge.

Table 7.2. Maximum deflections measured at the center of Girder No.5, Bridge US127/BD (B01-30071).

Run #	Vertical Deflection (mm)
1	1.0
2	0.3
3	0.9
4	0.2
5	0.9
6	0.9
7	1.8
8	0.6
9	N/A
10	0.5
11	2.0
12	1.8
13	2.8
14	3.0
15	N/A
16	1.5

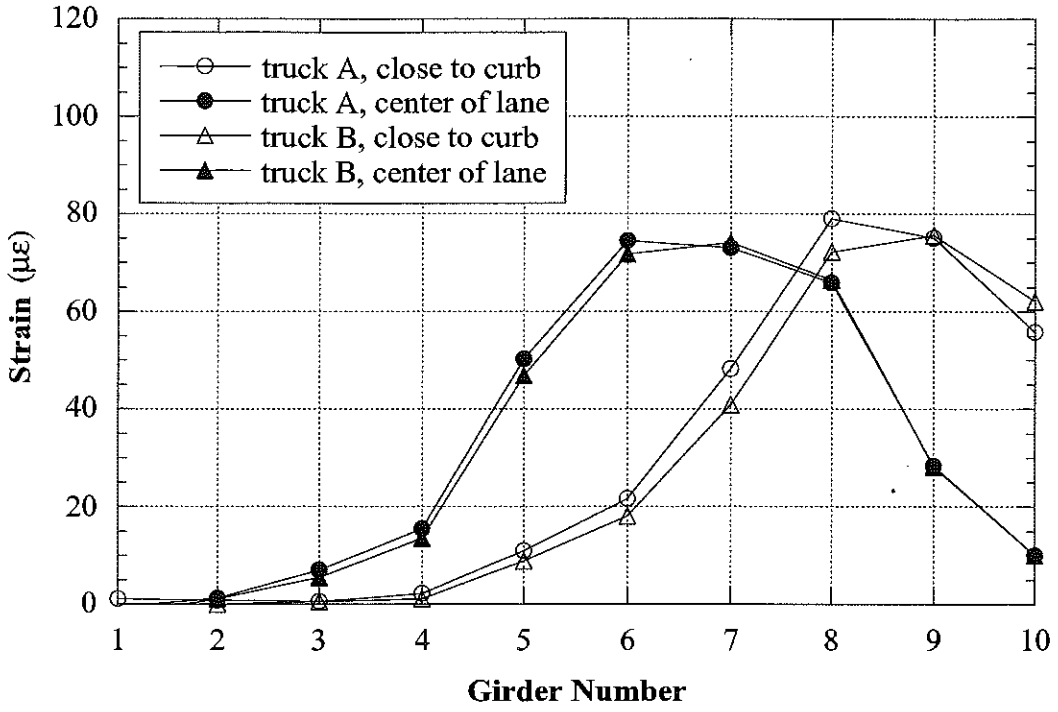

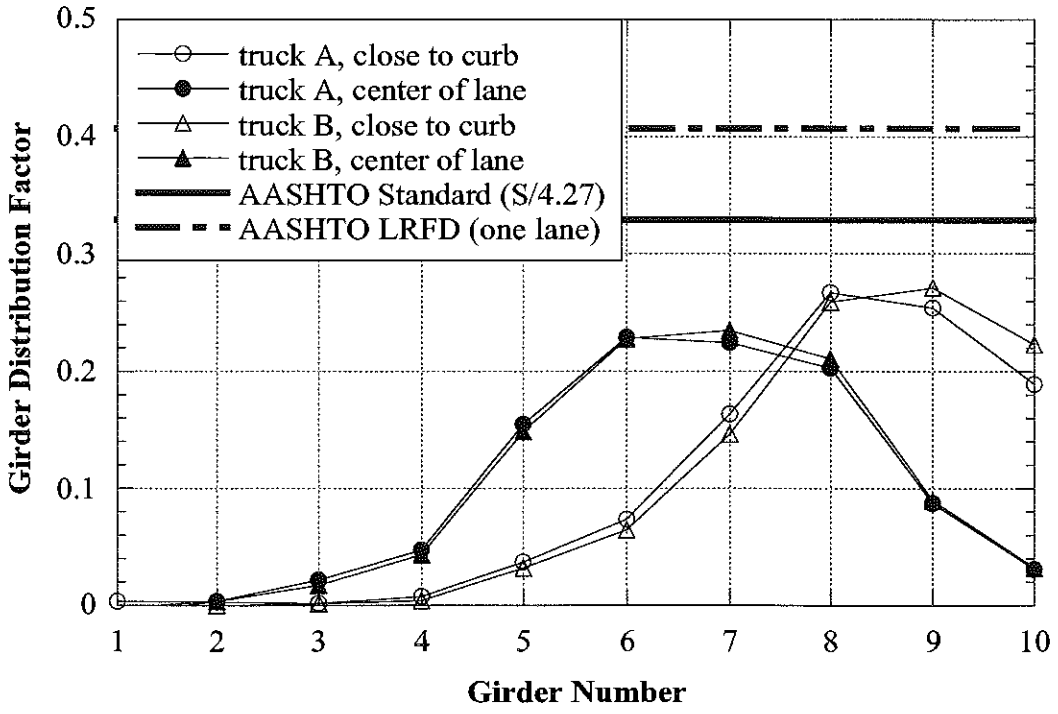

Figure 7.12. West Lane, Crawling Speed, US127/BD (B01-30071).

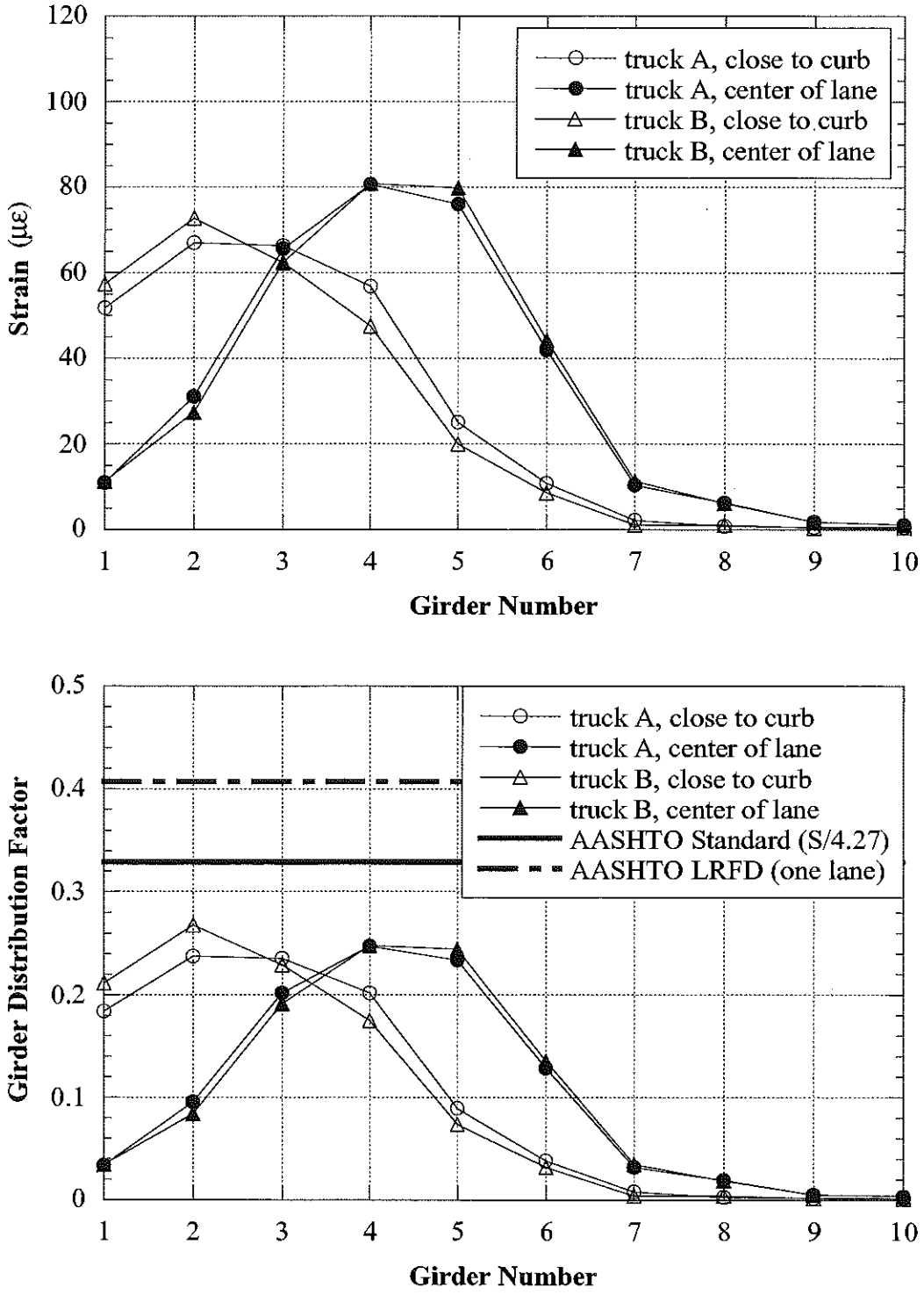

Figure 7.13. East Lane, Crawling Speed, US127/BD (B01-30071).

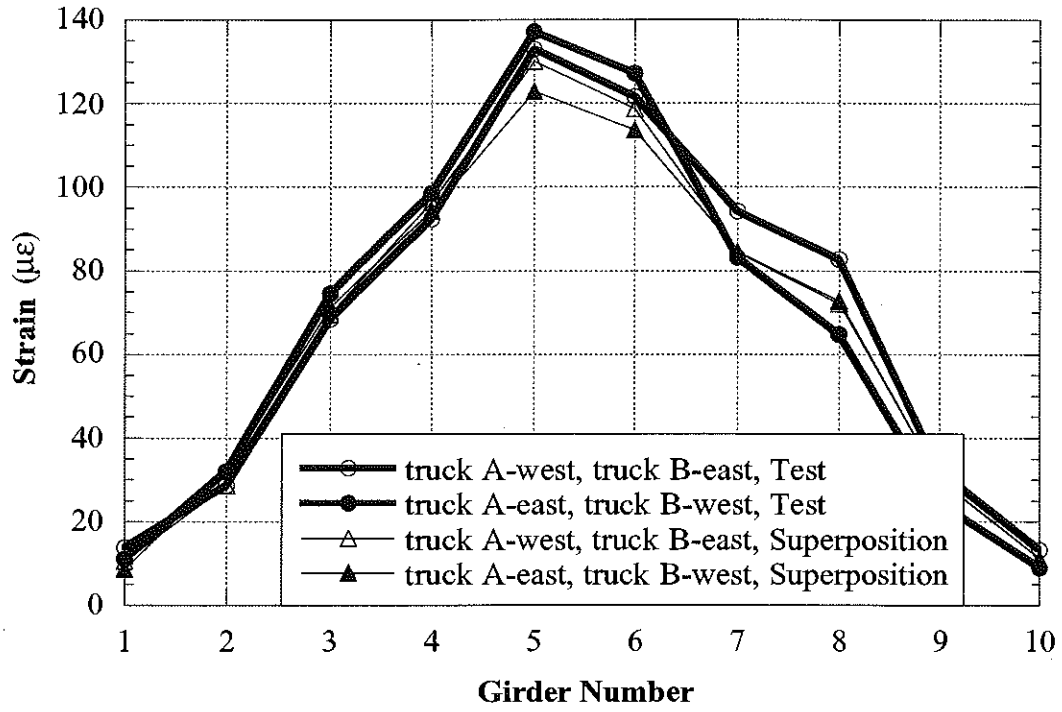

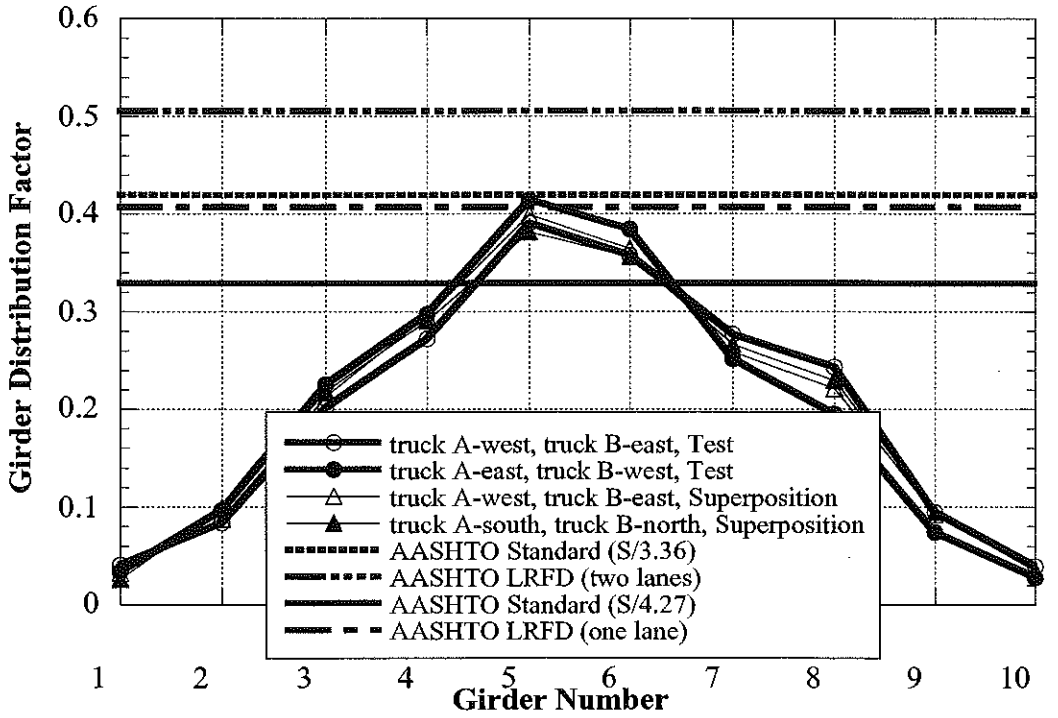

Figure 7.14. Side-by-Side Loading, Center of Lane, Crawling Speed, US127/BD (B01-30071).

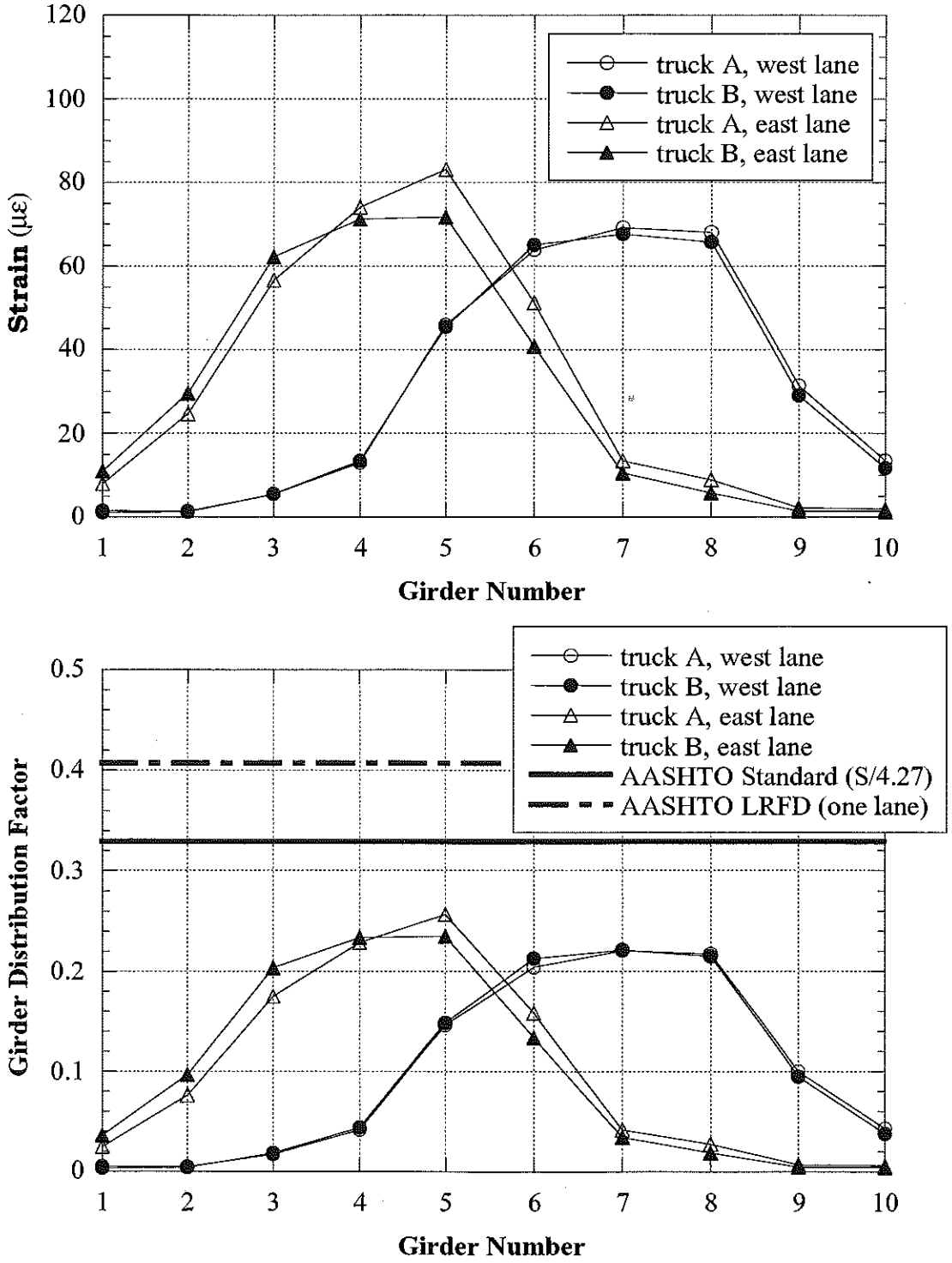

Figure 7.15. Strain and GDF under One Truck Loading at Regular Speed, US127/BD (B01-30071).

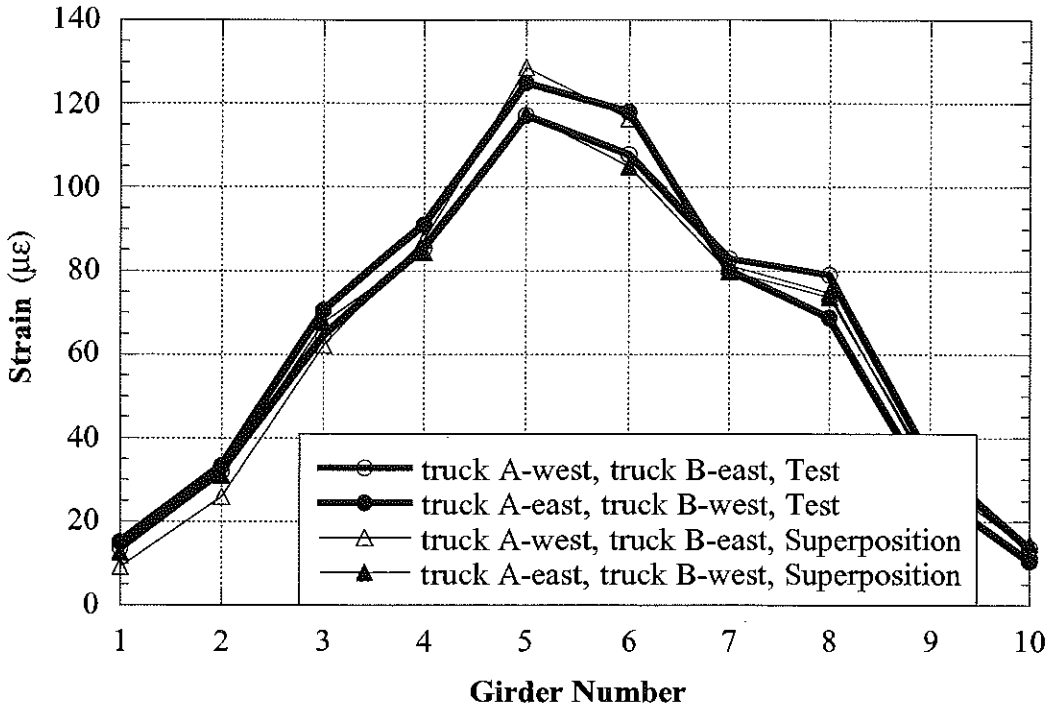

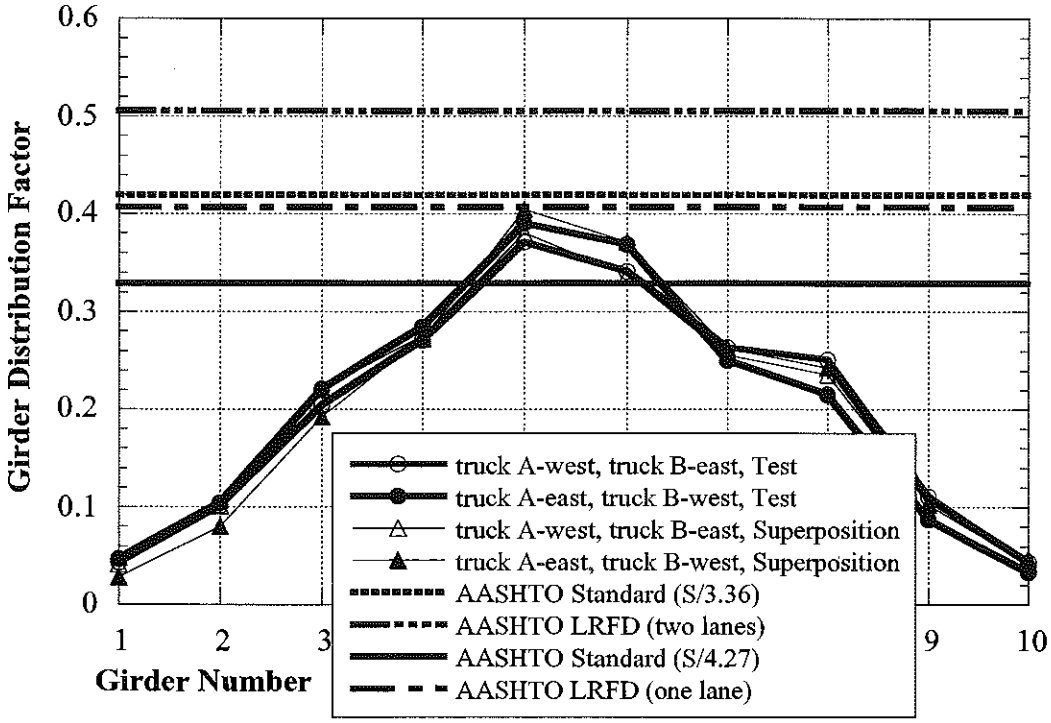

Figure 7.16. Strain and GDF under Side-by-Side Loading at Regular Speed, US127/BD (B01-30071).

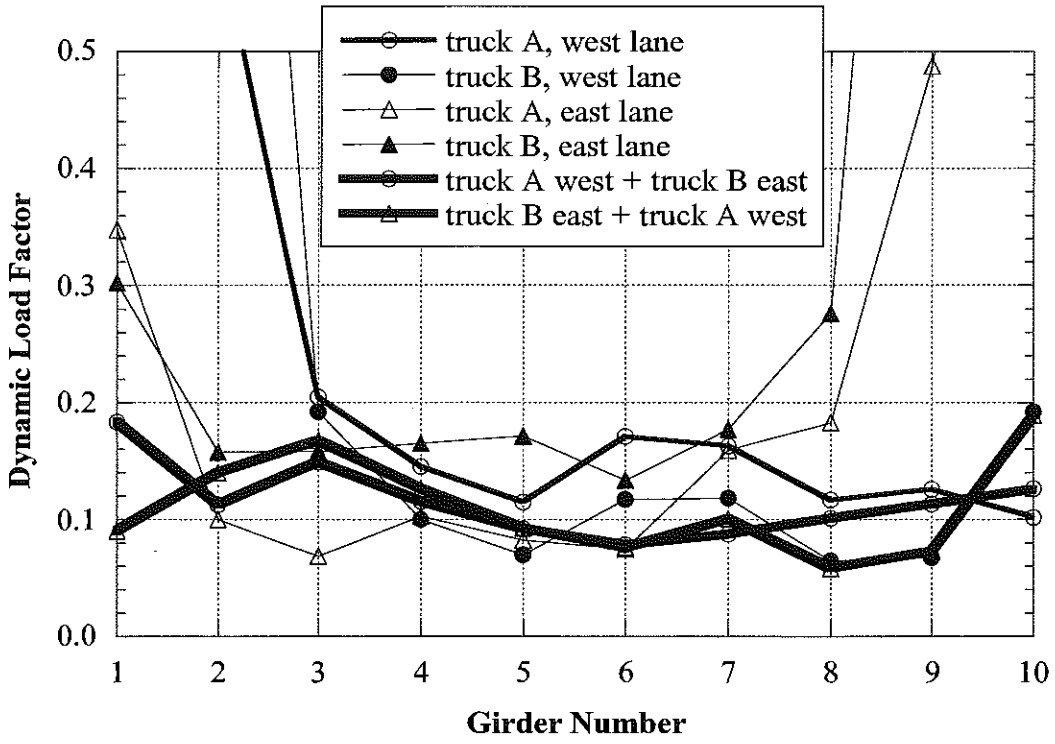

Figure 7.17. Dynamic Load Factors, US127/BD (B01-30071).

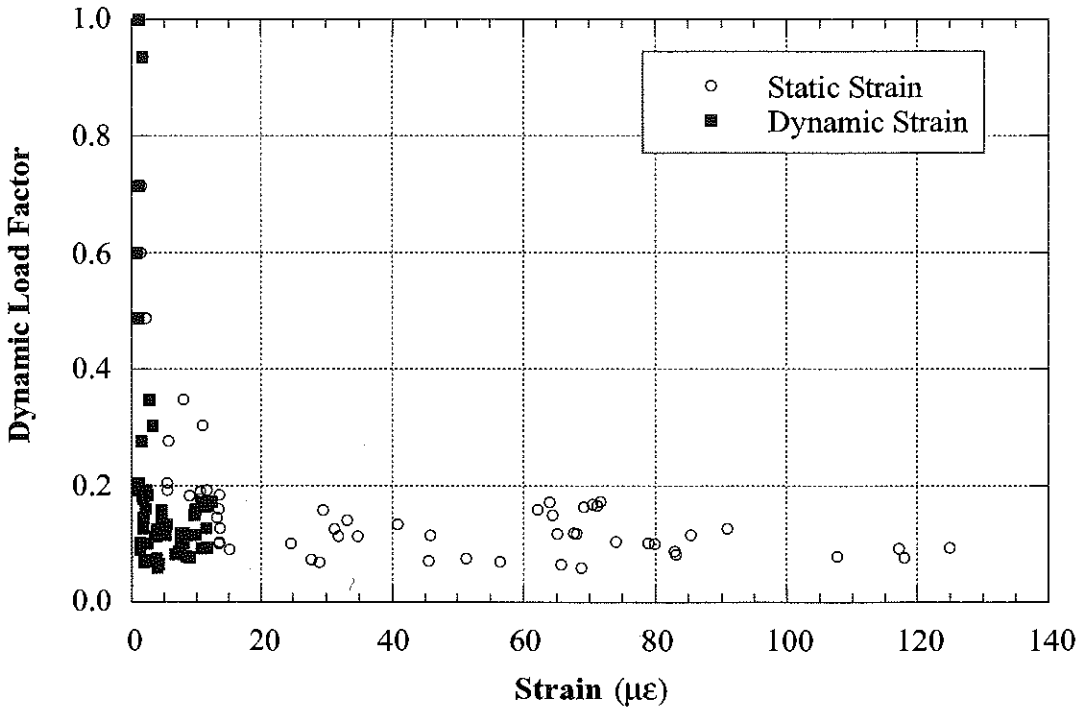

Figure 7.18. Strain vs. Dynamic Load Factors, US127/BD (B01-30071).

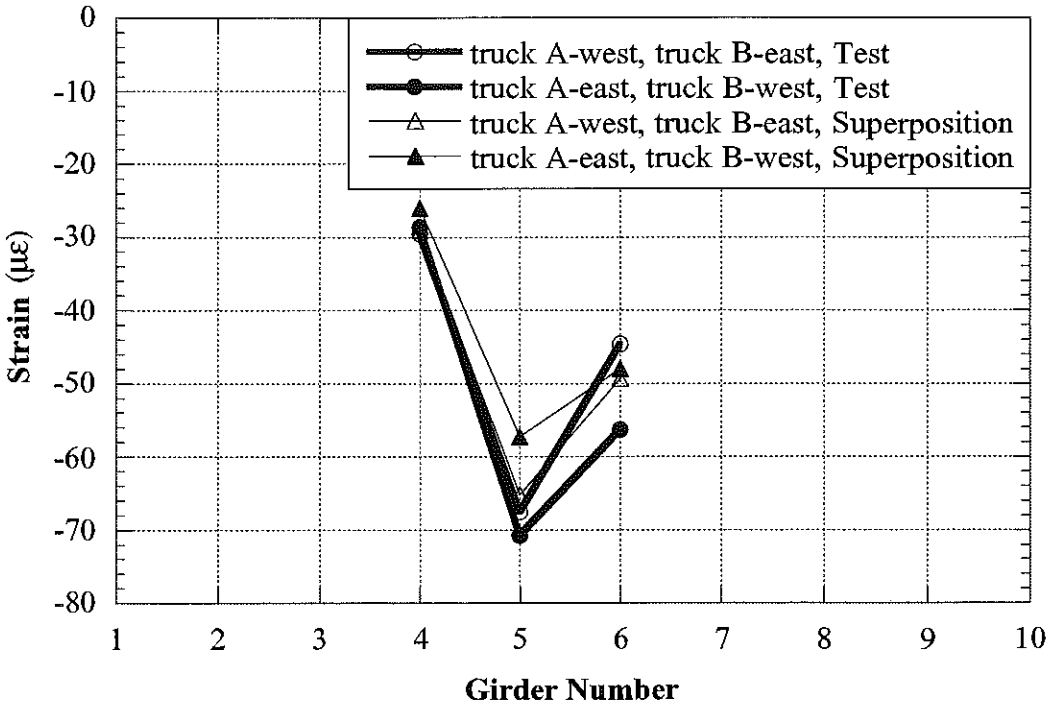

Figure 7.19. Strains at North End, Side-by-Side Loading, Crawling Speed, US127/BD (B01-30071).

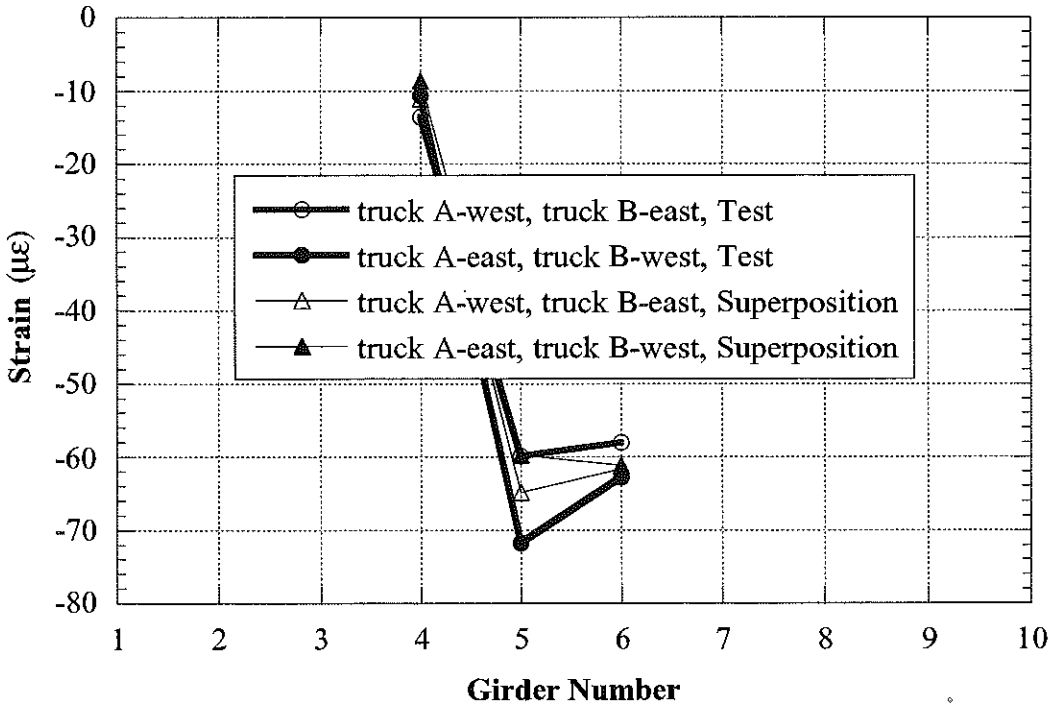

Figure 7.20. Strains at South End, Side-by-Side Loading, Crawling Speed, US127/BD (B01-30071).

8. BRIDGE ON M-50 OVER SOUTH BRANCH OF MACON RIVER, MONROE COUNTY (B01-58041, M50/MR)

8.1 Description

This bridge was built in 1953 and it is located on M-50 over South Branch of Macon River in Monroe County, Michigan. It is a single span, simply supported structure, designed as a composite section. The total span length is 16.7 m, with skew angle of 10 degrees. It has eight steel girders spaced at 1.79 m, as shown in Figure 8.1. The bridge has one lane in each direction and it carries an average daily traffic (ADT) of 4,400. The speed limit on this bridge is 89 km/h. The operating load rating is 1,237 kN, according to the Michigan Structure Inventory.

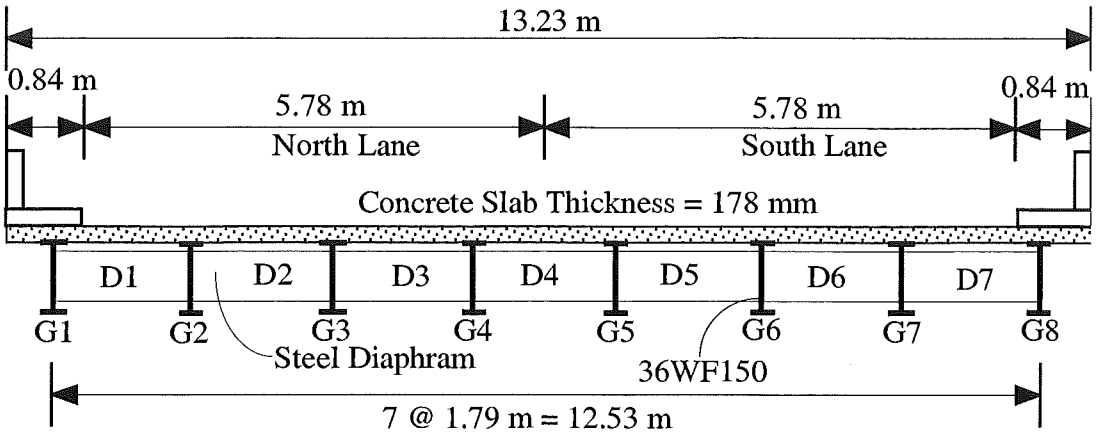

Figure 8.1. Cross-Section of the Bridge M50/MR (B01-58041).

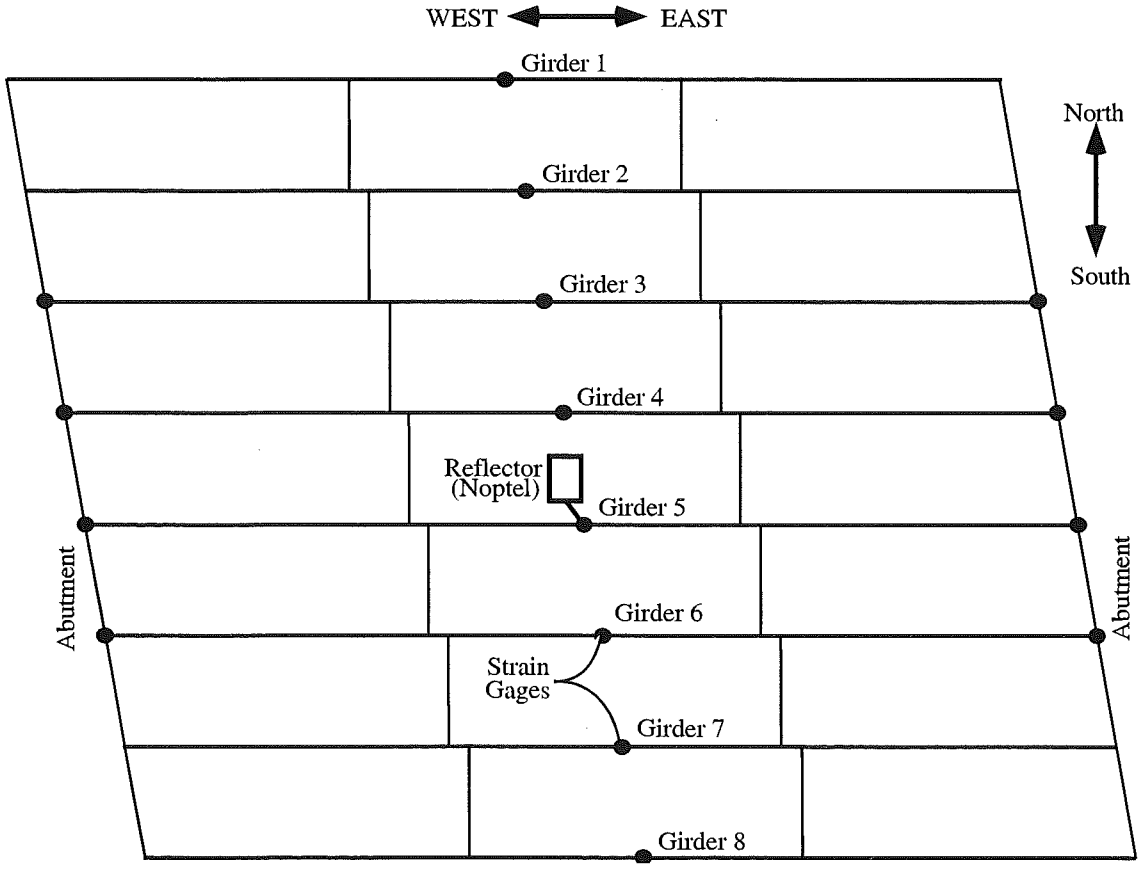

Figure 8.2. Strain Gage Locations in Bridge M50/MR (B01-58041).

8.2 Instrumentation

Strain transducers were installed on the bottom flanges of girders at midspan and at selected support locations, as shown in Figure 6.2. The test equipment was installed on August 16, 2000. The bridge test was performed on August 17, 2000.

8.3 Load Cases

The girder distribution factors (GDF) and dynamic load factors (DLF) were calculated using the strains measured at midspan. The bridge was loaded with two 11-axle trucks (three-unit vehicles).

The truck A and truck B have gross weights of 630 kN and 637 kN, with wheelbases of 15.40 m and 15.65 m, respectively. Truck configurations are shown in Figures 8.3 and 8.4.

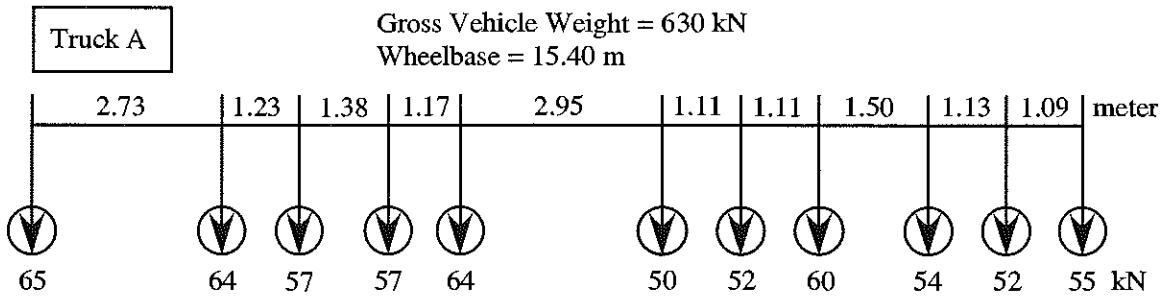

Figure 8.3. Truck A Configuration, Bridge M50/MR (B01-58041).

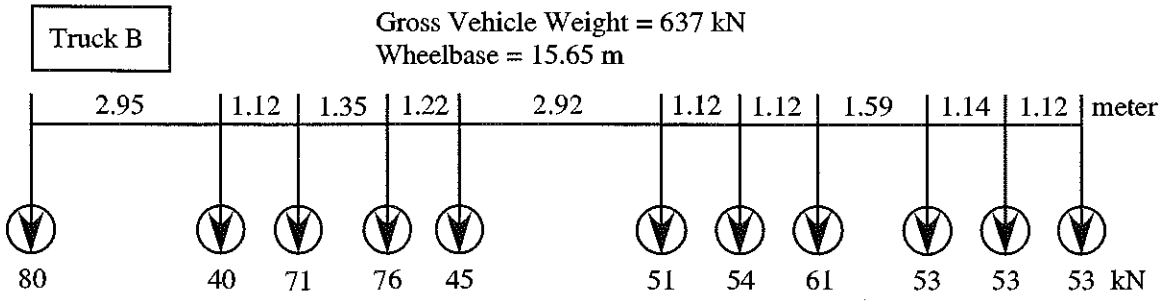

Figure 8.4. Truck B Configuration, Bridge M50/MR (B01-58041).

A total of 16 load cases were considered, as shown in Table 8.1. First each truck was driven by itself at the center of one lane, at crawling

speed. Then, the same truck was driven close to the curb. The runs in the center of the lane were repeated at a normal highway speed. The same was repeated for the other lane. Finally, two trucks were driven simultaneously, side-by-side, at crawling speed and normal highway speed. For side-by-side cases, the runs were repeated after the trucks switched lanes, i.e. first truck A was in South lane, and B in North lane, then truck A was in North lane, and B in South lane.

Table 8.1. Sequence of Test Runs, Bridge M50/MR (B01-58041).

Run#	Truck	Lane Side	Position in Lane	Truck Speed
1	Truck A	South	Center	Crawling
2	Truck A	South	Curb	Crawling
3	Truck B	South	Center	Crawling
4	Truck B	South	Curb	Crawling
5	Truck B	South	Center	57 km/h
6	Truck A	South	Center	52 km/h
7	Truck A	North	Center	Crawling
8	Truck A	North	Curb	Crawling
9	Truck B	North	Center	Crawling
10	Truck B	North	Curb	Crawling
11	Truck B	North	Center	57 km/h
12	Truck A	North	Center	57 km/h
13	Truck A and B	both	Center	Crawling
14	Truck B and A	both	Center	Crawling
15	Truck A and B	both	Center	53 km/h
16	Truck B and A	both	Center	53 km/h

8.4. Analysis results

A three-dimensional finite element method (FEM) was applied to investigate the structural behavior of the bridge M50/MR (B01-58041). The concrete slab was modeled with isotropic, eight node solid elements, with three degrees of freedoms at each node. The girder flanges and web were modeled using three-dimensional, quadrilateral, four node shell elements with six degrees of freedom at each node. The structural effects of the secondary members, such as the sidewalk and parapet, were also taken into account in the finite element analysis models.

Three cases of the boundary conditions are considered, as described earlier in this Report. The partially frozen supports were modeled using spring elements as shown in Figure 8.6.

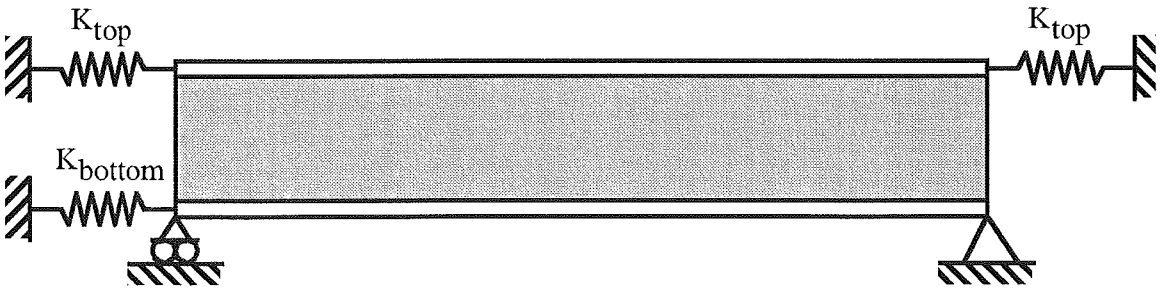

Figure 8.6. Modeing of Support Partial Fixity in Finite Element Analysis.

The mesh of the FEM model is shown in Figure 8.7. Figure 8.8 presents a deformed shape of the bridge loaded with two trucks side-by-side. Figure 8.9 illustrates the distribution of the loads simulating two truck side-by-side.

Strains calculated for the three considered models are shown in Figure 8.10 for two trucks side-by-side (Run 13). Also shown are the experimental results. The FEM results show that the maximum strain at the most heavily loaded girder is about 185 $\mu\varepsilon$ for the model with simple support, while the maximum strain recorded from the test is about 135 $\mu\varepsilon$. When the spring elements are used with the K constants adjusted

according to the test results (K_{top} = 60,000 kN/m and K_{bottom}=240,000 kN/m), then the FEM results become very close to the test results. This confirms the presence of some degree of fixity of supports.

Figure 8.11 presents the deflection obtained from the three different FEM models. It shows that the maximum deflection under two truck loading is about 5 mm, for the FEM model with the partial support fixity.

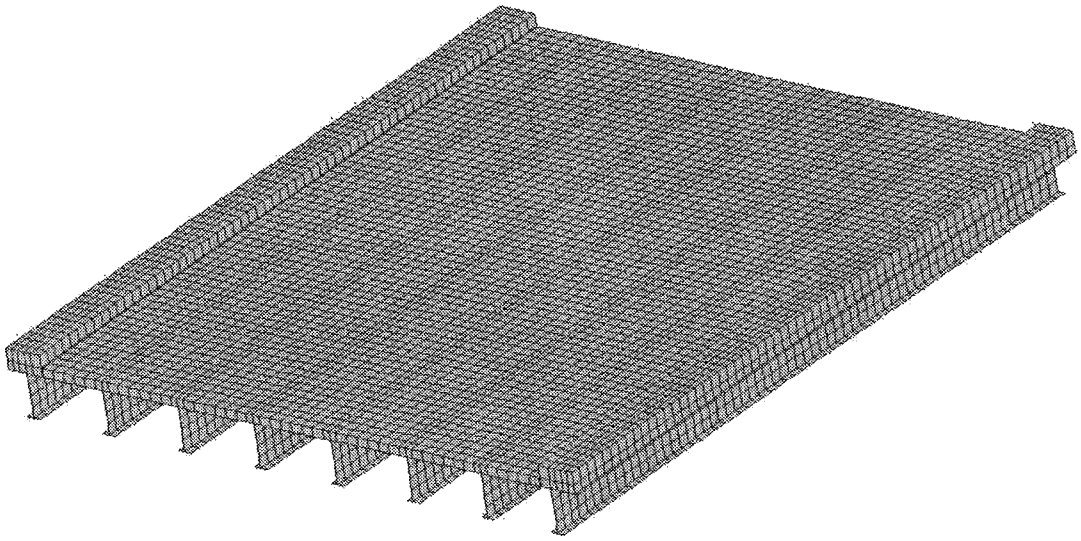

Figure 8.7. The Mesh of the Finite Element Model.
M50/MR (B01-58041).

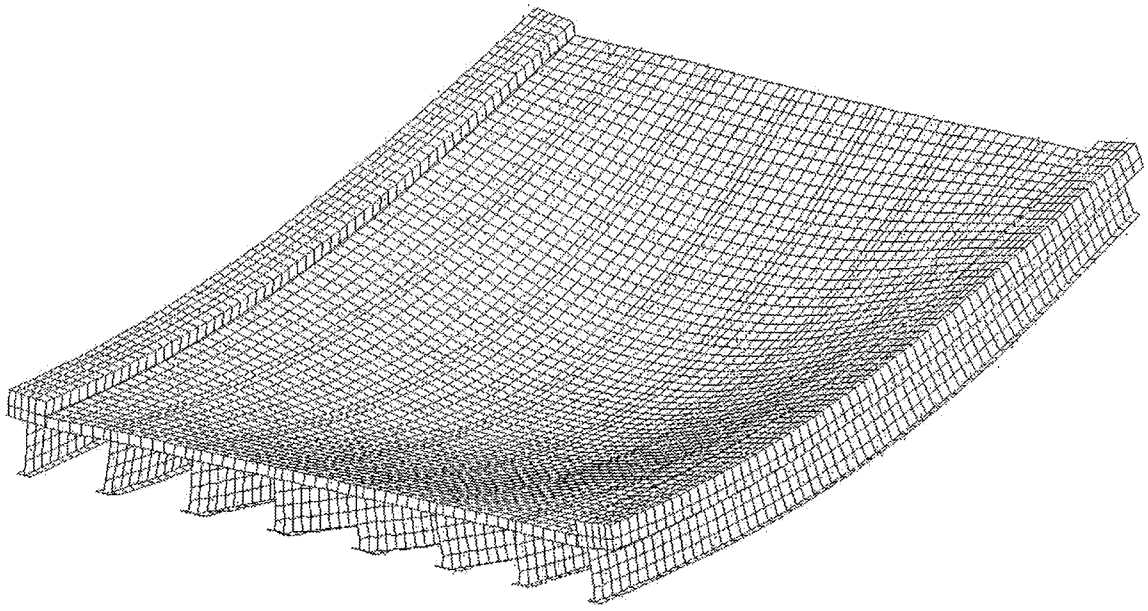

Figure 8.8. The Deformed Shape of the Bridge under Two Lane Loading. M50/MR (B01-58041).

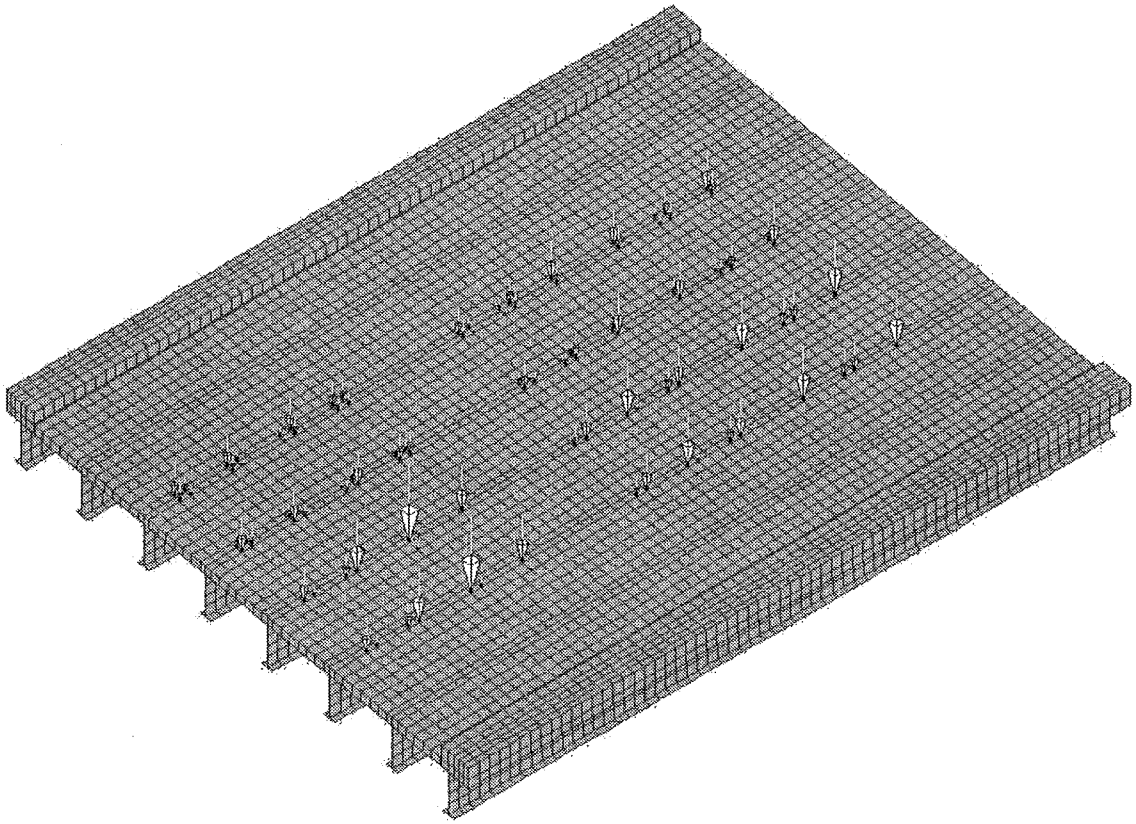

Figure 8.9. Configuration of Load Distribution under Two Lane Loading M50/MR (B01-58041).

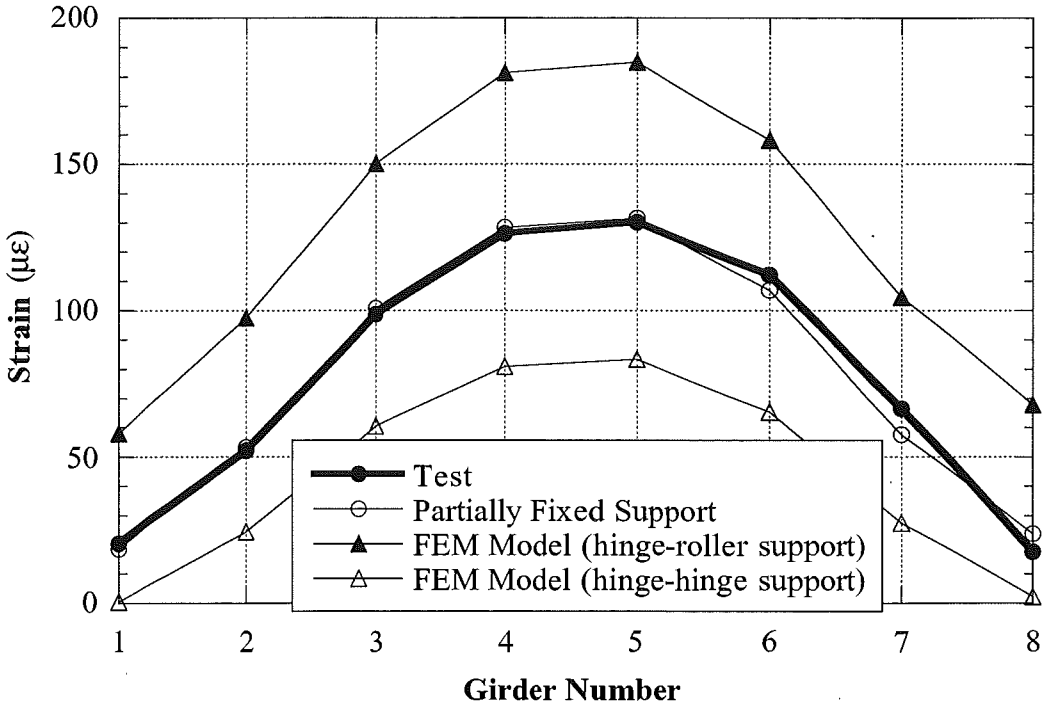

Figure 8.10. Strain from the FEM Analysis Compared with the Test Results for Two Lane Loading, M50/MR (B01-58041).

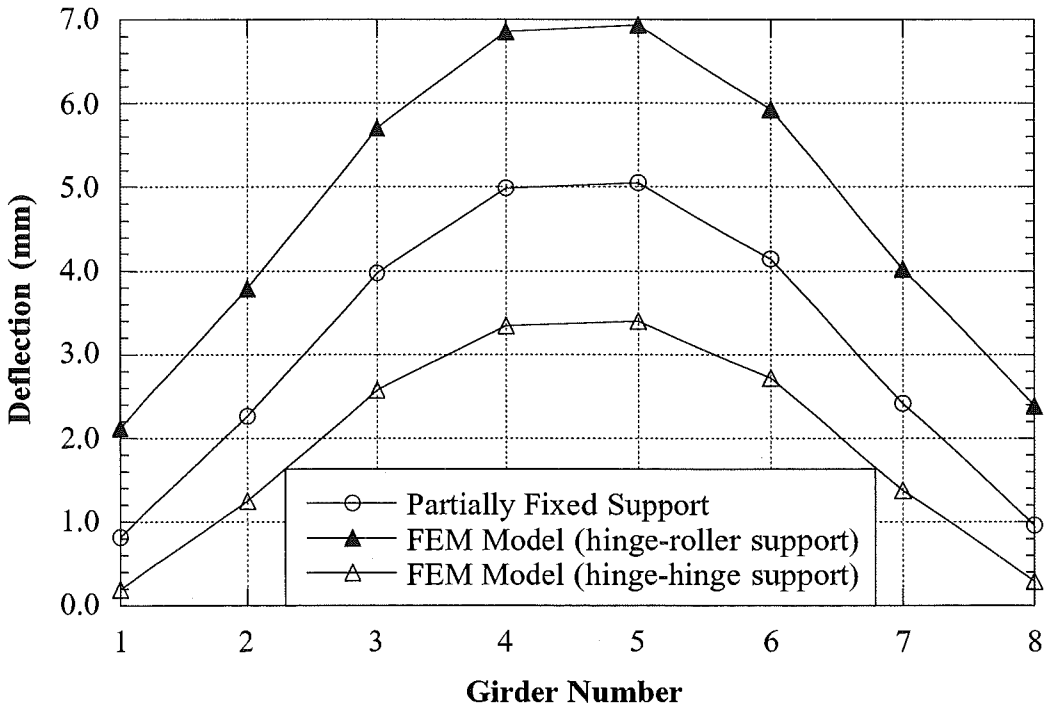

Figure 8.11. Deflection from the FEM Analysis for Two Lane Loading M50/MR (B01-58041).

8.5 Test results

The resulting strains and GDF's are shown in Figures 8.12 through 8.16. Figures 8.12 to 8.14 present the results of all crawling-speed (static) tests. Figures 8.12 to 8.13 present static strains and GDF's for one truck on the bridge. The maximum strain due to a single truck is about 90 με. This corresponds to about 18 MPa.

Figure 8.14 shows static strains and GDF's from side-by-side static load tests. For two vehicles side-by-side the maximum strain is about 130 με (which corresponds to 26 MPa). The superposition of strains due to a single truck in North and South lanes produces almost the same results as strain due to two trucks side-by-side.

For two trucks side-by-side, the girder distribution factor for girder i is determined using Eq. (3-1). For comparison, GDF are also calculated according to AASHTO Standard (1996) and AASHTO LRFD Code (1998). Two cases were considered, a single lane loaded, and two lanes loaded. The resulting GDF's are shown in Figures 8.12 through 8.16.

The results indicate that code-specified GDF's are conservative. Even single lane GDF's specified in both AASHTO Standard (1996) and AASHTO LRFD (1998) are also sufficient for two lane load cases for this bridge.

Figures 8.15 and 8.16 shows the resulting strain and distribution factors from normal speed tests. There is practically no difference between the crawling speed and normal speed results.

Dynamic load factor is defined in section 3.3. In Figure 8.17, DLF's are plotted for all load cases involving normal speed (no dynamic load was measured for crawling speed runs). Dynamic load factors for exterior girders are high because the static strains in these girders are

very low. In other words, large values of DLF in exterior girders correspond to load cases with a single truck in the opposite lane (resulting in very low static strain).

The relationship between DLF and static and dynamic strains is shown in Figure 8.18. The open circles correspond to static strain, ε_{stat}, and black solid squares correspond to dynamic strain, ε_{dyn}. For each static strain value (open circle), the corresponding dynamic strain is denoted by solid square (the numbers of circles and squares are same). Dynamic strains remain nearly constant, while static strains increase as truck loading increases. This results in large dynamic load factors for low static strains. It is clear from the Figure 8.18 that dynamic strains does not exceed 10 με for all the cases while the static strain can exceed 120 με in normal speed test. DLF corresponding to the maximum strain caused by two trucks side-by-side, is less than 0.10 at girder No. 4 and 5, the most heavily loaded girders.

The strains were also measured close to the support. The results are shown in Figures 8.19 and 8.20. Negative strain values indicate the strains recorded at the bottom flanges near supports were in compression, due to the partial fixity of support. The strain values near the support were measured when the loads caused the maximum strain at the midspan. As shown in the Figures, the levels of support fixity are highly unpredictable. Even in a same bridge, each girder has different support behavior.

Girder No. 5 was instrumented with a remote deflection measurement device manufactured by Noptel. The reflector was installed at midspan. However, the test results could not be retrieved due to the hard disk failure of the notebook computer used in the test.

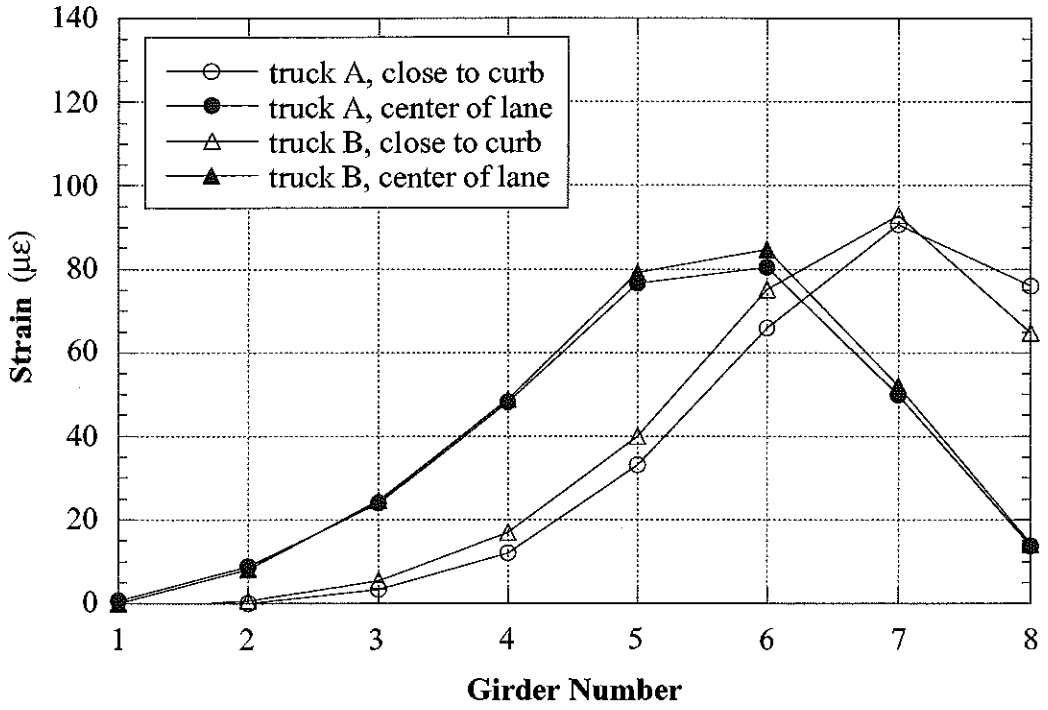

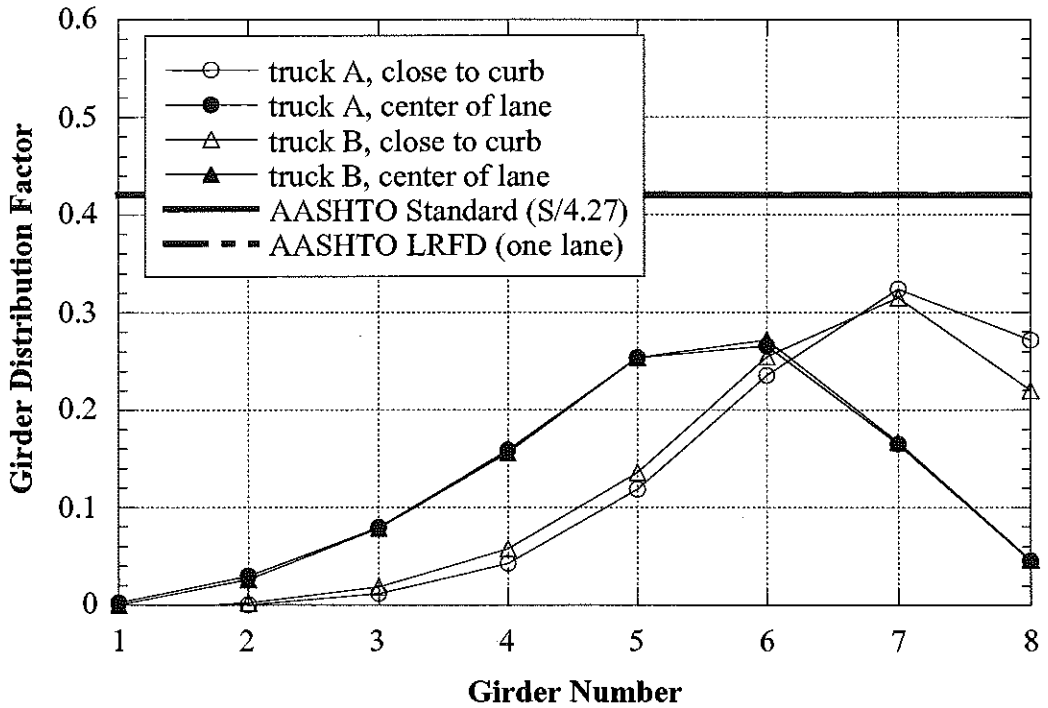

Figure 8.12. South Lane, Crawling Speed, M50/MR (B01-58041).

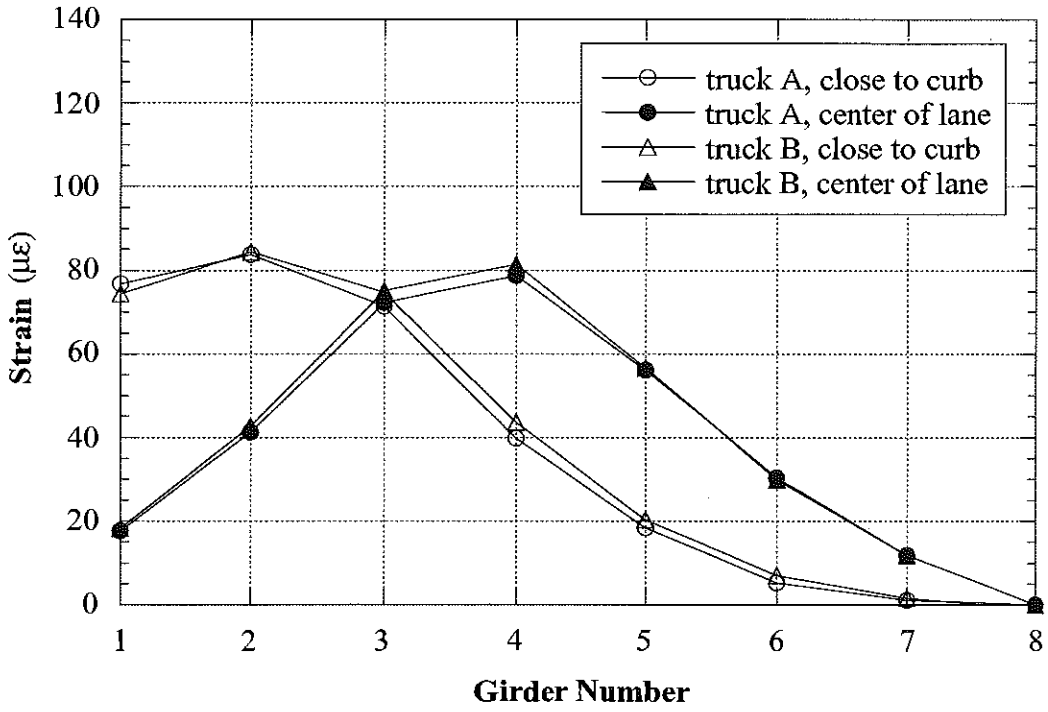

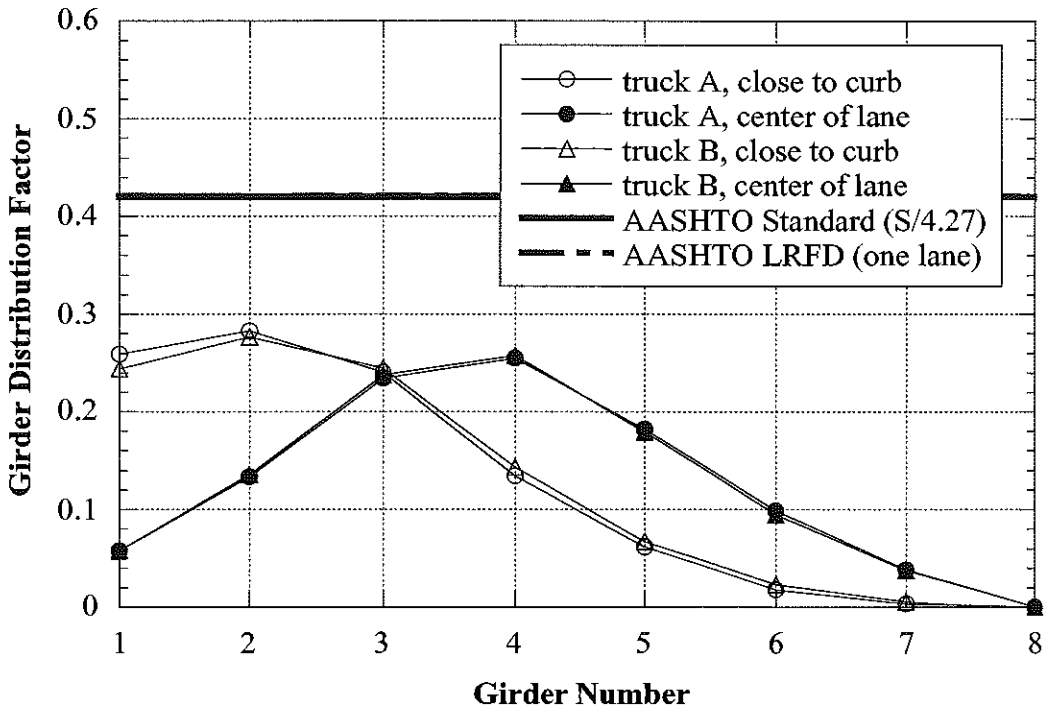

Figure 8.13. North Lane, Crawling Speed, M50/MR (B01-58041).

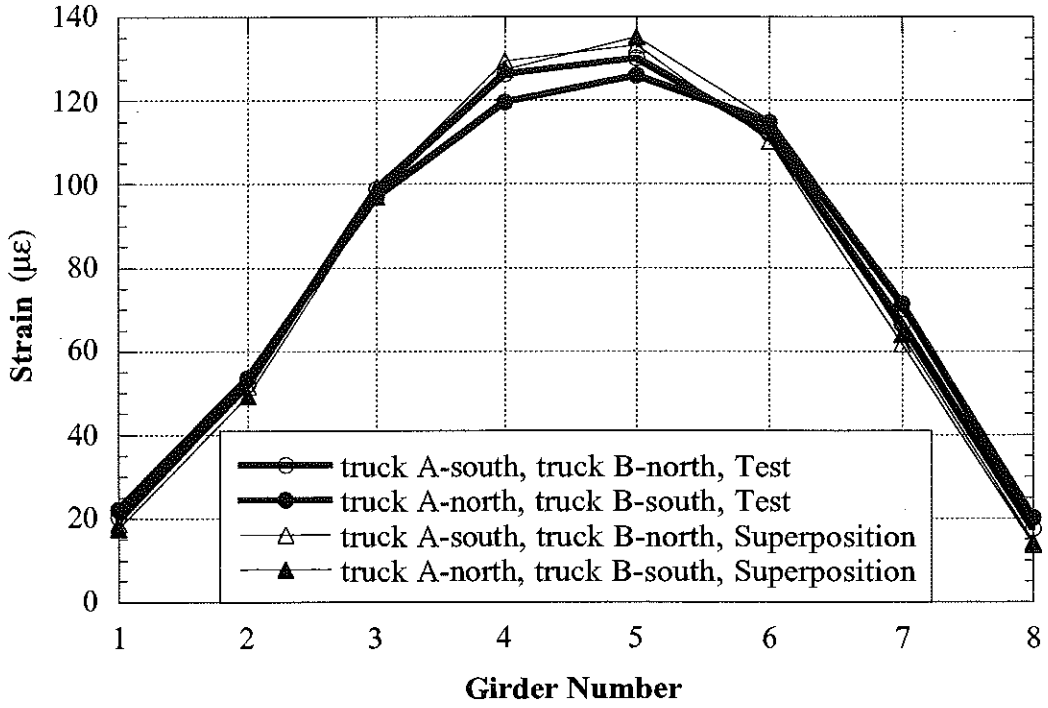

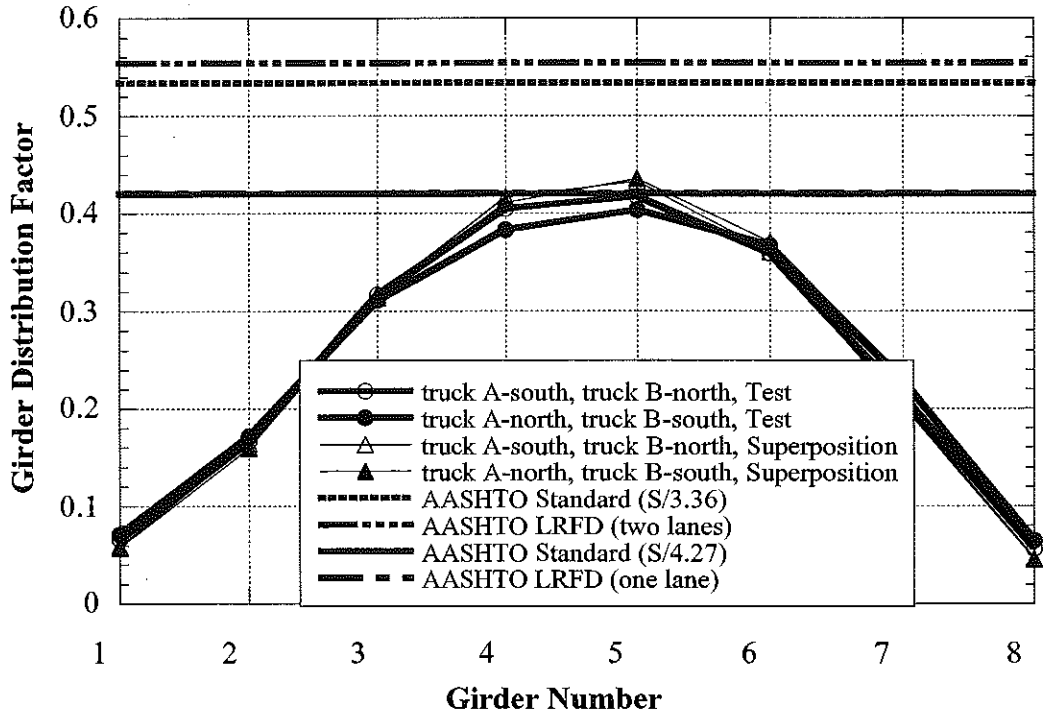

Figure 8.14. Side-by-Side Loading, Center of Lane, Crawling Speed, M50/MR (B01-58041).

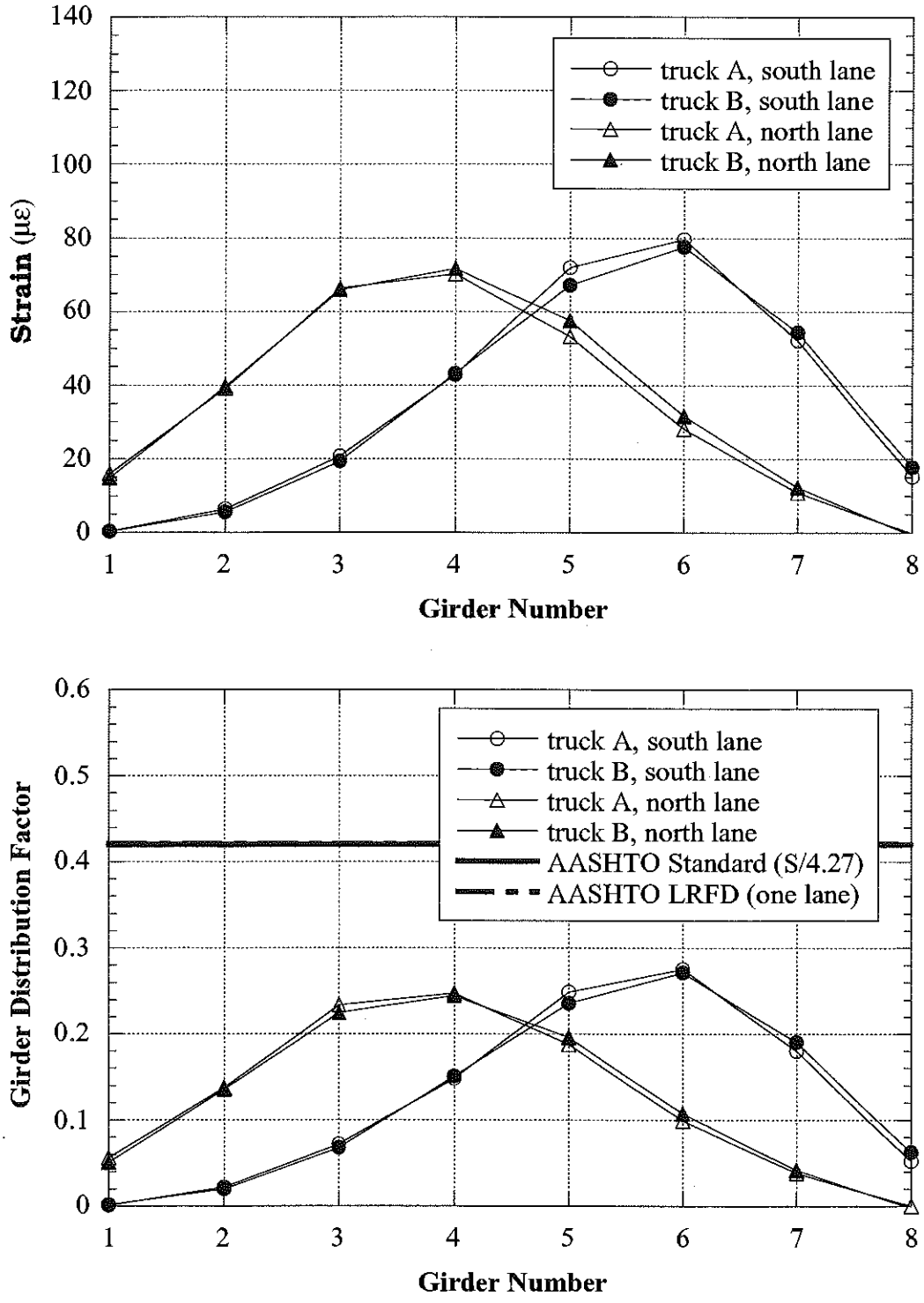

Figure 8.15. Strain and GDF under One Truck Loading at Regular Speed, M50/MR (B01-58041).

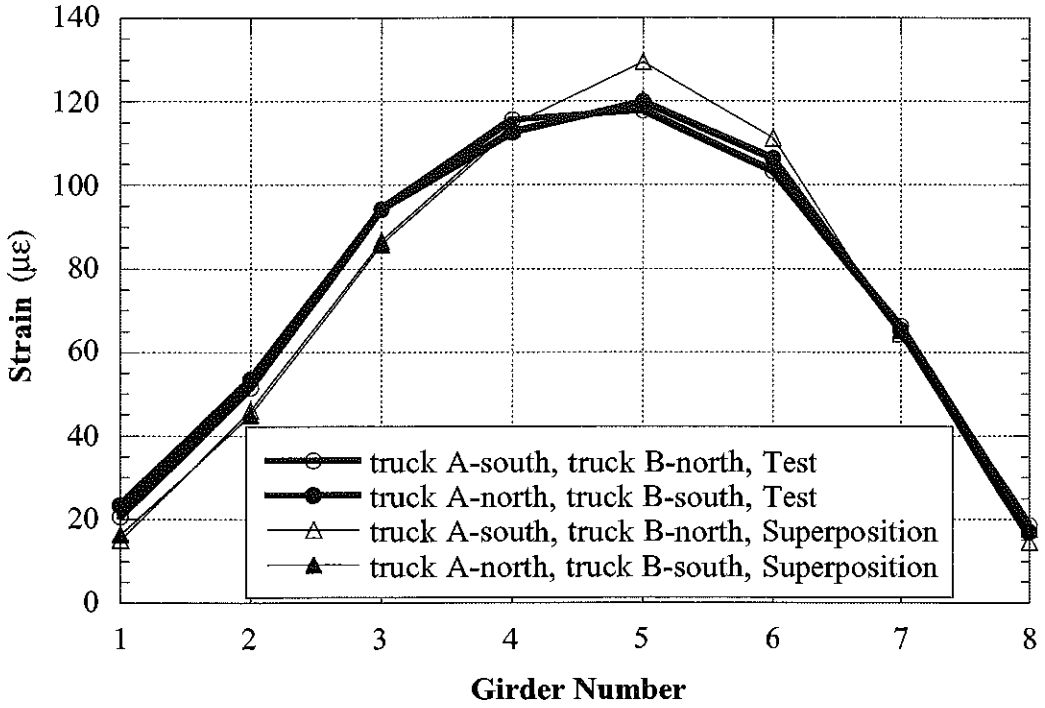

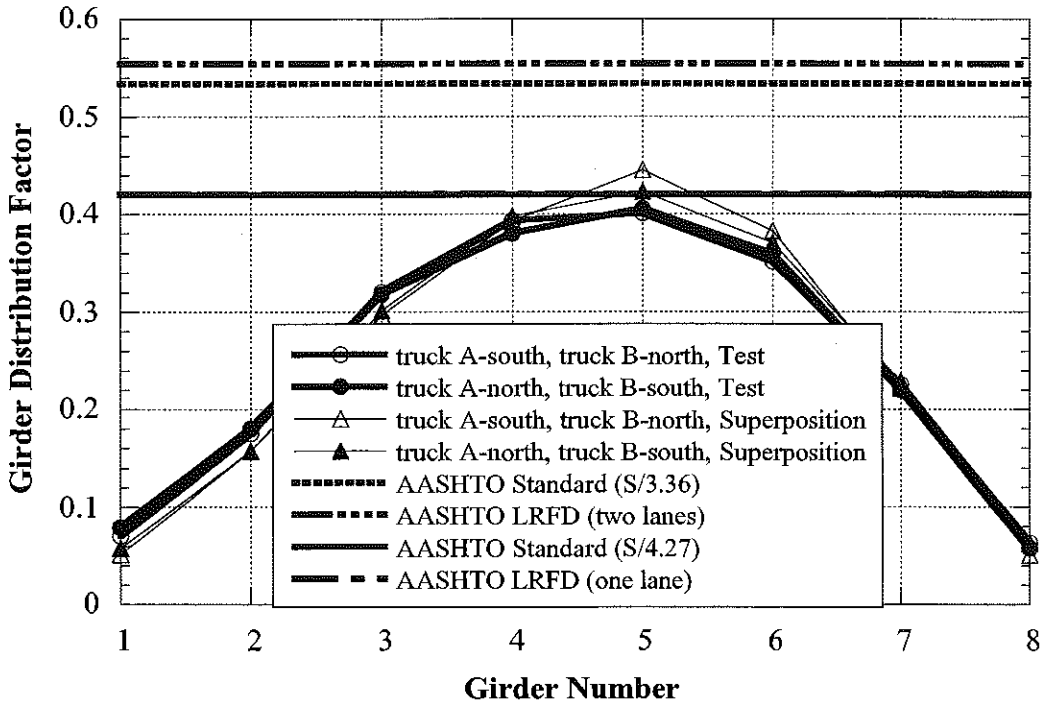

Figure 8.16. Strain and GDF under Side-by-Side Loading at Regular Speed, M50/MR (B01-58041).

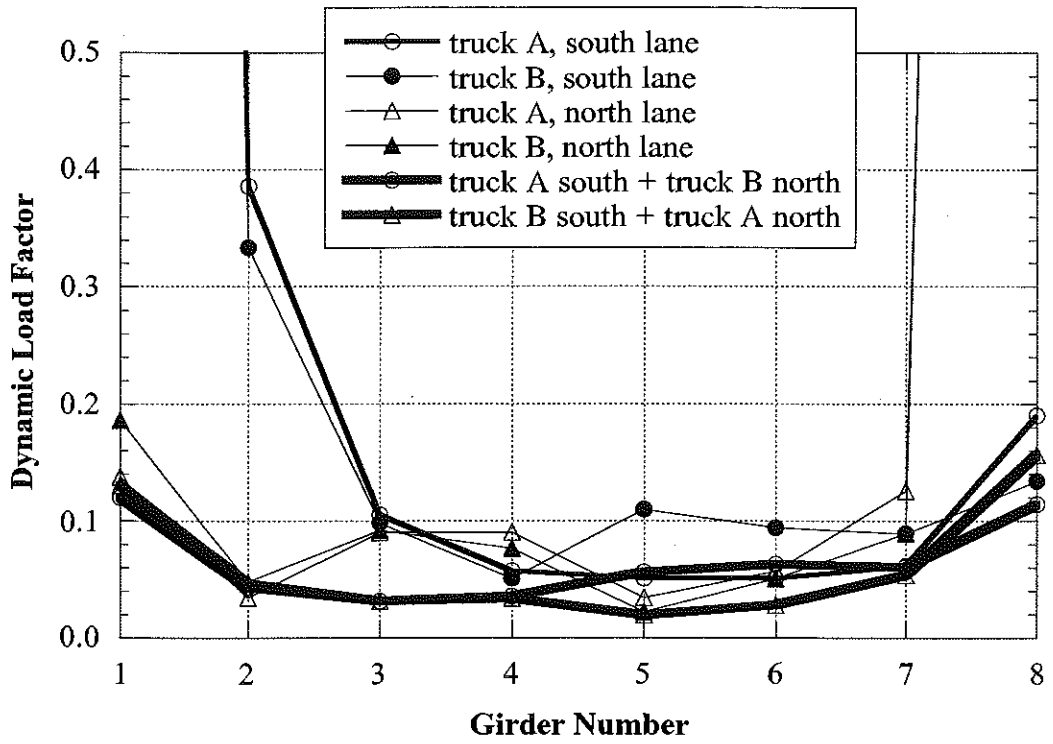

Figure 8.17. Dynamic Load Factors, M50/MR (B01-58041).

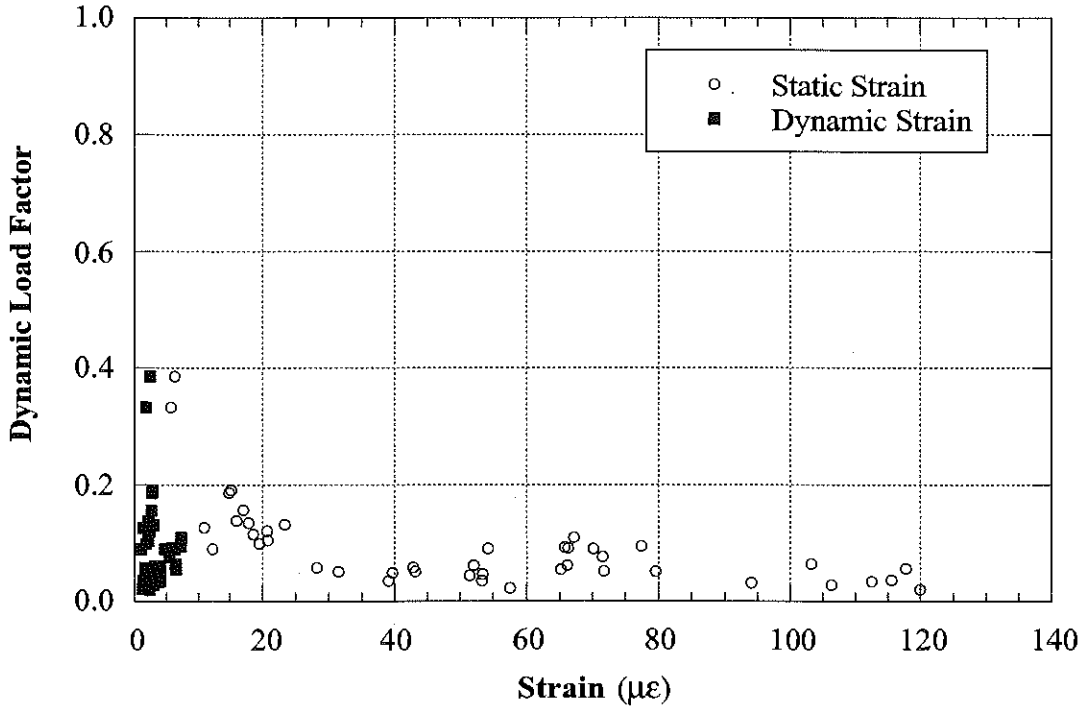

Figure 8.18. Strain vs. Dynamic Load Factors, M50/MR (B01-58041).

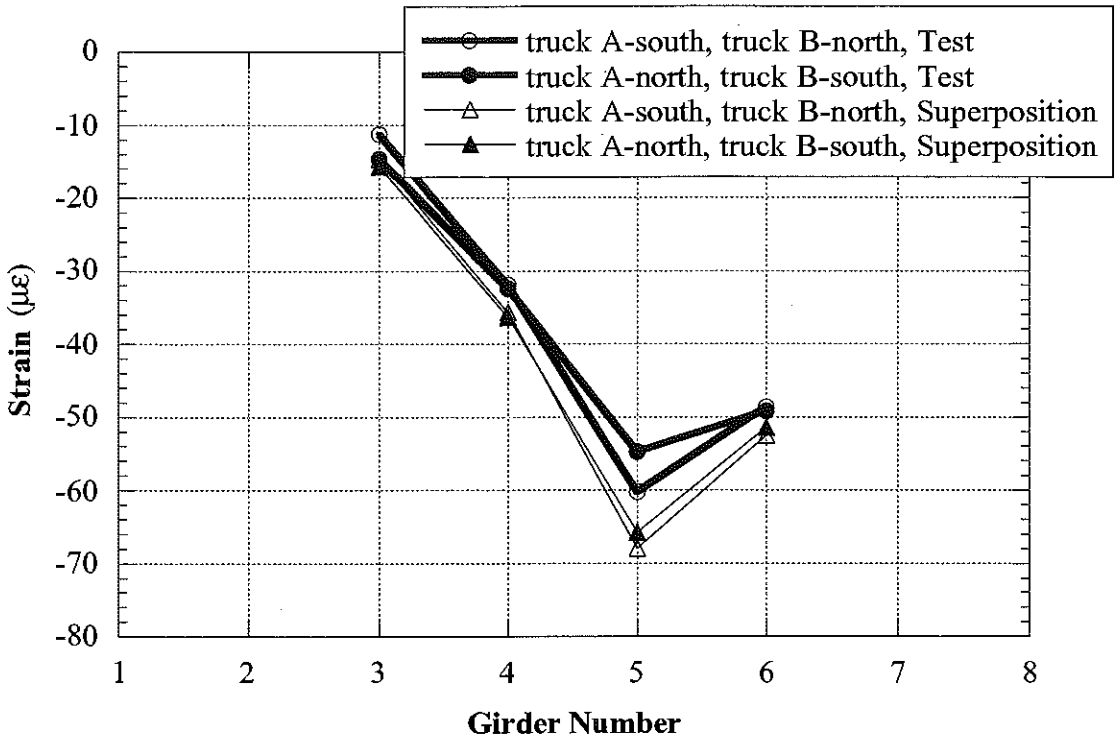

Figure 8.19. Strains at West End, Side-by-Side Loading, Crawling Speed, M50/MR (B01-58041).

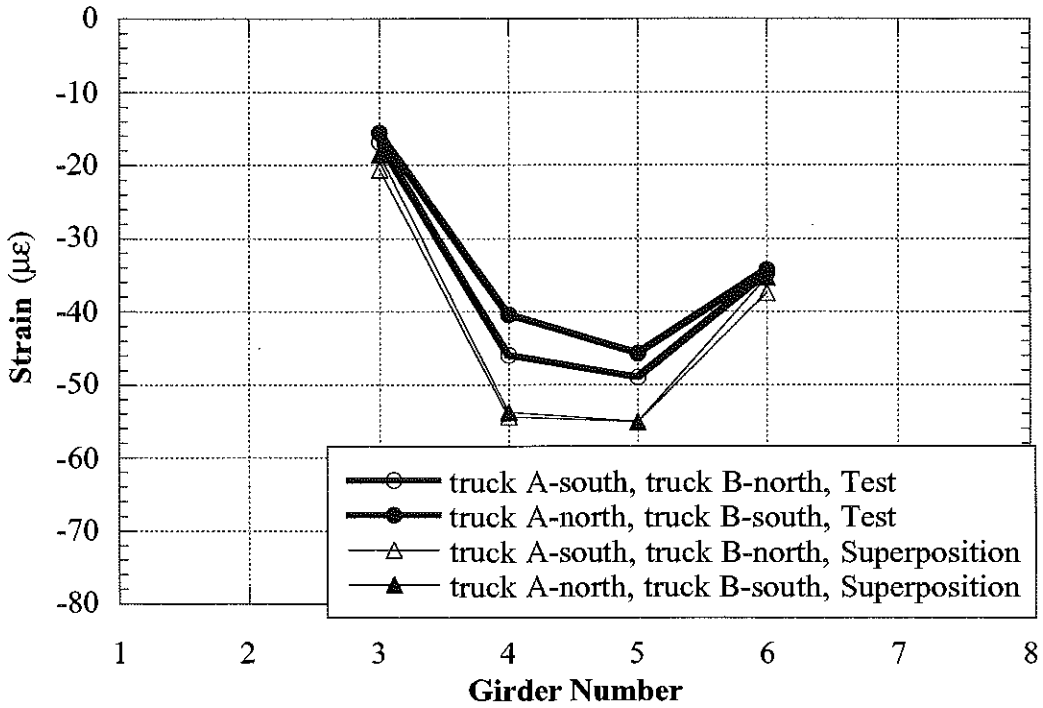

Figure 8.20. Strains at East End, Side-by-Side Loading, Crawling Speed, M50/MR (B01-58041).

Note:

Intentionally left blank

9. BRIDGE ON STANLEY ROAD OVER I-75, IN FLINT (S11-25032, ST/I75)

9.1 Description

This bridge was built in 1972 and it is located on Stanley Road over I-75 in Fint, Michigan. It is a three span, simply supported structure, designed as a composite section. The tested span is suspended by pin and hanger at each end. The total bridge length is 86.8 m. The total length of the tested span is 41.1 m with a cantilever overhang. The clear length of the tested span is 38.4 m without any skew. It has seven steel girders spaced at 2.21 m, as shown in Figure 9.1. The bridge has one lane in each direction and it carries an average daily traffic (ADT) of 2,000. The speed limit on this bridge is 89 km/h. The operating load rating is 1,023 kN, according to the Michigan Structure Inventory.

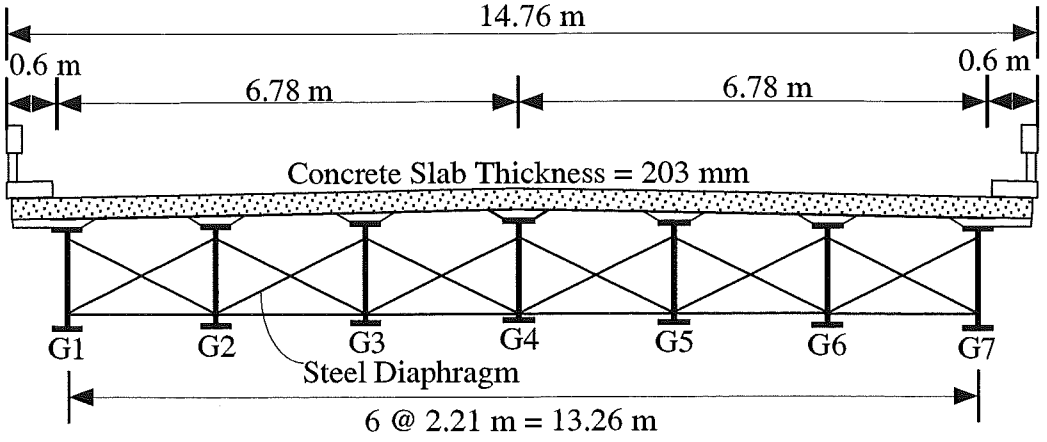

Figure 9.1. Cross-Section of the Bridge ST/I75 (S11-25032).

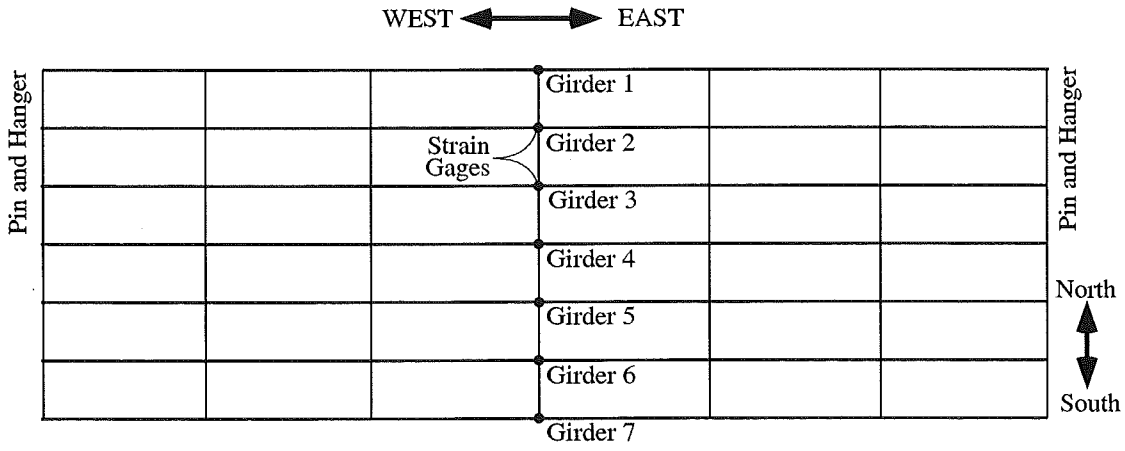

Figure 9.2. Strain Gage Locations in Bridge ST/I75 (S11-25032).

9.2 Instrumentation76

Strain transducers were installed on the bottom flanges of girders at midspan, as shown in Figure 9.2. The test equipment was installed on August 29, 2000. The bridge test was performed on August 30, 2000.

9.3 Load cases

The girder distribution factors (GDF) and dynamic load factors (DLF) were calculated using the strains measured at midspan. The bridge was loaded with two 11-axle trucks (three-unit vehicles).

The truck A and truck B have gross weights of 660 kN and 657 kN, with wheelbases of 15.67 m and 15.55 m, respectively. Truck configurations are shown in Figures 9.3 and 9.4.

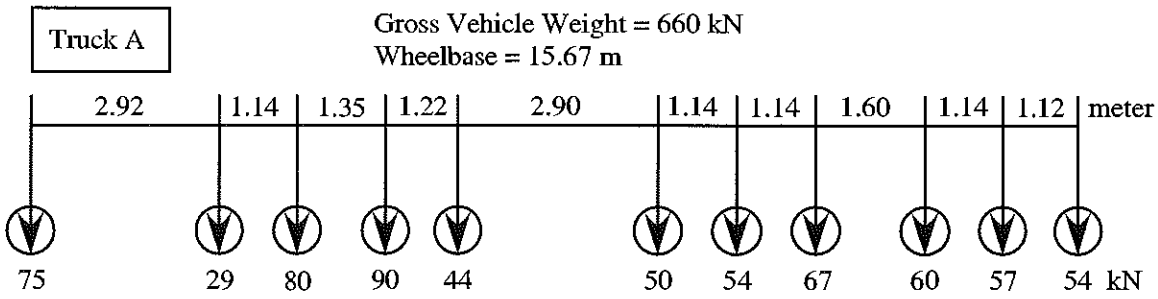

Figure 9.3. Truck A Configuration, Bridge ST/I75 (S11-25032).

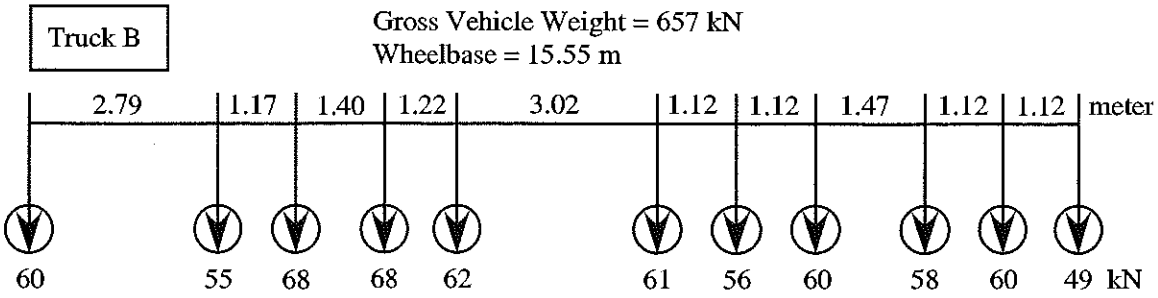

Figure 9.4. Truck B Configuration, Bridge ST/I75 (S11-25032).

A total of 16 load cases were considered, as shown in Table 9.1. First each truck was driven by itself at the center of one lane, at crawling speed. Then, the same truck was driven close to the curb. The runs in the center of the lane were repeated at a normal highway speed. The same was repeated for the other lane. Finally, two trucks were driven simultaneously, side-by-side, at crawling speed and normal highway speed. For side-by-side cases, the runs were repeated after the trucks

switched lanes, i.e. first truck A was in South lane, and B in North lane, then truck A was in North lane, and B in South lane.

Table 9.1. Sequence of Test Runs, Bridge Bridge ST/I75 (S11-25032).

Run#	Truck	Lane Side	Position in Lane	Truck Speed
1	Truck A	South	Center	Crawling
2	Truck A	South	Curb	Crawling
3	Truck B	South	Center	Crawling
4	Truck B	South	Curb	Crawling
5	Truck B	South	Center	32 km/h
6	Truck A	South	Center	26 km/h
7	Truck A	North	Center	Crawling
8	Truck A	North	Curb	Crawling
9	Truck B	North	Center	Crawling
10	Truck B	North	Curb	Crawling
11	Truck B	North	Center	32 km/h
12	Truck A	North	Center	26 km/h
13	Truck A and B	both	Center	Crawling
14	Truck B and A	both	Center	Crawling
15	Truck A and B	both	Center	26 km/h
16	Truck B and A	both	Center	25 km/h

9.4. Analysis results

A three-dimensional finite element method (FEM) was applied to investigate the structural behavior of the bridge ST/I75 (S11-25032). The concrete slab was modeled with isotropic, eight node solid elements, with three degrees of freedoms at each node. The girder flanges and web were modeled using three-dimensional, quadrilateral, four node shell elements with six degrees of freedom at each node. The structural effects of the secondary members, such as the sidewalk and parapet, were also taken into account in the finite element analysis models.

Three cases of the boundary conditions are considered, as described earlier in this Report. The partially frozen supports were modeled using spring elements as shown in Figure 9.6.

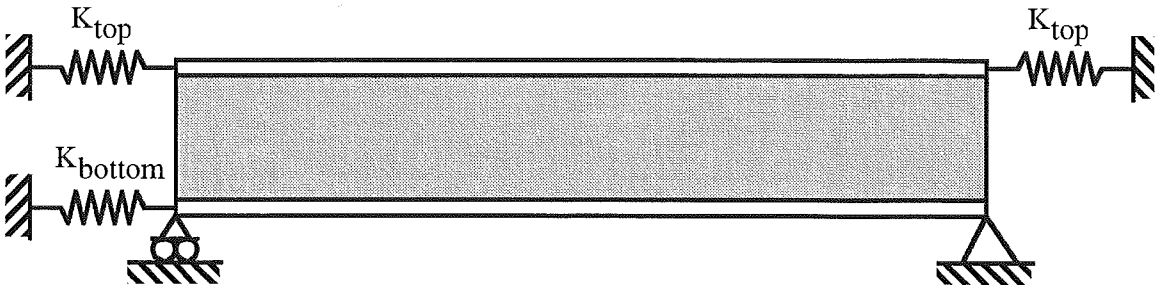

Figure 9.6. Modeing of Support Partial Fixity in Finite Element Analysis.

The mesh of the FEM model is shown in Figure 9.7. Figure 9.8 presents a deformed shape of the bridge loaded with two trucks side-by-side. Figure 9.9 illustrates the distribution of the loads simulating two truck side-by-side.

Strains calculated for the three considered models are shown in Figure 9.10 for two trucks side-by-side (Run 13). Also shown are the experimental results. The FEM results show that the maximum strain at the most heavily loaded girder is about 185 $\mu\varepsilon$ for the model with simple

support, while the maximum strain recorded from the test is about 150 με. When the spring elements are used with the K constants adjusted according to the test results (K_{top} = 60,000 kN/m and K_{bottom}=120,000 kN/m), then the FEM results become very close to the test results. This confirms the presence of some degree of fixity of supports.

Figure 9.11 presents the deflection obtained from the three different FEM models. It shows that the maximum deflection under two truck loading is about 29 mm, for the FEM model with the partial support fixity.

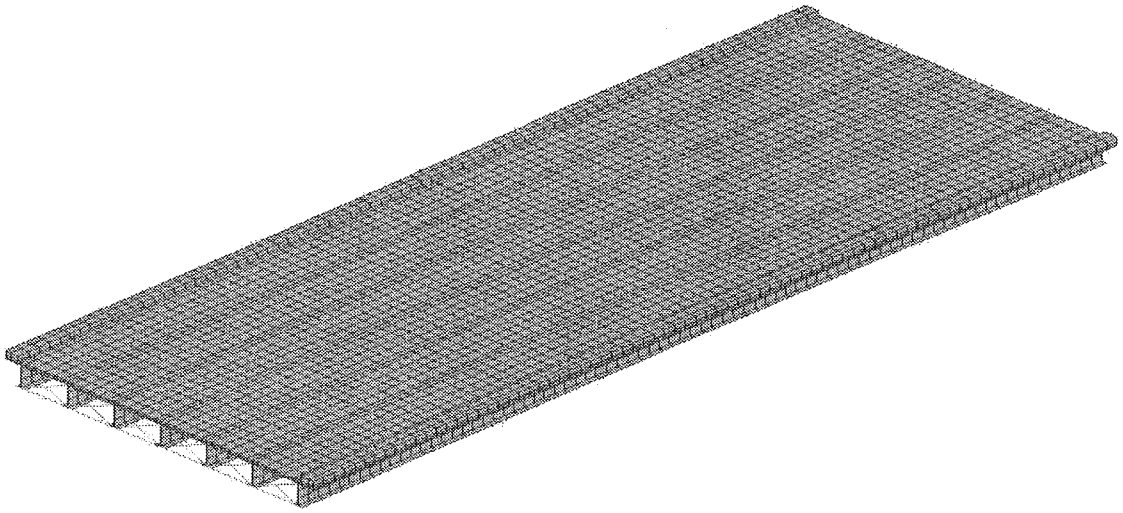

Figure 9.7. The Mesh of the Finite Element Model.
ST/I75 (S11-25032).

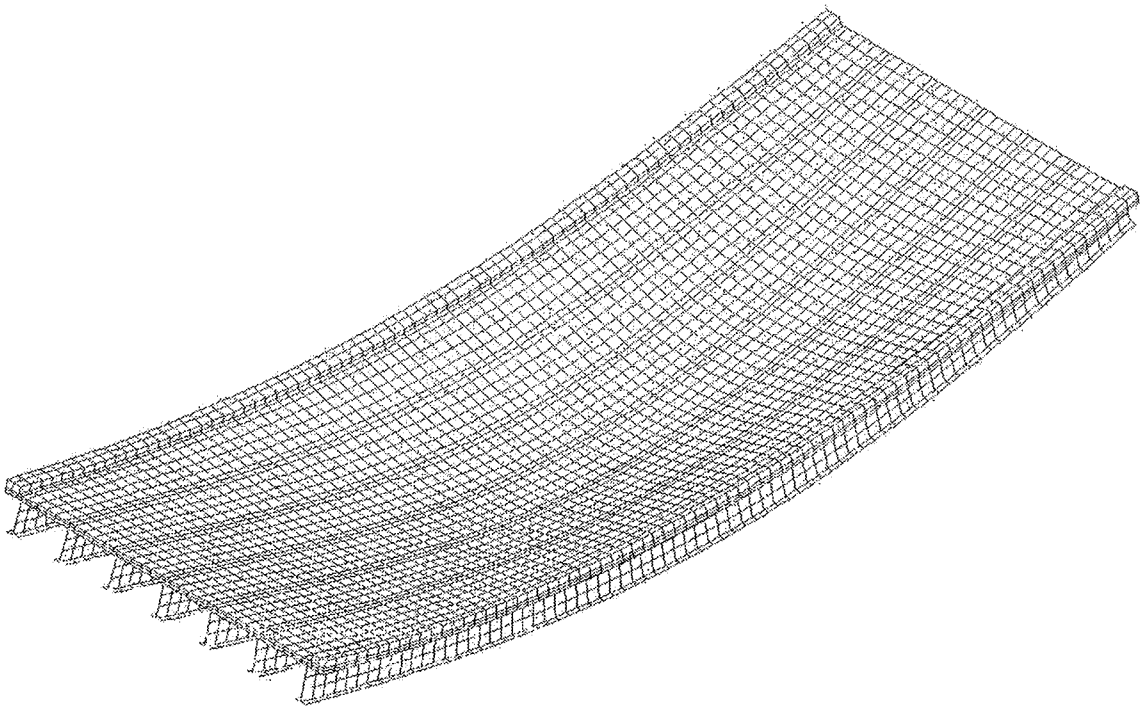

Figure 9.8. The Deformed Shape of the Bridge under Two Lane Loading. ST/I75 (S11-25032).

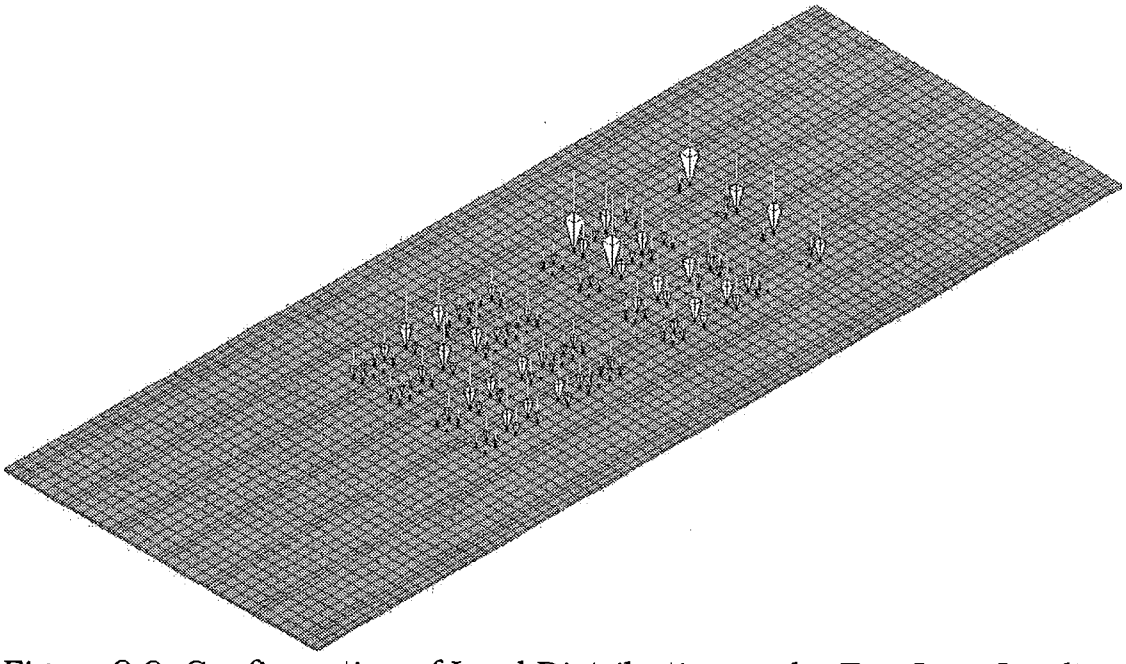

Figure 9.9. Configuration of Load Distribution under Two Lane Loading ST/I75 (S11-25032).

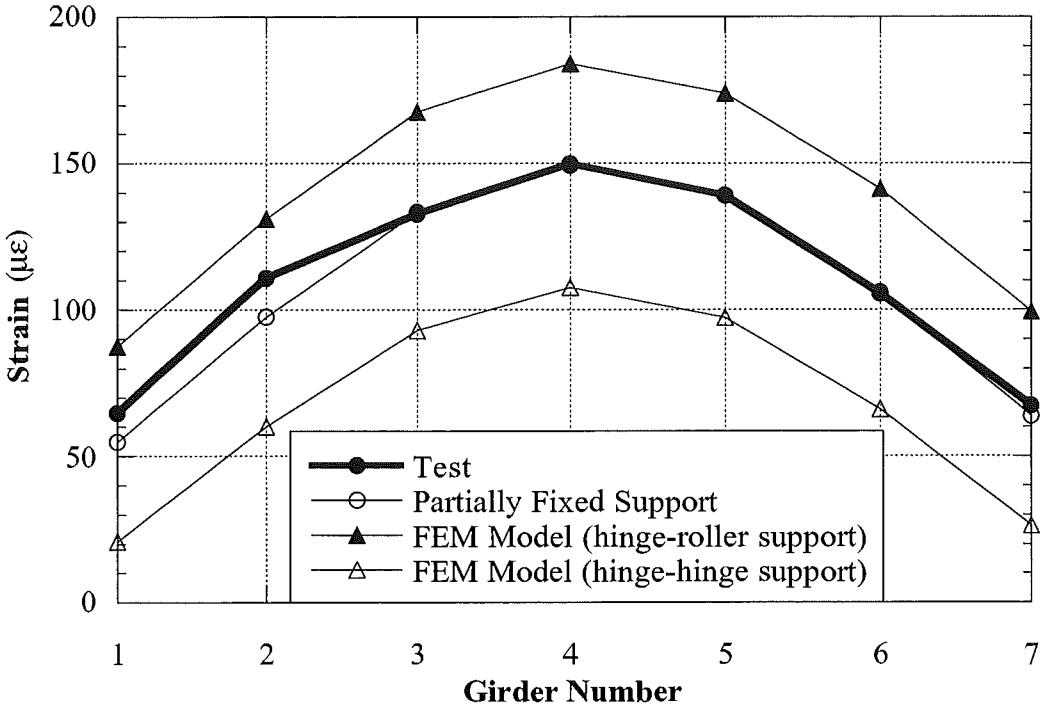

Figure 9.10. Strain from the FEM Analysis Compared with the Test Results for Two Lane Loading, ST/I75 (S11-25032).

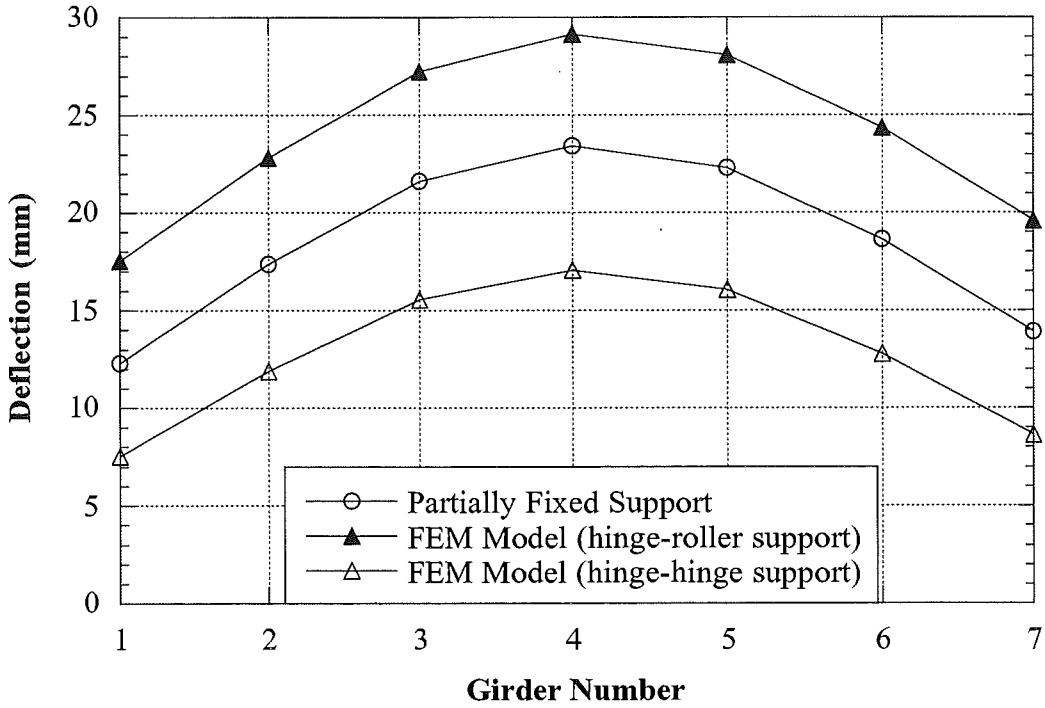

Figure 9.11. Deflection from the FEM Analysis for Two Lane Loading ST/I75 (S11-25032).

9.5 Test results

The resulting strains and GDF's are shown in Figures 9.12 through 9.16. Figures 9.12 to 9.14 present the results of all crawling-speed (static) tests. Figures 9.12 to 9.13 present static strains and GDF's for one truck on the bridge. The maximum strain due to a single truck is about 140 με. This corresponds to about 28 MPa.

Figure 9.14 shows static strains and GDF's from side-by-side static load tests. For two vehicles side-by-side the maximum strain is close to 160 με (which corresponds to 32 MPa). The superposition of strains due to a single truck in South and North lanes produces almost the same results as strain due to two trucks side-by-side.

For two trucks side-by-side, the girder distribution factor for girder i is determined using Eq. (3-1). For comparison, GDF are also calculated according to AASHTO Standard (1996) and AASHTO LRFD Code (1998). Two cases were considered, a single lane loaded, and two lanes loaded. The resulting GDF's are shown in Figures 9.12 through 9.16.

The results indicate that code-specified GDF's are conservative. Even single lane GDF's specified in both AAHSTO Standard (1996) and AASHTO LRFD (1998) are also sufficient for two lane load cases for this bridge.

Figures 9.15 and 9.16 shows the resulting strain and distribution factors from normal speed tests. There is practically no difference between the crawling speed and normal speed results.

Dynamic load factor is defined in section 3.3. In Figure 9.17, DLF's are plotted for all load cases involving normal speed (no dynamic load was measured for crawling speed runs). Dynamic load factors for exterior girders are high because the static strains in these girders are

very low. In other words, large values of DLF in exterior girders correspond to load cases with a single truck in the opposite lane (resulting in very low static strain).

The relationship between DLF and static and dynamic strains is shown in Figure 9.18. The open circles correspond to static strain, ε_{stat}, and black solid squares correspond to dynamic strain, ε_{dyn}. For each static strain value (open circle), the corresponding dynamic strain is denoted by solid square (the numbers of circles and squares are same). Dynamic strains remain nearly constant, while static strains increase as truck loading increases. This results in large dynamic load factors for low static strains. It is clear from the Figure 9.18 that dynamic strains does not exceed 10 με for all the cases while the static strain can exceed 150 με in normal speed test. DLF corresponding to the maximum strain caused by two trucks side-by-side, is less than 0.05 at girder No. 4, the most heavily loaded girder.

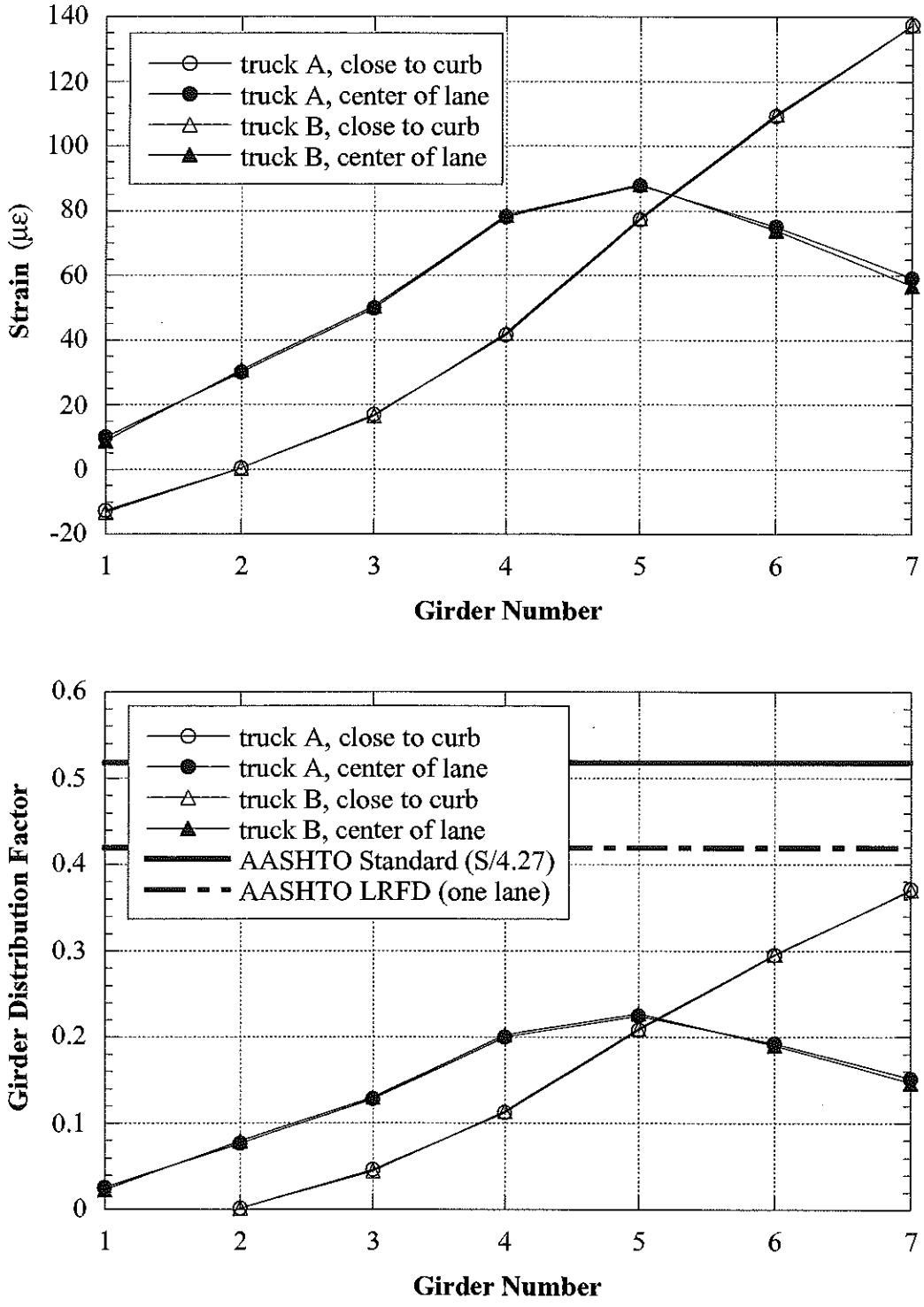

Figure 9.12. South Lane, Crawling Speed, ST/I75 (S11-25032).

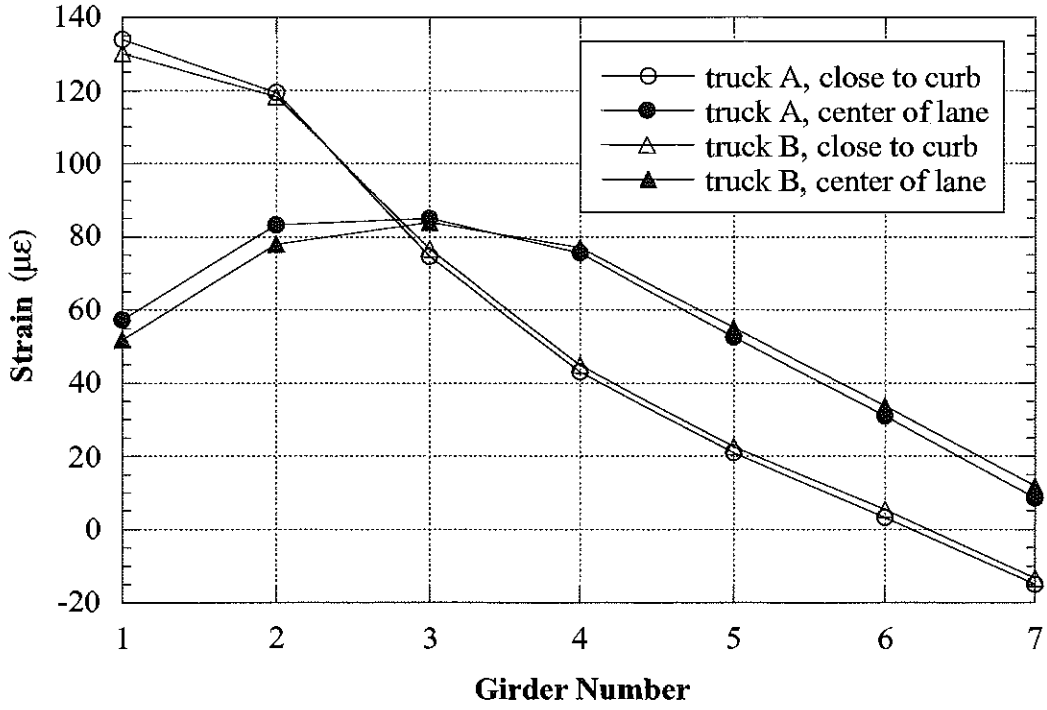

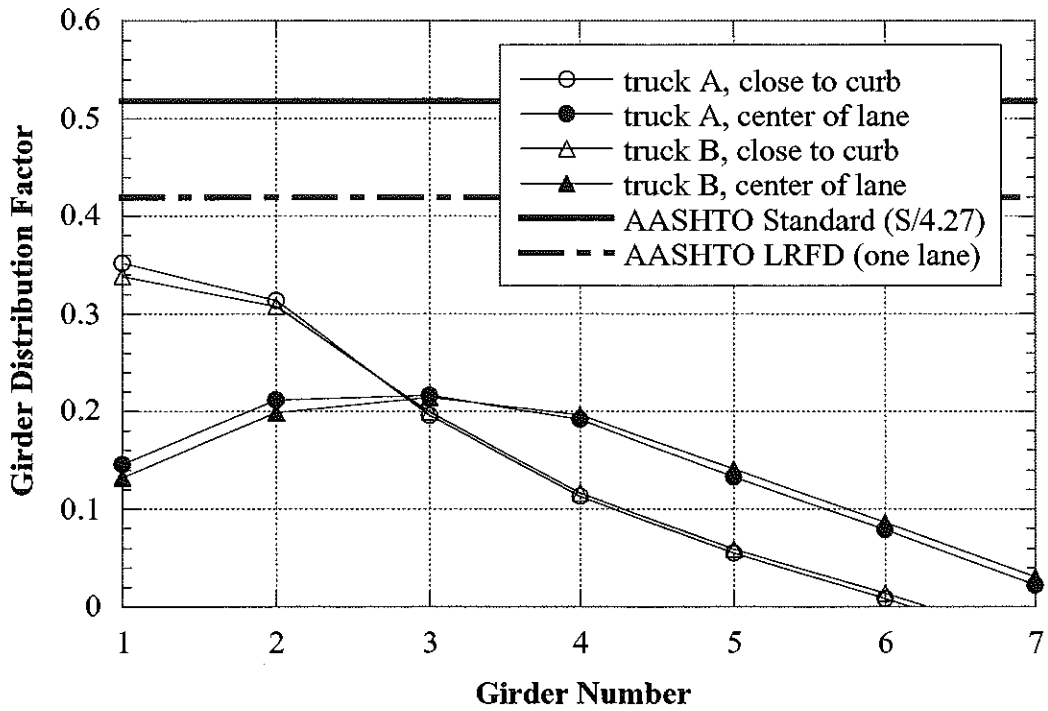

Figure 9.13. North Lane, Crawling Speed, ST/I75 (S11-25032).

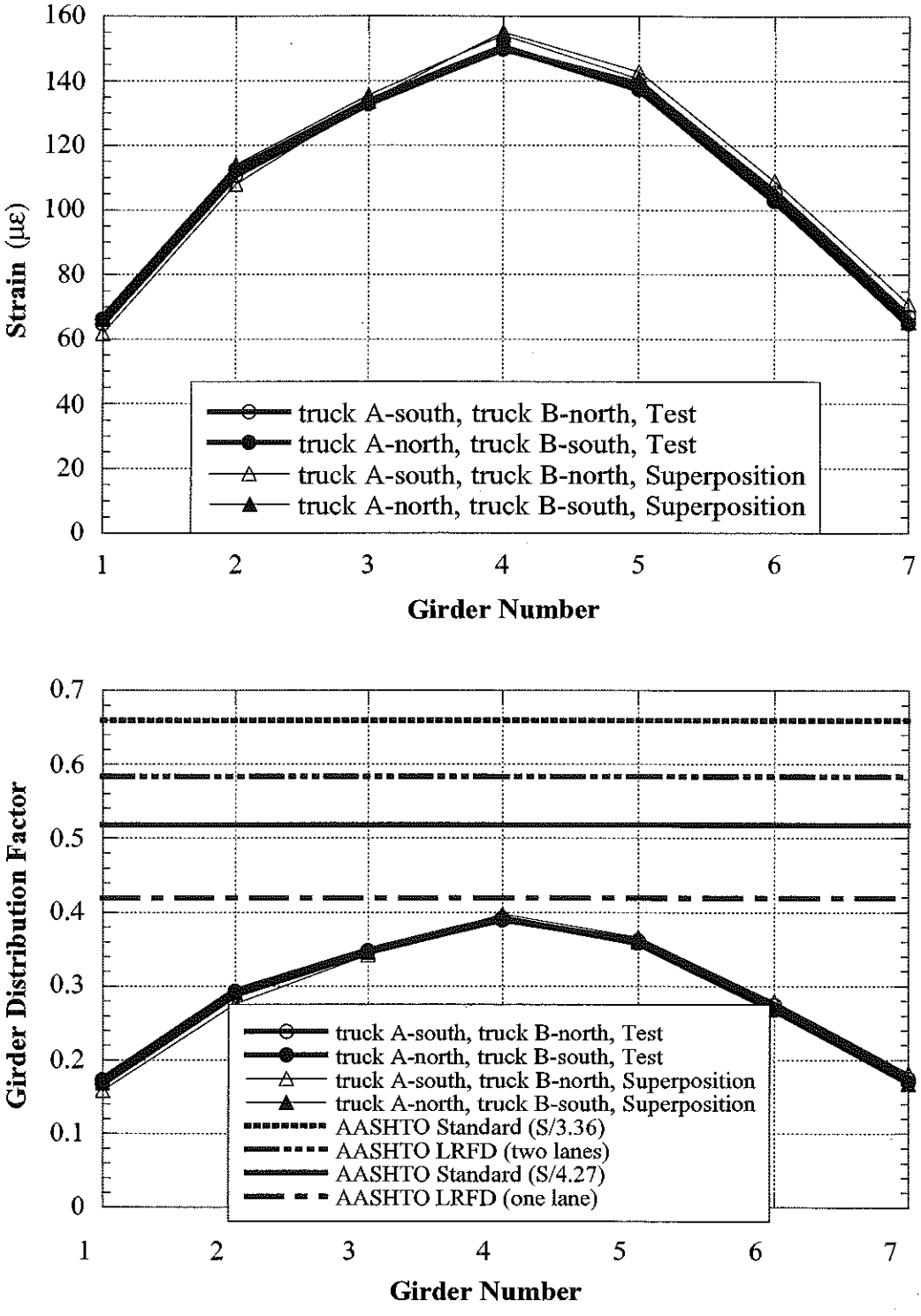

Figure 9.14. Side-by-Side Loading, Center of Lane, Crawling Speed, ST/I75 (S11-25032).

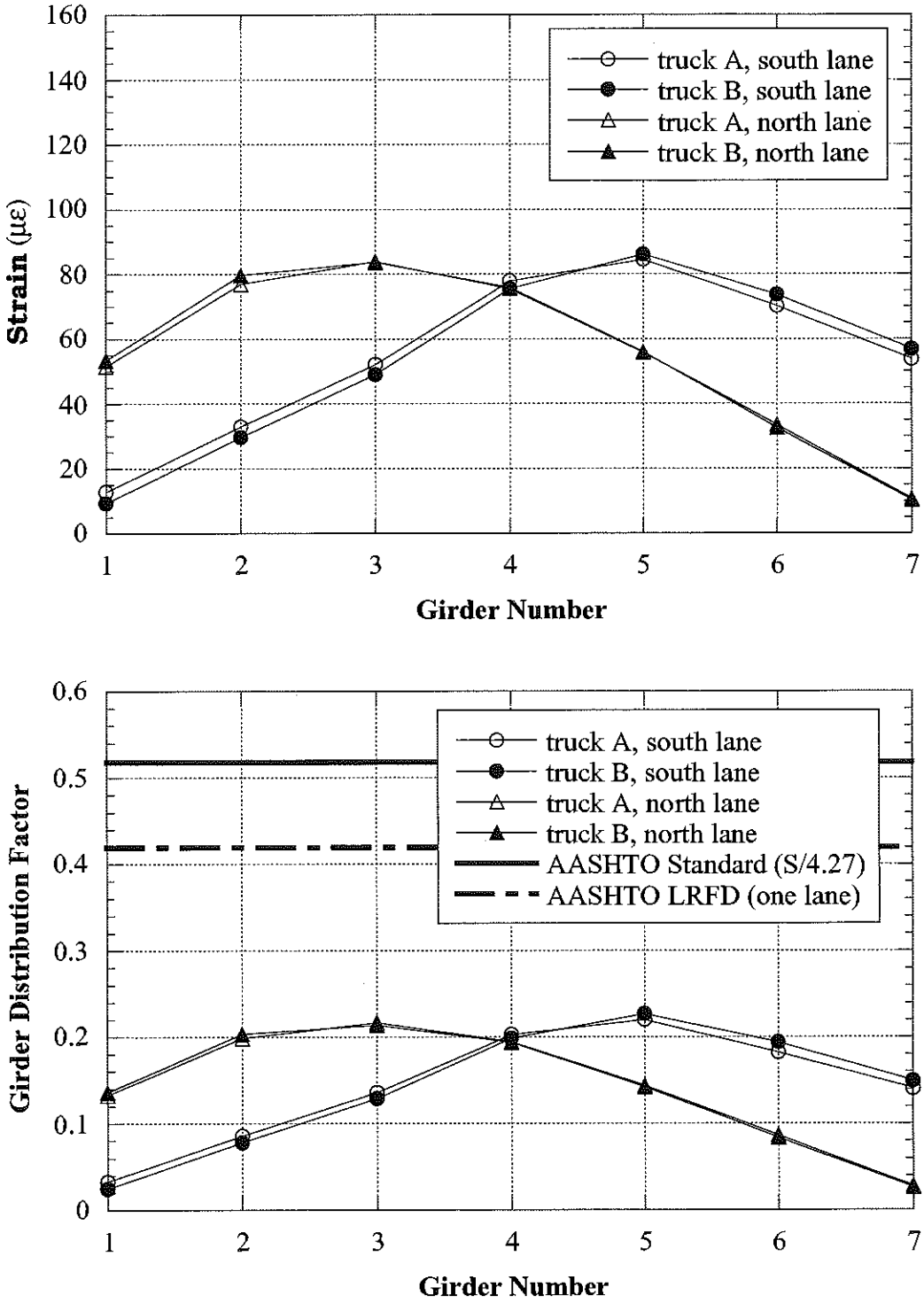

Figure 9.15. Strain and GDF under One Truck Loading at Regular Speed, ST/I75 (S11-25032).

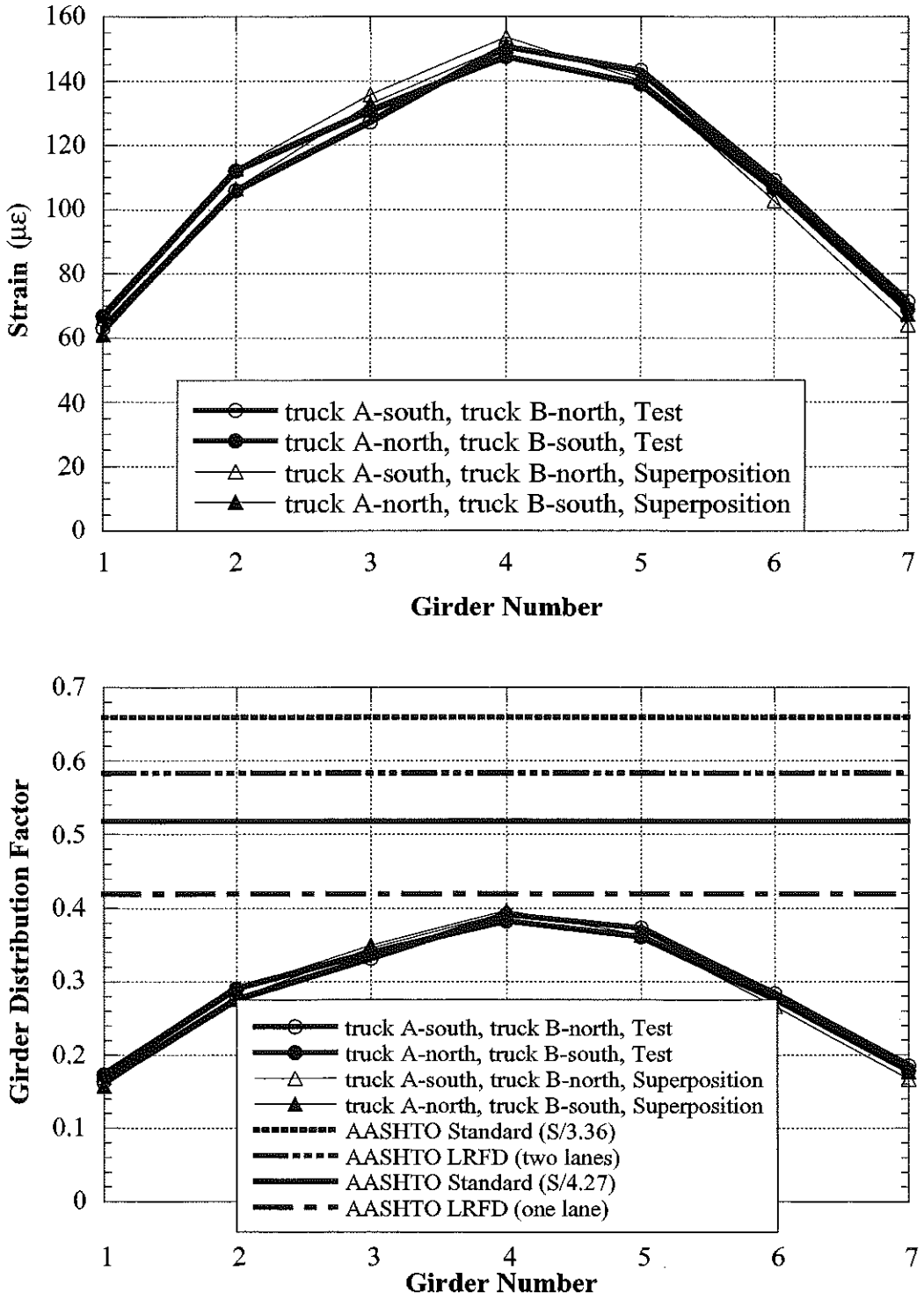

Figure 9.16. Strain and GDF under Side-by-Side Loading at Regular Speed, ST/I75 (S11-25032).

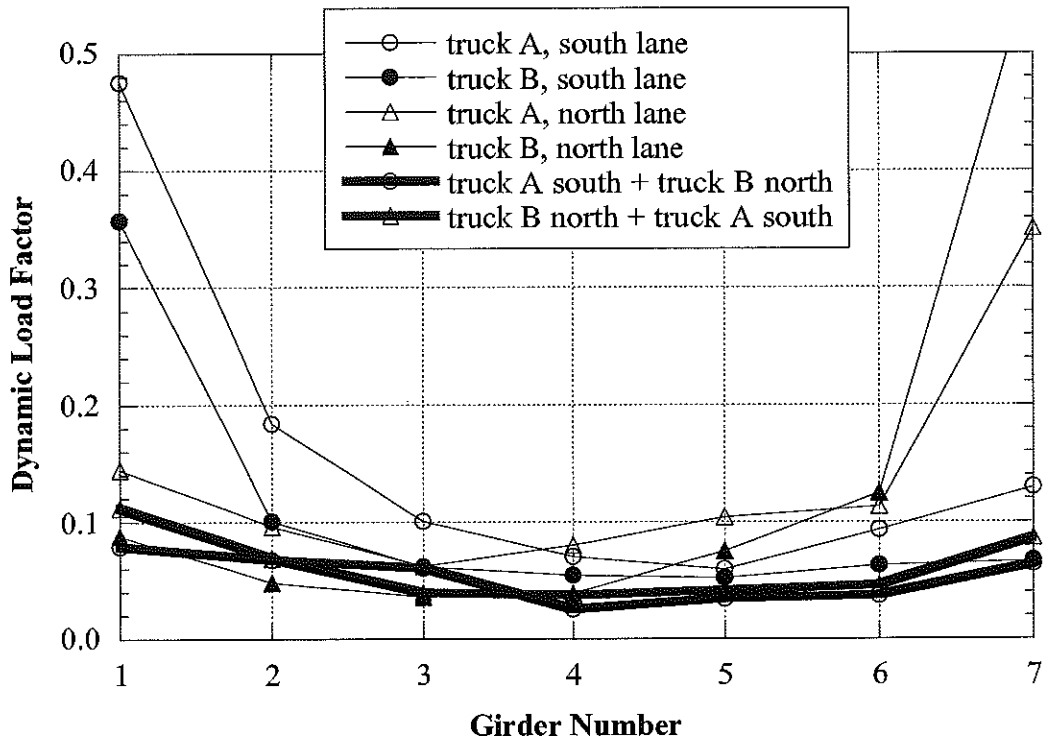

Figure 9.17. Dynamic Load Factors, ST/I75 (S11-25032).

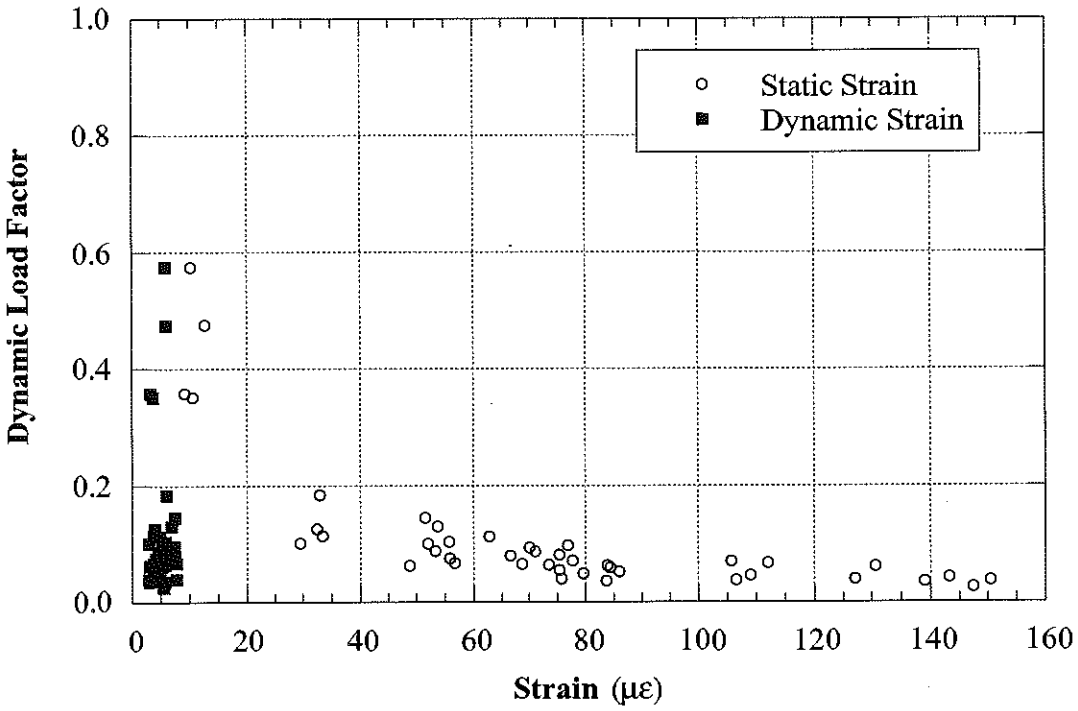

Figure 9.18. Strain vs. Dynamic Load Factors, ST/I75 (S11-25032).

10. BRIDGE ON M-43 OVER SEBEWA CREEK, EATON COUNTY (B02-23041, M43/SC)

10.1 Description

This bridge was built in 1949 and it is located on M-43 over Sebewa Creek in Eaton County, Michigan. It is a single span, simply supported structure, designed as a non-composite section. The total span length is 10.6 m, without any skew. It has nine steel girders spaced at 1.57 m, as shown in Figure 10.1. The bridge has one lane in each direction and it carries an average daily traffic (ADT) of 4,000. The speed limit on this bridge is 89 km/h. The operating load rating is 1,343 kN, according to the Michigan Structure Inventory.

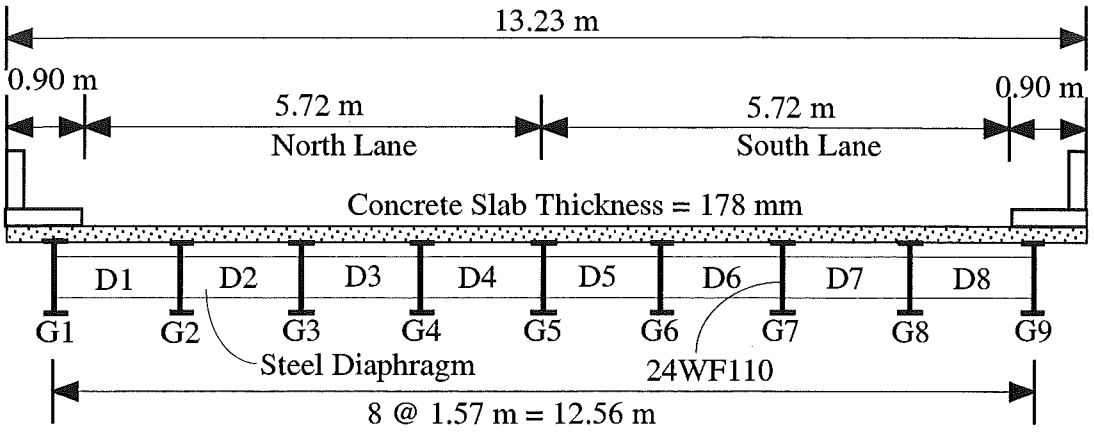

Figure 10.1. Cross-Section of the Bridge M43/SC (B02-23041).

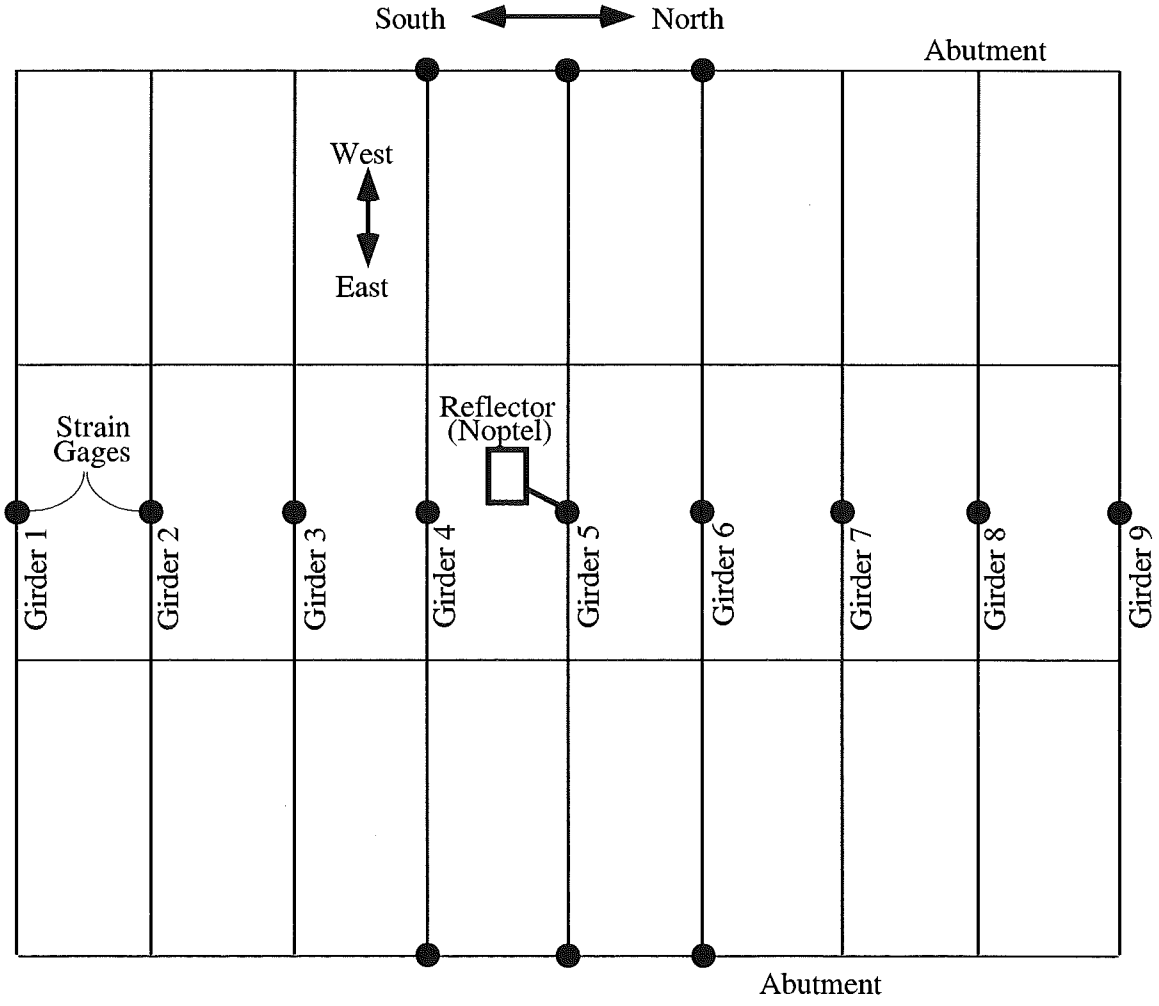

Figure 10.2. Strain Gage Locations in Bridge Bridge M43/SC (B02-23041).

10.2 Instrumentation

Strain transducers were installed on the bottom flanges of girders at midspan and at selected support locations, as shown in Figure 10.2. The test equipment was installed on September 13, 2000. The bridge test was performed on September 14, 2000.

10.3 Load cases

The girder distribution factors (GDF) and dynamic load factors (DLF) were calculated using the strains measured at midspan. The bridge was loaded with two 11-axle trucks (three-unit vehicles).

The truck A and truck B have gross weights of 657 kN and 629 kN, with wheelbases of 15.37 m and 15.48 m, respectively. Truck configurations are shown in Figures 10.3 and 10.4.

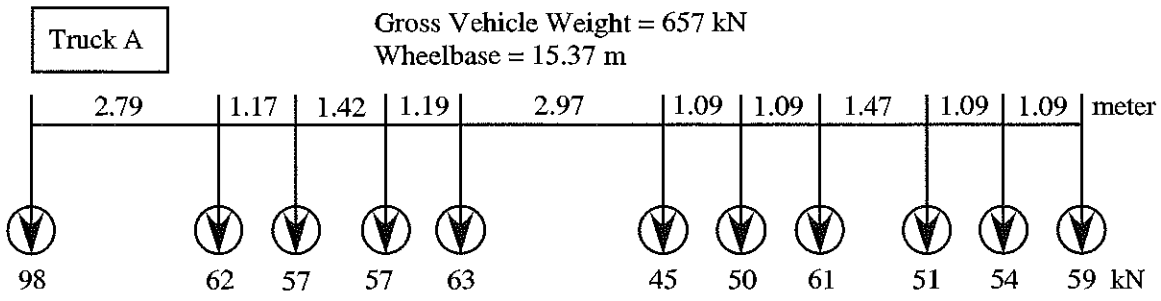

Figure 10.3. Truck A Configuration, Bridge M43/SC (B02-23041).

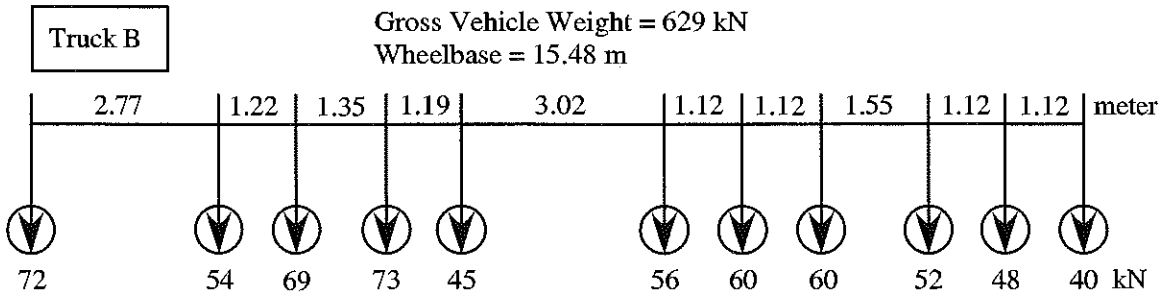

Figure 10.4. Truck B Configuration, Bridge M43/SC (B02-23041).

A total of 16 load cases were considered, as shown in Table 10.1. First each truck was driven by itself at the center of one lane, at crawling speed. Then, the same truck was driven close to the curb. The runs in the center of the lane were repeated at a normal highway speed. The same was repeated for the other lane. Finally, two trucks were driven simultaneously, side-by-side, at crawling speed and normal highway speed. For side-by-side cases, the runs were repeated after the trucks switched lanes, i.e. first truck A was in North lane, and B in South lane, then truck A was in South lane, and B in North lane.

Table 10.1. Sequence of Test Runs, Bridge M43/SC (B02-23041).

Run#	Truck	Lane Side	Position in Lane	Truck Speed
1	Truck A	North	Center	Crawling
2	Truck A	North	Curb	Crawling
3	Truck B	North	Center	Crawling
4	Truck B	North	Curb	Crawling
5	Truck B	North	Center	49 km/h
6	Truck A	North	Center	47 km/h
7	Truck A	South	Center	Crawling
8	Truck A	South	Curb	Crawling
9	Truck B	South	Center	Crawling
10	Truck B	South	Curb	Crawling
11	Truck B	South	Center	49 km/h
12	Truck A	South	Center	50 km/h
13	Truck A and B	both	Center	Crawling
14	Truck B and A	both	Center	Crawling
15	Truck A and B	both	Center	49 km/h
16	Truck B and A	both	Center	49 km/h

10.4. Analysis results

A three-dimensional finite element method (FEM) was applied to investigate the structural behavior of the bridge M43/SC (B02-23041). The concrete slab was modeled with isotropic, eight node solid elements, with three degrees of freedoms at each node. The girder flanges and web were modeled using three-dimensional, quadrilateral, four node shell elements with six degrees of freedom at each node. The structural effects of the secondary members, such as the sidewalk and parapet, were also taken into account in the finite element analysis models.

Three cases of the boundary conditions are considered, as described earlier in this Report. The partially frozen supports were modeled using spring elements as shown in Figure 10.6.

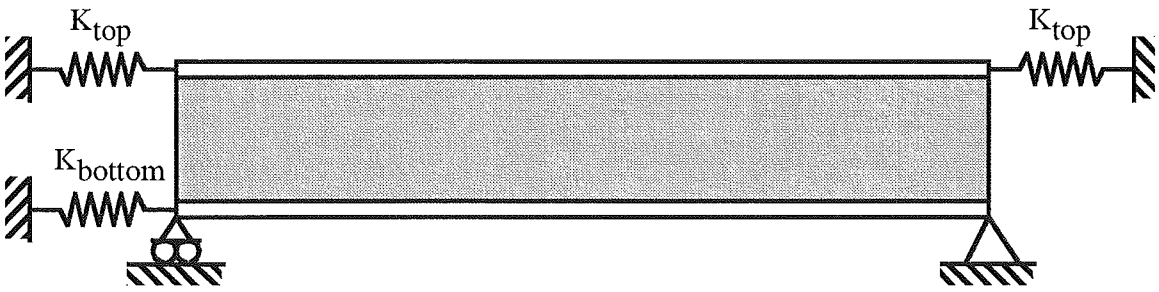

Figure 10.6. Modeing of Support Partial Fixity in Finite Element Analysis.

The mesh of the FEM model is shown in Figure 10.7. Figure 10.8 presents a deformed shape of the bridge loaded with two trucks side-by-side. Figure 10.9 illustrates the distribution of the loads simulating two truck side-by-side.

Strains calculated for the three considered models are shown in Figure 10.10 for two trucks side-by-side (Run 13). Also shown are the experimental results. The FEM results show that the maximum strain at the most heavily loaded girder is about 115 με for the model with simple support, while the maximum strain recorded from the test is about 95 με. When the spring elements are used with the K constants adjusted

according to the test results (K_{top} = 60,000 kN/m and K_{bottom}=120,000 kN/m), then the FEM results become very close to the test results. This confirms the presence of some degree of fixity of supports.

Figure 10.11 presents the deflection obtained from the three different FEM models. It shows that the maximum deflection under two truck loading is about 2.2 mm, for the FEM model with the partial support fixity.

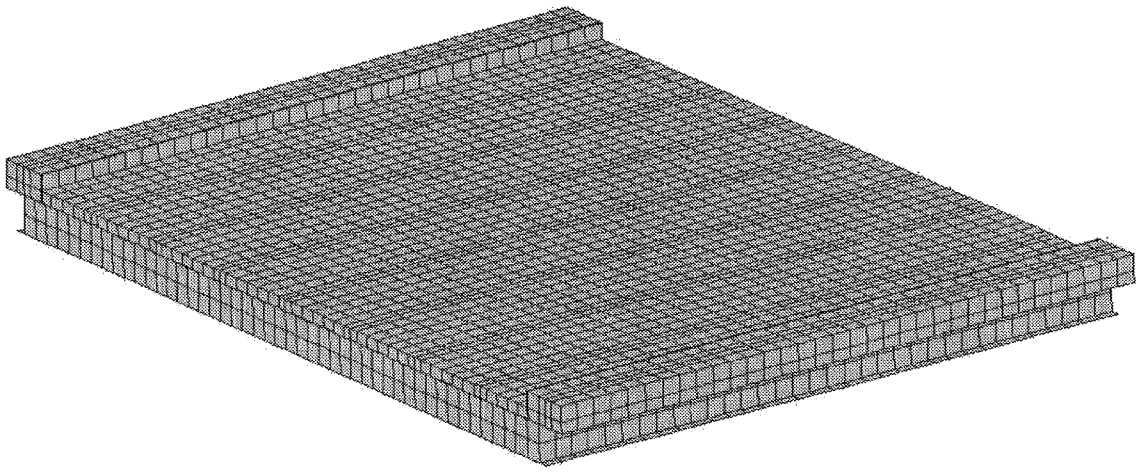

Figure 10.7. The Mesh of the Finite Element Model.
M43/SC (B02-23041).

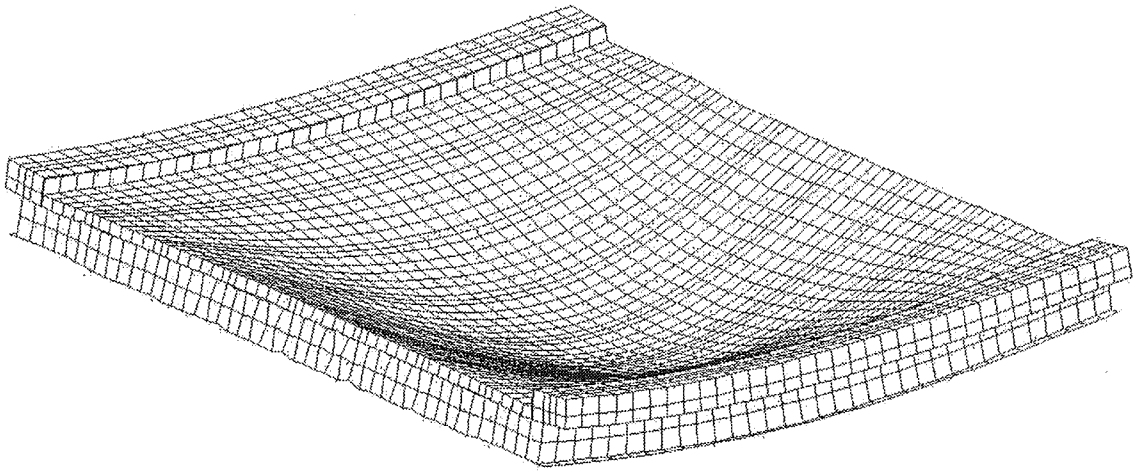

Figure 10.8. The Deformed Shape of the Bridge under Two Lane Loading. M43/SC (B02-23041).

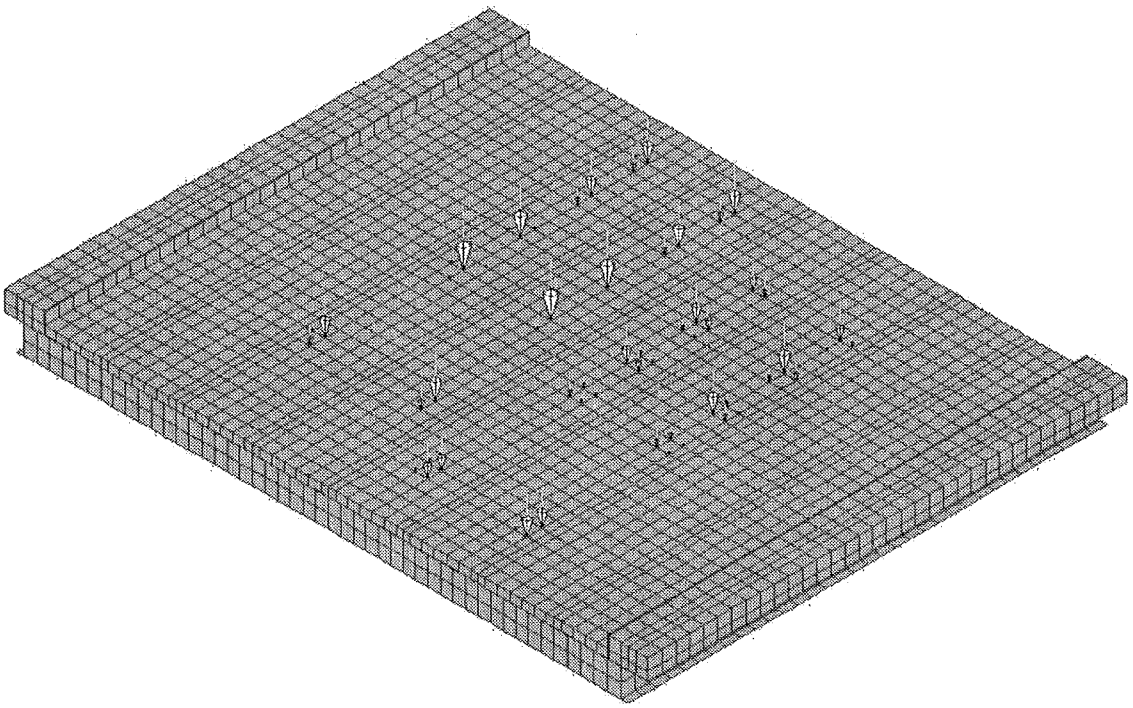

Figure 10.9. Configuration of Load Distribution under Two Lane Loading M43/SC (B02-23041).

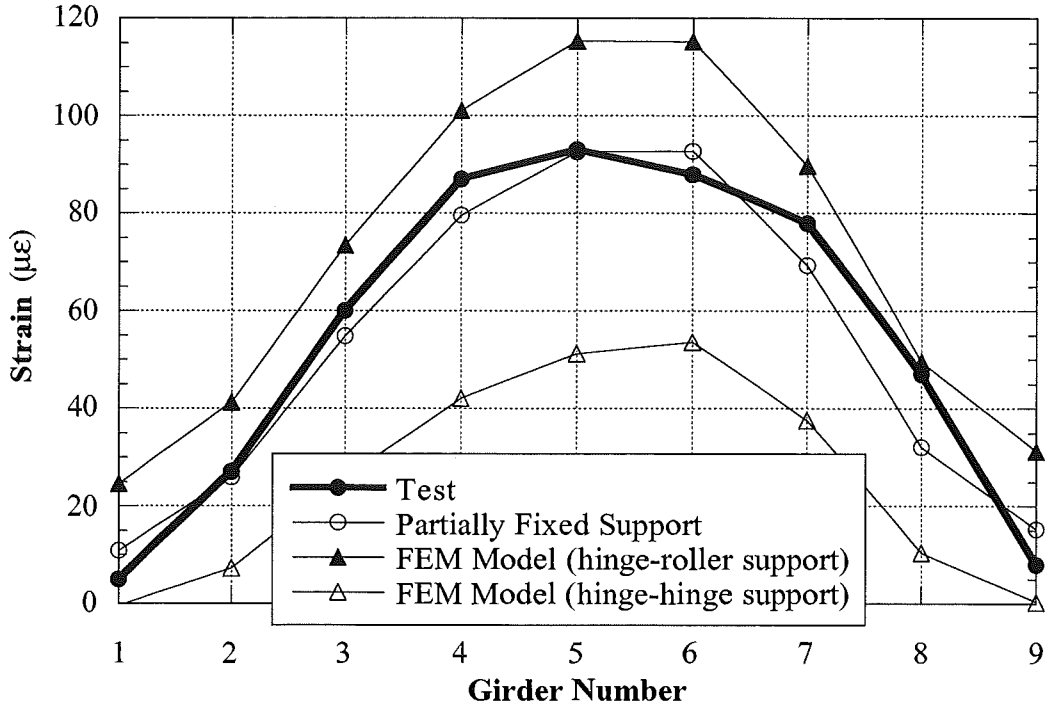

Figure 10.10. Strain from the FEM Analysis Compared with the Test Results for Two Lane Loading, M43/SC (B02-23041).

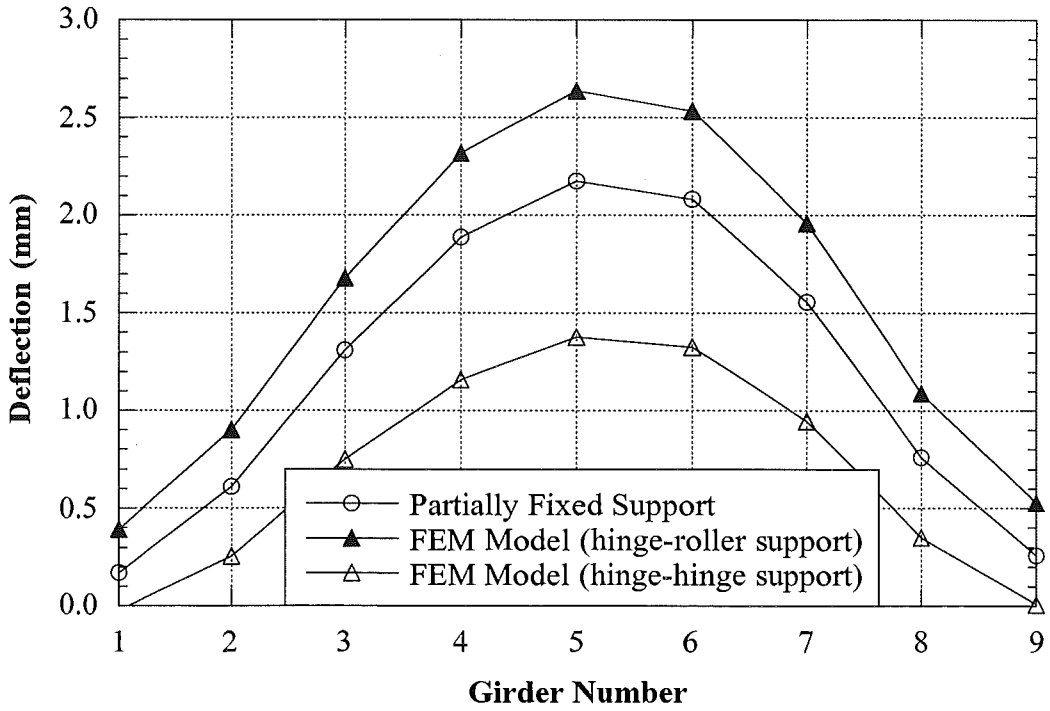

Figure 10.11. Deflection from the FEM Analysis for Two Lane Loading M43/SC (B02-23041).

10.5 Test results

The resulting strains and GDF's are shown in Figures 10.12 through 10.16. Figures 10.12 to 10.14 present the results of all crawling-speed (static) tests. Figures 10.12 to 10.13 present static strains and GDF's for one truck on the bridge. The maximum strain due to a single truck is less than 80 με. This corresponds to about 16 MPa.

Figure 10.14 shows static strains and GDF's from side-by-side static load tests. For two vehicles side-by-side the maximum strain is about 100 με (which corresponds to 20 MPa). The superposition of strains due to a single truck in North and South lanes produces almost the same results as strain due to two trucks side-by-side.

For two trucks side-by-side, the girder distribution factor for girder i is determined using Eq. (3-1). For comparison, GDF are also calculated according to AASHTO Standard (1996) and AASHTO LRFD Code (1998). Two cases were considered, a single lane loaded, and two lanes loaded. The resulting GDF's are shown in Figures 10.12 through 10.16.

The results indicate that code-specified GDF's are conservative. A single lane GDF specified in AASHTO LRFD (1998) is also sufficient for two lane load cases for this bridge. However, a single lane GDF specified in AASHTO Standard (1996) is not enough for two lane load cases for this bridge. However, the absolute values of the strains are less than 100 με for the heaviest load case (two fully-loaded trucks side-by-side). Therefore, the total load effect per girder estimated using GDF specified for single lane in AASHTO Standard (1996) is also conservative (less than design value).

Figures 10.15 and 10.16 shows the resulting strain and distribution factors from normal speed tests. There is practically no difference between the crawling speed and normal speed results.

Dynamic load factor is defined in section 3.3. In Figure 10.17, DLF's are plotted for all load cases involving normal speed (no dynamic load was measured for crawling speed runs). Dynamic load factors for exterior girders are high because the static strains in these girders are very low. In other words, large values of DLF in exterior girders correspond to load cases with a single truck in the opposite lane (resulting in very low static strain).

The relationship between DLF and static and dynamic strains is shown in Figure 10.18. The open circles correspond to static strain, ε_{stat}, and black solid squares correspond to dynamic strain, ε_{dyn}. For each static strain value (open circle), the corresponding dynamic strain is denoted by solid square (the numbers of circles and squares are same). Dynamic strains remain nearly constant, while static strains increase as truck loading increases. This results in large dynamic load factors for low static strains. It is clear from the Figure 10.18 that dynamic strains does not exceed 10 $\mu\varepsilon$ for all the cases while the static strain can be close to 100 $\mu\varepsilon$ in normal speed test. DLF corresponding to the maximum strain caused by two trucks side-by-side, is less than 0.05 at girder No. 5, the most heavily loaded girder.

The strains were also measured close to the support. The results are shown in Figures 10.19 and 10.20. Negative strain values indicate the strains recorded at the bottom flanges near supports were in compression, due to the partial fixity of support. The strain values near the support were measured when the loads caused the maximum strain at the midspan. As shown in the Figures, the levels of support fixity are highly unpredictable. Even in a same bridge, each girder has different support behavior.

Girder No. 5 was instrumented with a remote deflection measurement device manufactured by Noptel. The reflector was installed

at midspan. However, there was a communication error between the equipment and the notebook computer during the test. Consequently, the test results were not saved correctly, and cannot be used.

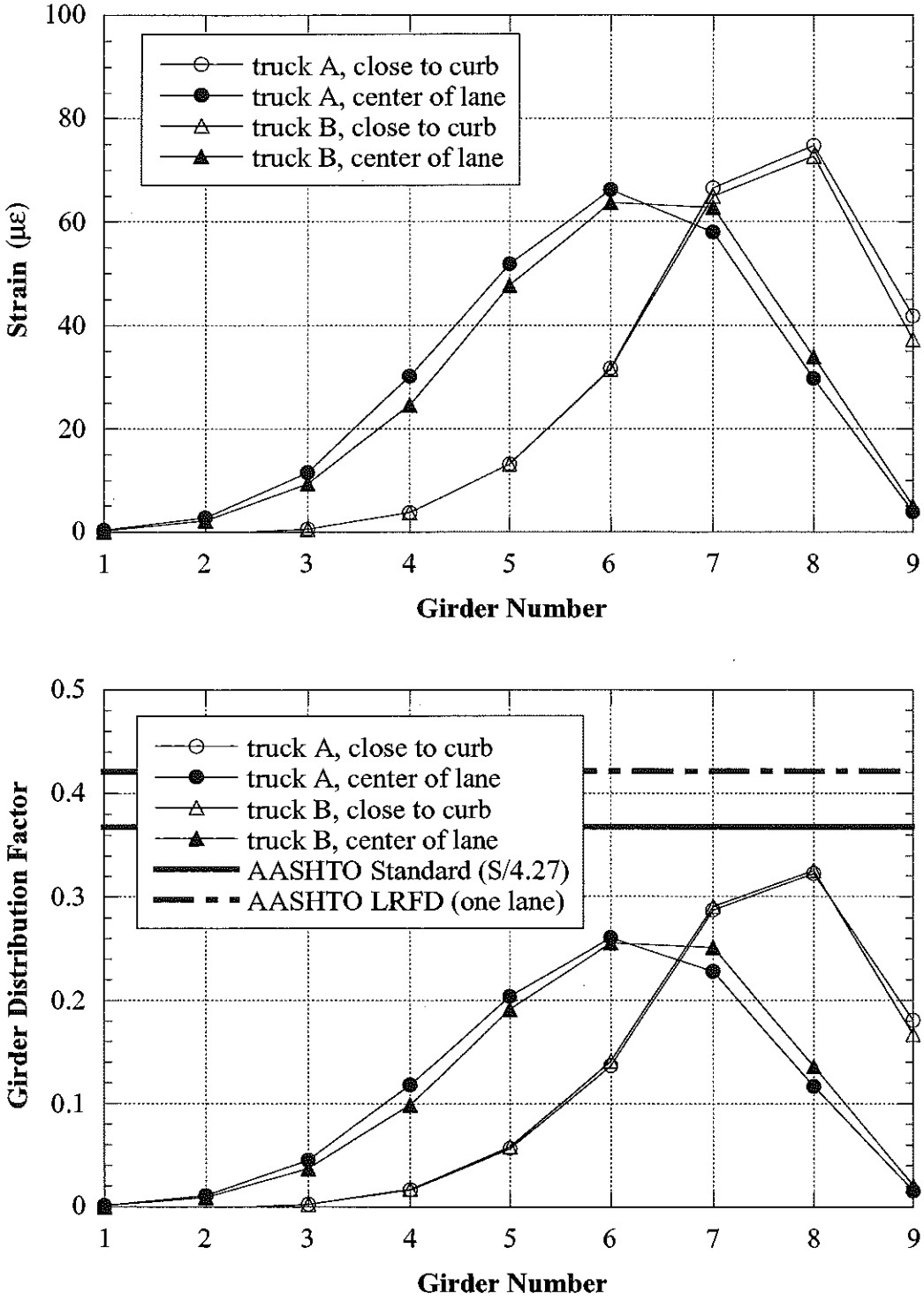

Figure 10.12. North Lane, Crawling Speed, M43/SD (B02-23041).

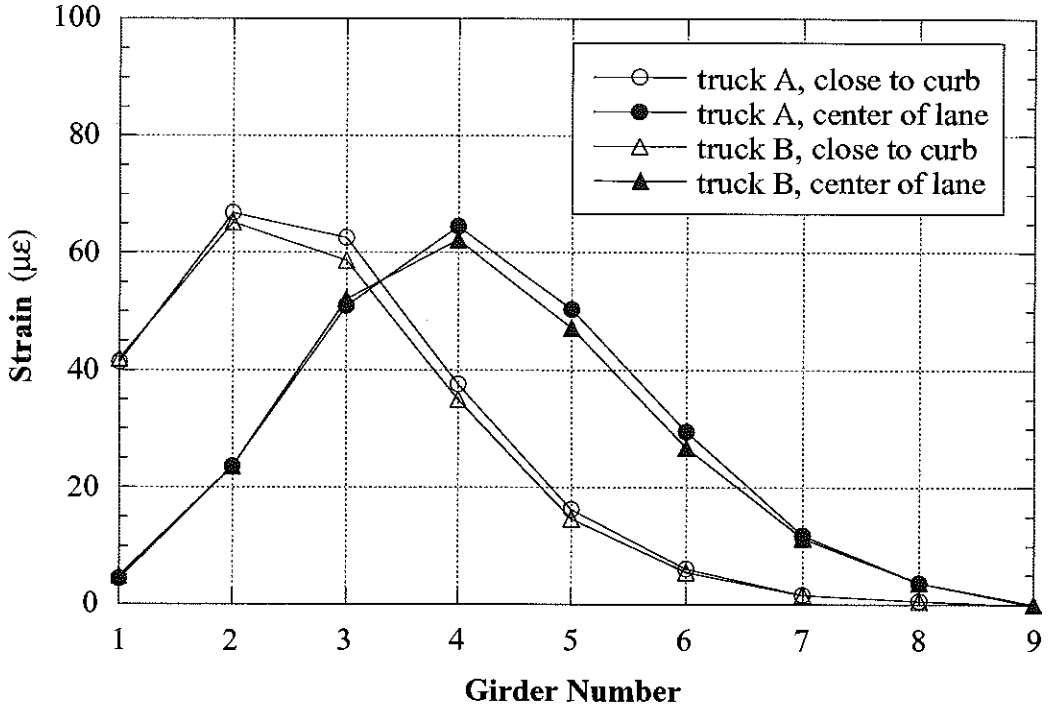

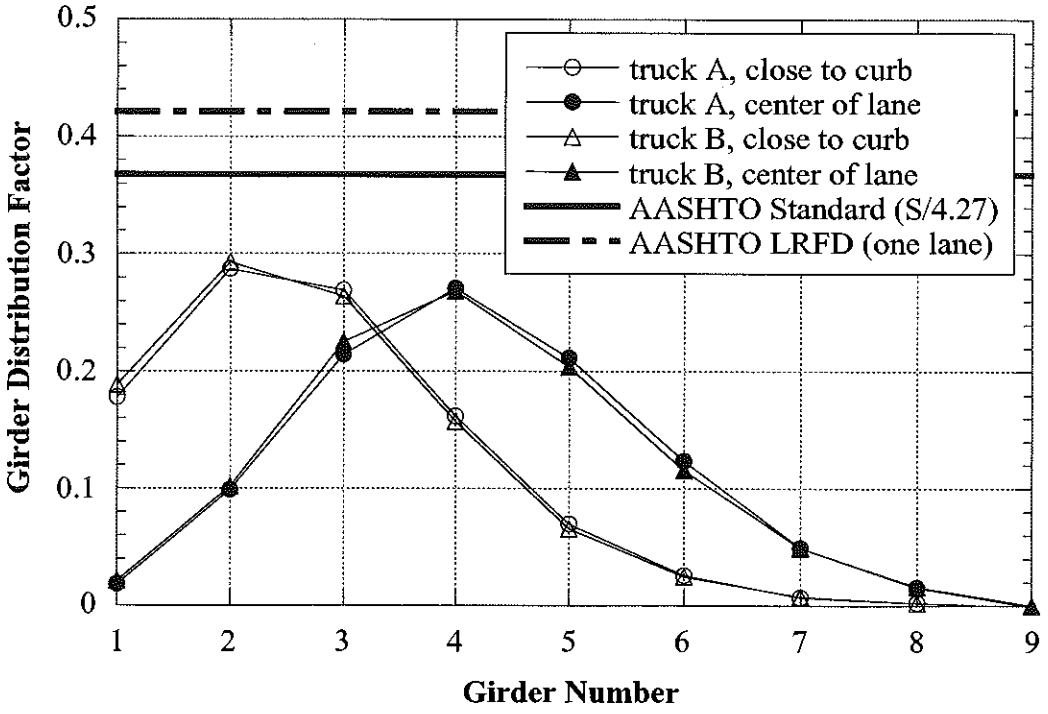

Figure 10.13. South Lane, Crawling Speed, M43/SD (B02-23041).

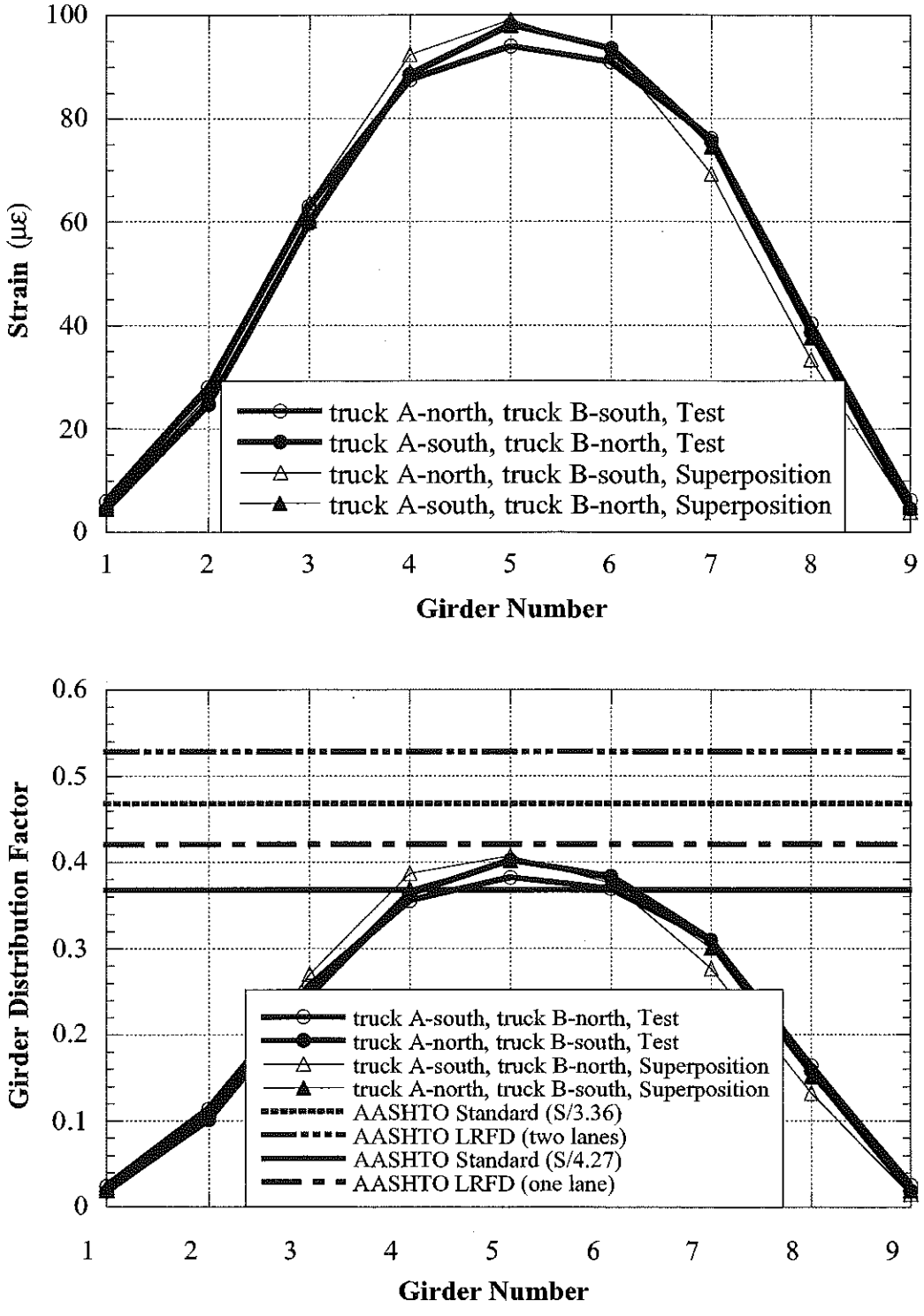

Figure 10.14. Side-by-Side Loading, Center of Lane, Crawling Speed, M43/SD (B02-23041).

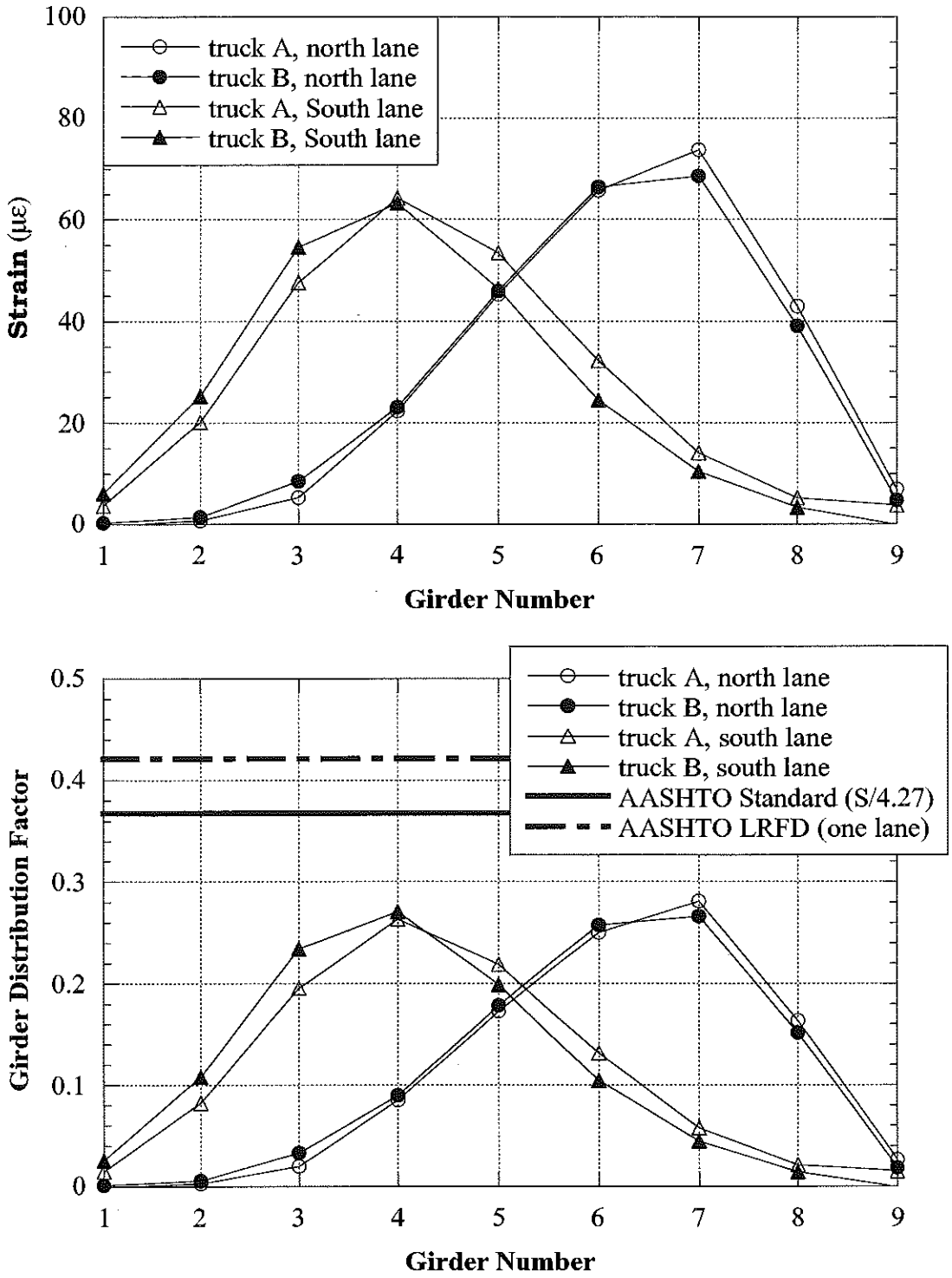

Figure 10.15. Strain and GDF under One Truck Loading at Regular Speed, M43/SD (B02-23041).

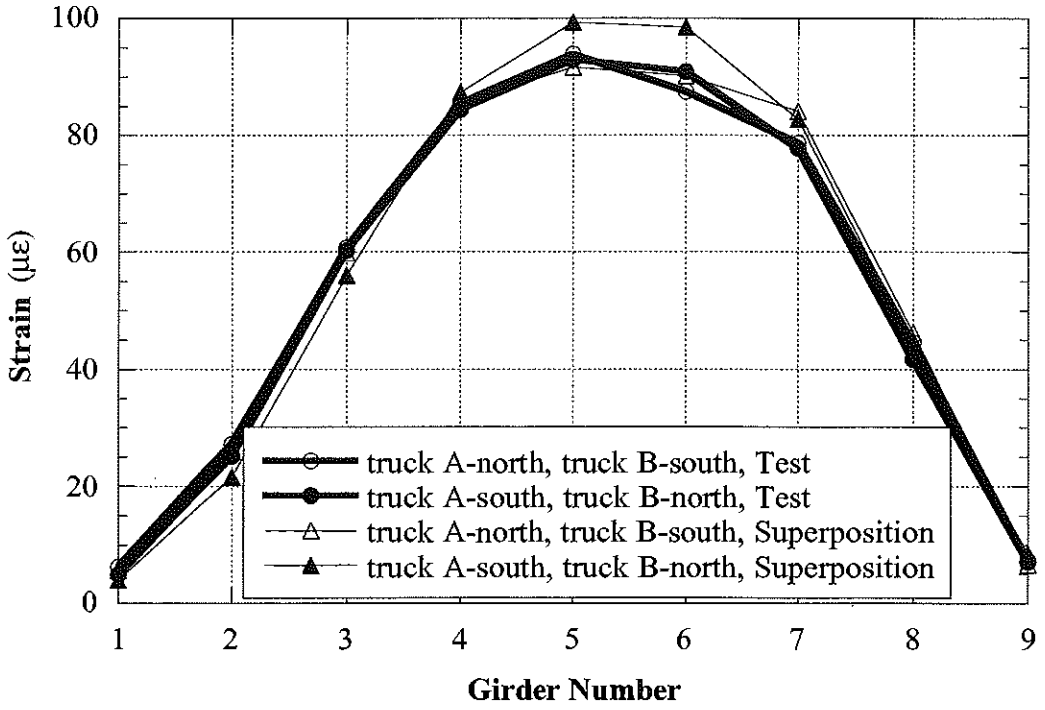

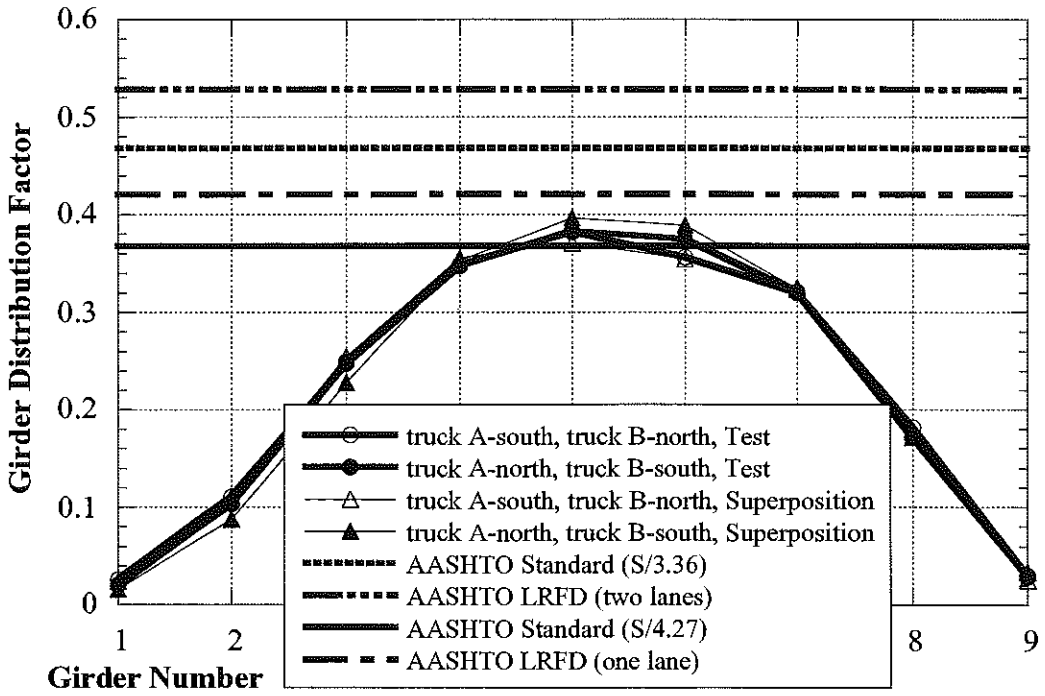

Figure 10.16. Strain and GDF under Side-by-Side Loading at Regular Speed, M43/SD (B02-23041).

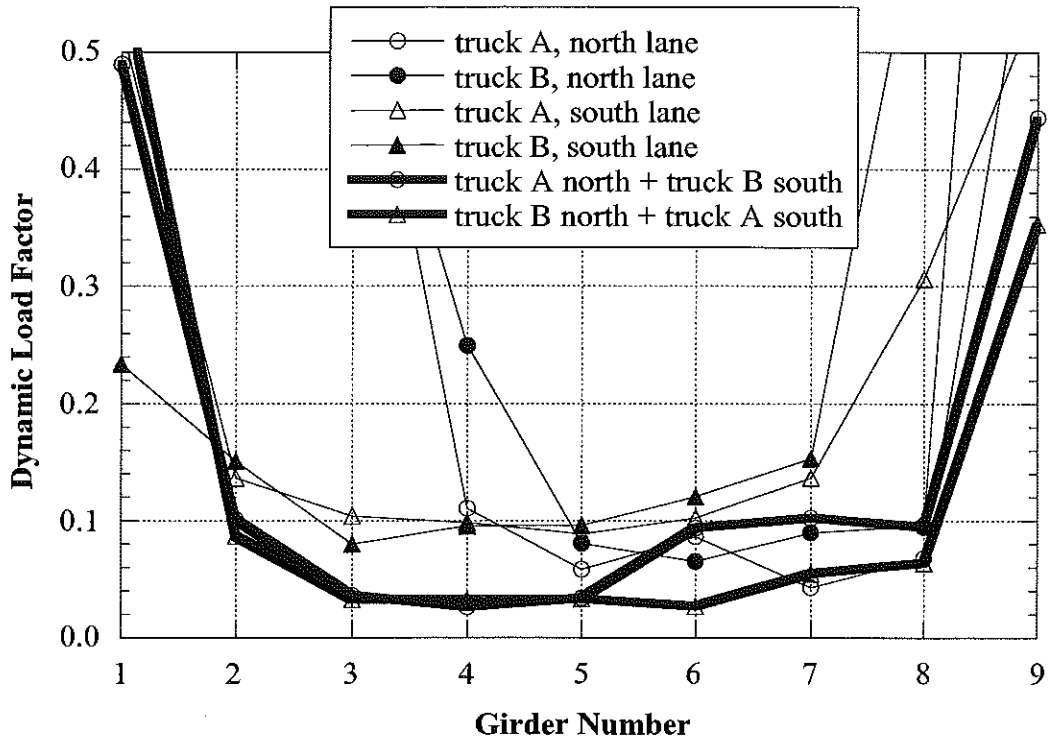

Figure 10.17. Dynamic Load Factors, M43/SD (B02-23041).

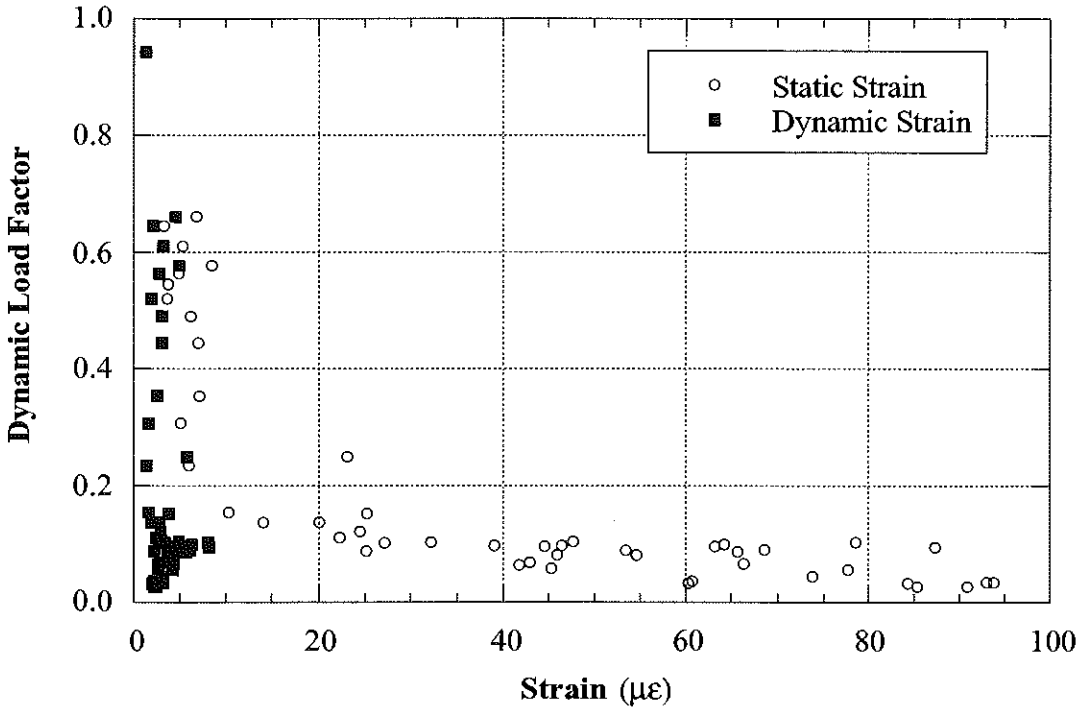

Figure 10.18. Strain vs. Dynamic Load Factors, M43/SD (B02-23041).

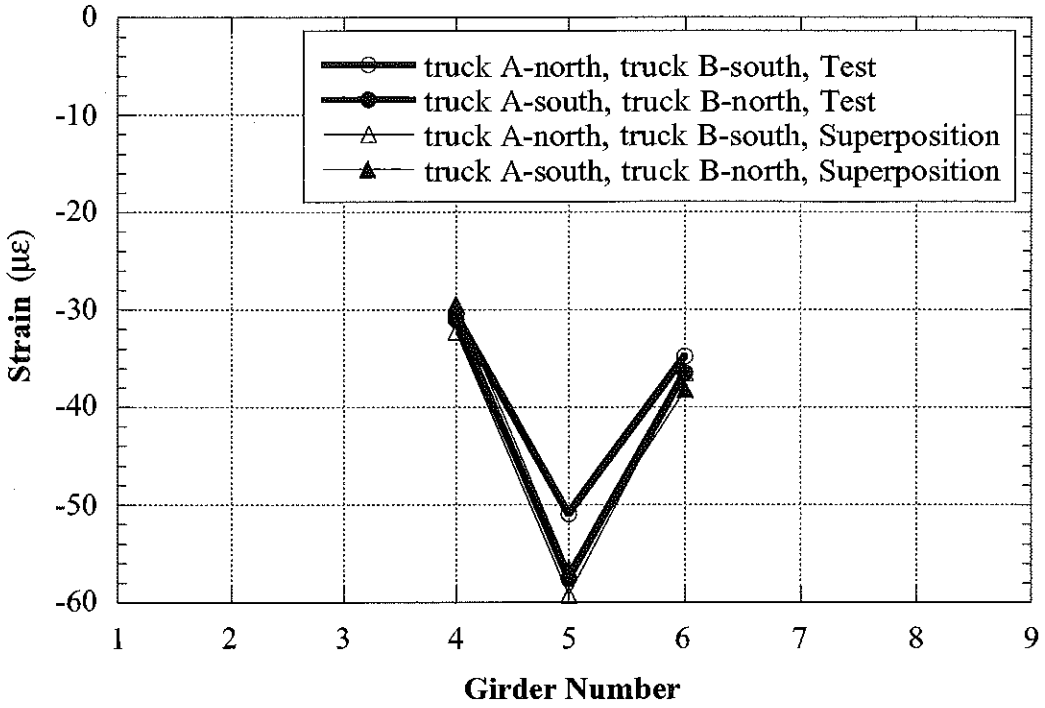

Figure 10.19. Strains at West End, Side-by-Side Loading, Crawling Speed, M43/SD (B02-23041).

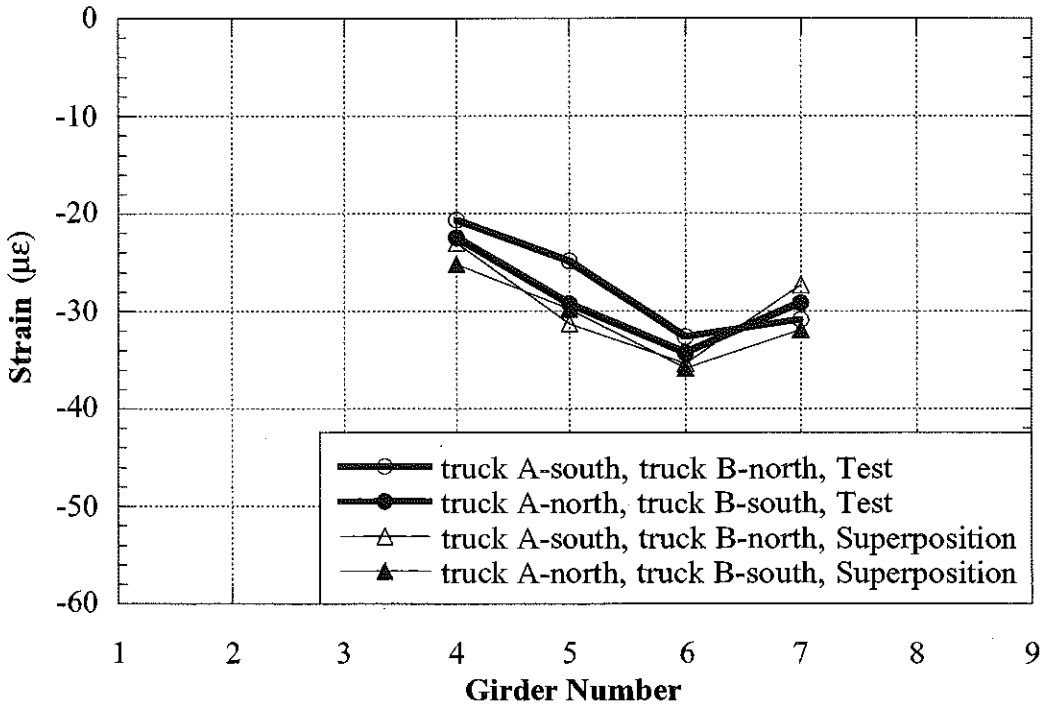

Figure 10.20. Strains at East End, Side-by-Side Loading, Crawling Speed, M43/SD (B02-23041).

Note:

Intentionally left blank

11. BRIDGE ON M-36 OVER HURON RIVER, LIVINGSTON COUNTY (B01-47041, M36/HR)

11.1 Description

This bridge was built in 1986 and it is located on M-36 over Huron River in Livingston County, Michigan. It is a single span, simply supported structure, designed as a composite section. The total span length is 42.6 m with skew of 15 degrees. It has six steel girders spaced at 2.85 m, as shown in Figure 11.1. The bridge has one lane in each direction and it carries an average daily traffic (ADT) of 12,000. The speed limit on this bridge is 89 km/h. The operating load rating is 1,050 kN, according to the Michigan Structure Inventory.

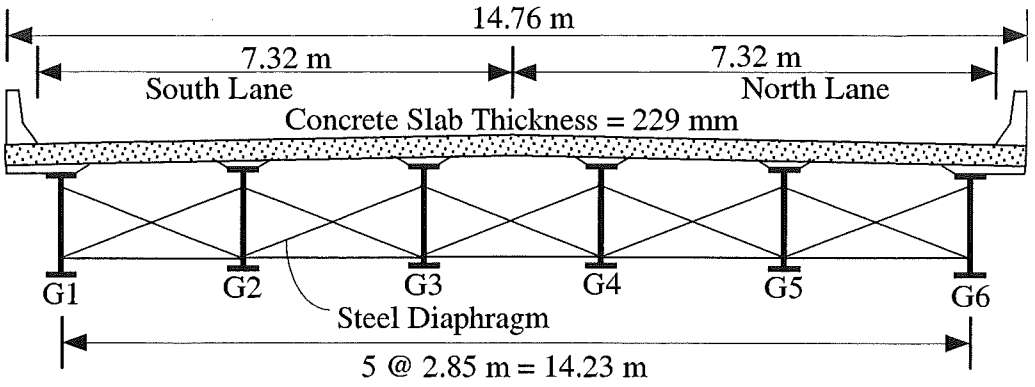

Figure 11.1. Cross-Section of the Bridge M36/HR (B01-47041).

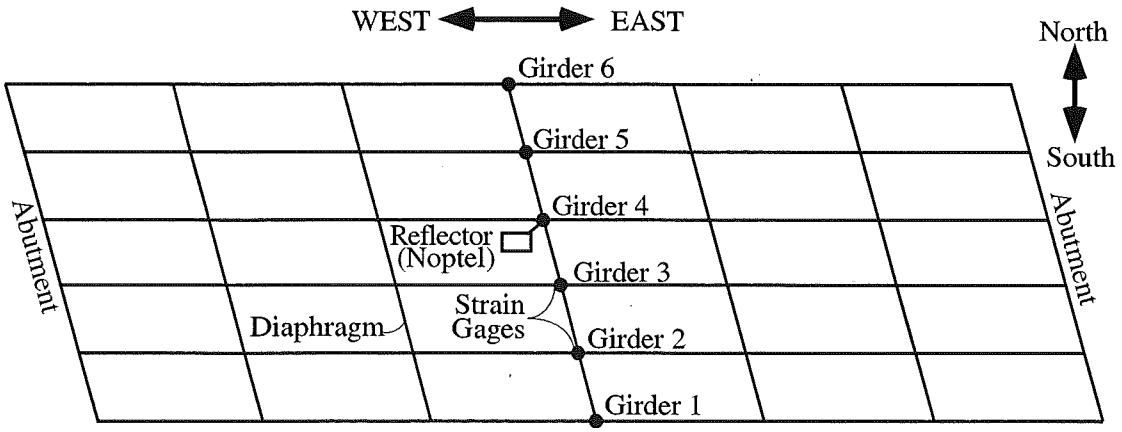

Figure 11.2. Strain Gage Locations in Bridge M36/HR (B01-47041).

11.2 Instrumentation

Strain transducers were installed on the bottom flanges of girders at midspan and at selected support locations, as shown in Figure 11.2. The reflector for the PSM-R device from Noptel was installed at the girder No. 4 to measure deflection. The installation of equipment and bridge test were both performed on October 12, 2000.

11.3 Load cases

The girder distribution factors (GDF) and dynamic load factors (DLF) were calculated using the strains measured at midspan. The bridge was loaded with two 11-axle trucks (three-unit vehicles).

The truck A and truck B have gross weights of 666 kN and 652 kN, with wheelbases of 17.66 m and 17.66 m, respectively. Truck configurations are shown in Figures 11.3 and 11.4.

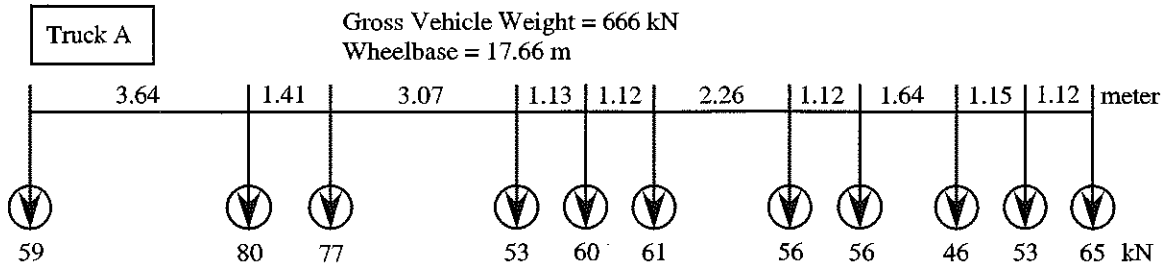

Figure 11.3. Truck A Configuration, Bridge M36/HR (B01-47041).

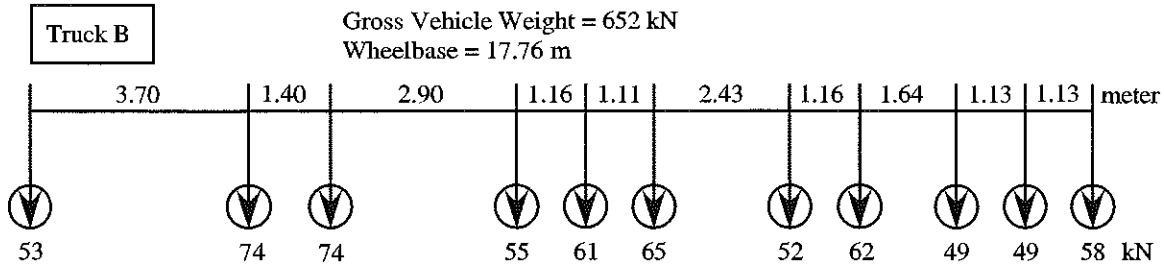

Figure 11.4. Truck B Configuration, Bridge M36/HR (B01-47041).

A total of 16 load cases were considered, as shown in Table 11.1. First each truck was driven by itself at the center of North lane, at crawling speed. Then, the same truck was driven close to the curb. The runs in the center of the lane were repeated at a normal highway speed. The same was repeated for the South lane. In addition, two trucks were driven simultaneously, side-by-side, at crawling speed and normal highway speed. For side-by-side cases, the runs were repeated after the trucks switched lane, i.e. first truck A was in North lane, and B in South lane, then truck A was in South lane, and B in North lane.

Table 11.1. Sequence of Test Runs, Bridge M36/HR (B01-47041).

Run#	Truck	Lane Side	Position in Lane	Truck Speed
1	Truck A	North	Center	Crawling
2	Truck A	North	Curb	Crawling
3	Truck A	South	Center	Crawling
4	Truck A	South	Curb	Crawling
5	Truck A and B	both	Center	Crawling
6	Truck B and A	both	Center	Crawling
7	Truck B	North	Center	Crawling
8	Truck B	North	Curb	Crawling
9	Truck B	South	Center	Crawling
10	Truck B	South	Curb	Crawling
11	Truck A	North	Center	39 km/h
12	Truck B	North	Center	45 km/h
13	Truck A	South	Center	50 km/h
14	Truck B	South	Center	52 km/h
15	Truck A and B	both	Center	49 km/h
16	Truck B and A	both	Center	55 km/h

11.4. Analysis results

A three-dimensional finite element method (FEM) was applied to investigate the structural behavior of the bridge M36/HR (B01-47041). The concrete slab was modeled with isotropic, eight node solid elements, with three degrees of freedoms at each node. The girder flanges and web were modeled using three-dimensional, quadrilateral, four node shell elements with six degrees of freedom at each node. The structural effects of the secondary members, such as the sidewalk and parapet, were also taken into account in the finite element analysis models.

Three cases of the boundary conditions are considered, as described earlier in this Report. The partially frozen supports were modeled using spring elements as shown in Figure 11.6.

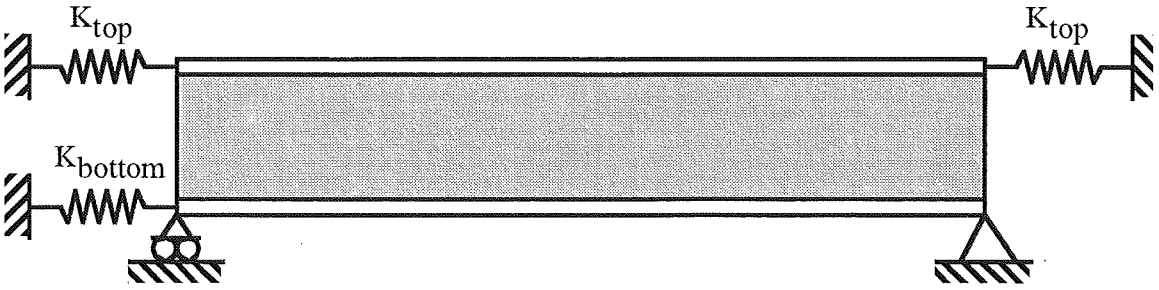

Figure 11.6. Modeing of Support Partial Fixity in Finite Element Analysis.

The mesh of the FEM model is shown in Figure 11.7. Figure 11.8 presents a deformed shape of the bridge loaded with two trucks side-by-side. Figure 11.9 illustrates the distribution of the loads simulating two truck side-by-side.

Strains calculated for the three considered models are shown in Figure 11.10 for two trucks side-by-side (Run 5). Also shown are the experimental results. The FEM results show that the maximum strain at the most heavily loaded girder is about 220 με for the model with simple

support, while the maximum strain recorded from the test is about 190 με. When the spring elements are used with the K constants adjusted according to the test results (K_{top} = 30,000 kN/m and K_{bottom}= 60,000 kN/m), then the FEM results become very close to the test results. This confirms the presence of some degree of fixity of supports.

Figure 11.11 presents the deflection obtained from the three different FEM models. It shows that the maximum deflection under two truck loading is about 27 mm, for the FEM model with the partial support fixity.

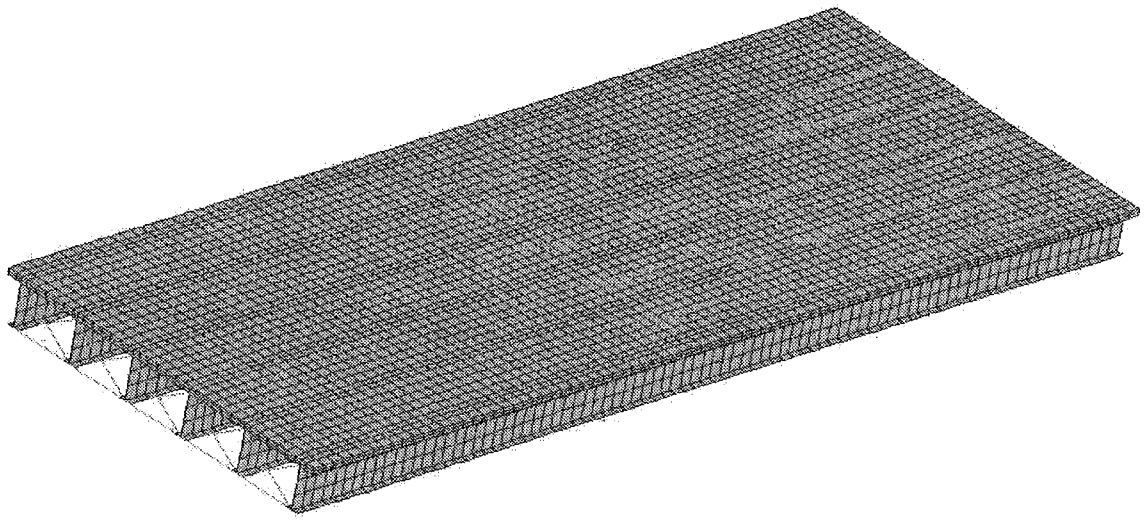

Figure 11.7. The Mesh of the Finite Element Model.
M36/HR (B01-47041).

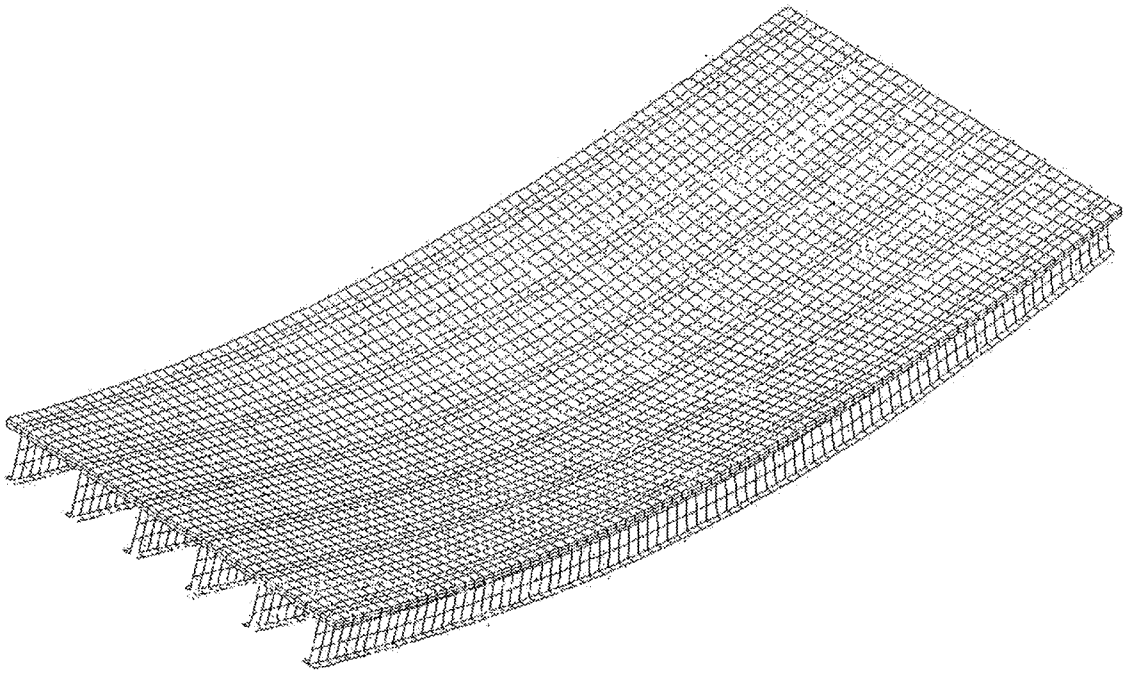

Figure 11.8. The Deformed Shape of the Bridge under Two Lane Loading. M36/HR (B01-47041).

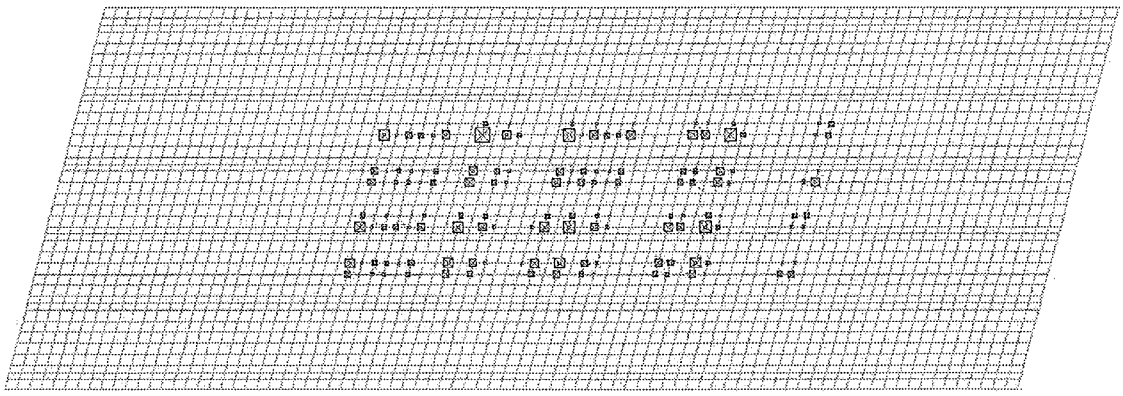

Figure 11.9. Configuration of Load Distribution under Two Lane Loading M36/HR (B01-47041).

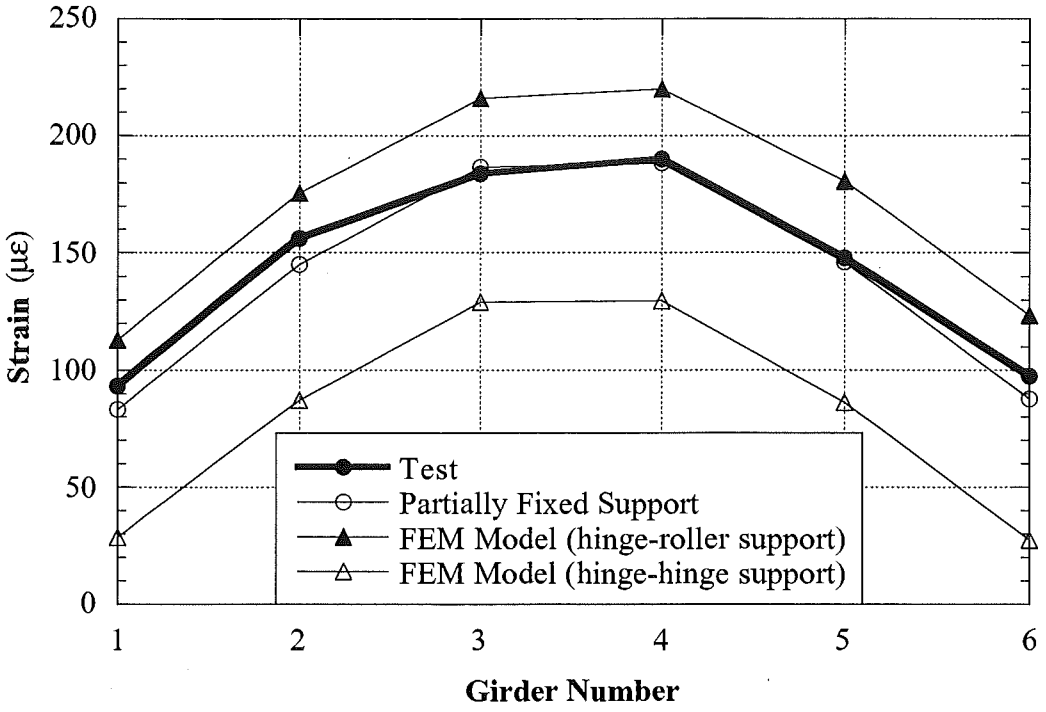

Figure 11.10. Strain from the FEM Analysis Compared with the Test Results for Two Lane Loading, M36/HR (B01-47041).

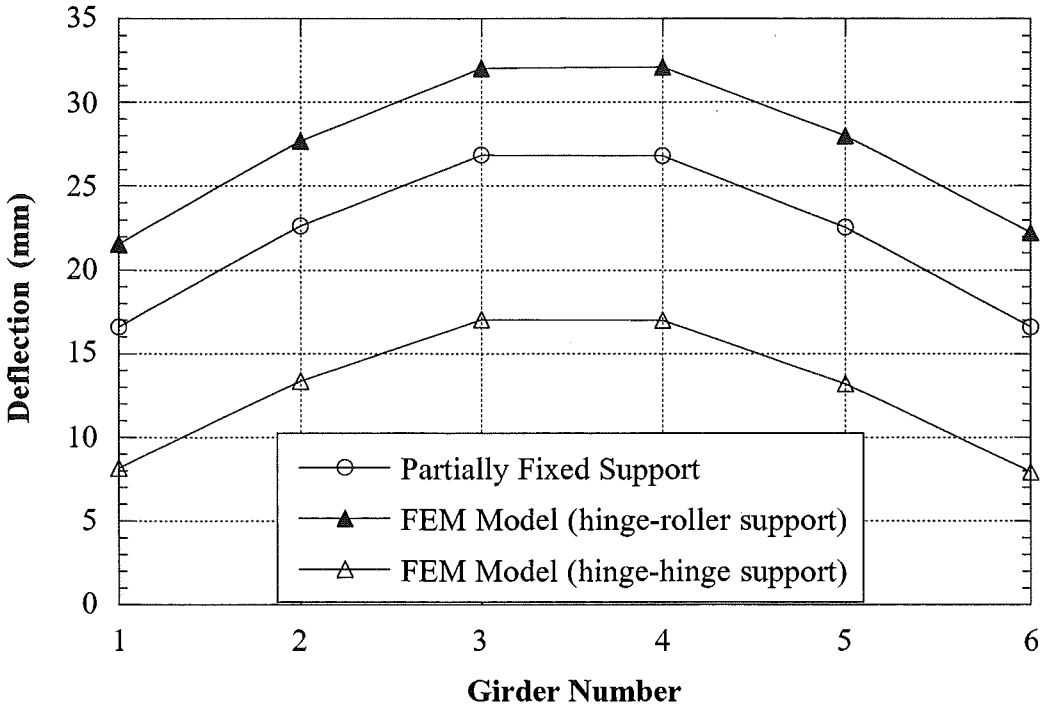

Figure 11.11. Deflection from the FEM Analysis for Two Lane Loading M36/HR (B01-47041).

11.5 Test results

The resulting strains and GDF's are shown in Figures 11.12 through 11.16. Figures 11.12 to 11.14 present the results of all crawling-speed (static) tests. Figures 11.12 to 11.13 present static strains and GDF's for one truck on the bridge. The maximum strain due to a single truck is about 160 με. This corresponds to about 32 MPa.

Figure 11.14 shows static strains and GDF's from side-by-side static load tests. For two vehicles side-by-side the maximum strain is about 190 με (which corresponds to 38 MPa). The superposition of strains due to a single truck in North and South lanes produces almost the same results as strain due to two trucks side-by-side.

For two trucks side-by-side, the girder distribution factor for girder i is determined using Eq. (3-1). For comparison, GDF are also calculated according to AASHTO Standard (1996) and AASHTO LRFD Code (1998). Two cases were considered, a single lane loaded, and two lanes loaded. The resulting GDF's are shown in Figures 11.12 through 11.16.

The results indicate that code-specified GDF's are conservative. Even a single lane GDF's specified in both AASHTO Standard (1996) and AASHTO LRFD (1998) are also sufficient for two lane load cases for this bridge.

Figures 11.15 and 11.16 shows the resulting strain and distribution factors from normal speed tests. There is practically no difference between the crawling speed and normal speed results.

Dynamic load factor is defined in section 3.3. In Figure 11.17, DLF's are plotted for all load cases involving normal speed (no dynamic load was measured for crawling speed runs). Dynamic load factors for exterior girders are high because the static strains in these girders are

very low. In other words, large values of DLF in exterior girders correspond to load cases with a single truck in the opposite lane (resulting in very low static strain).

The relationship between DLF and static and dynamic strains is shown in Figure 11.18. The open circles correspond to static strain, ε_{stat}, and black solid squares correspond to dynamic strain, ε_{dyn}. For each static strain value (open circle), the corresponding dynamic strain is denoted by solid square (the numbers of circles and squares are same). Dynamic strains remain nearly constant, while static strains increase as truck loading increases. This results in large dynamic load factors for low static strains. It is clear from the Figure 11.18 that dynamic strains does not exceed 20 με for all the cases while the static strain can exceed 200 με in normal speed test. DLF corresponding to the maximum strain caused by two trucks side-by-side, is less than 0.05 at girders No. 3 and 4, the most heavily loaded girders.

Girder No. 4 was instrumented with a remote deflection measurement device manufactured by Noptel. The reflector was installed at midspan. The result is shown in Table 11.2. However, for runs 5 and 6, the measurements could not be recorded because of the system buffer overflow. The maximum deflection recorded during the test is 24.5 mm for girder No. 4 for the normal speed and two side-by-side trucks. This value was obtained by filtering out the dynamic portion of the deflection for comparison with run 5. In FEM analysis, deflection was about 26.5 mm for run 5 with partially fixed supports, which is very close to test result (24.5 mm). This confirms a partial fixity at the supports.

Table 11.2. Maximum deflections measured at the center of Girder No.4, Bridge M36/HR (B01-47041).

Run #	Vertical Deflection (mm)
1	13.3
2	11.3
3	10.3
4	5.7
5	N/A
6	N/A
7	13.8
8	11.3
9	10.4
10	5.6
11	13.9
12	13.5
13	10.5
14	10.8
15	24.5
16	24.1

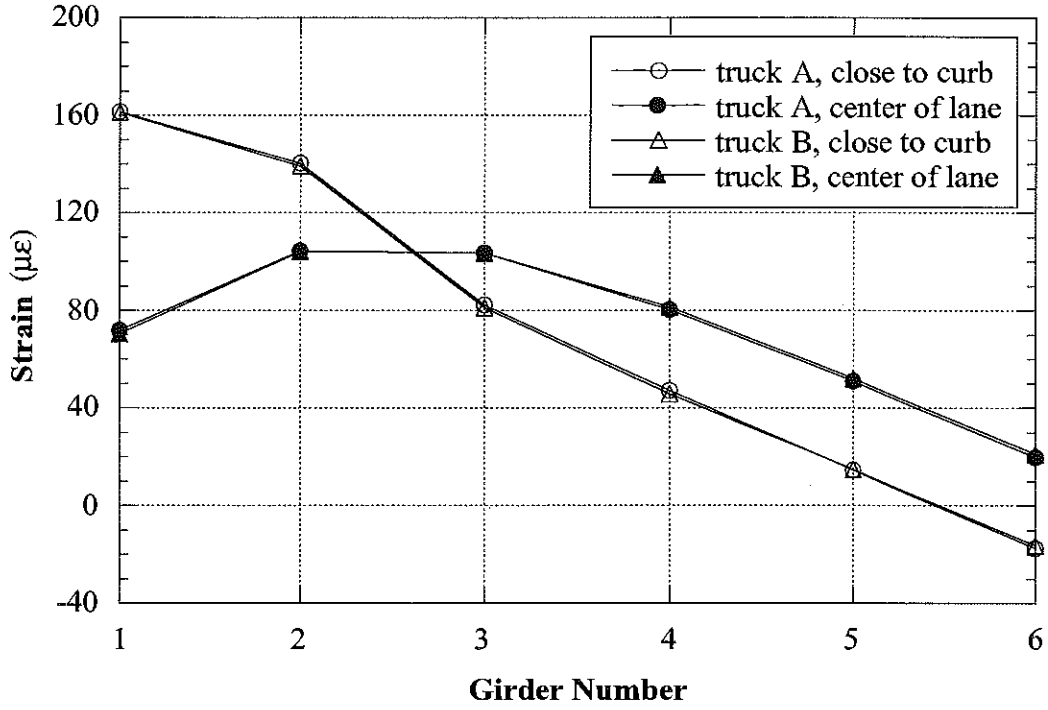

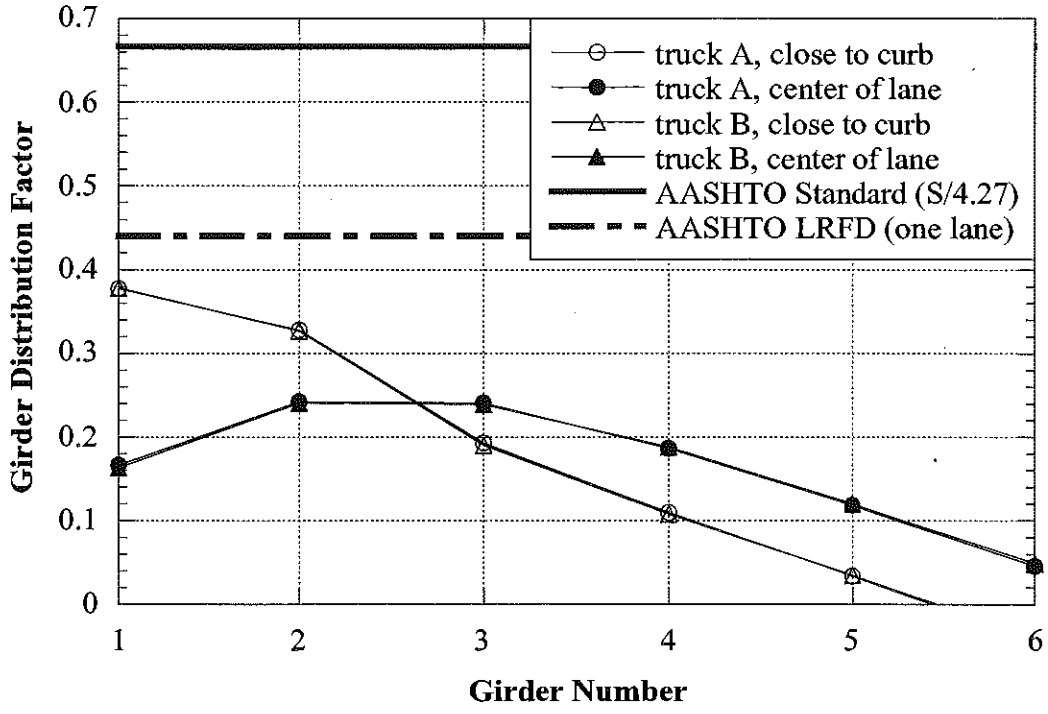

Figure 11.12. South Lane, Crawling Speed, M36/HR (B01-47041).

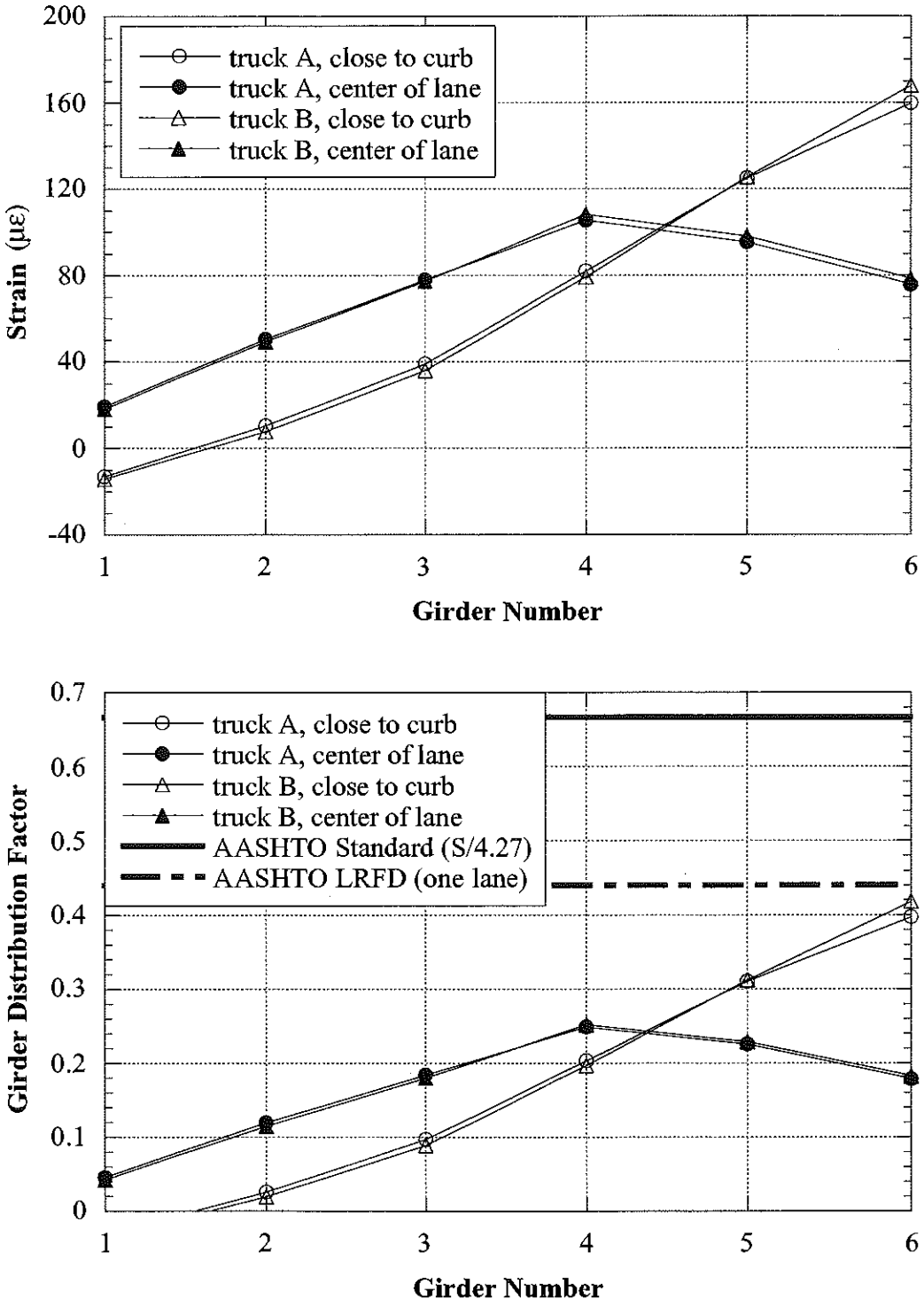

Figure 11.13. North Lane, Crawling Speed, M36/HR (B01-47041).

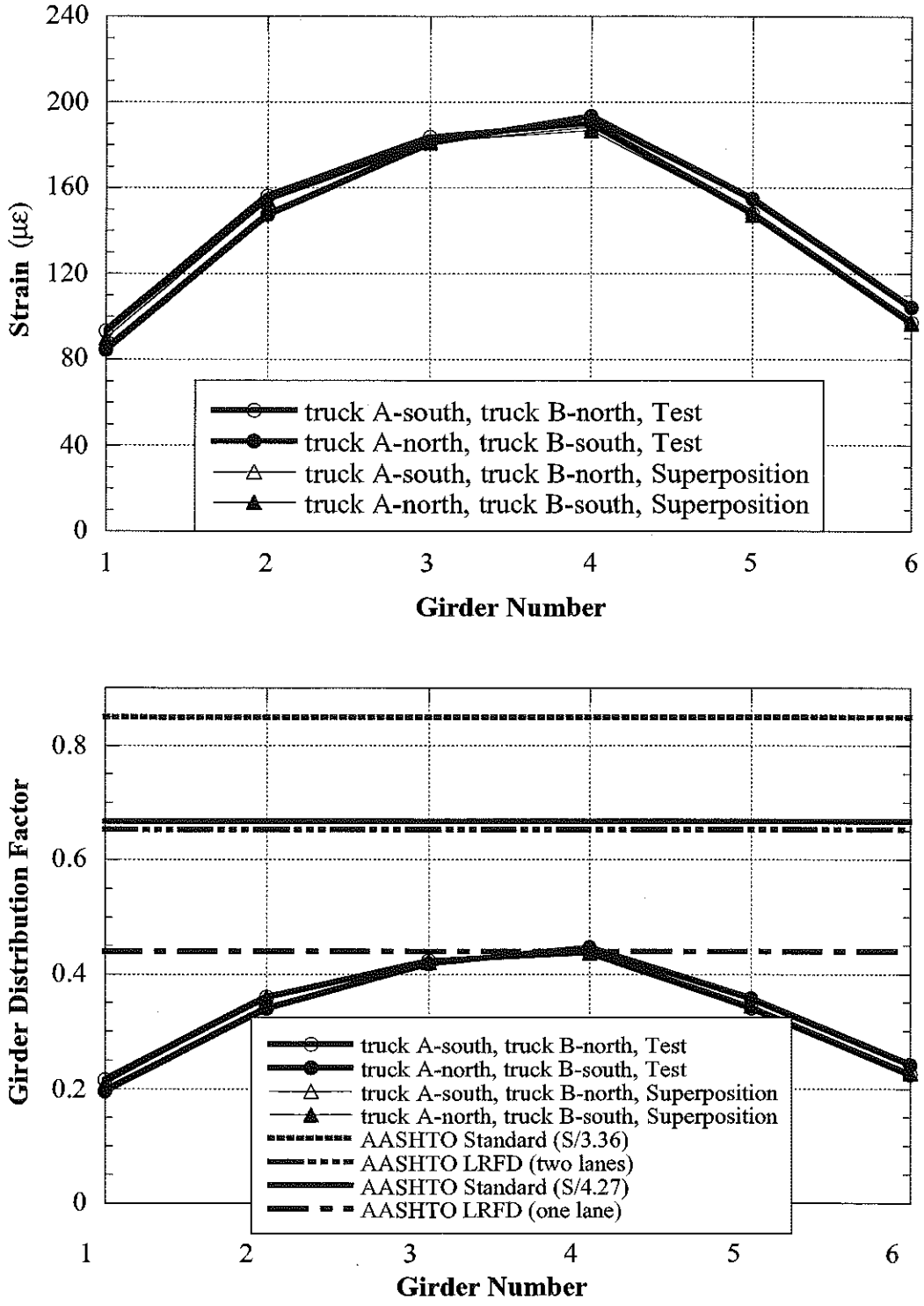

Figure 11.14. Side-by-Side Loading, Center of Lane, Crawling Speed, M36/HR (B01-47041).

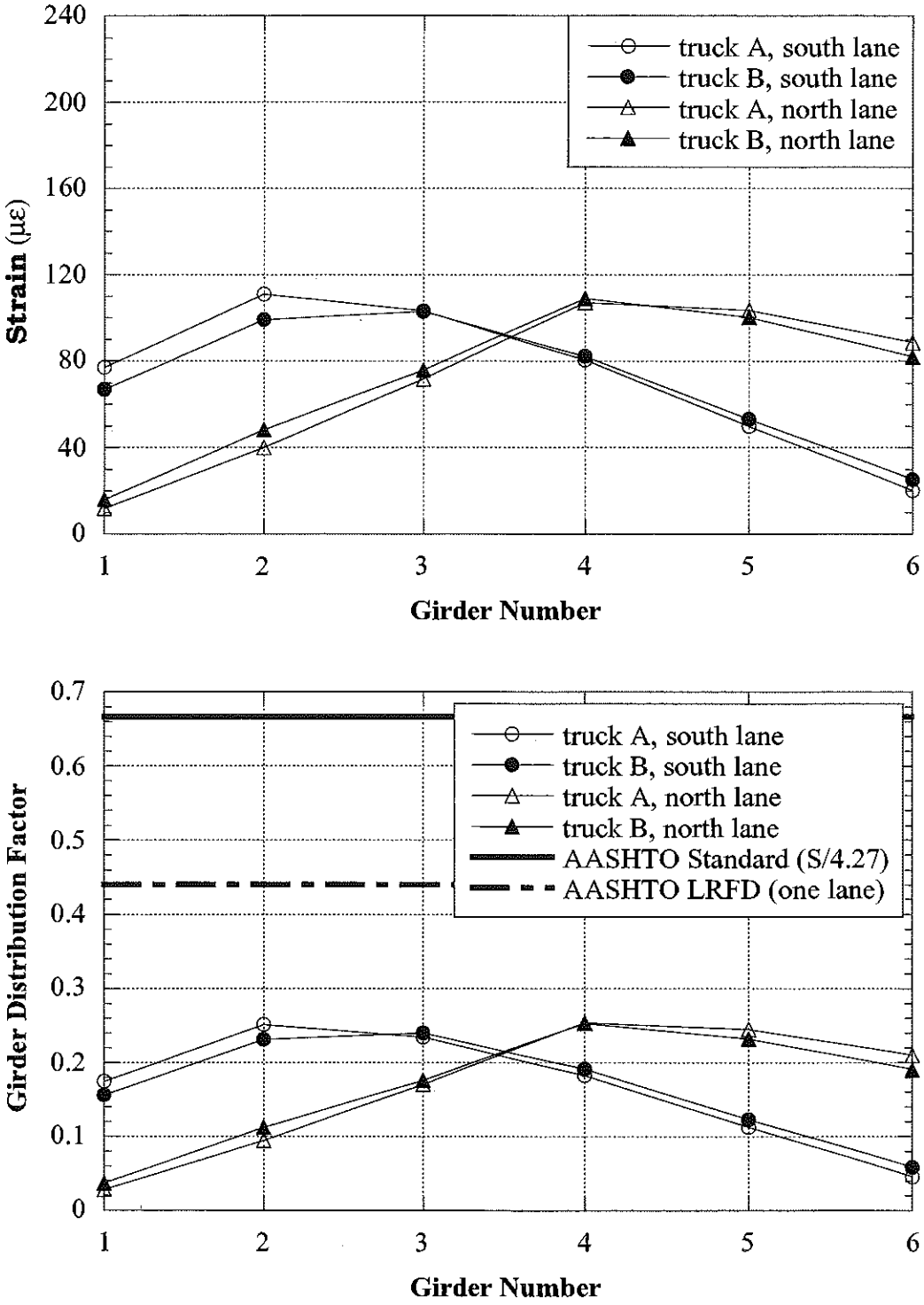

Figure 11.15. Strain and GDF under One Truck Loading at Regular Speed, M36/HR (B01-47041).

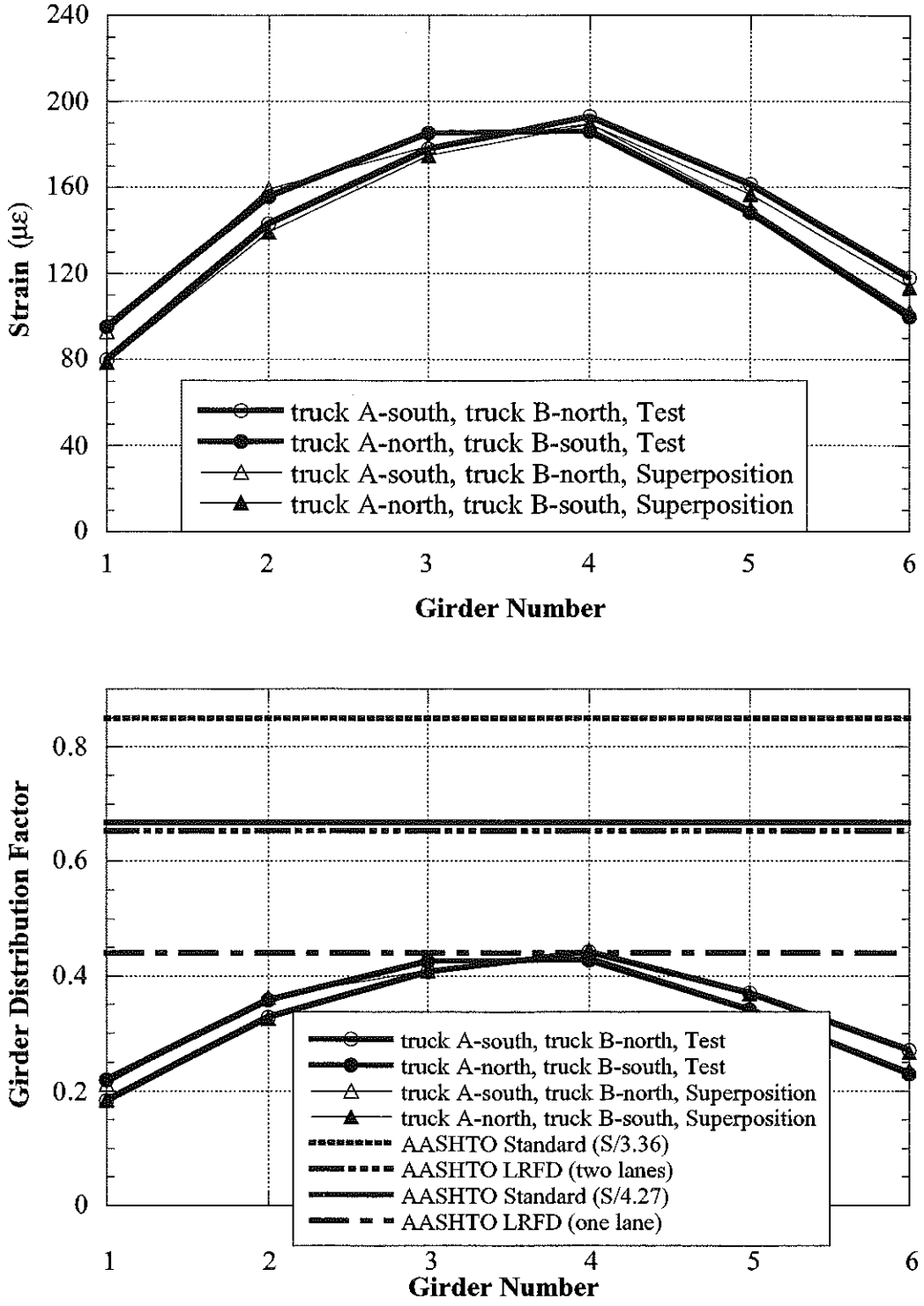

Figure 11.16. Strain and GDF under Side-by-Side Loading at Regular Speed, M36/HR (B01-47041).

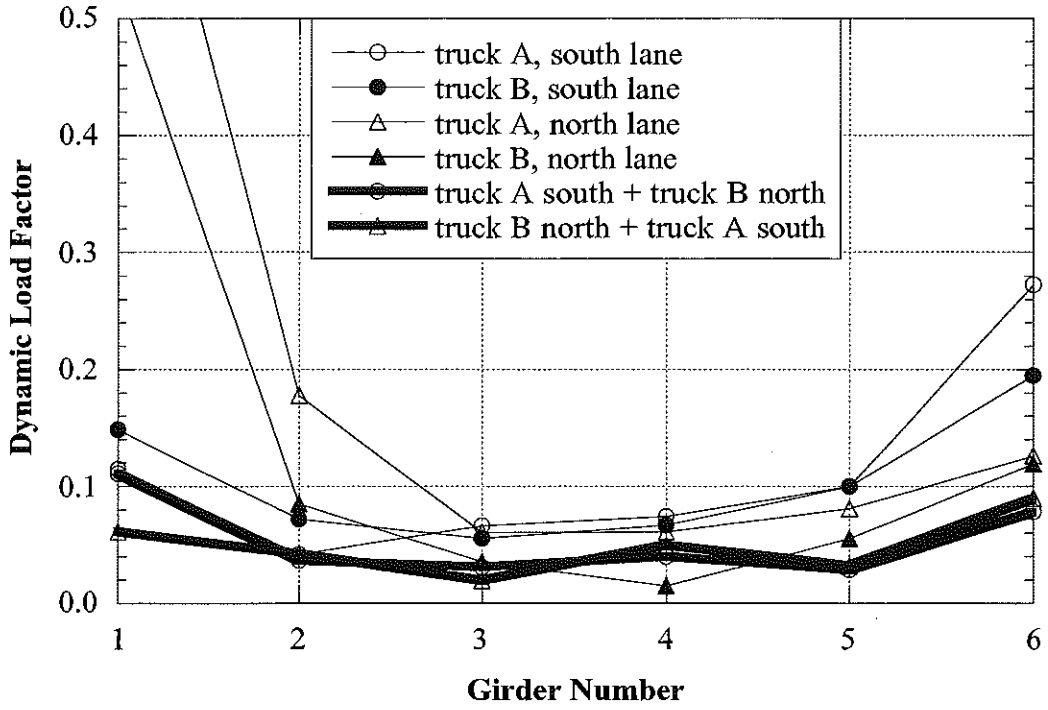

Figure 11.17. Dynamic Load Factors, M36/HR (B01-47041).

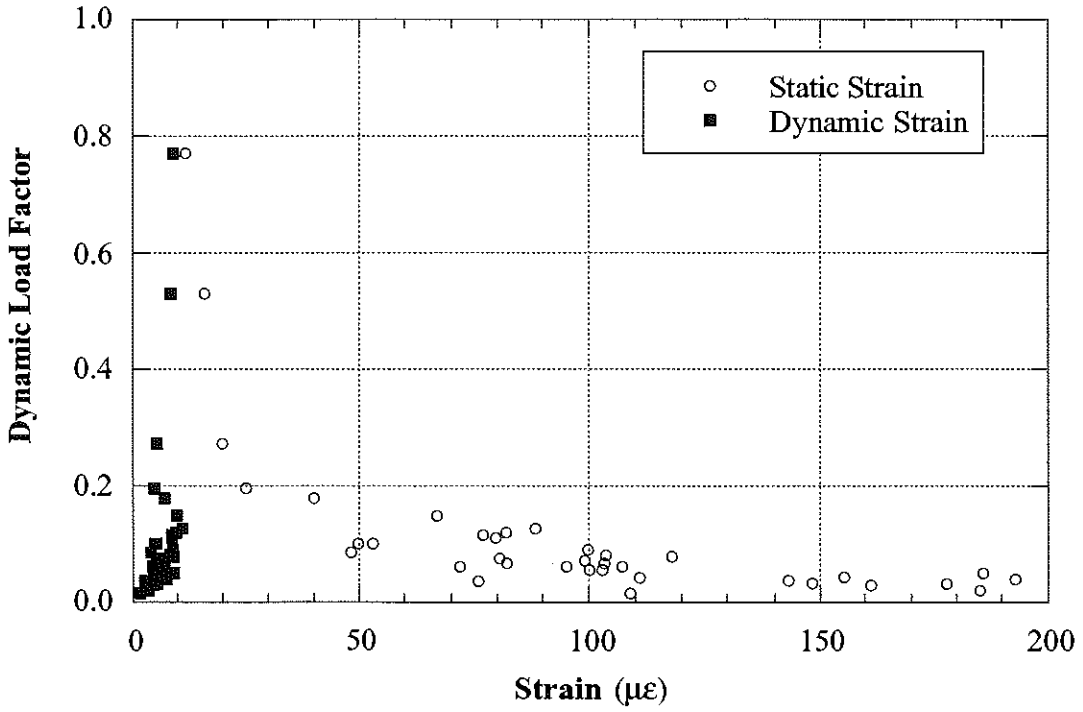

Figure 11.18. Strain vs. Dynamic Load Factors, M36/HR (B01-47041).

Note:

Intentionally left blank

12. MULTIPLE PRESENCE OF TRUCKS

Structural analysis and field tests indicate that the live load effect in bridge girders is most often governed by a simultaneous occurrence of two heavy vehicles side-by-side. Therefore, it is important to establish the statistical parameters for multiple presence of trucks on the bridge. The truck survey was performed in 1991 at two locations. Additional field observations were taken as part of this project in 2001 at four locations. The results are summarized taking into consideration the calculated probabilities of simultaneous occurrence events.

12.1 Truck Survey in 1991

The initial truck surveys were carried out in 1991 and the results were reported by Nowak et al. (1994). The objective was to determine the probability of a multiple presence of trucks on M-14 over the New York City Railroad in Ann Arbor and on I-94 about 1 mile East of Zeeb Road (Ann Arbor).

Three categories of multiple presence were considered:

(a) In-lane, with one truck following behind the other with headway distance less than 15m.

(b) Side-by-side, both trucks with front axles in the same longitudinal position on the bridge.

(c) Side-by-side, one truck behind the other with headway distance less than 15m.

The Average Daily Truck Traffic (ADTT) is estimated as 8,000 for I-94 and 6,000 for M-14. The numbers of observed cases (categories) of

multiple presence were recorded. However, the records do not include information on the number of axles for vehicles involved.

The probabilities of multiple presence were calculated as the ratio of number of multiple presence cases and total number of trucks observed at the location. For the combined data, approximately every 50th truck was in-lane with another truck with a headway distance of less than 15m. Every 35th truck was side-by-side with another truck with front axles aligned, and every 25th truck was side-by-side with another truck with headway distance less than 15m.

12.2 Truck Survey in 2001

The new truck survey was carried out at four locations:

(a) M-52 in Chelsea, Washtenaw County, (ADTT = 250, two lanes, one in each direction)
(b) M-36 over US-23, Livingston County (ADTT = 150, three lanes, one in each direction and a passing lane)
(c) US-12 in Saline, Washtenaw County (ADTT = 200, four lanes, two in each direction)
(d) I-94 at exit 159, West of Chelsea, Washtenaw County (ADTT = 9,000, four lanes, two in each direction)

ADTT values are estimated based on the survey results.

The objective of this survey was to observe the number of multiple presence occurrences. At the first three locations, all the trucks were recorded, while on I-94 only multiple presence cases were recorded.

At the first three locations, no case of side-by-side occurrence was observed.

On M-52, half of all trucks were 5 axle vehicles, and 11-axle trucks constituted 5% of the population. Just one in-lane event was observed, with a 2-axle truck following behind a 4-axle truck.

On M-36, 5-axle trucks constituted only 20% of the total population of trucks, with 30% being 11-axle trucks and 30% being 2-axle trucks. Four cases of in-lane multiple presence were observed; including two with both being 11-axle trucks, one with 11-axle truck and 3-axle truck, and one with 5-axle truck and 2-axle truck.

On US-12, 40% of the trucks were 2-axle vehicles, 25% were 4-axle trucks and 15% were 5-axle trucks. Not even a single 11-axle truck was observed. Three cases of multiple presence in-lane were observed, all involving only 2-axle trucks.

On I-94, the traffic volume was very heavy. The number of observed in-lane events was 21 and only 3 side-by-side (front-to-front within 5 m), none involving 11-axle trucks. These occurrences correspond to probabilities of 0.005 and 0.0005, respectively.

The results of observations are summarized in Table 12-1.

Table 12-1 Observed Multiple Presence Cases in the 2001 Truck Survey

Location	Percentage of Trucks by Axles				Probability of Multiple Presence	
	2	4	5	11	In-lane	Side-by-side
US-52	10	20	50	5	0.01	0
Hamburg Rd	35	7	20	30	0.04	0
US-12	40	25	15	0	0.03	0
I-94	not available				0.005	0.0005

The conclusion from the truck survey is that the probability of having two side-by-side trucks on a bridge is very low. It is even lower for heavily loaded trucks, and practically negligible for two fully loaded 11-axle trucks.

12.3 Summary of Multiple Presence and Recommendations

The field test data indicates that the code-specified GDF's are adequate for evaluation of existing bridges. The field tests also showed that in all cases, measured GDF's for two side-by-side trucks are less than the GDF's specified for one lane by AASHTO LRFD (1998). The test results also indicated that the measured GDF's for two side-by-side trucks can exceed the GDF's specified for one lane loading by AASHTO Standard (1996) by 20 %. The truck surveys confirm that the probability of such an event is negligible. Therefore, it is recommended that the existing bridges in Michigan can be evaluated using the girder distribution factors (GDF) corresponding to one lane loading.

In addition, the actual strains and stress in the girders are considerably lower than the values predicted by analytical evaluation using the code specified procedures. This is an extra safety reserve which can also be used to justify the use of GDF's for one lane loading.

13. SUMMARY AND CONCLUSIONS

The field test program documented in this report covered simply supported, steel girder bridges with span range between 10 m and 45 m. The objective of the tests was to verify girder distribution factors (GDF), and dynamic load factors (DLF).

13.1. Girder Distribution Factors

Six bridges were instrumented and loaded with fully loaded 11-axle trucks. The resulting strains are shown in Figures 13.1 to 13.5, for one truck and two trucks side-by-side.

In Figures 13.1 and 13.2, the strains are plotted for one lane loading at crawling speed. Two truck positions are considered for each case: close to the curb and at the center of the traffic lane. Strains for truck A and B are practically the same, which confirms the repeatability of the results. For a single truck, the maximum strain was recorded in the interior girder, about 160 $\mu\varepsilon$ for the bridge B01-47041. For two trucks side-by-side and crawling speed, the strains are shown in Figure 13.3. For two trucks side-by-side, the maximum strain is about 190 $\mu\varepsilon$ for the bridge B01-47041.

Similar results are obtained for strains measured at the regular speed, as shown in Figures 13.4 and 13.5. This confirms that the speed does not affect the accuracy of the results for GDF's.

The girder distribution factors are summarized in Figures 13.6 to 13.8 at crawling speed and Figures 13.9 and 13.10 for the regular speed.

For a one lane loaded, GDF's observed for interior girders are lower than GDF's specified in the code as shown in Figures 13.6 and 13.7 for crawling speed, and in Figure 13.9 for normal speed. For exterior

girders, the code specified GDF's are different than for GDF's for interior girders and the test results are not compared to code specified values in this study.

The code specified GDF's are conservative for two trucks side-by-side. As shown in Figure 13.8 and Figure 13.10, the GDF's from the tests are equal or less than the GDF's specified for two lanes loaded by the AASHTO LRFD (1998) and AASHTO Standard (1996). In many cases, even code specified GDF's for one lane loading are sufficient for, or very close to, the test results for the two truck side-by-side loading.

For comparison, the GDF's obtained in field tests as a part of this study are plotted versus analytical values calculated using AASHTO Standard (1996) and AASHTO LRFD Code (1998), as shown in Figures 13.11 through 13.13. The results are presented for a single truck (one lane loaded), and for two trucks (two lanes loaded), from the crawling speed tests. Figure 13.11 shows the results of the short span bridges (span < 20 m), and Figure 13.12 shows the results for the medium span bridges (span > 30 m).

In addition, Figure 13.13 shows the results for all of the short span bridges (span < 30 m) tested since 1997 (15 bridges), including the results of the previous projects.

The absolute values of measured strains are less than 200 με for all the tested bridges. There are two main reasons for low strain values:

- Partial fixity of supports. All of the considered bridges were designed with simple supports. Yet, the actual supports provide some resistance to horizontal movement and rotation. This is due to collection of debris, corrosion, and counter-balancing effect of weight of structural and non-structural components on the other end of the bearing center (cantilever portion of the girder, concrete

diaphragm over the support, portion of the deck slab, portion of the pavement adjacent to the bridge).

- More uniform girder distribution factors. The truck load is distributed on the girders and other components (deck slab, sidewalks, parapet, curbs). The latter are not considered in the design and their contribution to the overall stiffness of the bridge can be about 10%.

The measured maximum static strains for two trucks side-by-side are compared to the calculated static strains in Table 13.1. The maximum calculated strains were obtained by using the maximum bending moment due to legal truck load of 685 kN and GDF's specified in AASHTO Standard (1996) and AASHTO LRFD (1998). As shown in Table 13.1, the calculated strains corresponding to the AASHTO Standard (1996) and AASHTO LRFD (1998) are very large compared to the test results. Even for the code specified GDF values for one lane loading, the calculated strains are much larger than the maximum measured strains due to two side-by-side trucks. In addition, the truck survey confirmed that the probability of a simultaneous occurrence of two trucks side-by-side is negligible.

Based on the test results and truck survey, it is recommended to use the AASHTO LRFD (1998) code-specified values of GDF for the design of girder bridges. However, for evaluation of existing bridges, GDF's specified for a single lane can be used.

13.2. Dynamic Load Factors

The dynamic load factors (DLF) obtained from the tests are summarized in Figures 13.14 and 13.15. For a one lane loading, DLF corresponding to the maximum static strain, is less than 0.20. For two trucks side-by-side, DLF is less than 0.10 for all the tested bridges.

Therefore, in evaluation of existing steel girder bridges, it is recommended to use the DLF = 0.10 for two lane bridges, with both lanes loaded. For a single lane load, DLF = 0.20 can be used.

13.3. Finite Element Analysis

Figures 13.16 and 13.17 show the results of the finite element analysis for two truck side-by-side loading. Figure 13.16 presents the strain values from FEM analysis compared with test values. Figure 13.17 illustrates the deflection values from FEM analysis. Also shown are the experimental and analytical (FEM) results corresponding to three different models. The measured response lies between the results for the simply supported girders and the model with horizontal restraint for the girders. The actual behavior is very well modeled by partially fixed supports.

The maximum measured static strains are compared to strains from the FEM analysis in Table 13.1, for two trucks side-by-side. The effects of the secondary members, such as sidewalk and parapet, are also included in the finite element analysis models.

13.4. Optical Device for Measurement of Deflection

An important consideration in field testing is the access to the structural components without interfering with traffic. Therefore, the deflections were measured for bridges B01-30071 and B01-47041 by using the optical device by Noptel.

For verification, the measured deflections were compared with the FEM analysis results. For the bridge B01-30071, the maximum measured deflection was 2.8 mm while the FEM model with partially fixed supports showed the maximum deflection of 3.0 mm. For the bridge B01-47041, the maximum measured deflection was 24.5 mm

while for the FEM model with partially fixed supports, the maximum deflection is 26.5 mm. It confirms the accuracy of the measuring system. However, there were some problems with the computer attached to this device, and the measurements were not recorded for bridges B01-58041 and B02-23041.

13.5. Wireless Transmitters

The research team's experience with using the wireless transmitters is not very good. There were many problems, the system was not working properly (interference, poor connections, range), and it had to be returned to the manufacturer to be fixed. The installation time compared to the cable-based system is not much shorter.

Prior to the field tests in 2000, the wireless equipment was tested by University of Michigan research team, and it was found not functional. Therefore, it was returned to the manufacturer for further repair and modifications.

Table 13.1. Comparison of the Strain Values from the test and analysis.

MDOT ID #	Maximum Measured Strain (10^{-6})	Maximum Calculated Strain (10^{6})				Strain from Finite Element Analysis (10^{-6})		
		AASHTO Standard (S/4.27)	AASHTO Standard (S/3.36)	AASHTO LRFD (one lane)	AASHTO LRFD (two lanes)	Simple Supports	Hinged Supports	Partially Fixed Supports
B02-46071	126.2	337.9	430.1	392.5	506.5	166.2	75.5	128.1
B01-30071	132.9	338.5	430.8	418.4	520.2	165.8	73.8	126.4
B01-58041	130.2	261.1	332.3	261.4	344.8	185.0	83.4	131.4
S11-25032	149.7	285.4	363.2	230.9	321.3	184.1	107.5	149.4
B02-23041	93.0	267.8	340.9	306.8	384.7	115.4	51.2	92.5
B01-47041	190.1	395.3	503.1	266.2	396.1	220.2	129.4	188.3

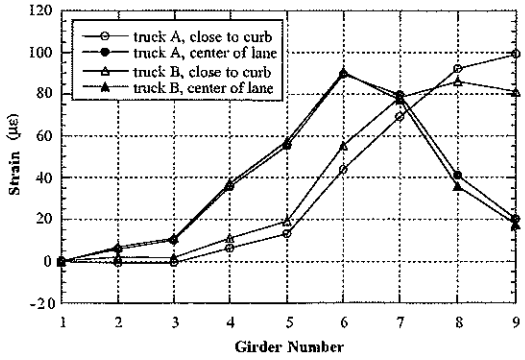

M52/BC (B02-46071)
West Lane Loaded

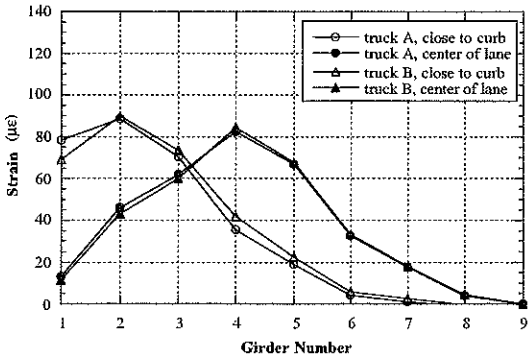

M52/BC (B02-46071)
East Lane Loaded

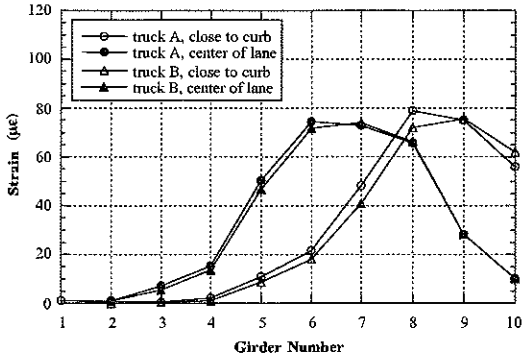

US127/BD (B01-30071)
West Lane Loaded

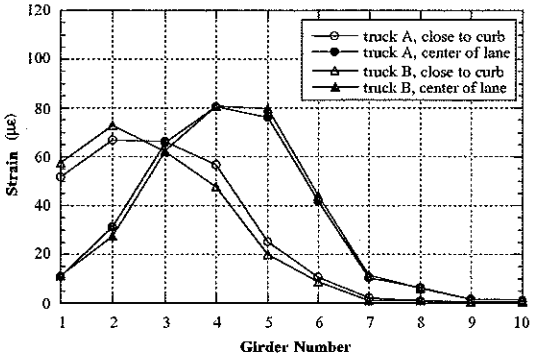

US127/BD (B01-30071)
East Lane Loaded

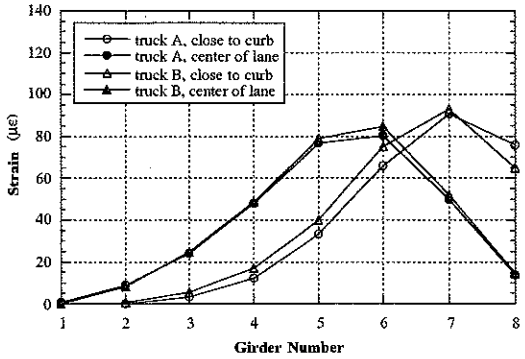

M50/MR (B01-58041)
South Lane Loaded

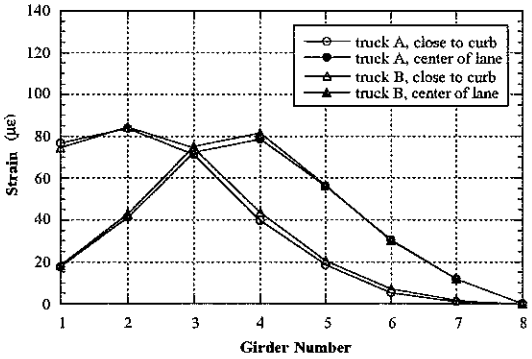

M50/MR (B01-58041)
North Lane Loaded

Figure 13.1. Strains under One Lane Loading at Crawling Speed

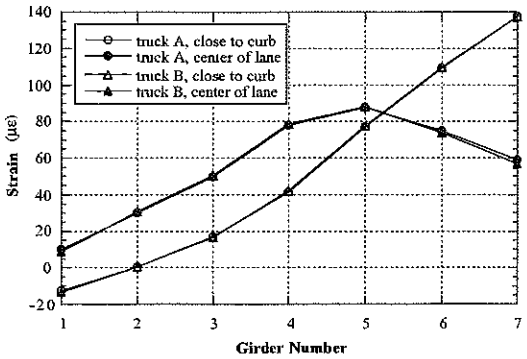

ST/I75 (S11-25032)
South Lane Loaded

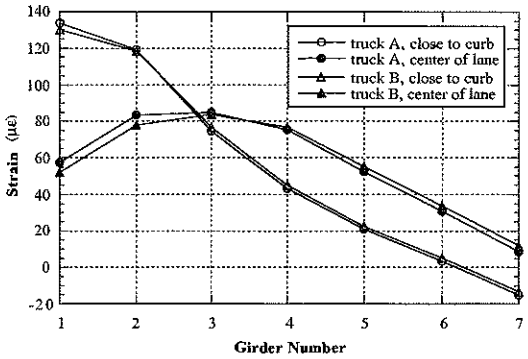

ST/I75 (S11-25032)
North Lane Loaded

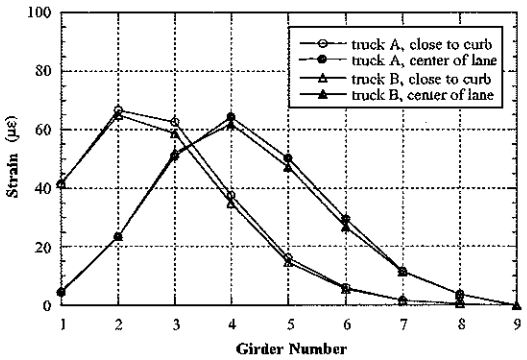

M43/SC (B02-23041)
South Lane Loaded

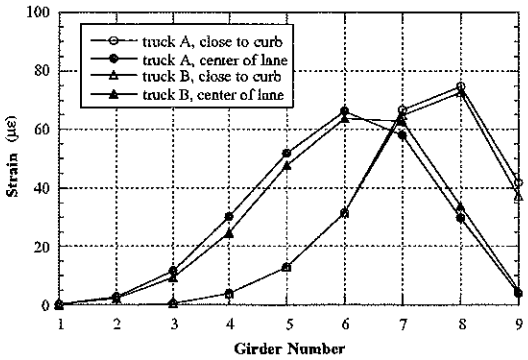

M43/SC (B02-23041)
North Lane Loaded

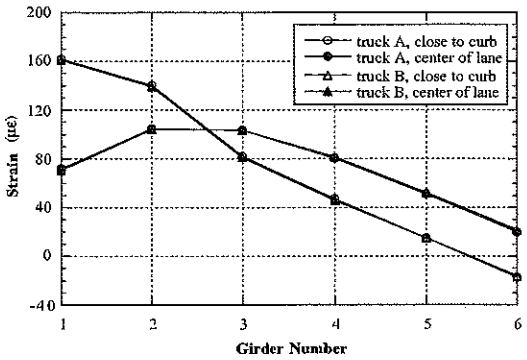

M36/HR (B01-47041)
South Lane Loaded

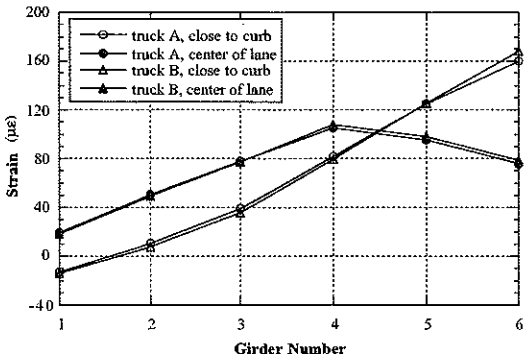

M36/HR (B01-47041)
North Lane Loaded

Figure 13.2. Strains under One Lane Loading at Crawling Speed (Continued).

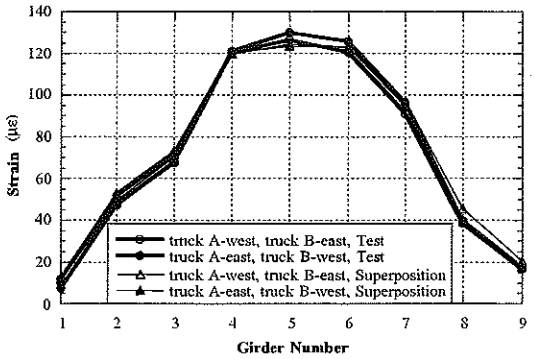

M52/BC (B02-46071)

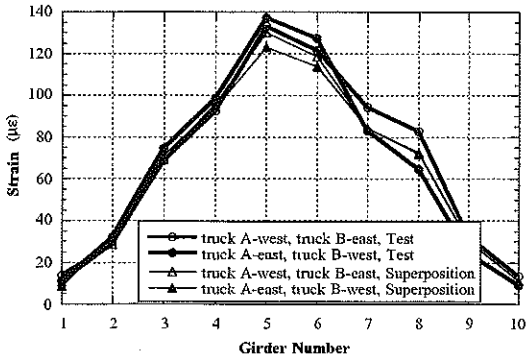

US127/BD (B01-30071)

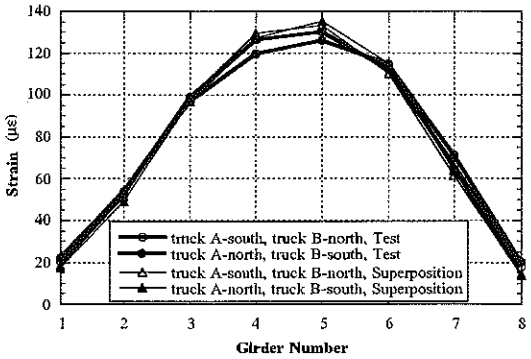

M50/MR (B01-58041)

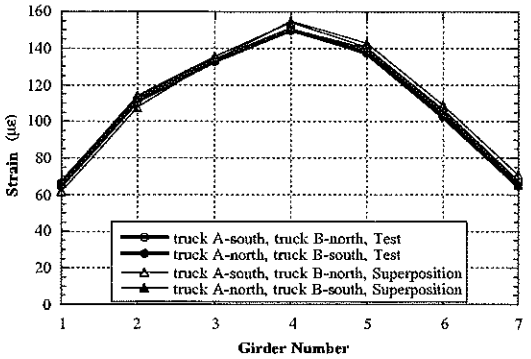

ST/I75 (S11-25032)

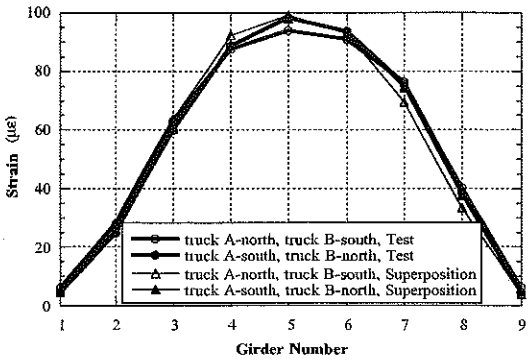

M43/SC (B02-23041)

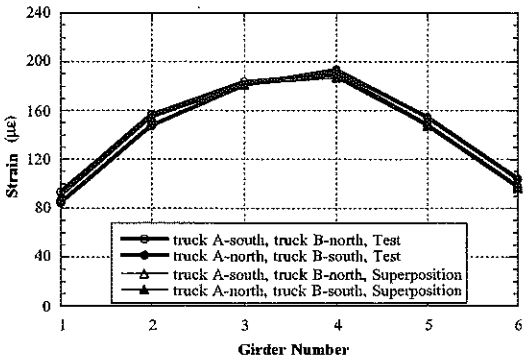

M36/HR (B01-47041)

Figure 13.3. Strains under Side-by-Side Truck Loading at Crawling Speed

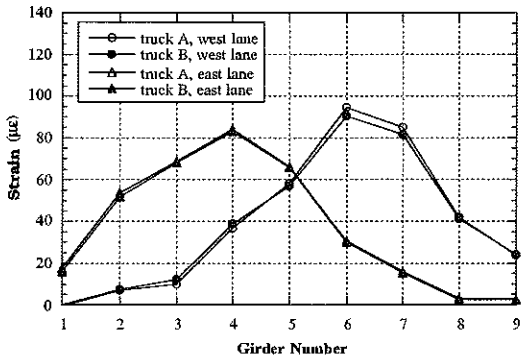

M52/BC (B02-46071)

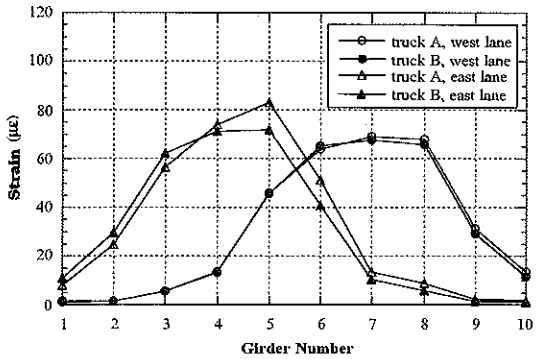

US127/BD (B01-30071)

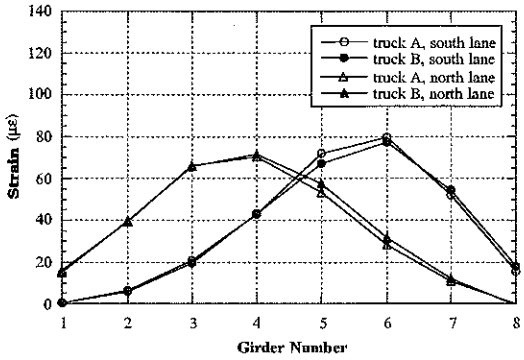

M50/MR (B01-58041)

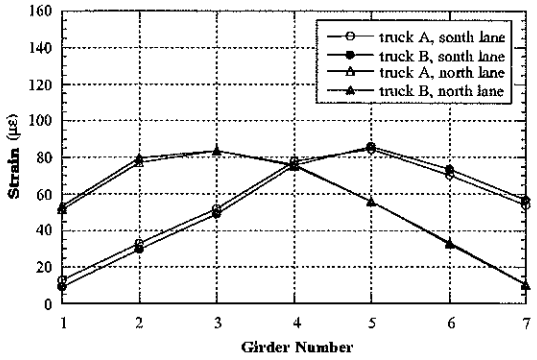

ST/I75 (S11-25032)

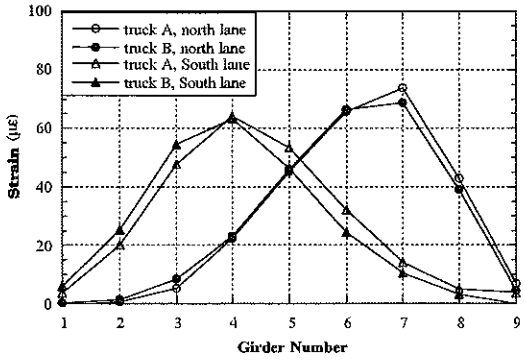

M43/SC (B02-23041)

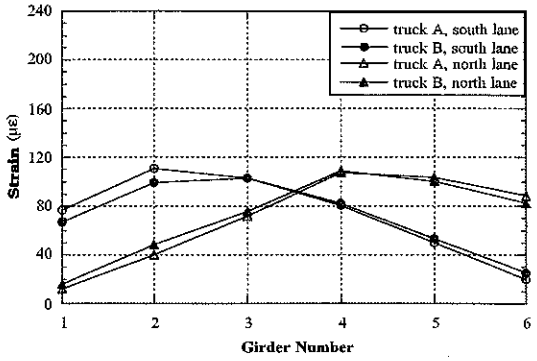

M36/HR (B01-47041)

Figure 13.4. Strains under One Lane Loading at Regular Speed.

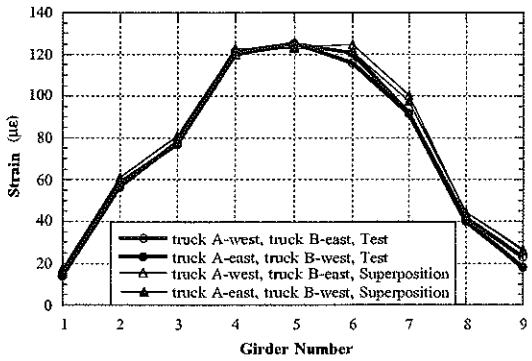

M52/BC (B02-46071)

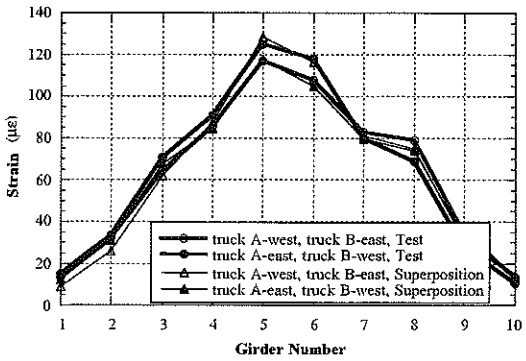

US127/BD (B01-30071)

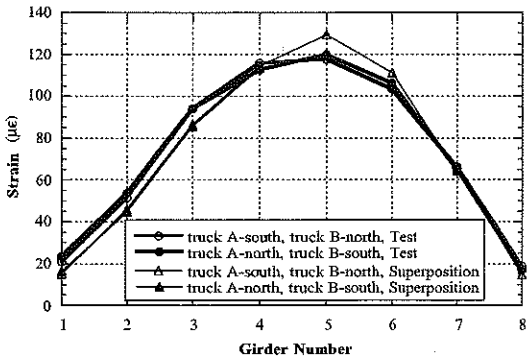

M50/MR (B01-58041)

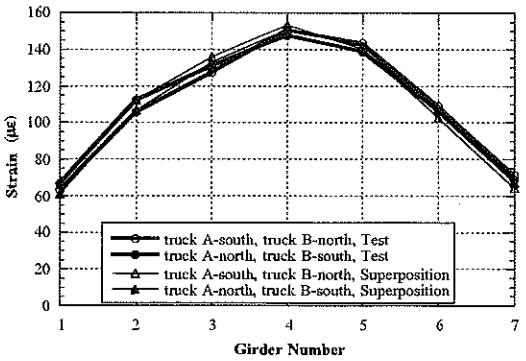

ST/I75 (S11-25032)

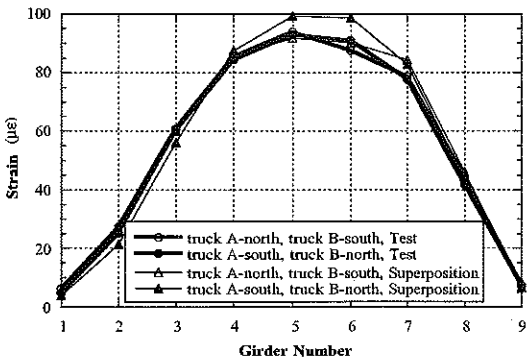

M43/SC (B02-23041)

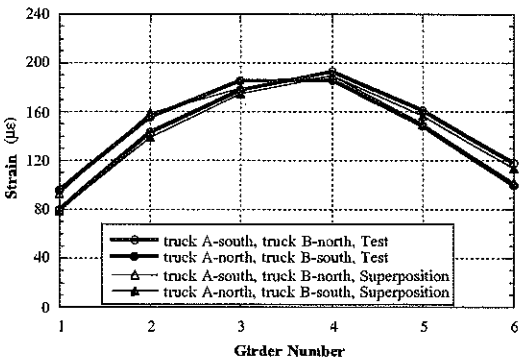

M36/HR (B01-47041)

Figure 13.5. Strains under Side-by-Side Truck Loading at Regular Speed.

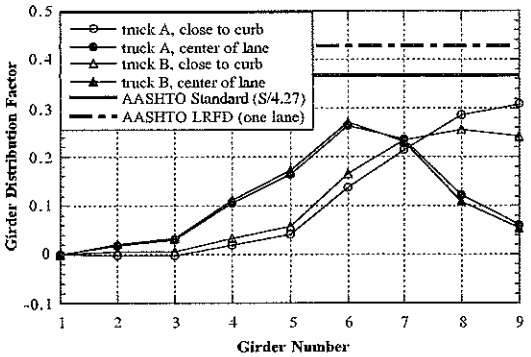

M52/BC (B02-46071)
West Lane Loaded

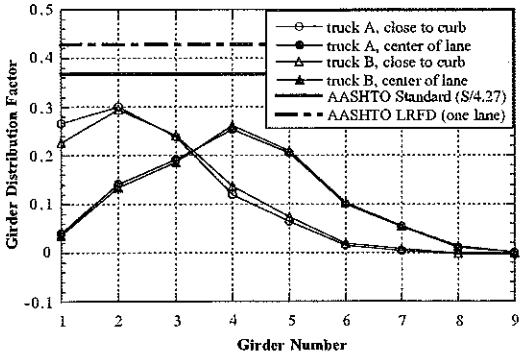

M52/BC (B02-46071)
East Lane Loaded

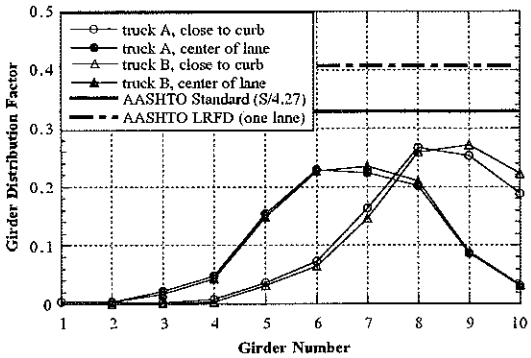

US127/BD (B01-30071)
West Lane Loaded

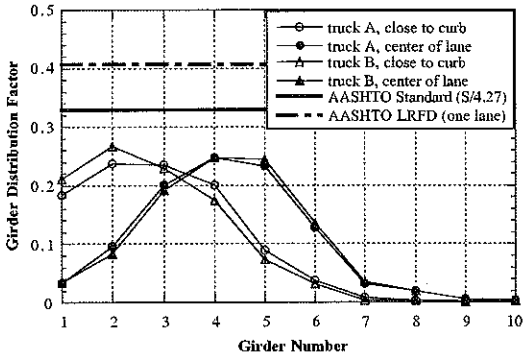

US127/BD (B01-30071)
East Lane Loaded

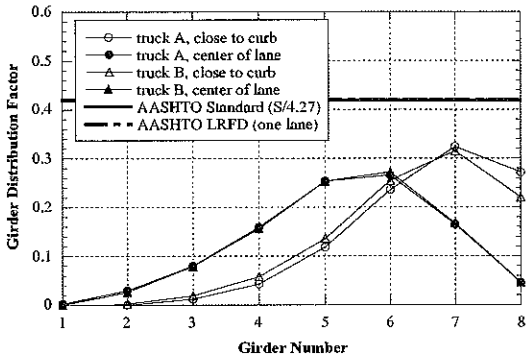

M50/MR (B01-58041)
South Lane Loaded

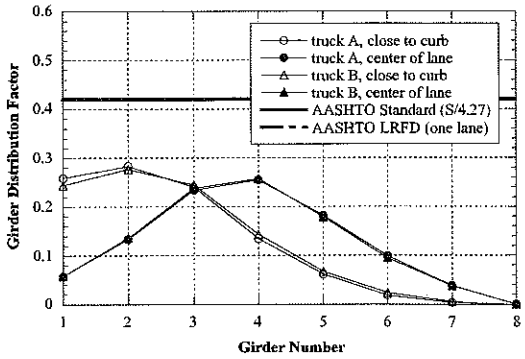

M50/MR (B01-58041)
North Lane Loaded

Figure 13.6. Girder Distribution Factor under One Truck Loading at Crawling Speed.

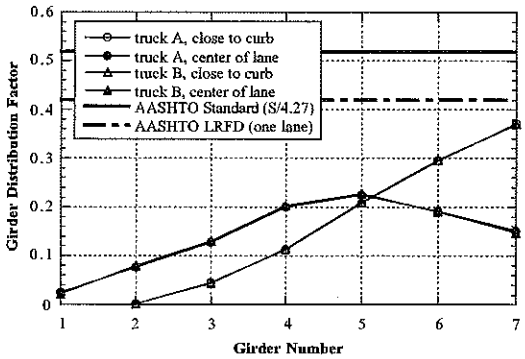

ST/I75 (S11-25032)
South Lane Loaded

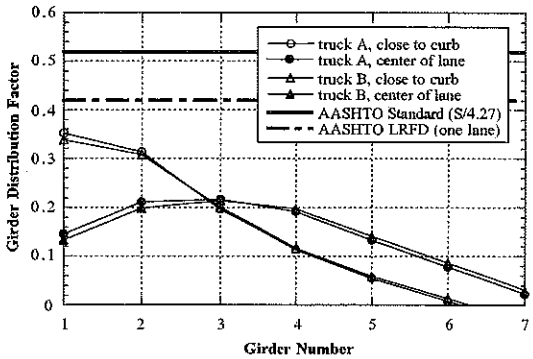

ST/I75 (S11-25032)
North Lane Loaded

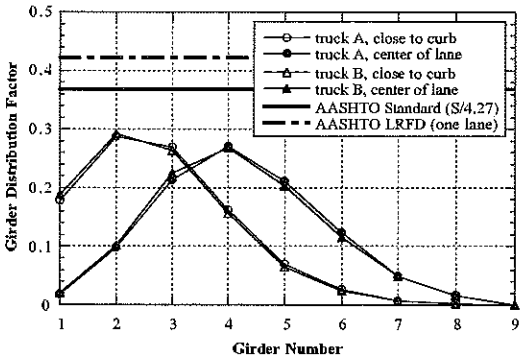

M43/SC (B02-23041)
South Lane Loaded

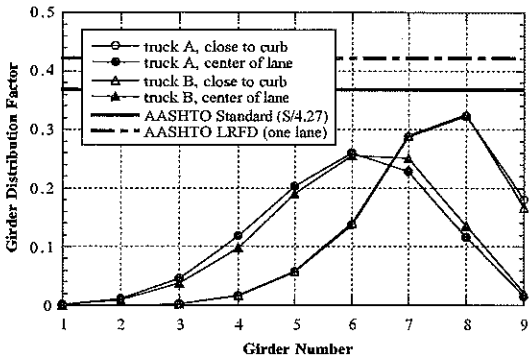

M43/SC (B02-23041)
North Lane Loaded

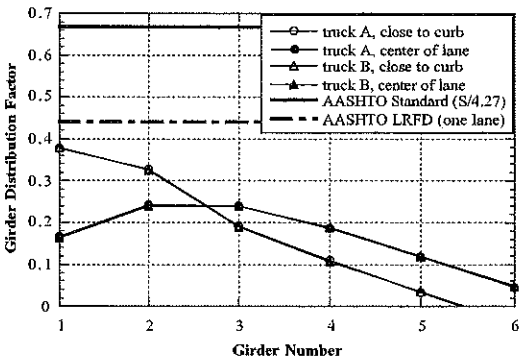

M36/HR (B01-47041)
South Lane Loaded

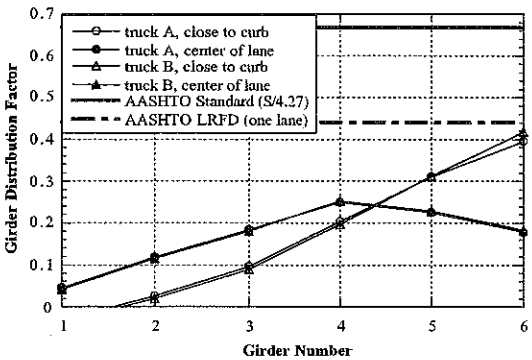

M36/HR (B01-47041)
North Lane Loaded

Figure 13.7. Girder Distribution Factor under One Truck Loading at Crawling Speed (continued).

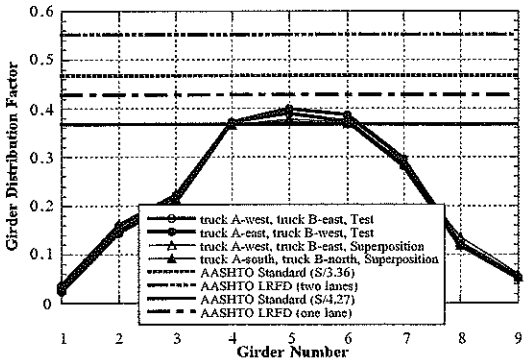

M52/BC (B02-46071)

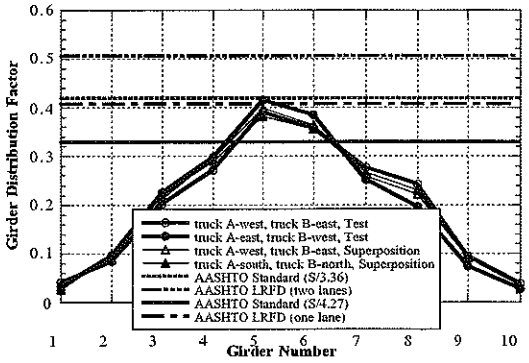

US127/BD (B01-30071)

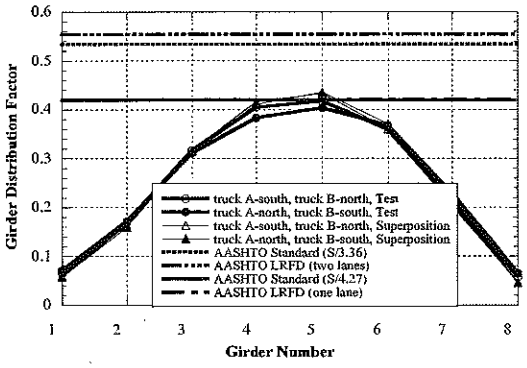

M50/MR (B01-58041)

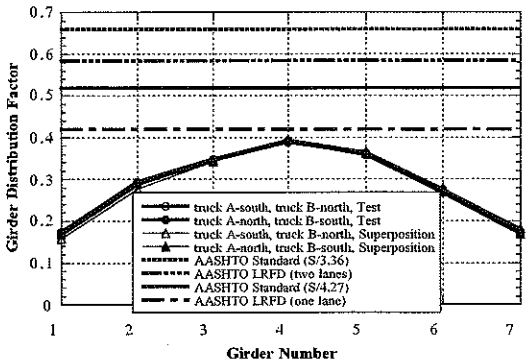

ST/I75 (S11-25032)

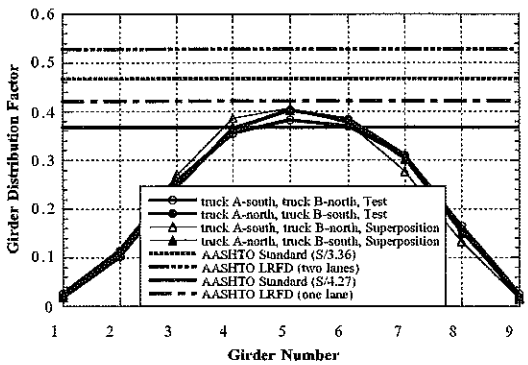

M43/SC (B02-23041)

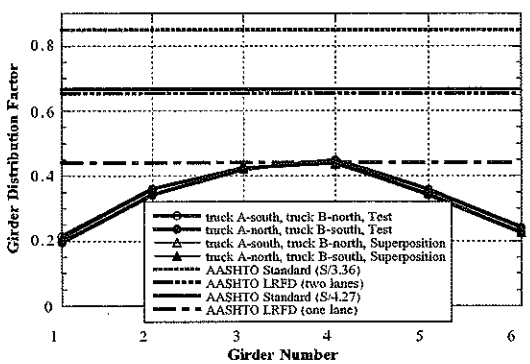

M36/HR (B01-47041)

Figure 13.8. Girder Distribution Factor under Two Truck Side-by-Side Loading at Crawling Speed.

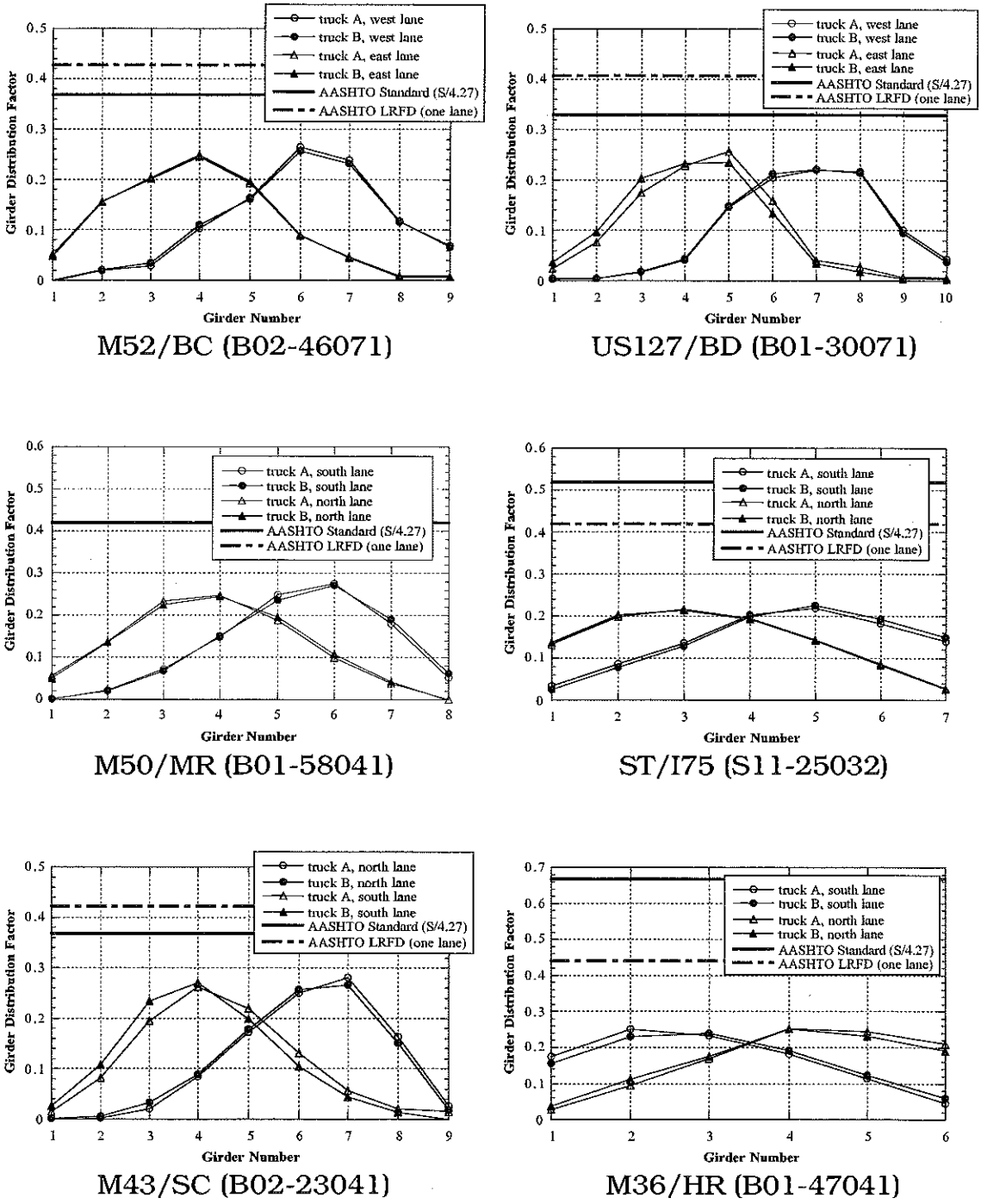

Figure 13.9. Girder Distribution Factor under One Truck Loading at Regular Speed.

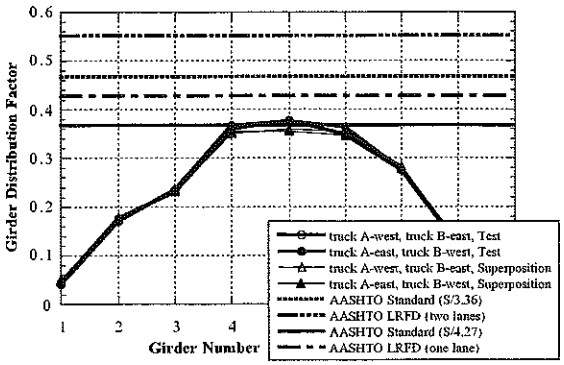

M52/BC (B02-46071)

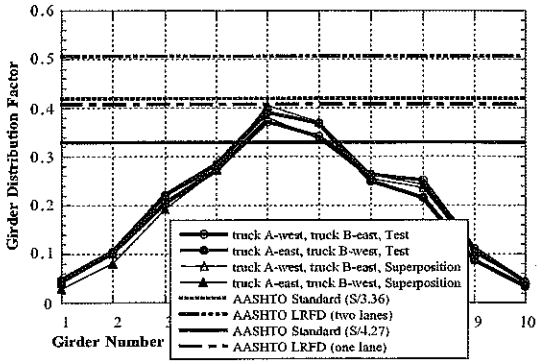

US127/BD (B01-30071)

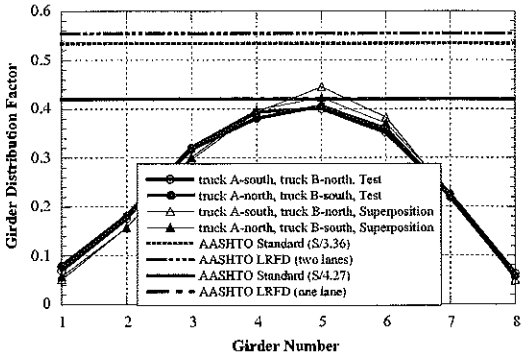

M50/MR (B01-58041)

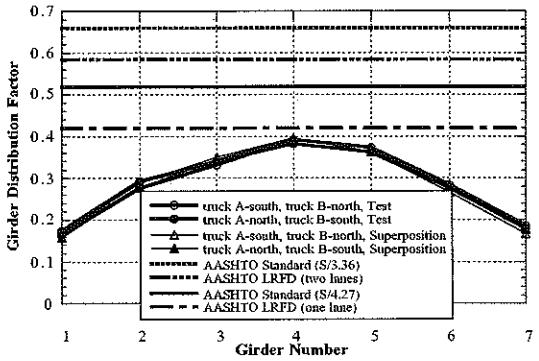

ST/I75 (S11-25032)

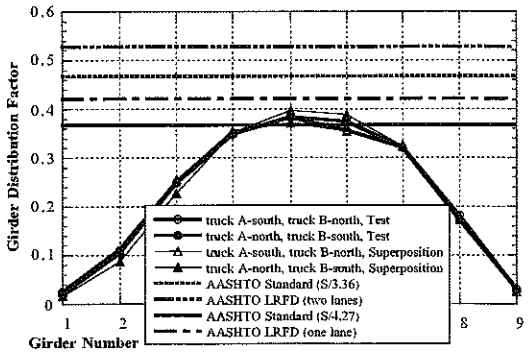

M43/SC (B02-23041)

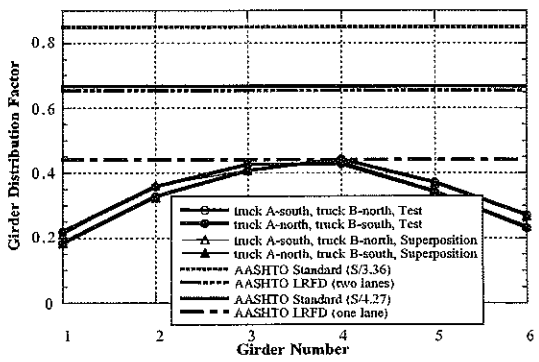

M36/HR (B01-47041)

Figure 13.10. Girder Distribution Factor under Two Truck Side-by-Side Loading at Regular Speed.

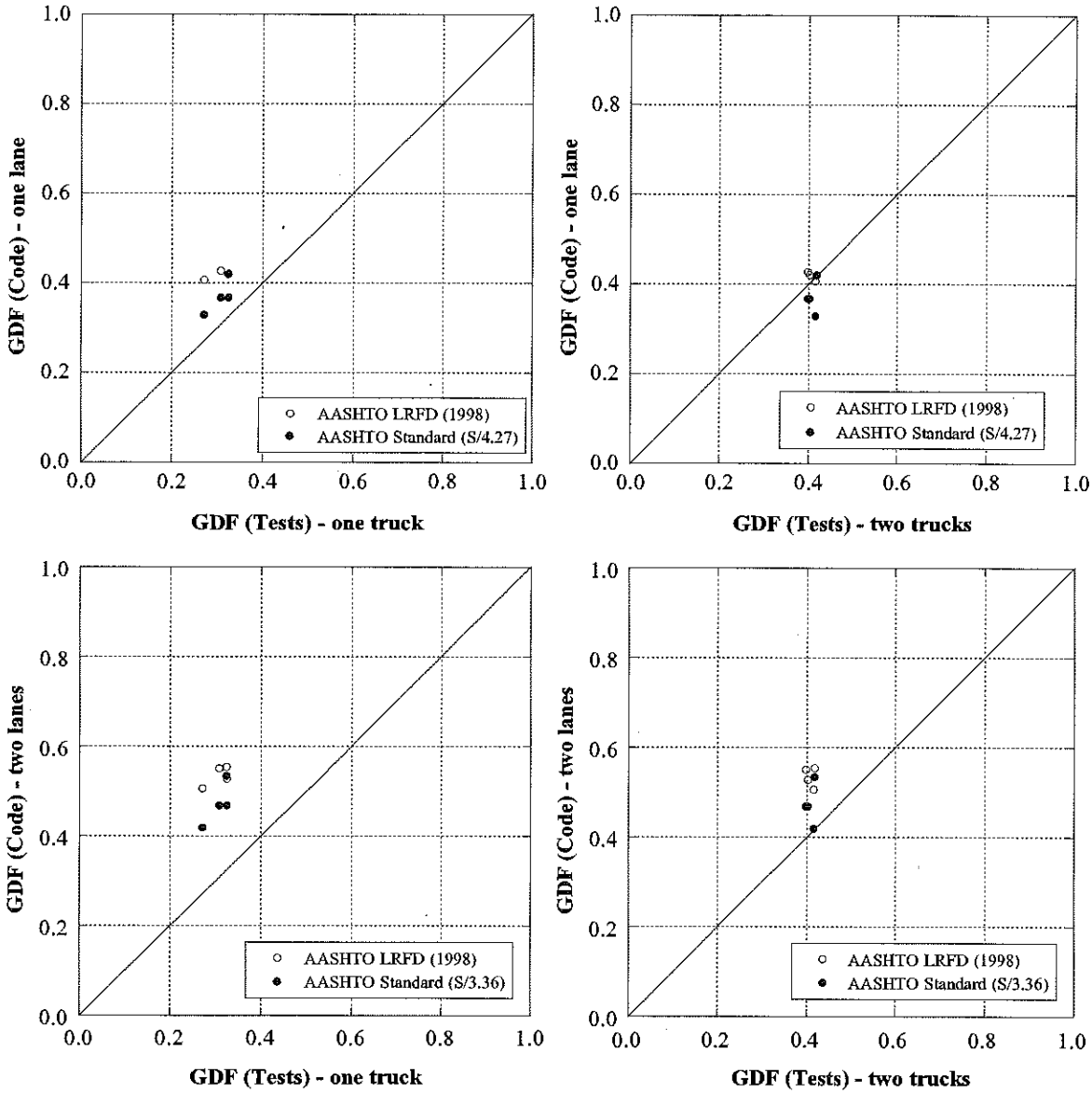

Figure 13.11. GDF (Test) Versus GDF (Code) for Bridge Span < 20 m (B02-46071, B01-30071, B01-58041,and B02-23041)

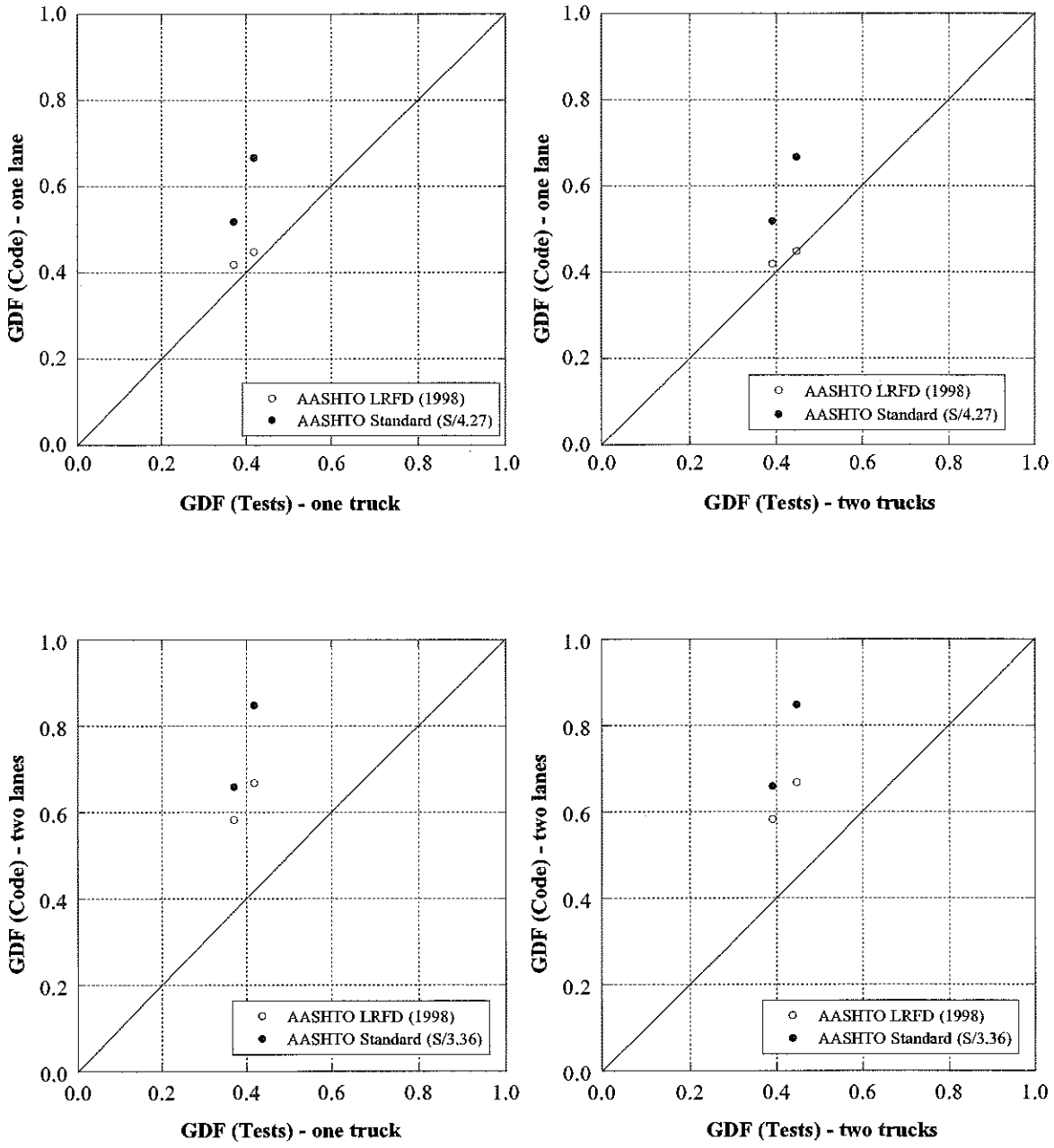

Figure 13.12. GDF (Test) Versus GDF (Code) for Bridge Span > 30 m (S11-25032, B02-23041, and B01-47041)

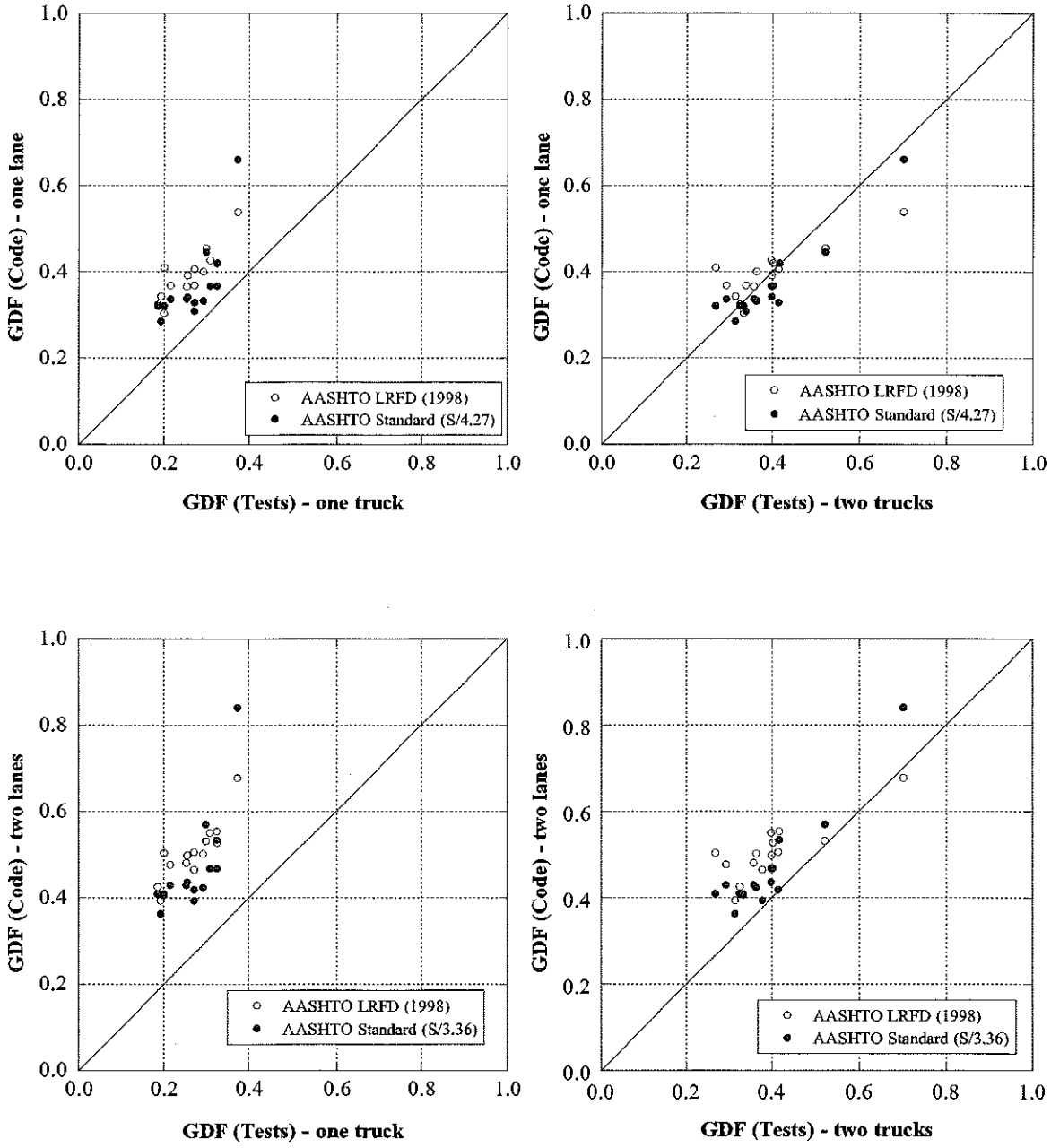

Figure 13.13. GDF (Test) Versus GDF (Code) for Bridge Span < 30 m
(All tested bridges since 1997)

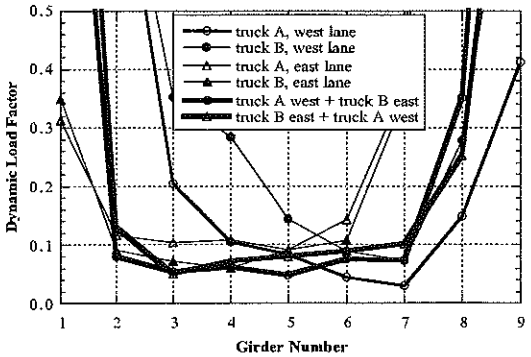

M52/BC (B02-46071)

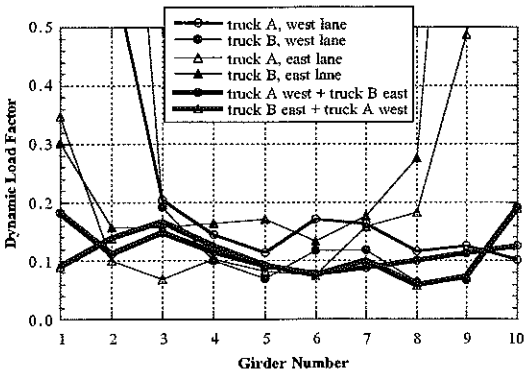

US127/BD (B01-30071)

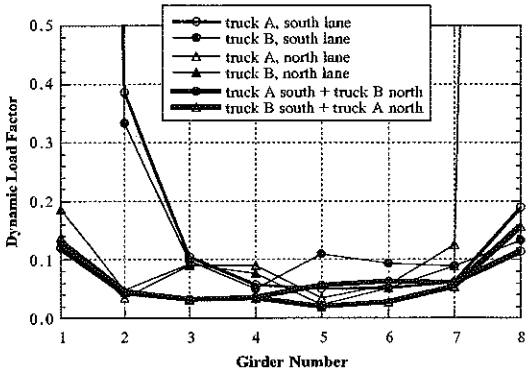

M50/MR (B01-58041)

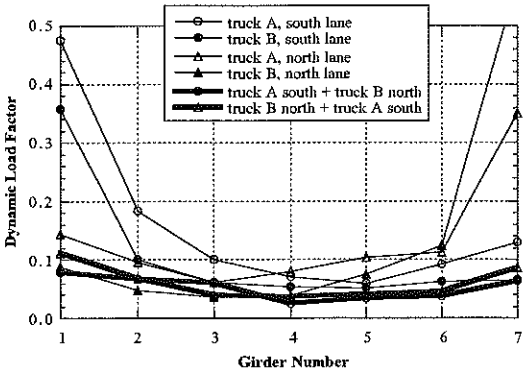

ST/I75 (S11-25032)

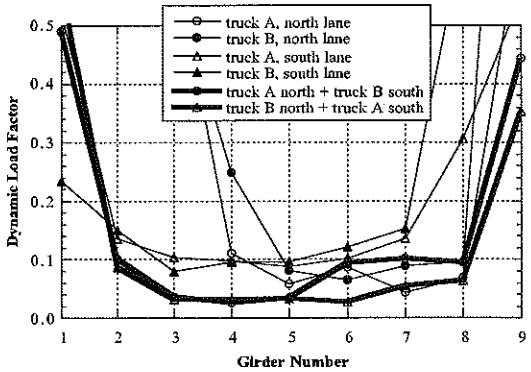

M43/SC (B02-23041)

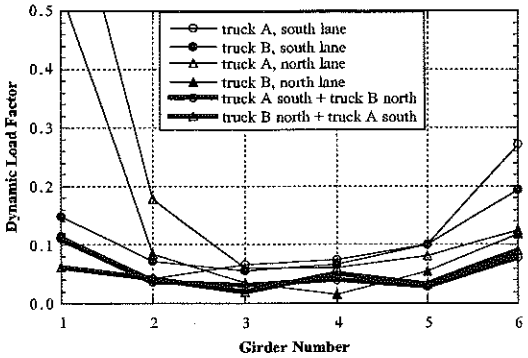

M36/HR (B01-47041)

13.14. Dynamic Load Factor.

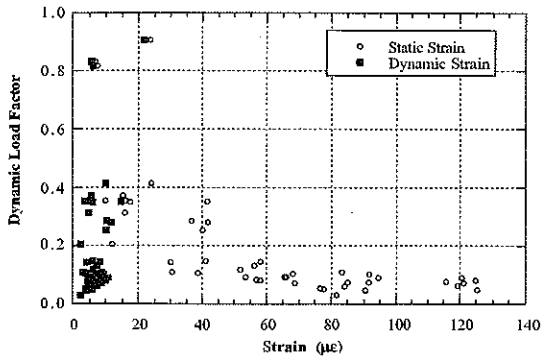

M52/BC (B02-46071)

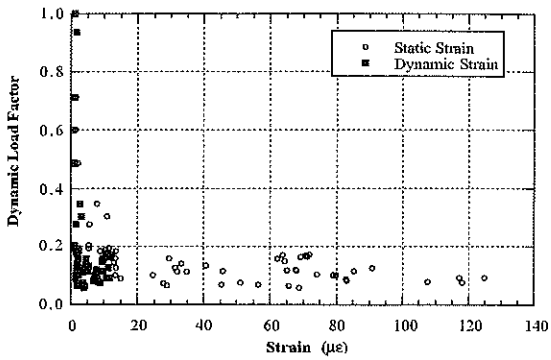

US127/BD (B01-30071)

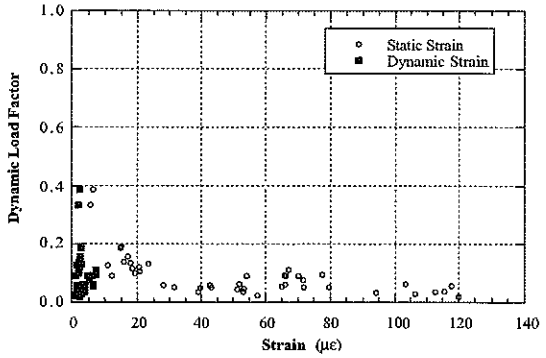

M50/MR (B01-58041)

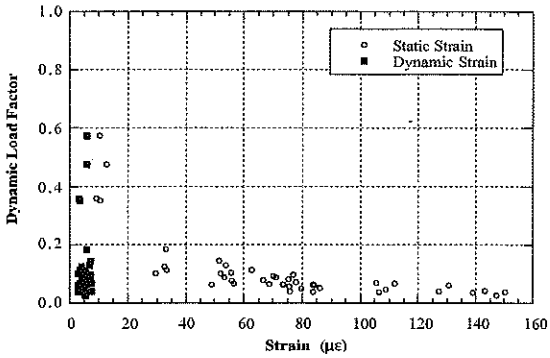

ST/I75 (S11-25032)

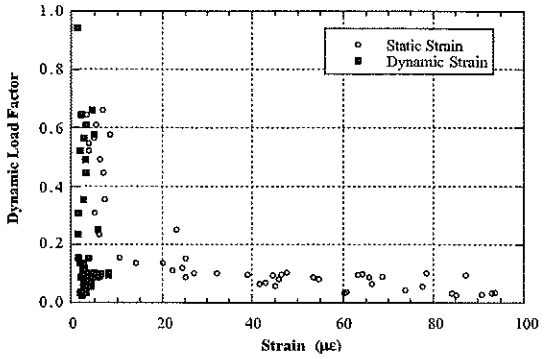

M43/SC (B02-23041)

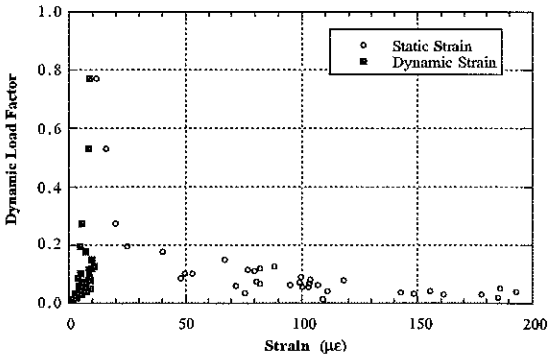

M36/HR (B01-47041)

13.15. Strain Vs. Dynamic Load Factor.

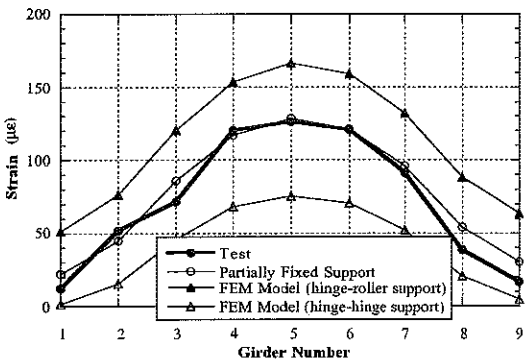

M52/BC (B02-46071)

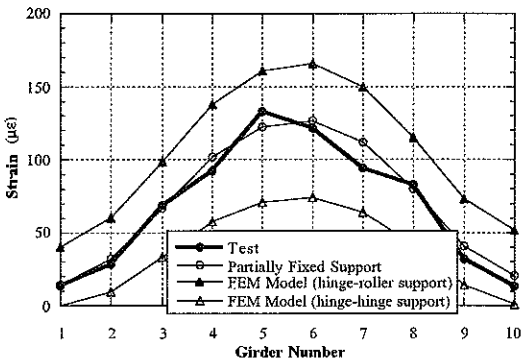

US127/BD (B01-30071)

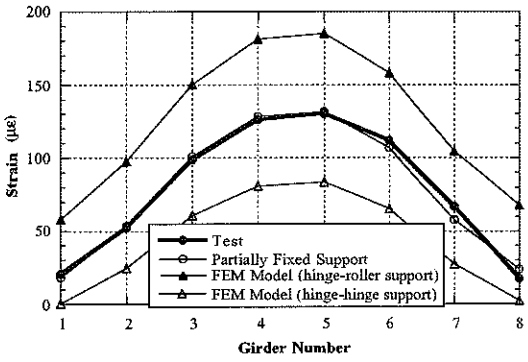

M50/MR (B01-58041)

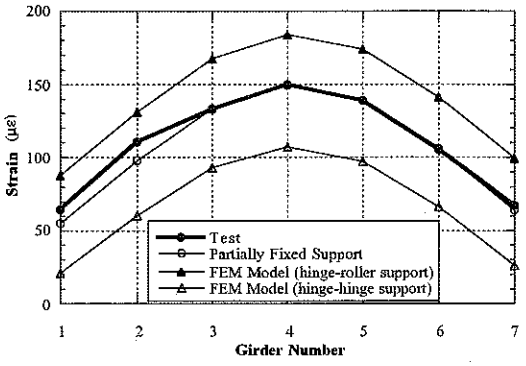

ST/I75 (S11-25032)

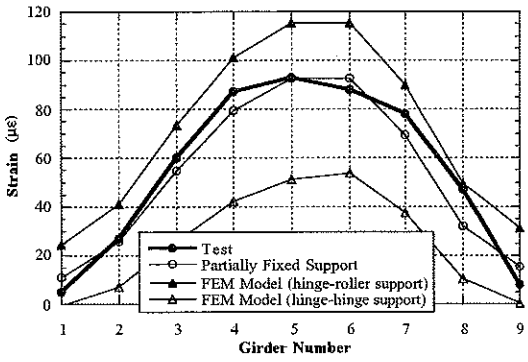

M43/SC (B02-23041)

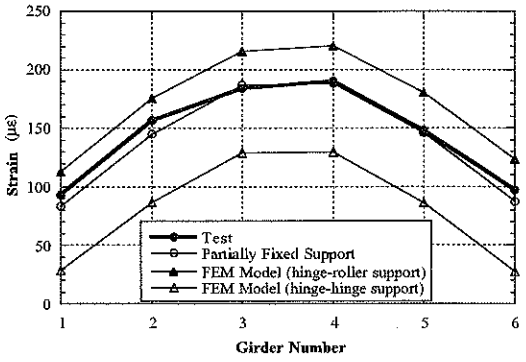

M36/HR (B01-47041)

13.16. Results of the Fimte Element Analysis, Strains.

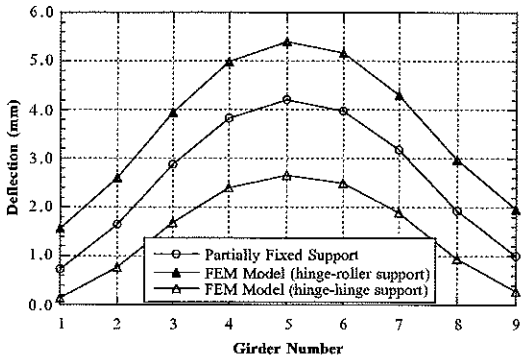

M52/BC (B02-46071)

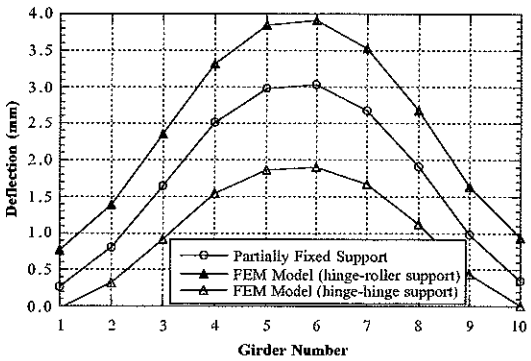

US127/BD (B01-30071)

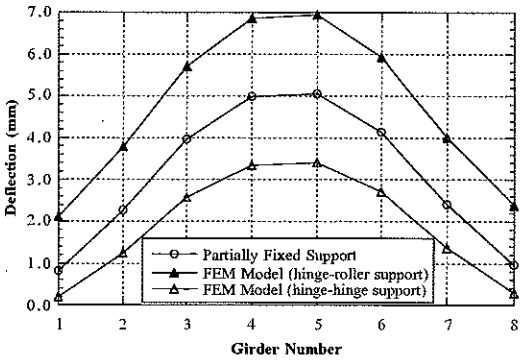

M50/MR (B01-58041)

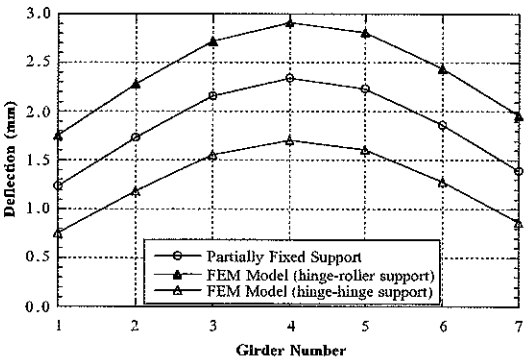

ST/I75 (S11-25032)

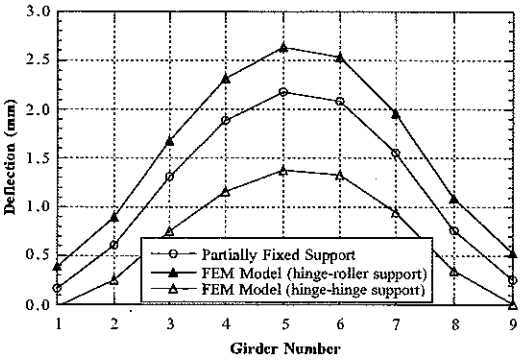

M43/SC (B02-23041)

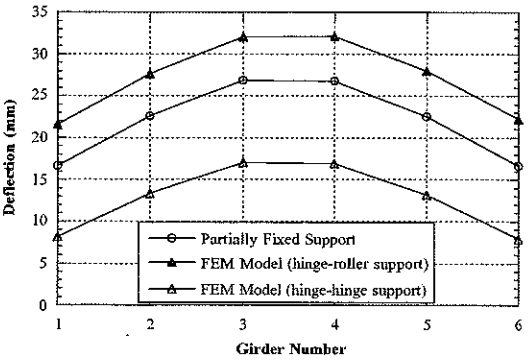

M36/HR (B01-47041)

13.17. Results of the Finite Element Analysis, Deflections.

14. References

1. AASHTO Standard Specifications for Highway Bridges, American Association of State and Transportation Officials, Washington, DC, 1996.

2. AASHTO LRFD Bridge Design Specifications. American Association of State Highway and Transportation Officials, Washington, D.C., 1998.

3. AASHTO Guide Specifications for Distribution of Loads for Highway Bridges, American Association of State Highway and Transportation Officials, Washington, D.C., 1994.

4. Bakht, B., and Pinjarkar, S.G., "Dynamic Testing of Highway Bridges-A Review." Transportation Research Record 1223, Transportation Research Board, National Research Council, Washington, D.C., pp. 93-100, 1989.

5. Brockenbrough, R.L., "Distribution factors for curved I-girder bridges." Journal of Structural Engineering, ASCE, Vol. 112, No. 5, 1986.

6. Croce, P. and Salvatore, W., "Stochastic Model for Multilane Traffic Effects on Bridges." Journal of Bridge Engineering, ASCE, Vol. 6, No.2, pp136-143, March/April, 2001.

7. Ghosn, M., Moses, F., and Gobieski, J., "Evaluation of Steel Bridges Using In-Service Testing." Transportation Research Record 1072, Transportation Research Board, National Research Council, Washington, D.C., pp. 71-78, 1986.

8. Hays, C.O., Sessions, L.M., and Berry, A.J. (1986), "Further studies on lateral load distribution using FEA." Transportation Research Record 1072, Transportation Research Board, National Research Council, Washington, 1986.

9. Hwang, E.S., and Nowak, A.S., "Simulation of Dynamic Load for Bridges." Journal of Structural Engineering, ASCE, Vol. 117, No.5, pp.1413-1434, July, 1991.

10. Imbsen, R.A., and Nutt, R.V., "Load Distribution Study on Highway Bridge using STRUDL FEA" Proceeding, Conference on Computing in Civil Engineering, ASCE, New York, 1978.

11. Lichtenstein, A. G., Manual for Bridge Rating Through Nondestructive Load Testing, NCHRP Report 12-28(13) A, 1998.

12. Mabsout, M.E., Tarhini, K.M., Frederick, G.R., and Tayar, C. "Finite-Element Analysis of Steel Girder Highway Bridges." Journal of Bridge Engineering. Vol. 2, No 3, August 1997.

13. Nassif, H.H. and Nowak, A.S., "Dynamic Load Spectra for Girder Bridges." Transportation Research Record 1476, Transportation Research Board, National Research Council, Washington, D.C., pp. 69-83, 1995

14. Nowak, A.S., Laman, J.A., and Nassif H., "Effect of Truck Loading on Bridges." Report UMCE 94-22. Department of Civil and Environmental Engineering, University of Michigan, Ann Arbor, 1994

15. O'Connor, C. and Shaw, P.A., "Bridge Loads", Spon Press, New York, 2000.

16. Paultre, P., Chaallal, O., and Proulx, J., "Bridge Dynamics and Dynamic Amplification Factors-A Review of Analytical and Experimental Findings." Canadian Journal of Civil Engineering, Vol. 19, pp. 260-278, 1992.

17. Schultz J.L., Commander B., Goble G.G., Frangpol D.M., Efficient field Testing and load Rating of Short – And Medium – Span Bridges, Structural Engineering review, Vol. 7, No 3 pp181-194, 1995.

18. Stallings, J.M., and Yoo, C.H., "Tests and Ratings of Short-Span Steel Bridges." Journal of Structural Engineering, ASCE, Vol. 119, No. 7, pp. 2150-2168, July, 1993.

19. Tarhini K.M and Frederick, G. R. 1992. "Wheel load distribution in I-girder highway bridges" Journal of Structural Engineering Vol 118, No 5, pp1285-1294.

20. Zokaie, T., Osterkamp, T.A., and Imbsen, R.A., Distribution of Wheel Loads on Highway Bridges, National Cooperative Highway Research Program Report 12-26, Transportation Research Board, Washington, D.C., 1991.